



UNIVERSITÀ DEGLI STUDI DI PADOVA

Dipartimento di Fisica e Astronomia “Galileo Galilei”

Corso di Laurea Magistrale in Fisica

Tesi di Laurea

Unitarity-based Methods for Muon-Electron Scattering in Quantum Electrodynamics

Relatore

Prof. Pierpaolo Mastrolia

Correlatori

Prof. Massimo Passera

Dr. William Javier Torres Bobadilla

Laureando

Giulio Dondi

Anno Accademico 2018/2019

Abstract

In this thesis we elaborate on the modern techniques for the evaluation of Scattering Amplitudes in Quantum Field Theory, and apply them to the calculation of $\mu^- e^- \rightarrow \mu^- e^- \gamma$ at one loop in Quantum Electrodynamics, within the Dimensional Regularization scheme. The corresponding Feynman diagrams contribute to the so called *real-virtual* term of the Next-to-Next-to-Leading-Order corrections to $\mu e \rightarrow \mu e$ scattering. Their calculation is crucial for a novel estimation of the leading Hadronic corrections to the muon's anomalous magnetic moment, which is the goal of the *MUonE* experiment, recently proposed at CERN.

First, we review the theoretical background behind the contributions to the muon's magnetic moment and the connection with $\mu^- e^-$ scattering. Then, we elaborate on the algorithmic steps required by the evaluation of multi-loop Feynman amplitudes, from the form-factor decomposition, to the reduction onto a basis of Master Integrals, and, finally, to the calculation of the latter by means of the Differential Equations method. We outline the modern frameworks based on Unitarity of the S -matrix, which employ amplitude cuts to construct a decomposition onto Master Integrals in the *Generalised Unitarity* framework. This includes *Integrand-level Decomposition methods* which take advantage of the polynomial properties of Feynman amplitude integrands and offer a higher level of automation for the calculation of complex amplitudes. Specifically we detail the more recent *Adaptive Integrand Decomposition* and its automated code implementation AIDA used to carry out the calculations presented.

We illustrate the *Momentum Twistor* parametrisation for particle kinematics used by AIDA, and introduce four and five-point twistor parametrisations suitable for our goals.

We present our results on the Master Integral decompositions of $\mu^- e^- \rightarrow \mu^- e^-$ and $\mu^- e^- \rightarrow \mu^- e^- \gamma$ at one-loop, both considering massive and massless electrons, and finally we review the evaluation of the Master Integrals for $\mu^- e^- \rightarrow \mu^- e^-$ in the $m_e \rightarrow 0$ limit with Differential Equations.

Contents

Introduction	1
1 The muon's intrinsic magnetic moment	5
1.1 Magnetic moments	5
1.1.1 The anomalous magnetic moment of the muon	6
1.2 The Standard Model prediction of a_μ	8
1.2.1 The QED contribution	8
1.2.2 The Electroweak contribution	11
1.2.3 The hadronic contribution	12
1.3 Extracting the leading hadronic contribution to a_μ	14
1.3.1 A novel approach: <i>MUonE</i>	17
2 Methods for one-loop Feynman integrals	23
2.1 Dimensional Regularisation	25
2.1.1 The $D = 4 - 2\epsilon$ prescription	26
2.1.2 The $D = D_{\parallel} + D_{\perp}$ prescription	28
2.2 Tensor integral reduction	31
2.2.1 Passarino-Veltman tensor reduction	32
2.2.2 D-dimensional amplitude decomposition	36
2.3 Master Integral Identities	38
2.3.1 Lorentz invariance identities	38
2.3.2 Integration-by-parts identities	39
2.4 Evaluating Master Integrals with Differential Equations	41
2.4.1 Differential equations in canonical form	43
2.4.2 The Magnus exponential method	44
2.4.3 General solution via Iterated Integrals	47
3 Unitarity methods for one-loop amplitudes	50
3.1 Unitarity and the Optical Theorem	50
3.2 Unitary cuts	53
3.3 The Feynman Tree Theorem	55
3.4 Multiple cuts and Generalised Unitarity	58
4 Integrand-level Decomposition methods	64
4.1 The OPP decomposition method	64
4.1.1 Parametric expansion of the residues	66
4.1.2 Extension to D dimensions	68
4.2 Integrand decomposition via Polynomial Division	70
4.2.1 Integrand recurrence	71
4.2.2 Division modulo Gröbner bases	72

5	Adaptive Integrand Decomposition	76
5.1	Preliminaries	76
5.2	The Divide-Integrate-Divide (DID) procedure	78
5.3	Adaptive Integrand Decomposition at one-loop	79
5.4	<i>AIDA</i> : ADAPTIVE INTEGRAND DECOMPOSITION ALGORITHM	83
6	N-point kinematics	88
6.1	Mandelstam variables	88
6.2	Spinor-Helicity Formalism	89
6.2.1	Massless fermion representation	90
6.2.2	Massless vector boson representation	93
6.2.3	Little-group scaling	94
6.3	Momentum twistors	94
6.3.1	Dual variables	94
6.3.2	Twistor parametrisation	97
7	The NNLO real-virtual corrections to muon-electron scattering	101
7.1	Calculations with FEYNCALC	102
7.1.1	Leading Order	102
7.1.2	Next-to-leading Order	103
7.2	Calculations with <i>AIDA</i>	107
7.2.1	Next-to-leading Order	107
7.2.1.1	Massive Electron case	107
7.2.1.2	Massless electron limit	111
7.2.2	Next-to-next-to-leading Order	113
7.2.2.1	Massive electron case	114
7.2.2.2	Numerical reduction of the Massive electron case	117
7.2.2.3	Massless electron limit	119
8	Evaluation of massive one-loop 4-point Master Integrals with Differential Equations	122
8.1	System of Differential Equations in canonical form	123
8.2	Boundary conditions	125
	Conclusions	128
	Appendix A Construction of a massless basis for loop momenta	131
	Appendix B Parametric expansion of Integrand Decomposition residues on the cut solutions	134
	Appendix C Complete NLO Virtual corrections to μ-e scattering	141
	Appendix D Feynman rules for counterterm diagrams	145
	Appendix E Detailed results for massive one-loop 4-point Master Integrals	147
	References	150

Introduction

Fundamental particles and their interactions are at the very heart of all physical phenomena we experience. The form of these interactions and the way we describe them depend on the typical energies at which they occur. One of the goals of Particle physics is to uncover and describe the interactions of fundamental particles during the very early universe, in a state of extreme heat and density and, consequently, very high energy. Describing the early universe through the behaviour of its constituents may give the answer to the question of its very origin, which puzzled mankind for millennia.

Our best way to probe these conditions is through collision experiments carried out in particle accelerators at many locations worldwide. These experiments established two key concepts in high-energy physics: that matter can be converted into energy and particles may be produced out of energy according to Special Relativity, and that the outcome of any process of particle physics is probabilistic in nature as Quantum Mechanics describes. These ideas are unified in the framework of Quantum Field Theory (QFT) which is the foundation for the accepted modern theory of fundamental particles, the *Standard Model of Particle Physics (SM)*.

Quantum Field theory describes interactions between particles as the evolution of a *particle field* $|i\rangle$ via the so-called *S-matrix*, which encodes all the processes possible within the theory. In a collision experiment one may wish to probe one specific outcome of the interaction, expressed as a specific final particle field $|f\rangle$. The transition matrix element $\langle f|S|i\rangle$ represents the probability density for the initial particles to interact in the specific fashion desired. In the language of QFT this transition probability is expressed in terms of the so-called *Feynman Amplitude* $\mathcal{M}(i \rightarrow f)$. The amplitude squared is directly related to the *scattering differential cross-section*, the physical quantity of interest which can be extracted from experimental data. Through experiment one can determine the Feynman amplitude of a given process $|i\rangle \rightarrow |f\rangle$ and, by extension, shed light on the validity of the underlying Quantum Theory. To produce a theoretical prediction that can shed light on new physics, the objective is then to evaluate the Feynman amplitude of a candidate process to very high precision.

An explicit expression for the Feynman amplitude is most often obtained by evaluating the *S-matrix* in a *perturbative series*, where each term is a combination of the basic interactions of the theory and carries powers of the *coupling constant* of the theory, which sets the perturbative order.

The mathematical expression of each term is represented pictorially by *Feynman Diagrams*, which depicts the initial, final and intermediate particles as lines, whose intersections represent the basic interaction blocks of the theory. Such diagrams look like tree-like graphs in the simpler cases with few interactions, but as the perturbative expansion progresses they evolve into complex lattices, possibly with so-called *loops* of internal particles.

Despite the external particles carrying very definite relativistic momenta (they are forced to lie on the so-called *mass shell*), intermediate particles running in a loop evade this constraint and may have any generic momentum, since they are inaccessible and subject to the Indetermination principle. These loops lead to *loop integrals* that account for all the possible momenta running, and these constitute the major difficulty in the evaluation of all but the simplest Feynman amplitudes.

The development of ground-breaking calculation techniques from the late '90s and throughout the

2000s [1, 2] was stimulated by the then-upcoming collision experiments at the *Large Hadron Collider*, purpose-built by CERN to perform scattering experiments at energies between 100 GeV to several TeV, with the goal of testing the validity of the Standard Model in this range.

For the first time in particle physics it became possible to carry out high-precision theoretical calculations at *Next-to-Leading Order (NLO)* in perturbation theory in a fully-automated fashion [3–6], particularly useful given the complexity and abundance of processes. During the so-called *NLO Revolution* [7] most $2 \rightarrow 3$ particle interaction processes of interest to LHC physics were calculated, as well as the first $2 \rightarrow 4$ and $2 \rightarrow 5$ particles interactions.

These theoretical achievements have enabled the validation of the Standard Model to very high degree, most remarkably with the recent first detection of the Higgs Boson in 2012. Nevertheless there is good evidence that the Standard Model is not the ultimate theory for high-energy physics since, to give a few prominent examples, it does not include a description for the gravitational interaction nor it provides an explanation for Dark Energy or conclusive candidates for Dark Matter.

Evidence for *Beyond-the-Standard-Model (BSM)* physics can be gathered by accurate measurements of the discrepancies between the current model and experimental observations. The *gyromagnetic ratio a_μ of the Muon μ* is a prime candidate for studying BSM physics since it is one of the most accurately measured quantities in particle physics and it already diverges from the SM prediction by $3 \sim 4$ standard deviations. Determining the contribution of BSM physics relies on improving the accuracy of the SM contributions, especially those coming from Hadronic physics. A recent experimental proposal, *MUonE* [8], aims to extract a $\sim 1\%$ estimate of these contributions from measurements of the Hadronic corrections to $\mu^\pm e^- \rightarrow \mu^\pm e^-$ scattering to 10 parts-per-million [9], an unprecedented level of accuracy.

The theoretical challenge is then to determine the Hadronic Leading Order contributions to μe scattering with comparable precision. To this aim, the contributions due to Quantum Electrodynamics (QED) alone need to be determined to *Next-to-Next-to-Leading Order (NNLO)* in perturbation theory. Ground-breaking work has already been conducted on the two-loop virtual radiative corrections [10–12].

In this thesis we take the first steps towards the calculation of the *real-virtual one-loop radiative corrections* to this process, namely we examine the amplitudes for the process $\mu^- e^- \rightarrow \mu^- e^- \gamma$ at one-loop, which constitute part of the NNLO contributions and are complementary to the aforementioned two-loop results.

This thesis work is organised as follows. In Chapter 1 we review the theoretical background behind the gyromagnetic ratio of the muon a_μ and the main contributions from the various sectors of the Standard Model. We focus on the most uncertain contributions to the final result, namely the Hadronic corrections given by the so-called *Hadronic Vacuum Polarisation (HVP)* function. We then describe the novel theoretical ideas behind the proposed *MUonE* experiment, in particular how the HVP may be extracted from the Hadronic contributions to the running of the QED coupling constant, and how this can itself be extracted from $\mu e \rightarrow \mu e$ scattering data.

In Chapter 2 we outline the principal theoretical techniques used for the computation of one-loop Feynman amplitudes.

First, we introduce the concept of *Dimensional Regularisation* both in the $D = 4 - 2\epsilon$ prescription by 't Hooft and Veltman [13] as well as the so-called $D = D_\parallel + D_\perp$ prescription [14–16] which entails splitting the D -dimensional space-time in a *parallel space* spanned by the independent external momenta, and an *orthogonal space* spanned by the remaining vectors.

In the rest of the chapter we outline the three-step approach to the evaluation of Feynman amplitudes:

1. *Tensor Decomposition* of a generic loop Feynman amplitude as a linear combinations of a finite number *scalar loop integrals*, effectively constituting an integral basis for the amplitude;

2. reduction of this set of integrals to the minimal number of independent integrals, at this stage called *Master Integrals*;
3. evaluation of the Master Integrals themselves

Long ago it was realised that, since Special Relativity constrains the form of the factors appearing in the expression of a Feynman integral, it is possible to manipulate the integral and re-write it as a sum of a finite number of scalar integrals. This can be done with the *Passarino-Veltman method* [17] which we outline in this chapter, although more advanced techniques for obtaining a Scalar Integral decomposition are introduced later on. We shall also touch on how the scalar integral decomposition is affected by working in Dimensional Regularisation.

We then deal with the reduction of this set of integrals to the minimal basis of *Master Integrals* by taking advantage of remarkable relations between Feynman integrals, known as *Lorentz-Invariance* and *Integration-by-Parts* identities. The former arise from the invariance of scalar integrals under Lorentz transformations, the latter come from the D -dimensional divergence theorem. The *Laporta algorithm* [18] is capable, given a set of scalar integrals, to identify a minimal basis of Master Integrals and generate relations to map all elements to that basis. The size of the basis depends exclusively on the nature of the problem (e.g. the external kinematics and number of loops) while the exact scalar integrals are not uniquely defined. Many code suites implement this algorithm, such as KIRA [19] and REDUZE [20].

Lastly, we describe the *Differential Equations method* [21, 22], which involves setting up coupled systems of Differential Equations in the kinematic invariants whose solution yields an analytical expression for the Master Integrals in powers of ϵ . We introduce the concept of a system in the so-called *Canonical basis* [23] and the *Magnus Exponential* [24] method used to obtain it, and lastly how it is possible to construct the solution to the coupled systems algorithmically as a Dyson series of iterated integrals and written in terms of the *Goncharov (or Generalised) PolyLogarithms (GPLs)* [25].

In Chapter 3 we introduce some of the powerful techniques developed in the last couple of decades [1, 2] concurrently with the need for highly-precise and automatic evaluation codes to carry out the complex theoretical calculations to be paired up with experiments at LHC.

These theoretical breakthroughs are founded upon a powerful consequence of the Unitarity property of the S -matrix: the *Optical Theorem*. This essentially relates the imaginary part of a loop Feynman amplitude to simpler amplitudes at a *lower order* in perturbation theory: the key idea is that by severing a loop amplitude into two tree amplitudes in all the possible ways one basically obtains the imaginary part of the loop amplitude itself. The act of severing an amplitude can be seen as the act of turning intermediate particles into external states by applying on-shell conditions on them. This procedure is formalised by the *Cutkosky rule* [1].

We briefly describe how these ideas can be put into practice in the *Generalised Unitarity* [26, 27] scheme which takes advantage of Unitarity to express a whole loop Feynman amplitude in terms of complete and partial cuts of simpler amplitudes [28], yielding a decomposition into scalar integrals in a procedural way. These methods have also been extended and applied to Feynman loop amplitudes in the framework of Dimensional Regularisation [29–37].

In Chapter 4 we introduce the related Integrand Decomposition technique [38–42] which, at one-loop, can obtain virtually the same scalar-integral decomposition given by Generalised Unitarity without the need to perform any integration. This approach is also known as the *OPP method* from the initials of its creators: the key idea is to obtain an *integrand level* expression for the Feynman amplitude by introducing so-called *spurious terms* which preserve the equivalence of the two expressions and which vanish upon integration, restoring the original integral-level expression. This is done by parametrising the loop momentum on a basis of external momenta and thence studying the numerator as the most general polynomial in the kinematic variables, which entails identifying all the monomials that can be written in terms of the amplitude's denominators and simplified, and the remaining *Irreducible Scalar*

Products (ISP) which make up the parametrisation. The simplified denominators are essentially integrands of smaller scalar integrals, and thus a decomposition is obtained by resorting on the algebraic properties of the integrand rather than computing a cut integral. We also describe how this method can be made compatible with Dimensional Regularisation [1, 41, 43–45].

We finally highlight that Integrand-reduction methods are essentially equivalent to performing the *Polynomial Division* between the numerator and any combination of denominators that defined the original loop integral. The algebraic properties of the method lead to a re-formulation using general results provided by *Algebraic Geometry* such as *Multivariate Polynomial Division modulo Gröbner bases* [46, 47], which enabled the implementation of these ideas in yet more automated code suites [47–49], suitable to extend the applicability of integrand methods to complex amplitudes and even beyond the one-loop level.

In chapter 5 we briefly touch on the issues with the multi-loop extension of integrand-decomposition methods, which revolve around the proliferation of ISPs arising from the most general parametrisation of polynomials in the kinematic variables: many of these are spurious but do not vanish trivially as for the one-loop case. The presence of ISPs which in fact are not independent leads to an over-abundance of scalar integrals in the final decomposition, which is needlessly complicated.

We then detail *Adaptive Integrand Decomposition* [14, 16], a recent proposal to overcome these technical hurdles. It still is an algebraic integrand decomposition method, but formulated within the $D = D_{\parallel} + D_{\perp}$ prescription for Dimensional regularisation. Building the most general parametrisation for the integrands and their scalar products in this framework leads to remarkable simplifications, namely that the spurious terms are parametrised by the variables belonging to the transverse space, and it is possible to detect and remove them with efficient integration techniques limited to this subspace. We then outline its algorithmic implementation: the automatic code package AIDA [15] for MATHEMATICA which is the main tool used in this thesis to obtain the Scalar Integral decomposition of $2 \rightarrow 3$ amplitudes.

Chapter 6 is devoted to kinematics, or the parametrisation of the external momenta of Feynman amplitudes. One seeks to write amplitudes in terms of as few parameters as possible but, all the while, it is desirable to have a formalism that encodes naturally properties such as momentum conservation. We introduce the *Momentum Twistor Formalism* used by AIDA which solves all these requirements, along with the *Spinor-Helicity* formalism upon which it is based.

In Chapter 7 we present our computations for $\mu^- e^- \rightarrow \mu^- e^-$ scattering in QED, starting with calculations at Leading-Order and Next-to-Leading Order done using the standard tools provided by the MATHEMATICA package FEYN CALC [50, 51]. We then report the fully-analytical decomposition of the Next-to-Leading order contributions done with AIDA: to apply this tool to the NLO one-loop amplitudes with two mass scales we introduce novel twistor parametrisations for massive momenta used to parametrise the kinematics, and show the resulting Master Integrals both in massive-electron and in the massless-electron limits.

We then tackle the main goal of this thesis: the evaluation of the amplitudes for $\mu^- e^- \rightarrow \mu^- e^- \gamma$ at one-loop, part of the Next-to-Next-to-Leading Order radiative corrections. Once again we present a twistor parametrisation for five-point kinematics with two mass scales, and detail the fully-analytical decomposition result obtained with AIDA and, again, we provide results for the massless electron limit for comparison. These constitute the first steps towards a complete, fully-analytical result for these corrections.

Finally, in Chapter 8, we show a practical implementation of the theoretical techniques for the evaluation of Master Integrals with Differential Equations, obtaining an analytical expression for the integrals of $\mu^- e^-$ scattering at NLO, namely one-loop four-point integrals in the $m_e \rightarrow 0$ limit, along the lines of [10, 52]: this calculation may serve as a first step toward the study of the Master Integrals for the massive-electron cases.

Chapter 1

The muon's intrinsic magnetic moment

1.1 Magnetic moments

The connection between orbiting charged particles and magnetic properties is well understood since the days of classical electromagnetism. If one can define the orbital angular momentum of a particle spinning about an axis as $\vec{l} := m \vec{r} \times \vec{v}$ then the resulting magnetic moment is¹ :

$$\vec{\mu}_l = \frac{q}{2m} \vec{l} \quad (1.1)$$

From a quantum-mechanical perspective, elementary particles possess a quantised intrinsic angular-momentum known as *spin* which generates itself a magnetic moment:

$$\vec{\mu}_s = \frac{q}{2m} g \frac{\vec{\sigma}}{2} = \mu_B g \vec{\Sigma} \quad (1.2)$$

where we wrote the moment in terms of the spin- $\frac{1}{2}$ operator Σ (itself dependent in the Pauli matrices σ_i , $i = 1, 2, 3$), the *Bohr magneton* $\mu_B := \frac{q}{2m}$ and the proportionality constant g .

Spin- $\frac{1}{2}$ particles obey the relativistic Dirac equation which naturally includes spin as a fundamental property. Considering the coupling to an external electromagnetic four-potential and taking the non-relativistic limit, this equation gives an explicit expression for the particle's spin magnetic moment, yielding in turn a prediction for the g -factor which turns out to be 2.

The Dirac equation is superseded by the frameworks of Quantum Field Theory (QFT) and Gauge theory, which describe interactions between fundamental particles as mediated by the so-called gauge bosons. In this framework, the electromagnetic coupling between spin- $\frac{1}{2}$ leptons (the class of particles to which the muon belongs) and an external electromagnetic field is described by Feynman diagrams with three external lines:

$$\text{Diagram} = \text{Diagram} + \text{Diagram} + \text{Diagram} + \dots \quad (1.3)$$

¹In this thesis natural units are employed, therefore factors of c and \hbar are omitted.

The shaded blob indicates a perturbative series of increasingly more complex internal processes. The simplest process is the naïve scattering of a muon and a photon, the so-called *tree-level* which is captured by classical scattering theory. The more complicated diagrams are instead inherently quantum-mechanical in nature, and are collectively referred to as *radiative corrections*. They often involve internal loops of particles as indicated, and each loop order entails more powers of the coupling constant, which in the case of electromagnetism is the fine-structure constant α .

It is thus more convenient to work in terms of $a_l = (g_l - 2)/2$ (where $l = e, \mu, \tau$), which is the discrepancy of the factor from this value, known as *anomaly*. This effectively measures the anomaly with respect to the "classical" tree-level contribution arising directly from the higher-order corrections. Given that the rest of the objects composing the definition of the intrinsic magnetic moment are either fixed or well-known, the quantity a_l is often taken directly as a stand-in for the magnetic moment itself, especially when referring to experiments and predictions. Radiative corrections can involve processes typical of energies much higher than that of the external particles, since these corrections are quantum-mechanical in nature and nothing in QFT restricts the four-momentum of the particles which participate in some of them.

Accurate predictions and measurements of a_l can thus shed light on the fundamental interactions that can play a role in the radiative corrections; the match between prediction and measurement serves as verification of the validity of the Standard Model of fundamental interactions (SM) or as evidence for new physics lying beyond.

The first a_l factor tackled was the electron's, given the ease with which it can be produced and accelerated in cyclotrons and synchrotrons. The first accurate measurement of its magnetic moment was performed in 1948 by Kusch and Foley [53] by studying the hyperfine splitting within atomic emission spectra, yielding $g_e = 2.00238(6)$. The lowest-order theoretical prediction given by Quantum Electrodynamics (QED) was calculated by Schwinger [54]:

$$\begin{aligned} g_e &= 2 \left(1 + \frac{\alpha}{2\pi} \right) \approx 2.00232 \\ \rightarrow a_e &= \frac{\alpha}{2\pi} \approx 0.00116 \end{aligned} \tag{1.4}$$

This early result provided compelling evidence for the validity of QED as the QFT of electromagnetic interactions, and energised research into techniques to compute higher-order corrections to a_e and test these predictions more and more accurately. The state-of-the-art measurement is to 0.22 ppb [55], which matches the most accurate prediction for the QED correction [56]².

1.1.1 The anomalous magnetic moment of the muon

The rest of the SM contributions to the electron's anomalous magnetic, namely the Weak and Quantum Chromodynamics (QCD) contributions, are highly suppressed since they are highly suppressed at the energy scales typical of electronic processes.

The muon μ , on the other hand, is a lepton ~ 206 times more massive than the electron. As such, it participates in QED interactions with itself and indirectly with its lighter relative, as well as electroweak interactions and QCD indirect contributions. Given the higher mass, the latter are important in determining a_μ and an accurate estimate must be given to assemble a complete prediction.

Moreover, a general study of a wide range of beyond-the-Standard-Model interactions (BSM) [57, 58]

²The theoretical correction is estimated up to order 10, which in terms of Feynman diagrams corresponds to a perturbative expansion up to and including 5 loops.

found that the expected sensitivity of some leptonic g -factor to new short-range interactions ought to scale as follows:

$$\frac{\delta a_l}{a_l} \sim \frac{m_l^2}{\Lambda^2} \quad (1.5)$$

Given that $(m_\mu/m_e)^2 \approx 4 \times 10^4$, the muon is expected to be 40000 times more sensitive than the electron to new BSM physics given the same experimental accuracy.

This feature of the muon's magnetic moment make it a prime candidate to study not only the validity of the Standard Model at high precision (given the smallness of the EW and QCD corrections, as we shall see) but also new physics beyond.

As we mentioned, the muon's magnetic moment arises from the coupling between its spin and an external magnetic field. This can be studied experimentally by studying the spin motion of a polarised muon trapped in a homogeneous magnetic field, more precisely measuring the *Larmor precession* of the spin direction ω_S caused by its motion in the field and proportional to g_μ [59]. Such an experiment requires highly-polarised muons, and for a long time there was no known way to produce these in the first place.

However, in 1957, the seminal discovery of Parity violations by the weak interactions [60] provided a way to accomplish this. One can exploit the decay $(\pi^- \rightarrow \bar{u}d \rightarrow W^- \rightarrow \mu^- \bar{\nu}_\mu)$ since, due to parity violation in the latter weak-mediated steps of the decay, the final muon's handedness (and consequently polarisation) is shown to be closely related to its electric charge [59]. Consequently, one can collect the muons emitted in the direction of travel of the original pion using magnetic quadrupoles, and even select the desired polarisation of muons with bending dipoles.

This decay, and the methodology outlined above, have been the basis of the experimental measurement of a_μ in many occasions. The most recent measure comes from the E821 experiment carried out at the BNL [61, 62], their final result is:

$$a_\mu^{exp} = 116592091(63) \times 10^{-11} \quad (1.6)$$

with a relative precision of 0.54 parts-per-million. The best SM theoretical prediction for a_μ turns out to be significantly different [63]:

$$a_\mu^{SM} = 116591776(44) \times 10^{-11} \quad (1.7)$$

the discrepancy checks out at $\sim 4\sigma$.

This large gap between theory and experiment points towards the existence of new unseen effects at play, be BSM physics such as SuperSymmetry (SUSY) or new features of the current Standard Model. Research is being conducted both to refine the experimental measurement and also to pinpoint more accurately the Standard Model prediction. Two new experiments are underway: E989 at Fermilab replicates the techniques of E821 but aiming to reduce the uncertainty by a factor 4, while E34 at J-PARC will employ a different technique altogether, providing an important independent cross-check of the measure.

Finally, the MUonE proposal aims to provide an independent determination of the leading hadronic contributions to a_μ^{SM} by using muon-electron scattering data, as will be detailed in section 1.3.1.

1.2 The Standard Model prediction of a_μ

The new experimental goals for measuring a_μ must be paired up with equally sophisticated theoretical predictions coming from the SM as established. This section is devoted to reviewing the main SM contributions to a_μ^{SM} and to comparing their importance to the final result.

The SM prediction of a_μ is composed of several contributions:

$$a_\mu^{SM} = a_\mu^{QED} + a_\mu^{EW} + a_\mu^{HAD} \quad (1.8)$$

We shall examine each term separately in the following. Figure 1.1 summarises the various contributions and is useful to compare their importance.

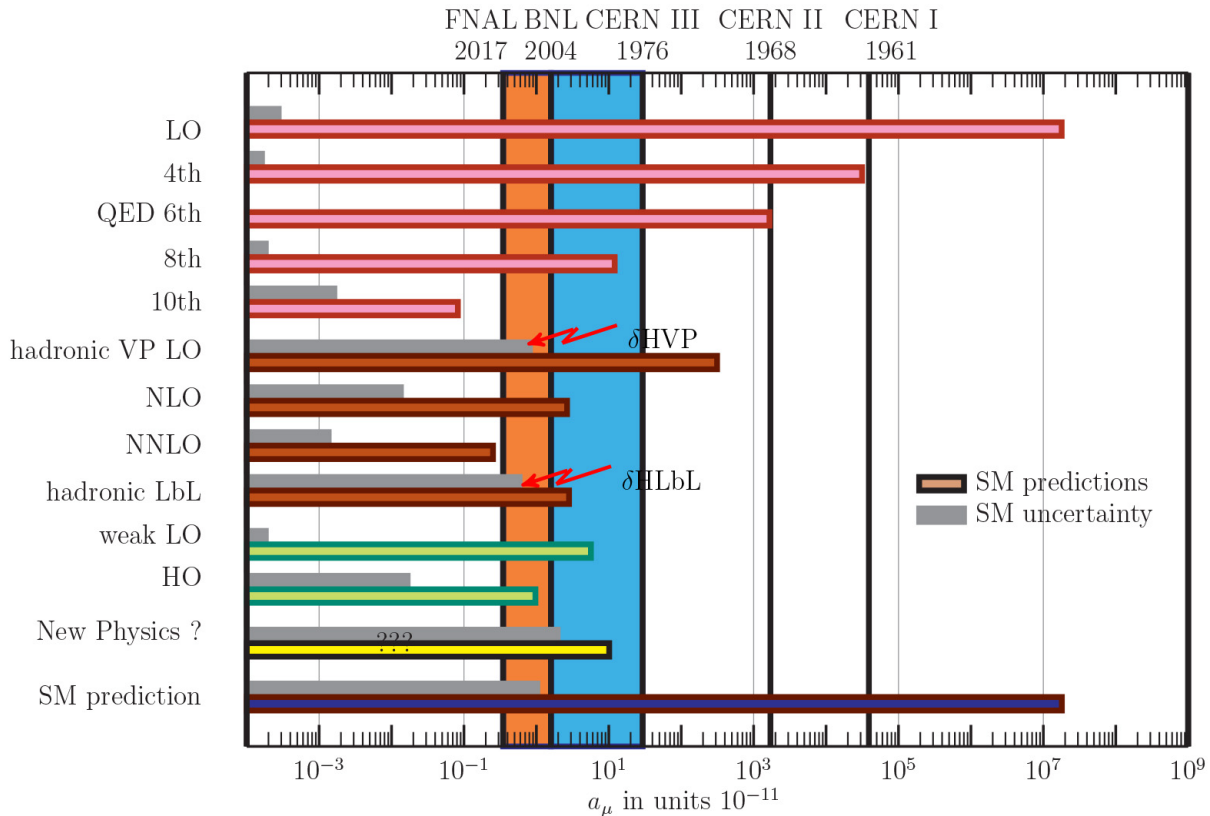


Figure 1.1: SM contributions to a_μ compared against past and future experiments testing various contributions. The red bars are relevant to a_μ^{QED} , the brown ones to a_μ^{HAD} and the green ones to a_μ^{EW} . "new physics" displays actually the deviation $(a_\mu^{exp} - a_\mu^{SM})/a_\mu^{exp}$. The grey bars indicate uncertainties, the two largest ones being highlighted by red arrows [63].

1.2.1 The QED contribution

Quantum Electrodynamics provides the largest fraction of the contribution by far. It can be further subdivided as follows [64]:

$$a_\mu^{QED} = A_1 + A_2 \left(\frac{m_\mu}{m_e} \right) + A_2 \left(\frac{m_\mu}{m_\tau} \right) + A_3 \left(\frac{m_\mu}{m_e}, \frac{m_\mu}{m_\tau} \right) \quad (1.9)$$

where A_1 encompasses the contributions from diagrams involving solely the muon and the photon, therefore identical to the corresponding A_1 contribution to the electron's magnetic moment from QED.

A_2 and A_3 correspond to diagrams involving two or all three kinds of leptons (e, μ, τ) and are functions of the mass ratios with the muon.

All contributions can be expanded out as a power series in α/π :

$$A_i = A_i^{(2)} \left(\frac{\alpha}{\pi}\right) + A_i^{(4)} \left(\frac{\alpha}{\pi}\right)^2 + A_i^{(6)} \left(\frac{\alpha}{\pi}\right)^3 + \dots \quad (1.10)$$

which enables us to write the QED contributions to the muon magnetic moment order-by-order:

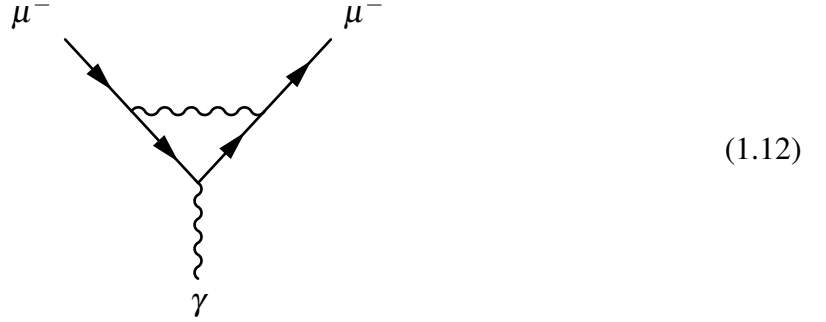
$$a_{\mu}^{QED} = \sum_L C_L \left(\frac{\alpha}{\pi}\right)^L \quad (1.11)$$

$$C_L = A_1^{(2L)} + A_2^{(2L)} \left(\frac{m_{\mu}}{m_e}\right) + A_2^{(2L)} \left(\frac{m_{\mu}}{m_{\tau}}\right) + A_3^{(2L)} \left(\frac{m_{\mu}}{m_e}, \frac{m_{\mu}}{m_{\tau}}\right)$$

In [64] a detailed review of the state-of-the-art estimates for these terms up to $L = 5$ is presented, here we will highlight the main results:

- **One-loop level**

At one-loop the only diagram present is the vertex correction involving exclusively muons:



This corresponds to the Schwinger calculation, therefore $C_1 = A_1^{(2)} = \frac{1}{2}$ with $A_2^{(2)} = A_3^{(2)} = 0$.

- **Two-loop level**

At two loops nine diagrams are generated in QED. Seven of them are composed of muons and photons only, comprising the A_1 contribution, while the remaining two involve the vacuum-polarisation of the virtual photon with a fermionic loop (respectively with an electron and a tauon).

All these contributions were computed analytically; $A_1^{(4)}$ was computed in [65, 66], while the remaining two were obtained in [67] and are affected by uncertainties on the masses of the particles involved:

$$A_1^{(4)} = 0.32847896557919378\dots \quad (1.13)$$

$$A_2^{(4)} \left(\frac{m_{\mu}}{m_{\tau}}\right) = 1.0942583092(72) \quad (1.14)$$

$$A_3^{(4)} \left(\frac{m_{\mu}}{m_{\tau}}\right) = 0.000078079(14) \quad (1.15)$$

yielding the second coefficient:

$$C_2 = 0.765857423(16) \quad (1.16)$$

- **Three-loop level**

At three-loops more than 100 diagrams participate. The $A_1^{(6)}$ contributions comprises 70 diagrams which were calculated in [68–76], while the $A_2^{(6)}$ contribution comprises 36 vacuum-polarisation diagrams as well as 12 light-by-light diagrams where an even number of photons interact³ [77, 78]. Finally, for the first time the contribution $A_2^{(6)}$ appears [79], which comprises diagrams of all three massive leptons.

The results are:

$$A_1^{(6)} = 1.181241456587\dots \quad (1.17)$$

$$A_2^{(6)} \left(\frac{m_\mu}{m_e} \right) = 22.86838000(17) \quad (1.18)$$

$$A_2^{(6)} \left(\frac{m_\mu}{m_\tau} \right) = 0.00036063(12) \quad (1.19)$$

$$A_3^{(6)} \left(\frac{m_\mu}{m_e}, \frac{m_\mu}{m_\tau} \right) = 0.00052776(10) \quad (1.20)$$

yielding the third coefficient:

$$C_3 = 24.05050982(28) \quad (1.21)$$

- **Four-loop level**

The computation of the more than 1000 diagrams appearing at four loops has only been completed by employing numerical and Monte Carlo techniques, as only few diagrams are known analytically. The term comprises 891 diagrams and has been computed by Laporta in [80], while the remaining coefficients are estimated in [81]:

$$A_1^{(8)} = -1.912245764926\dots \quad (1.22)$$

$$A_2^{(8)} \left(\frac{m_\mu}{m_e} \right) = 132.6852(60) \quad (1.23)$$

$$A_2^{(8)} \left(\frac{m_\mu}{m_\tau} \right) = 0.04234(12) \quad (1.24)$$

$$A_3^{(8)} \left(\frac{m_\mu}{m_e}, \frac{m_\mu}{m_\tau} \right) = 0.06272(4) \quad (1.25)$$

the estimate of the fourth coefficient is then:

³Under the rules of QED, loop scattering amplitudes ought to be invariant under the application of the charge conjugation operator upon a diagram, corresponding to reversing the flow of charge along the internal fermionic lines. The electromagnetic current flips sign as a result, and the whole amplitude will also flip sign in the case of odd-number of internal fermionic lines (which corresponds to the case of odd-number of external photons). If the amplitude is to stay invariant then the odd-photon amplitudes have to cancel out, this result is known as *Furry's theorem*.

$$C_4 = 130.8734(60) \quad (1.26)$$

- **Five-loop level** At this level more than 12000 diagrams appear. Their numerical evaluation was performed in [82] and yields:

$$C_5 = 751.917(932) \quad (1.27)$$

The final value for the total QED contribution to the muon's g -factor is given as:

$$a_\mu^{QED} = 116584718.859(.026)(.009)(.017)(.006) \times 10^{-11} \quad (1.28)$$

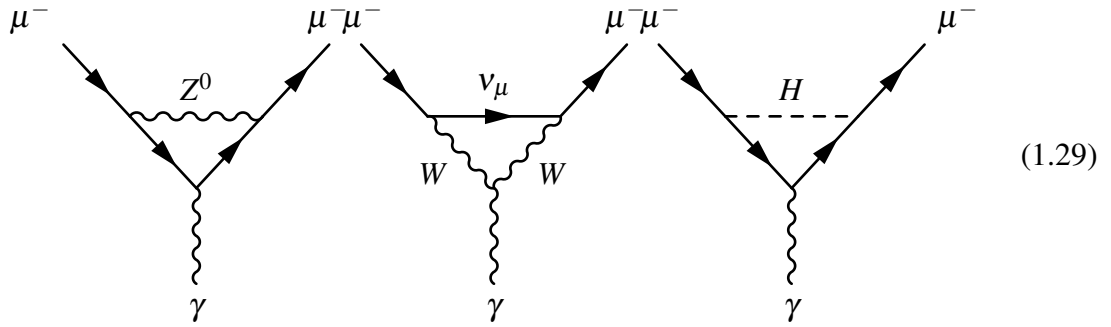
The uncertainties are respectively related to the experimental errors in the measurement of α and of the lepton masses, and to the numerical errors accumulated in the computation of the four- and five-loop terms.

1.2.2 The Electroweak contribution

An important difference between the electroweak interactions and electromagnetism is the presence of massive force carriers: the W and Z bosons. The factor $(m_\mu/m_W)^2$ suppressed the electroweak (EW) contribution to the g -factor beyond experimental uncertainty for a long time, although the BNL experiment were able to measure a_μ^{EW} with an uncertainty of about a third of the one-loop contribution.

- **One-loop level**

The one-loop electroweak diagrams involve the W and Z bosons, the neutrinos and the Higgs boson H , as shown explicitly:



Their contributions were computed analytically in the 1970s [83–87], after it was confirmed that non-abelian Gauge theories like the Electroweak model were renormalisable, and consists in the following expression:

$$a_\mu^{EW} = \frac{5}{24\pi^2} \frac{G_F m_\mu^2}{\sqrt{2}} \left[1 + \frac{1}{5} (1 - 4 \sin^2 \theta_W) + \mathcal{O} \left(\frac{m_\mu^2}{m_{W,Z,H}^2} \right) \right] \quad (1.30)$$

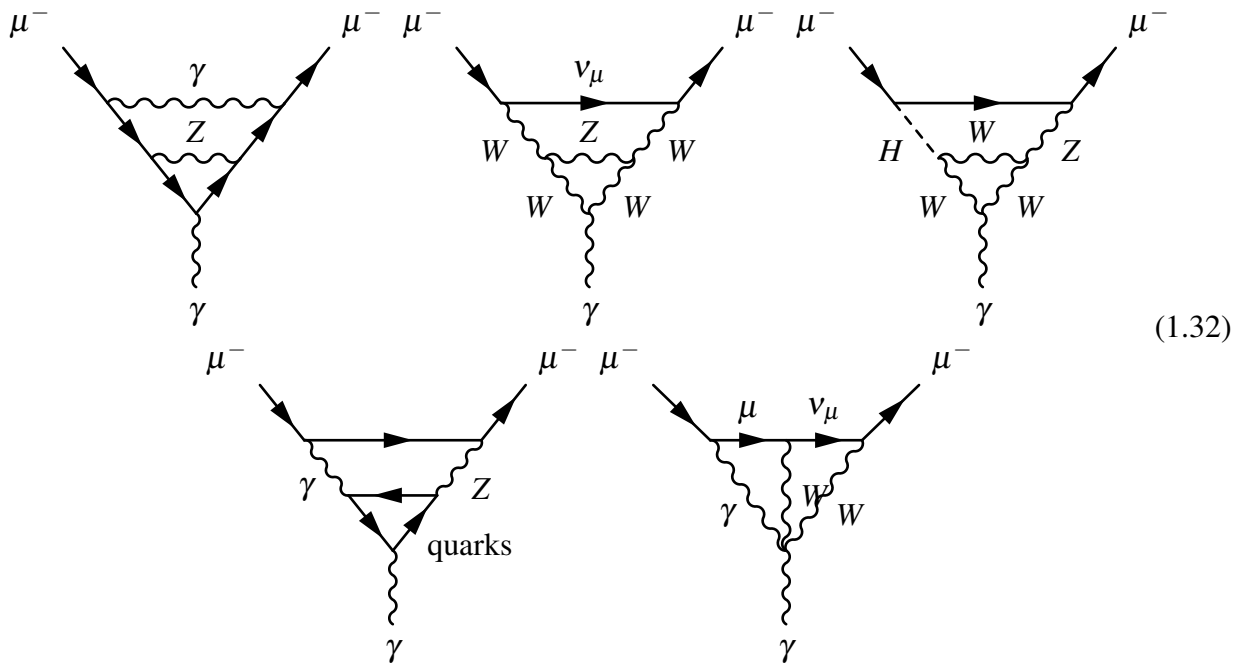
where G_F is the Fermi weak decay constant and θ_W is the Weinberg angle. This formula is accurate up to corrections of the order of $\left(\frac{m_\mu^2}{m_{W,Z,H}^2} \right)$ which are taken as negligible. This yields:

$$a_{\mu}^{(2)EW} = (194.81 \pm 0.01) \times 10^{-11} \quad (1.31)$$

the uncertainty comes mainly from the measurement of the Weinberg angle.

• **Two-loop level**

The contributing diagrams number in the hundreds. The diagrams can be thought of as the one-loop diagrams augmented by vacuum polarisations, self-energies or vertex corrections composed of various kinds of particles⁴. One therefore finds loops such as $\gamma WW, \gamma\gamma Z, \gamma ZZ$ and others. In addition, a few diagrams feature the quartic interaction between two W bosons, one Z and the photon or two W and two γ . Present are also diagrams with hadronic quark loops inserted in 2-loop electroweak diagrams (HEW). A few of these diagrams are:



The leading-order two-loop contribution was obtained in 1992 in [89]. In there it was shown that the diagrams containing a fermionic triangle loop yield at amplitude level a factor $\log(M_{W,Z}/M_f)$ with f indicating the kind of fermion in question. These factors, rather counter-intuitively, boost the 2-loop contribution to the g factor to the same order as the 1-loop one but with an opposite sign, thus diminishing greatly the electroweak contribution to the muon $g - 2$.

In [90–92] the following value is given:

$$a_{\mu}^{(4)EW} = (-42.7(2)(1.8)) \times 10^{-11} \quad (1.33)$$

The first uncertainty is due to the precision in the value of the Higgs boson and t quark masses, while the second arises from hadronic effects in quark loops.

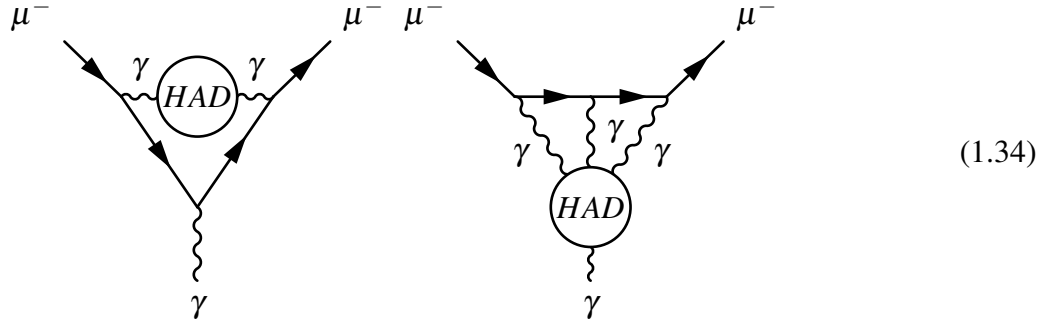
1.2.3 The hadronic contribution

Naïvely, the strong interactions should influence the g -factor simply by augmenting the QED diagrams with quark loops, the leading contribution (a_{μ}^{HLO}) being the hadronic vacuum polarisation (HVP) at

⁴It should be noted that there is no analogous of Furry's theorem for the electroweak interactions. This is due to the violation of parity [88] which, in turn, spoils charge-conjugation invariance and, by extension, the cancellation between a triple-particle loop and its conjugate.

leading order inserted in the internal photon propagator, represented by the first diagram of 1.34. The second diagram shows the subsequent most important contribution, the so-called Hadronic light-by-light scattering (HLbL). Additionally, HVP effects at higher orders have been computed but they are at least 10^2 times smaller than the leading order effects [63].

The leading hadronic contributions are shown compared with all the other main contributions in figure 1.1, showing that the HVP and HLbL are also the main sources of uncertainty in a_μ as a whole. This uncertainty is due to the fact that giving a theoretical estimate for hadronic contributions is not at all straightforward: at the energy scales typical of pair-production of the lightest hadrons, the quarks interact at long range, and the QCD coupling becomes so strong that the perturbation-based methods of QFT cannot be applied.



There are various alternative ways to extract these contributions:

- HVP contributions can be extracted indirectly by examining the e^+e^- annihilation process. In [93–95] these two seemingly-unrelated processes were related by a dispersion integral, a result based on analyticity and unitarity⁵ of the quantum scattering matrix S . We will detail this method in the subsequent section.

The contribution is estimated as [63, 99, 100]:

$$a_\mu^{(1)HVP} = 6880.7 \pm 41.4 \times 10^{-11} a_\mu^{(1)HVP} = 6939 \pm 40 \times 10^{-11} \quad (1.35)$$

$$a_\mu^{(1)HVP} = 6932.7 \pm 24.6 \times 10^{-11} \quad (1.36)$$

where the uncertainties are dominated by experimental uncertainties on the $(e^+e^- \rightarrow x)$ cross-section.

- HLbL have been extracted by using the so-called Resonance Lagrangian Approach. This is based on *Chiral Perturbation theory* (the Effective Quantum Field Theory of quark-confined states in accordance with the Chiral symmetry of QCD) extended to higher energies and augmented with vector resonances. They are estimated as [63]:

$$a_\mu^{HLbL} = (103 \pm 29) \times 10^{-11} \quad (1.37)$$

Both these theoretical techniques can be compared with the bare-bones approach of Lattice QCD (LQCD), that aims to obtain this contribution by directly calculating the path-integrals of the confined quarks and gluons using the rules of high-energy QCD ([101] and references therein).

This technique is naturally all-inclusive regarding the hadronic processes but is limited by computational complexity, and therefore still lacking precision. To be competitive with the more traditional approaches, the coming LQCD calculations aim to achieve a relative precision of sub-percent for HVP processes and 10% for HLbL processes [63, 102]. The latter process is much more difficult to compute in LQCD (being a four-point process instead of a two-point one) and its smaller overall contributions means that a higher uncertainty is acceptable.

⁵Unitarity and the Optical theorem can be found in chapter 3.1. For dispersion relations applied to Feynman amplitudes see, for example, [96–98].

1.3 Extracting the leading hadronic contribution to a_μ

This section is devoted to describing the techniques employed in the past to extract indirectly the hadronic VP contribution to a_μ at leading order, as mentioned previously, and subsequently to lay out a novel method [8] that forms the basis of the proposed *MUonE* experiment [103].

A generic vacuum polarisation function is often denoted as $\Pi(q^2)$, and as a direct consequence of causality it is analytical. Furthermore, for renormalisable QFTs such as the Standard Model, its asymptotic behaviour at large momenta is regulated by the introduction of a *counterterm* which generates an analogous diagram, only with the special symbol \otimes indicating the counterterm insertion in place of the vacuum polarisation function:

$$(1.38)$$

and only by considering the vacuum polarisation diagram together with its counterterm partner does one have a "complete" picture devoid of any unphysical divergences at large momenta. By imposing that the loop correction be vanishing in the low-momentum transfer limit (consistency with the classical limit) this counterterm can be computed to be $-\Pi(0)$.

Therefore in the following we shall consider the *renormalised* vacuum polarisation function⁶

$$\bar{\Pi}(q^2) = \Pi(q^2) - \Pi(0) = \frac{q^2}{\pi} \int_{s_0}^{+\infty} ds \frac{\text{Im}[\Pi(s)]}{s(s - q^2 - i\epsilon)} \quad (1.39)$$

and we wrote its spectral representation as it is both analytical and well-behaved at large momenta, and s_0 is the starting point of the lightest branch cut.

Let us now examine e^+e^- annihilation with a vacuum-polarisation insertion. Let us take its imaginary part and apply the optical theorem, essentially writing down an analogous form of equation 3.6:

$$(1.40)$$

This diagrammatic equation is basically saying that the imaginary part of the vacuum polarisation function (up to coupling, momentum and spin factors coming from the rest of the amplitude) is related to the cross-section of the process ($e^+e^- \rightarrow \gamma \rightarrow$ *generic particles*). We will consider the particular case of ($e^+e^- \rightarrow \gamma \rightarrow$ *hadrons*), as our goal is to obtain the hadronic vacuum polarisation.

⁶It should be noted that, at this stage, we are dealing with a *generic* vacuum polarisation function, not specifically the hadronic one.

It is common practice to measure the hadron-production cross-section in units of the cross-section of the process $(e^+e^- \rightarrow \gamma \rightarrow \mu^+\mu^-)$ in the massless muon limit. One then defines the $\mathcal{R}_\gamma(s)$ factor⁷, which can be written as [63]:

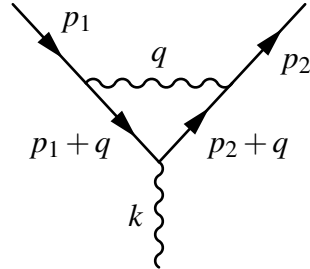
$$\mathcal{R}_\gamma(s) := \frac{\sigma(e^+e^- \rightarrow \gamma \rightarrow \text{hadrons})}{\sigma(e^+e^- \rightarrow \gamma \rightarrow \mu^+\mu^-)} = \frac{\sigma(e^+e^- \rightarrow \gamma \rightarrow \text{hadrons})}{\frac{4\pi\alpha^2}{3s}} \quad (1.41)$$

where the cross-section $(e^+e^- \rightarrow \gamma \rightarrow \mu^+\mu^-)$ acts as a numerical normalisation factor. Since the optical theorem relates the imaginary part of the vacuum-polarisation function to the hadron-production cross-section, this can be re-expressed in terms of $\mathcal{R}_\gamma(s)$ and plugged into the dispersion integral 1.39:

$$\bar{\Pi}(q^2) = \Pi(q^2) - \Pi(0) = \frac{\alpha q^2}{3\pi} \int_{4m_\pi^2}^{+\infty} ds \frac{\mathcal{R}_\gamma(s)}{s(s - q^2 - i\varepsilon)} \quad (1.42)$$

It should be noted that the branch cut now starts at the π mass, given that the pions are the lightest hadrons that can be produced out of a photon (specifically the process $(\gamma \rightarrow \pi^- \pi^+)$ has the lowest threshold).

Let us now derive an expression for the HVP corrections to a_μ^{HLO} . First we write down the Feynman amplitude associated with the basic vertex correction of diagram 1.12:



$$(1.43)$$

$$\begin{aligned} & -ie \bar{u}(p_2) \Gamma^\alpha(p_1, p_2) u(p_1) = \\ & (-ie\mu^{\varepsilon/2}) \int \frac{d^D q}{(2\pi)^D} \frac{-ig_{\alpha\beta}}{q^2} \bar{u}(p_2) \left[\gamma^\beta \frac{i[(\not{q} + \not{p}_2) + m_\mu]}{(q + p_2)^2 - m_\mu} \gamma^\alpha \frac{i[(\not{q} + \not{p}_1) + m_\mu]}{(q + p_1)^2 - m_\mu} \gamma^\delta \right] u(p_1) \end{aligned} \quad (1.44)$$

where we used Dimensional regularisation⁸ to regulate the divergence. To account for the hadronic vacuum polarisation we correct the internal photon propagator by inserting the renormalised VP function as a multiplicative factor (the result corresponds to diagrams 1.38), and thereafter we plug in the dispersion relation obtained above:

⁷Chapter 5.1 of Peskin & Schroeder provides an introduction to this ratio.

⁸we will introduce it properly in chapter 2.1

$$\begin{aligned}
 & -ie \bar{u}(p_2) \Gamma^\alpha(p_1, p_2) u(p_1) = \\
 & \left(-ie\mu^{\varepsilon/2}\right) \int \frac{d^D q}{(2\pi)^D} \frac{-ig_{\alpha\beta}}{q^2} [-\bar{\Pi}(q^2)] \bar{u}(p_2) \left[\gamma^\beta \frac{i[(\not{q} + \not{p}_2) + m_\mu]}{(q+p_2)^2 - m_\mu} \gamma^\alpha \frac{i[(\not{q} + \not{p}_1) + m_\mu]}{(q+p_1)^2 - m_\mu} \gamma^\delta \right] u(p_1)
 \end{aligned} \tag{1.45}$$

$$\begin{aligned}
 & -ie \bar{u}(p_2) \Gamma^\alpha(p_1, p_2) u(p_1) = \left(-ie\mu^{\varepsilon/2}\right) \frac{\alpha}{3\pi} \int_{4m_\pi^2}^{+\infty} \frac{ds}{s} \mathcal{R}_\gamma(s) \times \\
 & \times \int \frac{d^D q}{(2\pi)^D} \frac{-ig_{\alpha\beta}}{q^2 - s} \bar{u}(p_2) \left[\gamma^\beta \frac{i[(\not{q} + \not{p}_2) + m_\mu]}{(q+p_2)^2 - m_\mu} \gamma^\alpha \frac{i[(\not{q} + \not{p}_1) + m_\mu]}{(q+p_1)^2 - m_\mu} \gamma^\delta \right] u(p_1)
 \end{aligned} \tag{1.46}$$

where q^2 at the numerator of 1.39 cancelled with the internal photon propagator. Meanwhile, within the integral the photon has acquired a new propagator factor from the VP insertion: a massive one with mass \sqrt{s} .

We will momentarily treat s as an infra-red regulating factor in the loop integral, which enables us to carry out its textbook calculation. Let us remember that this fictitious mass is not really a regulator, and so no limit $s \rightarrow 0$ will be taken.

$$\begin{aligned}
 & -ie \bar{u}(p_2) \Gamma^\alpha(p_1, p_2) u(p_1) = \\
 & \frac{\alpha^2}{3\pi^2} \int_{4m_\pi^2}^{+\infty} \frac{ds}{s} \mathcal{R}_\gamma(s) \bar{u}(p_2) \left[F_1(k^2, s) \gamma^\alpha + \frac{i}{2m_\mu} F_2(k^2, s) \sigma^{\alpha\beta} \gamma_\beta \right] u(p_1)
 \end{aligned} \tag{1.47}$$

the result is expressed in terms of the *Dirac and Pauli form factors* $F_{1,2}$. To find the g -factor one sends $k \rightarrow 0$ and recalls that in this limit $F_1(0, s) = 1$ for consistency with the renormalisation conditions. The F_1 factor reproduces the tree-level contribution, therefore to find the anomaly one focusses on the $F_2(0, s)$ contribution. The standard way in literature to express such a result is:

$$\begin{aligned}
 a_\mu^{HLO} &= \frac{\alpha^2}{3\pi^2} \int_{4m_\pi^2}^{+\infty} \frac{ds}{s} \mathcal{R}_\gamma(s) K_\mu^{(2)}(s) \\
 K_\mu^{(2)}(s) &= \int_0^1 dx \frac{x^2(1-x)}{x^2 + (1-x)s/m_\mu^2}
 \end{aligned} \tag{1.48}$$

This formula relates the HVP contributions to the muon anomalous $g-2$ to a factor $\mathcal{R}_\gamma(s)$, but it could be extended to any kind of VP corrections, owing to the generality of the principles at its core.

The way to make practical use of this result would be to split the s -integral in two [59]:

$$a_\mu^{HLO} = \frac{\alpha^2}{3\pi^2} \left[\int_{4m_\pi^2}^{s_{cut}} \frac{ds}{s} \mathcal{R}_\gamma^{exp}(s) K_\mu^{(2)}(s) + \int_{s_{cut}}^{+\infty} \frac{ds}{s} \mathcal{R}_\gamma^{pQCD}(s) K_\mu^{(2)}(s) \right] \tag{1.49}$$

The second integral represents the high-energy contribution from an energy threshold s_{cut} upwards; in this region the known techniques of perturbative QCD (pQCD) would be reliable enough to compute the \mathcal{R}_γ factor analytically, and the range of validity of perturbation theory would set the energy threshold itself.

The first integral is instead the low-energy portion below s_{cut} , and in which the \mathcal{R}_γ factor could be measured experimentally by annihilating e^+e^- pairs and measuring the relative cross-sections or calculated by relying on LQCD.

The successful application of these theoretical techniques to actual measurements have come in spite of several difficulties.

First, by relying on experimental data to obtain a value for R_γ , the theoretical uncertainty on the HLO contribution is in fact *experimental* in nature. The prediction for R_γ is actually a compounded quantity: one sets up the measurement of a particular hadronic channel ($e^+e^- \rightarrow \gamma \rightarrow \text{particular hadrons}$) and then gathers the contributions of all possible channels. This is known as *exclusive measurement*.

The employment of different experimental techniques, the difficulties in selecting the desired final hadronic states and the comparison of systematic uncertainties [104] all worsen the overall accuracy of the experimental prediction. The energy region $[1.2; 2.0] \text{ GeV}$ is particularly problematic since more than 30 decay channels contribute to R_γ , and although it accounts for only 20% of the final HLO contribution it constitutes 50% of the uncertainty [63]. The low-energy limit below 1.0 GeV comprises π and ω -production channels, and also carries a large fraction of the uncertainty while accounting for more than 3/4 of the total contribution.

1.3.1 A novel approach: *MUonE*

The simplest way to solve the problems with the previous approach is to set up an *inclusive* measurement for HVP effects: a single process that can capture the contributions from all possible hadronic states running in loops in a single measurement.

This may be achieved by a new proposal [8] recently put forth, building up on the previously-established results to relate a_μ^{HLO} to the hadronic contribution to the running of α_{QED} in the space-like region. If one switches the s and x integrations [105] in equation 1.48:

$$a_\mu^{HLO} = \frac{\alpha}{\pi} \int_0^1 dx (x-1) \bar{\Pi}_{HAD} [t(x)] \quad (1.50)$$

$$t(x) = \frac{x^2 m_\mu^2}{(x-1)} < 0$$

the integral is expressed in terms of the renormalised HVP function with a *space-like* variable t , as opposed to the time-like variable s of the previous relation.

Let us now take a look at the running of the QED coupling constant α , another well-understood effect of radiative corrections. It is written down at a specified squared momentum transfer q^2 in terms of α measured at a different squared momentum transfer and the general VP function:

$$\alpha(q^2) = \frac{\alpha(0)}{1 - \Delta\alpha(q^2)} \quad (1.51)$$

$$-\Delta\alpha(q^2) = \text{Re} [\bar{\Pi}(q^2)]$$

$\Delta\alpha$ has various contributions coming from the various kinds of VP functions at play. $\Delta\alpha_{QED}$, given by the QED corrections to the photon propagator, is known up to at least three loops in perturbation theory, and its contribution can be factorised from the whole running to isolate the hadronic contribution $\Delta\alpha_{HAD}$.

The corrections to α ought to depend only on the real part of $\bar{\Pi}$ since the VP function can acquire a non-vanishing imaginary part if $q^2 > 4m_{particle}^2$ for some massive particle involved in the VP, in accordance with the Optical Theorem. But if the transferred momentum q^2 were to be space-like then $\bar{\Pi}(q^2)$ could safely be identified with its real part, since by the same unitarity-based reasoning the imaginary part would vanish trivially in that kinematic region.

Based on these considerations, it is possible to lay out a procedure to measure the Hadronic VP correction to a_μ by actually measuring the hadronic contribution to the running of α . One first measures $\Delta\alpha$ with space-like square momentum transfer t , subtracts the known QED contribution and the result ($\Delta\alpha_{HAD}(t) = Re[\bar{\Pi}_{HAD}(t)] \equiv \bar{\Pi}_{HAD}(t)$) is then substituted for the HVP function in 1.50:

$$a_\mu^{HLO} = \frac{\alpha}{\pi} \int_0^1 dx (1-x) \Delta\alpha_{HAD}[t(x)] \quad (1.52)$$

This is a very different approach, with an important advantage: the radiative corrections under advisement keep the hadrons fully-virtual in an internal blob, as opposed to having final hadronic states which can in general give rise to very complex children processes. This would provide a clean, inclusive and independent cross-check as compared to the traditional approach.

The advantage of studying space-like momentum transfer over time-like is evident from figure 1.2. The space-like momentum forbids resonances, which in turn makes the photonic VP function smooth in its domain. On the contrary, the time-like region opens up the possibility for resonances, pair-production and threshold behaviour that all cause spikes and troths in the VP function.

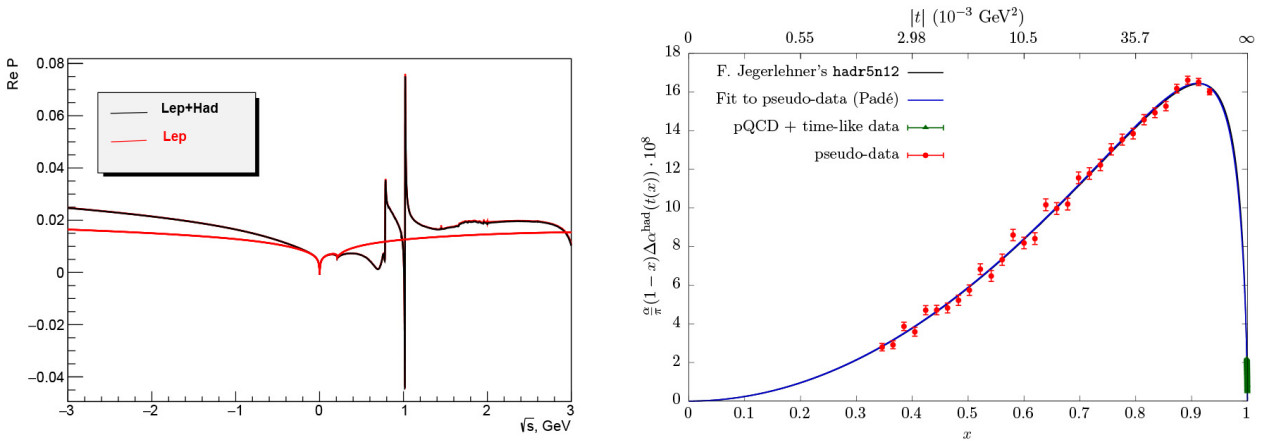


Figure 1.2: **Left:** Real part of the photon vacuum polarization ($\Delta\alpha(q^2)$) in the space-like and time-like region (Black line: leptonic plus hadronic contributions; Red line: only leptonic contribution); **Right:** The integrand $(1-x) \Delta\alpha_{HAD}[t(x)] \times 10^5$ as a function of x and $t(x) = \frac{x^2 m_\mu^2}{(x-1)} < 0$ [103].

Measuring 1.52 entails measuring accurately $\alpha(t)$ in the space-like region by measuring the cross-section of some physical process. An option could be Bhabha scattering ($e^+e^- \rightarrow e^+e^-$) which, however, always entails an s -channel contribution in addition to the desired t -channel one:

The diagram shows two Feynman diagrams for the process $e^+e^- \rightarrow e^+e^-$. The left diagram represents the s -channel, where an electron (e^-) and a positron (e^+) annihilate into a virtual photon (γ), which then splits into an electron and a positron. The right diagram represents the t -channel, where an electron and a positron exchange a virtual photon in the t -channel, resulting in an electron and a positron. A plus sign between the diagrams indicates they are summed. The equation number (1.53) is on the right.

The contribution from the s -channel and the resonance effects which it entails may be minimised by cleverly choosing the phase-space point of the colliding particles, in order to instead maximise the contribution from the t -channel. Since the time-like channel cannot be completely suppressed, a method of phase-space separation would be needed.

The insurmountable difficulty is related to accuracy: to be competitive with time-like measurements, a space-like estimate of a_μ^{HLO} must be given at an accuracy of $\sim 1\%$ [8]. Given the peak value of $\Delta\alpha_{HAD}$ (10^{-3}) the experimental precision in the cross-section measurement needs to be on the order of 10^{-5} or 10 parts-per-million [9]. Currently, no existing e^+e^- collider can provide such a dauntingly high level of accuracy.

A more practical alternative could be muon-electron scattering $\mu^\pm e^- \rightarrow \mu^\pm e^-$: not only is this process exclusively t -channel and naturally all-encompassing of the hadronic corrections, but the required precision could potentially already be achievable at existing facilities.

The diagram shows a Feynman diagram for muon-electron scattering. A muon (μ^-) and an electron (e^-) interact in the t -channel via a virtual photon (γ). The muon line is shown as a double line, and the electron line is shown as a single line. The diagram is labeled (1.54) on the right.

In the diagram above we only depicted the process $\mu^- e^- \rightarrow \mu^- e^-$ as it will be the principal focus of this thesis, the partner process $\mu^+ e^- \rightarrow \mu^+ e^-$ features virtually identical diagrams related by charge-conjugation.

The experiment would take the form of a fixed-target collision [9]: a high-energy (150-200 GeV) muon beam is already available at CERN's North area and could be directed on a target of low-atomic-number atoms⁹, enabling the measurement of the differential cross-section of muons scattering off the electrons in the atomic orbitals. The *MUonE* experiment [103] aims to extract the running $\alpha(t)$ by measuring the cross-section with a precision of ~ 10 ppm to provide a $\sim 1\%$ estimate of a_μ^{HLO} , in order to be competitive with the new upcoming $g-2$ experiments.

⁹The target needs to be thick enough to provide frequent scattering events in a reasonable time-frame, but not too thick that the outgoing electrons are affected by atomic-scale phenomena. Choosing low-atomic number atoms would minimise the the impact of multiple scattering and the background due to bremsstrahlung and pair production processes [9]. The incident beam energy is much larger than the typical electron binding energy ~ 10 eV, but since the scale of electron-nucleus interactions should be the electron mass this may not mean that atomic physics is completely negligible in this experimental set-up, even for light atoms. Further analysis is underway.

Extracting $\bar{\Pi}_{HAD}(t)$ from the scattering cross-section at the level of accuracy sought by the *MUonE* proposal requires a theoretical prediction of the μe cross-section up to at least next-to-next-to-leading order (NNLO), encompassing both QED and hadronic contributions.

Hadronic contributions to $\mu^- e^-$ scattering

In the context of the *MUonE* experiment the relevant EW contributions to muon-electron scattering are known. The main contributions are thus pure-QED diagrams and mixed QED-hadronic diagrams, the latter entering the stage only at NLO.

Let us momentarily assume that the complete set of QED-governed amplitudes up to NNLO can be computed in the space-like region. By subtracting their contribution to the $\mu^- e^-$ cross-section from measured data the amplitudes containing hadronic VP contributions are isolated.

Evaluating these remaining amplitudes and comparing them with the subtracted data enables the extraction of the hadronic VP, the goal of the *MUonE* experiment. In 1.55 they are laid out in five distinct groups, where each diagram should be taken as a representative for a larger class of similar diagrams:

- a) is the same diagram of 1.54 and represents the only hadronic contribution at NLO, being thus the leading contribution to the running of α . The contribution coming from $\bar{\Pi}_{HAD}(t)$ is accounted for as a simple multiplicative factor in front of the tree-level electron-muon scattering cross-section, in other words it can be factorised.
- b) stands for the diagrams with a double vacuum-polarisation insertion, either two hadronic VPs or one hadronic, one leptonic. They can be inserted either together along the same photon propagator or one in each of the two diagrams that make up the squared amplitude. The VP contribution is once again factorisable, this time the factor is $\bar{\Pi}_{HAD}(t) [\bar{\Pi}_{HAD}(t) + \bar{\Pi}_{LEP}(t)]$ up to combinatorial factors counting the diagrams.
- c) represents the QED one-loop diagrams with a HVP insertion on the photon propagator. This contribution is proportional to the factorised $\bar{\Pi}_{HAD}(t)$ and the one-loop integral in QED, which can be computed with techniques described in chapter 2.
- d) These are the *real correction* diagrams in QED, with an extra low-energy photon emitted as a final particle, plus the HVP insertion. The contribution is once again factorised into the QED cross-section and the VP factor $\bar{\Pi}_{HAD}(t_l)$. We point the reader's attention to the space-like photon momentum t_l whose definition depends on which external leg radiates the real photon.
- e) One-loop QED corrections of box and triangle-type with a HVP insertion. Contrary to the cases above it is not possible to factorise away the contribution of the HVP factor as the momentum variable will depend in the loop momentum and ought to be integrated upon.

The NLO and NNLO (i-iii) contributions can be computed independently of the HVP function, which is factorised in front, and in principle would enable one to extract the HVP itself by comparing the result with the measured cross-section minus the QED contribution (alternatively one could use prior experimental data for $\bar{\Pi}_{HAD}$ and obtain a numerical estimate for the $\mu^- e^-$ cross-section). The inclusion of class (iv) amplitudes, a requirement for a full NNLO calculation of electro-muon scattering, nullifies this procedure since extracting the HVP function from cross-section measurements is no longer a matter of calculating a multiplicative factor.

This issue was solved (in the context of computing the hadronic corrections to $e^+ e^-$ scattering) by writing $\bar{\Pi}_{HAD}(t)$ using the dispersion relation 1.42 within the class (iv) amplitudes, using time-like measurements for the r_γ factor and from there compute the whole amplitude as usual. This approach was undertaken by Passera, Fael [106] and M. Vitti [107].

NLO

NNLO (i)

NNLO (ii)

NNLO (iii)

NNLO (iv)

(1.55)

An alternative approach [108] does away with dispersion relations and experimental inputs. One could momentarily neglect the NNLO hadronic corrections altogether, compute the NLO + QED amplitudes and obtain a first approximation for $\bar{\Pi}_{HAD}(t)$. The NNLO corrections are subsequently switched back on, the approximate result is fed back in and the amplitudes computed (in [108] the class (iv) amplitudes were treated using *hyperspherical integration*, which enables the use of HVP data in the space-like region without resorting to any time-like input). This yields a corrected estimate for the hadronic HVP function, and the cycle repeats until the approximation converges. This technique uses space-like data exclusively and, paired up with results from the *MUonE* experiment and lattice calculations, produces an estimate for a_μ^{HLO} independent of any time-like inputs.

QED contributions to $\mu^- e^-$ scattering

At this point it should be evident that the aforementioned procedure to determine the hadronic VP function hinges not only on precise experimental data, but also on an equally precise estimate of the QED contribution up to NNLO which ought to be removed. A fully-analytical result is desirable, for it would ensure complete freedom in analysing the kinematics of the process through Monte Carlo simulations.

These corrections have not been fully determined yet. The NLO differential cross-section were calculated in [109–111], with improvements and a full differential Monte Carlo result obtained in [112]. At NNLO some results can be re-cycled from NNLO Bhabha scattering [113–117] and from some QCD processes [118, 119], while [10–12] show the first results towards a complete NNLO $\mu^- e^-$ evaluation, calculating the two-loop planar and non-planar Feynman diagrams (in particular, the loop integrals were decomposed onto a so-called *Master Integral* basis, which will be introduced later on in this thesis). It is important to mention that many of these NNLO results have been obtained in the approximation $m_e = 0$ [10], which is physically justifiable (as μ^- is ~ 200 times more massive than e^-) and since it simplifies the evaluation of the Master Integrals.

This thesis focusses particularly on the QED NNLO real-virtual corrections to $\mu^- e^-$ scattering, i.e. the process $\mu^- e^- \rightarrow \mu^- e^- \gamma$ at one-loop, where the photon γ is produced as real radiation.

$$\begin{array}{ccccccc}
 \mu^- & & \mu^- & & \mu^- & & \mu^- \\
 \swarrow & & \swarrow & & \swarrow & & \swarrow \\
 & \text{1L} & & & & & \\
 \searrow & & \searrow & & \searrow & & \searrow \\
 e^- & & e^- & & e^- & & e^- \\
 \uparrow & & \uparrow & & \uparrow & & \uparrow \\
 \gamma & & \gamma & & \gamma & & \gamma
 \end{array}
 \quad = \quad
 \begin{array}{ccccccc}
 \mu^- & & \mu^- & & \mu^- & & \mu^- \\
 \swarrow & & \swarrow & & \swarrow & & \swarrow \\
 & & & & & & \\
 \searrow & & \searrow & & \searrow & & \searrow \\
 e^- & & e^- & & e^- & & e^- \\
 \uparrow & & \uparrow & & \uparrow & & \uparrow \\
 \gamma & & \gamma & & \gamma & & \gamma
 \end{array}
 \quad + \quad
 \begin{array}{ccccccc}
 \mu^- & & \mu^- & & \mu^- & & \mu^- \\
 \swarrow & & \swarrow & & \swarrow & & \swarrow \\
 & & & & & & \\
 \searrow & & \searrow & & \searrow & & \searrow \\
 e^- & & e^- & & e^- & & e^- \\
 \uparrow & & \uparrow & & \uparrow & & \uparrow \\
 \gamma & & \gamma & & \gamma & & \gamma
 \end{array}
 \quad + \dots
 \quad (1.56)$$

These corrections comprise diagrams with five internal lines, the so-called *pentagons*, four-internal-lines diagrams (*boxes*) with a photon radiated from the external legs and similar combinations of possible loops and radiations.

The computation of their related Feynman amplitudes will be computed keeping track of both muon and electron masses, in order to assess the importance of the electron mass contribution and, hopefully, ascertain that the assumption of massless electron is a good one.

In preparation for this task, the following chapters will be devoted to introducing some advanced techniques employed in the evaluation of Feynman loop amplitudes.

Chapter 2

Methods for one-loop Feynman integrals

Feynman Integrals and Regularisation

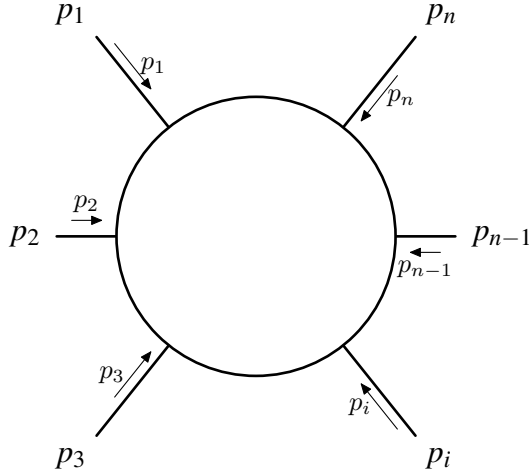


Figure 2.1: A generic n -point one-loop integral

Beyond tree-level, the standard techniques used to write out Feynman amplitudes given the rules of the theory invariably lead to momentum integrals over a closed loop, internal to the related Feynman diagram. One can isolate a loop momentum variable q^μ , independent of the external particle momenta, which is unbound.

This produces divergences in these loop integrals, which need to be treated somehow to produce meaningful physical predictions.

A generic n -point one-loop integral like the one in figure 2.1, with incoming momenta p_i obeying the momentum-conservation relation $\sum_{i=1}^n p_i = 0$ is of the form:

$$I_n[\mathcal{N}] = \int \frac{d^4 q}{(2\pi)^4} \frac{\mathcal{N}(q)}{D_1^{a_1} D_2^{a_2} \dots D_n^{a_n}} \quad (2.1)$$

The denominators D_i are defined as:

$$D_i = (q + r_i)^2 - m_i^2 + i\epsilon \quad (2.2)$$

$$r_i = p_1 + p_2 + \dots + p_i, \quad r_n = 0 \quad (2.3)$$

The powers a_j are most often set to 1 (at least for the cases commonly encountered at one-loop), but nothing forbids the same propagator from appearing twice in a diagram, and therefore the corresponding amplitude denominator being raised to a higher power.

Based on this realisation, it is useful to define a *topology* (or *sector*) as an integral like 2.1 where all powers a_j are strictly positive integers. Different sectors are identified based on the distinct denominators appearing within, rather than their the powers. Immediately one could define a number of *sub-topologies* of each sector by setting one or more powers to zero, all the while making sure that momentum conservation is not affected.

This operation is commonly referred to as *pinching* an internal propagator, and will play an important role later on.

Integrals like these are often transpose from 4-dimensional Minkowski space to 4-dimensional Euclidean space using a procedure known as *Wick rotation*. This has the effect of changing the sign of the mass parameters in every inverse propagator. The now Euclidean integration measure can be written, using 4-dimensional spherical coordinates, as:

$$d^4q = q^3 d\Omega_3 dq \quad (2.4)$$

and the integration over the 3-dimensional solid angle can be performed immediately, yielding a numerical pre-factor.

By naïve dimensional analysis it is easy to see how an integral like 2.1 can diverge both in the ultra-violet (UV) limit $q \rightarrow +\infty$ and in the infra-red (IR) limit $q \rightarrow 0$. If r is the rank, or highest power, in q of the numerator $\mathcal{N}(q)$, then one has:

$$I_n \sim \int dq \frac{q^{3+r}}{q^{2n}} \quad (2.5)$$

If we define the integer quantity $\delta := 3 + r - 2n$ then we have:

- for $\delta \geq 0$:

$$I_n \sim q^{\delta+1}$$

which is UV-divergent;

- for $\delta = -1$:

$$I_n \sim \log(q)$$

which is UV and IR-divergent and is known as *log-divergent*;

- for $\delta < -1$:

$$I_n \sim q^{-|\delta|+1}$$

which is IR-divergent.

Regularisation is in essence a mathematical prescription to momentarily remove the divergence, often with the introduction of some artificial quantity known as the regulator.

Regulators often used include a cut-off Λ on the loop momentum, bounding an UV-divergent integral from above. For infra-red divergences one could introduce an unphysical parameter λ , interpreted as a fictitious mass, used to shift the infra-red pole so that the integral is no longer divergent at the point $q \rightarrow 0$. Other techniques entail manipulating the loop propagators with parameters or power

coefficients to alter their ultraviolet behaviour and make the integral finite; one of these is known as *Pauli-Villars*.

These regulators are kept around until the very end of the calculation, at which point the divergent parts of the integral in question will all depend on them¹⁰. The parameters are then removed with appropriate limits (such as $\Lambda \rightarrow +\infty$ and $\lambda \rightarrow 0$) which bring back physical meaning to the object. This is done at the very end of the calculation of a measurable quantity such as a cross-section; the hope is that, if all the contributions have been accounted for and all "bare" parameters have been properly renormalised, there will be perfect cancellation of these divergences and the result will be finite at either end.

This is indeed the case for theories such as QED.

2.1 Dimensional Regularisation

Dimensional regularisation is a more sophisticated regularisation technique, It amounts to promoting the space-time in which the integrals are computed from 4 dimensions to D , where D is a continuous complex variable, making the integral finite by dimensional arguments as a result. The dimension should thus be sufficiently shifted from four to avoid all singularities. This dimensional replacement affects not only the integration measure, but also the objects appearing at the numerator and denominator.

The integral is calculated in D dimensions to obtain an expression explicitly dependent on D , and divergent in the $D \rightarrow 4$ limit.

The concept of a continuous dimension was introduced by Wilson and Fisher [120] for statistical physics and then further developed by 't Hooft and Veltman [13] in the context of the renormalisability of non-abelian Yang-Mills theories where all other regularisation prescriptions failed. This technique is advantageous for several reasons:

- since it preserves the character of all the objects in the theory and it avoids unphysical parameters, it doesn't spoil gauge symmetries crucial to the Standard Model;
- it separates the finite part of an integral from the divergent pole, and thus is naturally suited to renormalisation schemes such as *Minimal Subtraction (MS)* and the related \overline{MS} ;
- it works equally well for UV and IR divergences

We shall now introduce two prescriptions used to carry out computations in dimensional regularisation. We will need to distinguish between objects living in 4 and in generic D dimensions. D -dimensional quantities will henceforth will be denoted with a bar. These prescriptions are applicable to integrals at one loop or higher, and therefore are usually formulated in the generic case.

Let us write down, in D space-time dimensions, a generic n -point, l -loop Euclidean Feynman integral with m internal lines¹¹:

$$I_m^{n,l}[\mathcal{N}] = \int \prod_{j=1}^l \frac{d^D \bar{q}_j}{(\pi)^{D/2}} \frac{\mathcal{N}(\bar{q}_i)}{\bar{D}_1 \bar{D}_2 \dots \bar{D}_m} \quad (2.6)$$

¹⁰One could say that, in general, the resulting objects are *meromorphic* functions of the regulators, i.e. holomorphic everywhere on the complex plane of each parameter except at certain points (poles) at which the physical limit is restored and the result diverges as it used to.

¹¹in case of ≥ 1 loops, the number of internal lines is in general not equal to the number of external ones

where the numerator is a function of all the loop momenta \bar{q}_i^α , and where the denominators are kept as arbitrary D -dimensional objects until we define a prescription.

2.1.1 The $D = 4 - 2\varepsilon$ prescription

The key idea of this prescription is to split the D -dimensional space-time into a four-dimensional sector and a remainder (a “ (-2ε) -dimensional” subspace).

The metric tensor shows this decomposition explicitly:

$$\bar{g}^{\alpha\beta} = \begin{pmatrix} g^{\alpha\beta} & 0 \\ 0 & \tilde{g}^{\alpha\beta} \end{pmatrix} \quad (2.7)$$

where $g^{\alpha\beta}$ is the usual space-time metric and $\tilde{g}^{\alpha\beta}$ is the euclidean metric of the rest of our space-time. The trace over the two metrics are:

$$g^{\alpha\beta} g_{\alpha\beta} = 4 \quad (2.8)$$

$$\bar{g}^{\alpha\beta} \bar{g}_{\alpha\beta} = D \quad (2.9)$$

Lorentz vectors are similarly split:

$$\bar{v}^\alpha = v^\alpha + \tilde{v}^\alpha \quad (2.10)$$

Conventional practice is to keep the incoming particle momenta, external to the loop, strictly in four-dimensional space. This is as per the original formulation of Dimensional Regularisation by 't Hooft and Veltman.

Therefore:

$$\bar{p}_i^\alpha = p_i^\alpha \quad (2.11)$$

Although this thesis will focus mainly on one-loop Feynman integrals we temporarily consider more general integrals and assume an arbitrary number of loop momenta q_i . These momenta are D -dimensional and are split as follows:

$$\bar{q}_i^\alpha = q_i^\alpha + \mu_i^\alpha \quad (2.12)$$

where we introduced the vectors $\mu_i^\alpha = \tilde{q}_i^\alpha$ that live in (-2ε) -dimensions.

The Dirac- γ matrices are not extended from their four-dimensional counterpart like the metric, but instead defined conventionally using the Clifford Algebra:

$$\{ \bar{\gamma}^\alpha, \bar{\gamma}^\beta \} = 2\bar{g}^{\alpha\beta} \quad (2.13)$$

$$\bar{\gamma}^\alpha \bar{\gamma}_\alpha = \bar{\gamma}^\alpha \bar{\gamma}^\beta \bar{g}^{\alpha\beta} = \frac{1}{2} \left(\bar{\gamma}^\alpha \bar{\gamma}^\beta + \bar{\gamma}^\beta \bar{\gamma}^\alpha \right) \bar{g}^{\alpha\beta} = \bar{g}_{\alpha\beta} \bar{g}^{\alpha\beta} = D \quad (2.14)$$

$$\bar{\gamma}^\alpha \bar{\gamma}^\beta \bar{\gamma}_\alpha = (2 - D) \bar{\gamma}^\beta \quad (2.15)$$

where we used the symmetry of the metric to compute the trace.
Other useful relations are:

$$Tr[\mathbb{1}] = 2^{(D/2)} \quad (2.16)$$

$$\bar{g}^{\alpha\beta} \tilde{g}_{\alpha\beta} = -2\varepsilon \quad (2.17)$$

and the scalar products between the external and loop momenta, which make use of the orthogonality between the 4-dimensional and the (-2ε) -dimensional sectors:

$$p_i^\alpha \tilde{g}_{\alpha\beta} = 0 \quad (2.18)$$

$$\bar{q}_i \cdot \bar{q}_j = q_i^\alpha q_j^\beta g_{\alpha\beta} + \mu_i^\alpha \mu_j^\beta \tilde{g}_{\alpha\beta} = q_i \cdot q_j + \mu_{ij} \quad (2.19)$$

$$\bar{q}_i^2 = q_i^2 - \mu_i^2 \quad (2.20)$$

$$\bar{q}_i \cdot p_j = \bar{q}_i^\alpha p_j^\beta g_{\alpha\beta} = q_i \cdot p_j \quad (2.21)$$

where $\mu_{ij} = \mu_i \cdot \mu_j$.

These definitions enable us to write down explicitly the loop momentum l_i^α and denominators D_i of integral 2.6 :

$$\begin{aligned} \bar{D}_i &= l_i^2 + \sum_{j,k} \alpha_{ij} \alpha_{ik} \mu_{jk} + m_i^2 + i\varepsilon \\ l_i^\alpha &= \sum_j \alpha_{ij} q_j^\alpha + \sum_j \beta_{ij} p_j^\alpha \end{aligned} \quad (2.22)$$

the introduction of the α and β coefficients just means that the denominators can carry an arbitrary combination of loop momenta and external momenta flowing through.

Finally, the i -th integration measure can be split between the four-dimensional and the (-2ε) -dimensional sectors of our space-time:

$$\int \frac{d^D \bar{q}_i}{(2\pi)^D} = \int \frac{d^4 q_i}{(2\pi)^4} \int \frac{d^{-2\varepsilon} \mu_i}{(2\pi)^{-2\varepsilon}} \quad (2.23)$$

By virtue of orthogonality and the scalar products above, the extra-dimensional vector μ_i^α cannot appear linearly at the denominator, but only quadratically through μ_{ij} , and the same can be said for the numerator. This, in turn, means that for the integral over the (-2ε) -dimensional Euclidean space one can employ spherical coordinates and immediately integrate over the solid angle. Thus, after some work, 2.6 is rewritten as follows:

$$I_m^{n,l}[\mathcal{N}] = \Omega_D^l \int \prod_{i=1}^l d^4 q_j \int \prod_{1 \leq i \leq j \leq l} d\mu_{ij} \text{Det}[\mathbb{G}_{ij}(\mu_1 \dots \mu_l)]^{\frac{D-5-l}{2}} \frac{\mathcal{N}(q_i, \mu_{ij})}{\prod_{k=1}^m \bar{D}_k(q_i, \mu_{ij})} \quad (2.24)$$

where $\mathbb{G}_{ij} = \mu_{ij}$ is the gram matrix of the μ_i^α vectors and Ω_D^l is the product of all the solid angles:

$$\begin{aligned}\Omega_n &= \frac{2\pi^{\frac{n+1}{2}}}{\Gamma\left(\frac{n+1}{2}\right)} \\ \Omega_D^l &= \prod_{i=1}^l \frac{\Omega_{d-4-i}}{2\pi^{D/2}}\end{aligned}\tag{2.25}$$

We will discuss various practical techniques to simplify and compute Feynman loop integrals and we will often resort to writing the four-dimensional part of the loop momentum q_i in terms of an arbitrary basis $\mathcal{E} = \{e_1, e_2, e_3, e_4\}$:

$$q_i^\mu = \sum_{j=1}^4 x_{ij} e_j^\mu\tag{2.26}$$

arbitrariness entails that for the time being we will not say anything about its properties. Parametrising in this way the loop momenta within the integral yields:

$$I_m^{n,l}[\mathcal{N}] = \Omega_D^l \mathcal{J} \int \prod_{i=1}^l \prod_{j=1}^4 dx_{ij} \int \prod_{1 \leq i \leq j \leq l} d\mu_{ij} \text{Det}[\mathbb{G}_{ij}(\mu_1 \dots \mu_l)]^{\frac{D-5-l}{2}} \frac{\mathcal{N}(q_i, \mu_{ij})}{\prod_{k=1}^m \bar{D}_k(q_i, \mu_{ij})}\tag{2.27}$$

where \mathcal{J} is the Jacobian of the parametrisation.

The gist of this discussion is that, by adopting a dimensional regularisation scheme with external particles in four dimensions, one can represent a Feynman integral in D continuous dimensions as an integral over a finite set of variables:

$$\mathbf{z} = \{x_{j1}, x_{j2}, x_{j3}, x_{j4}, \mu_{ij}\}, \quad 1 \leq i \leq j \leq l\tag{2.28}$$

and their total number is $4l + l(l+1)/2 = l(l+9)/2$. Moreover, the dependence of the integrand on the whole set of variables turns out to be *polynomial*, which will play a crucial role later on.

2.1.2 The $D = D_{\parallel} + D_{\perp}$ prescription

An interesting and useful representation of Feynman integrals such as 2.27 can be obtained by a particular choice of basis \mathcal{E} .

The starting point is to consider, among all the n external momenta p_i , a subset of independent momenta. In principle there would be $n-1$ such vectors, having the one constraint of momentum conservation. However in a 4-dimensional space-time one can have at most 4 independent vectors.

We therefore define the *longitudinal space* as the space spanned by one such subset of momenta. This space has dimensions:

$$D_{\parallel} = \min[4, n-1]\tag{2.29}$$

and the remaining sector shall be spanned by vectors *orthogonal* to these momenta. These will span the so-called *transverse space* of dimensions D_{\perp} .

The metric of the combined space-time will once again be block-diagonal:

$$\bar{g}^{\alpha\beta} = \begin{pmatrix} g_{D_{\parallel}}^{\alpha\beta} & 0 \\ 0 & g_{D_{\perp}}^{\alpha\beta} \end{pmatrix} \quad (2.30)$$

The trace over the two metrics are:

$$g_{D_{\parallel}}^{\alpha\beta} g_{D_{\parallel}} \alpha\beta = D_{\parallel} \quad (2.31)$$

$$g_{D_{\perp}}^{\alpha\beta} g_{D_{\perp}} \alpha\beta = D_{\perp} \quad (2.32)$$

In this new prescription we will still aim to keep the external momenta in 4 dimensions and split the D -dimensional loop momenta, this time onto parallel and transverse components, and we will introduce a new vector λ to span the transverse sector. It is understood that part of the transverse components will correspond to the ones formerly labelled as μ_i^α , but since the space is now split with reference to the independent external moments, some of the components formerly carried by the four-dimensional q_i^α will appear within λ_i^α .

The \mathcal{E} basis will therefore contain D_{\parallel} elements which span the parallel space (and therefore be related to the independent external momenta) and between 1 and $(4 - d_{\parallel})$ transverse vectors defined to be orthogonal to the former. An example of such a basis which is used multiple times in this thesis can be found in appendix A.

The parametrisation of an arbitrary number of loop momenta in this parallel-perpendicular prescription can be found in [14, 15]. Based on this we split q_i^α as follows:

$$\bar{q}_i^\alpha = q_{\parallel i}^\alpha + \lambda_i^\alpha \quad (2.33)$$

with:

$$q_{\parallel i}^\alpha = \sum_{j=1}^{D_{\parallel}} x_{ij} e_j^\alpha \quad (2.34)$$

$$\lambda_i^\alpha = \sum_{j=D_{\parallel}+1}^4 x_{ij} e_j^\alpha + \mu_i^\alpha \quad (2.35)$$

Once again some useful scalar product relations can be obtained:

$$\bar{q}_i \cdot \bar{q}_j = q_{\parallel i}^\alpha q_{\parallel j}^\beta g_{D_{\parallel}} \alpha\beta + \lambda_i^\alpha \lambda_j^\beta g_{D_{\perp}} \alpha\beta = q_{\parallel i} \cdot q_{\parallel j} + \lambda_{ij} \quad (2.36)$$

$$\bar{q}_i^2 = q_{\parallel i}^2 - \lambda_i^2 \quad (2.37)$$

$$\bar{q}_i \cdot p_j = \bar{q}_i^\alpha p_j^\beta g_{\alpha\beta} = q_{\parallel i} \cdot p_j \quad (2.38)$$

where we introduced the symbol λ_{ij} :

$$\lambda_{ij} = \lambda_i \cdot \lambda_j = \sum_{k=D_{\parallel}+1}^4 x_{ik} x_{jk} + \mu_{ij} \quad (2.39)$$

We shall refer to the x_i variables that parametrise the parallel components of \vec{q} as $x_{\parallel i}$ and we will label the remaining ones as $x_{\perp i}$.

Let us apply this new parametrisation for the loop momenta to the denominators of 2.6:

$$\begin{aligned}\bar{D}_i &= l_{\parallel i}^2 + \sum_{j,k} \alpha_{ij} \alpha_{ik} \lambda_{jk} + m_i^2 + i\varepsilon \\ l_{\parallel i}^\alpha &= \sum_j \alpha_{ij} q_{\parallel j}^\alpha + \sum_j \beta_{ij} p_j^\alpha\end{aligned}\tag{2.40}$$

and from the scalar rules it is easy to see how the loop denominators are independent of the x_{\perp} components, except for their contribution to λ_{ij} . This further reduces the number of variables needed to parametrise an inverse propagator, from $l(l+9)/2$ to $4d_{\parallel} + l(l+1)/2 = l(l+2d_{\parallel}+1)/2$. However, the numerator can generally still depend on these components, but their dependence is once more *polynomial* and it is in fact possible to easily integrate over these components, thanks to this parametrisation.

The full procedure can be found in [14–16] and their appendices. In short, angular variables Θ_{Λ} and Θ_{\perp} are introduced, which depend exclusively on the external kinematic quantities, and the existing transverse variables ($x_{\perp i}$ and λ_{ij}) are mapped to polynomials in these variables:

$$\begin{aligned}\lambda_{ij} &\longrightarrow P[\lambda_{kk}, \sin(\Theta_{\Lambda}), \cos(\Theta_{\Lambda})], \quad i \neq j, k = \{1, \dots, l\} \\ x_{ij} &\longrightarrow P[\lambda_{kk}, \sin(\Theta_{\perp}), \cos(\Theta_{\perp}), \theta_{\Lambda}], \quad j \geq D_{\parallel}, k = \{1, \dots, l\}\end{aligned}\tag{2.41}$$

The Feynman integral 2.27 can be thus rewritten as:

$$I_m^{n,l}[\mathcal{N}] = \Omega_D^l \mathcal{J} \int \prod_{i=1}^l \prod_{j=1}^{D_{\parallel}} dx_{ij} \int \prod_{i=1}^l d\lambda_{ii} \lambda_{ii}^{\frac{D_{\perp}-2}{2}} \int d^{\frac{l(l-1)}{2}} \Theta_{\Lambda} \int d^{l(4-D_{\parallel})} \Theta_{\perp} \frac{\mathcal{N}(q_{\parallel i}, \lambda_{ij}, \Theta_{\perp})}{\prod_{k=1}^m \bar{D}_k(q_{\parallel i}, \lambda_{ij})}\tag{2.42}$$

where now the integration is performed over the longitudinal components x_{\parallel} , the norm of the transverse vectors λ_{ii} , the angles Θ_{Λ} related to the relative orientations of the transverse vectors and the Θ_{\perp} , which parametrise $x_{\perp i}$. \mathcal{J} is the Jacobian of the variable change from q_{\parallel} to x_{ij} .

The remarkable result is that the definition of the transverse angles $\Theta_{\Lambda}, \Theta_{\perp}$ (which depends on the choice of four-dimensional basis) is influenced solely by the external kinematics, and not on the specific denominators of the integral at hand.

The integration over the transverse variables, thanks to the mappings above, can be expressed as spherical integrals of trigonometric functions:

$$\begin{aligned}\int d^{\frac{l(l-1)}{2}} \Theta_{\Lambda} &= \int_{-1}^{+1} \prod_{1 \leq i < j \leq l} d \cos \theta_{ij} (\sin \theta_{ij})^{(D_{\perp}-2-i)} \\ \int d^{l(4-D_{\parallel})} \Theta_{\perp} &= \int_{-1}^{+1} \prod_{i=1}^{4-D_{\parallel}} \prod_{j=1}^l d \cos \theta_{(i+j-1)j} (\sin \theta_{(i+j-1)j})^{(D_{\perp}-1-i-j)}\end{aligned}\tag{2.43}$$

Thanks to the polynomial dependence of any numerator on the transverse components, to the mappings and to the possibility of factorising each independent transverse parameter, it turns out that integrating over the transverse space boils down to solving a number of factorised one-dimensional trigonometric integrals of the type:

$$\int_{-1}^{+1} d \cos \theta (\sin \theta)^a (\cos \theta)^b \quad (2.44)$$

where a, b depend on D in a way fixed by the topology of the amplitude. Moreover, it is possible to define a procedure [14, 16] to map any integral numerator in to a product of such simple trigonometric integrals via an expansion on the so-called *Gegenbauer Polynomials* $C_n^\alpha \cos \theta$ and, at the same time, exploit the properties of these polynomials to efficiently perform the integration of each term in the expansion.

Appendices A.2 and A.3 of [15] present a collection of general results for one- and two- loop integrals in various kinematic configurations, as well as the integrals over the transverse directions. Thanks to these results, integrating over transverse components is usually never more difficult than looking up the relevant case from such a list, which is particularly advantageous for automatic algorithms employing this mathematical technology.

To conclude this section, we mention that in recent years the understanding of regularisation schemes has been greatly advanced, and new prescriptions have been proposed. These include dimensional schemes such as *Four-Dimensional Helicity (FDH)*, its *Four-Dimensional formulation (FDF)* and schemes designed to work strictly in four-dimensions such as *FOUR-DIMENSIONAL REGULARISATION (FDR)*. These new schemes have been developed both to broaden the theoretical foundations of regularisation but also for best applicability to numerical and analytical automated tools. A compact review and comparison of these and other schemes can be found in [121]

2.2 Tensor integral reduction

Let us go back to considering one-loop Feynman integrals. Once a Feynman integral is properly regulated (using techniques such as the aforementioned Dimensional Regularisation) much of the difficulty in calculating dimensionally-regulated integrals is actually given by the tensor structure of the numerator. In the QFTs one most often encounters, it will contain one or more objects $T_{i_1, i_2, \dots, i_n}^{\mu_1, \mu_2, \dots, \mu_r}(\bar{q})$ composed of products of various non-trivial tensor objects (such as the γ^μ matrices for spinors) and kinematic objects with the loop D -dimensional vector \bar{q}^μ .

The generic integrals are of the form:

$$I_{i_1, i_2, \dots, i_n}^{\mu_1, \mu_2, \dots, \mu_r} = \int d^D \bar{q} \frac{T_{i_1, i_2, \dots, i_n}^{\mu_1, \mu_2, \dots, \mu_r}(\bar{q})}{\bar{D}_{i_1} \bar{D}_{i_2} \dots \bar{D}_n} \quad (2.45)$$

\bar{D}_i are the inverse propagators, their explicit form is prescription-dependent as evidenced in 2.22 or 2.40. We also forwent any normalisation factors, momentarily.

As it turns out, in a renormalisable theory one does not encounter tensor objects of rank r greater than the number of denominators:

$$r \leq n$$

Moreover, the external momenta live in 4-dimensional space-time and thus we have at any one time at most four independent such vectors. Keeping this in mind, it can be shown [122] that integrals with $n \geq 5$ can always be reduced into a combination of simpler integrals with fewer points. Therefore the actual integrals one encounters are all of the following form:

$$\begin{aligned}
 I_i, I_i^\mu &= \int d^D \bar{q} \frac{1, \bar{q}^\mu}{\bar{D}_i} \\
 I_{ij}, I_{ij}^\mu, I_{ij}^{\mu\nu} &= \int d^D \bar{q} \frac{1, \bar{q}^\mu, \bar{q}^\mu \bar{q}^\nu}{\bar{D}_i \bar{D}_j} \\
 I_{ijk}, I_{ijk}^\mu, I_{ijk}^{\mu\nu}, I_{ijk}^{\mu\nu\rho} &= \int d^D \bar{q} \frac{1, \bar{q}^\mu, \bar{q}^\mu \bar{q}^\nu, \bar{q}^\mu \bar{q}^\nu \bar{q}^\rho}{\bar{D}_i \bar{D}_j \bar{D}_k} \\
 I_{ijkl}, I_{ijkl}^\mu, I_{ijkl}^{\mu\nu}, I_{ijkl}^{\mu\nu\rho}, I_{ijkl}^{\mu\nu\rho\sigma} &= \int d^D \bar{q} \frac{1, \bar{q}^\mu, \bar{q}^\mu \bar{q}^\nu, \bar{q}^\mu \bar{q}^\nu \bar{q}^\rho, \bar{q}^\mu \bar{q}^\nu \bar{q}^\rho \bar{q}^\sigma}{\bar{D}_i \bar{D}_j \bar{D}_k \bar{D}_l}
 \end{aligned}$$

Let us, however, examine I_i^μ in detail. We can add and subtract r_i^μ to the numerator:

$$\int d^D \bar{q} \frac{\bar{q}^\mu}{(\bar{q} + r_i)^2 - m_i^2} = \int d^D \bar{q} \frac{(\bar{q}^\mu + r_i^\mu) - r_i^\mu}{(\bar{q} + r_i)^2 - m_i^2} = -r_i^\mu I_i$$

The first term at the numerator yields a vanishing integral by symmetry arguments, and thus the result is proportional to the scalar tadpole integral. I_i^μ is therefore always decomposed immediately.

The evaluation of these integrals is made much simpler by re-writing them as a linear combination of simpler *Scalar Integrals*, with coefficients depending on the external kinematic objects of the problem. This integral basis is sometimes referred to as a *Master Integral basis*, its elements are known as *Master Integrals (MIs)*¹², will be of the form:

$$I_{ij\dots n} = \int d^D \bar{q} \frac{1}{\bar{D}_i \bar{D}_j \dots \bar{D}_n} \tag{2.46}$$

Master-Integral reduction prescriptions are useful since they split a difficult task in two simpler steps: one is able to carry out the rest of the physical calculation under advisement as simple momentum traces and scalar products, leaving the MIs as "black-box" objects to be evaluated separately.

2.2.1 Passarino-Veltman tensor reduction

The *Passarino-Veltman method* (PV) [17] is a long-standing tool to reduce tensor integrals as a sum of scalar integrals.

¹²We will use the term *Master Integrals* to denote any set of integrals acting as a basis for a more complex integral. More precisely it refers specifically to the *minimal* basis of integrals that describe a process. This is relevant because some integrals can be related to others by identities or vanish outright, thus simplifying the expansion. We will say more about this in later chapters.

Let us describe the scheme with a few examples. If we take a generic rank-1 integral $I_{ij\dots n}^\mu$, then we expect this to transform as a four-vector under the Lorentz group. A basis for the vector space in which this quantity lives is given by the independent four-momentum vectors p_i^μ carried by the incoming particles interacting through the diagram. Keeping in mind momentum-conservation, for n incoming particles we will have $n - 1$ four-momentum vectors at our disposal. We therefore decompose as thus:

$$I_{ij\dots n}^\mu = \sum_{\alpha=1}^{n-1} p_\alpha^\mu C_n^\alpha \quad (2.47)$$

This sum encompasses all possible rank-1 tensors at our disposal given the independent external momenta. The coefficient B_1^α is called *form factor*, the superscripts (ij) indicate to which denominator (and particle masses) the coefficient is related. Let us now contract 2.47 with one of the independent vectors p_β :

$$I_{ij\dots n} \cdot p_\beta = \int d^D \bar{q} \frac{\bar{q} \cdot p_\beta}{\bar{D}_i \bar{D}_j \dots \bar{D}_n} = \sum_{\alpha=1}^{n-1} \mathbb{G}_{\alpha\beta} C_n^\alpha \quad (2.48)$$

$\mathbb{G}_{\alpha\beta}$ is the $(n-1) \times (n-1)$ Gram matrix of independent momenta, whose entries are $p_\alpha \cdot p_\beta$. Realising that we can write $p_\beta = r_\beta - r_{\beta-1}$ we can decompose the dot product $\bar{q} \cdot p_\beta$ as a combination of D-dimensional denominators and masses:

$$\bar{q} \cdot p_\beta = \frac{1}{2} \left[\bar{D}_\beta - \bar{D}_{\beta-1} - \left(r_\beta^2 - m_\beta^2 \right) + \left(r_{\beta-1}^2 - m_{\beta-1}^2 \right) \right] \quad (2.49)$$

This formula enables us to write out 2.48 in terms of simpler quantities. In detail, the two denominator factors will cancel out with the respective ones present in the original integral, yielding two scalar integrals with one fewer denominator, whereas the remaining constants will multiply the scalar integral $I_{ij\dots n}$:

$$\sum_{\alpha=1}^{n-1} \mathbb{G}_{\alpha\beta} C_n^\alpha = \frac{1}{2} \left[I_{ij\dots\beta\dots n} - I_{ij\dots\beta\cancel{1}\dots n} + \left(r_{\beta-1}^2 - m_{\beta-1}^2 - r_\beta^2 + m_\beta^2 \right) I_{ij\dots n} \right] \quad (2.50)$$

This constitutes an $(n-1)$ -dimensional system of equations in the unknown form factors. We can extract all of them by multiplying by the inverse Gram matrix and summing over the columns:

$$C_n^\alpha = \sum_{\beta=1}^{n-1} \frac{\mathbb{G}_{\alpha\beta}^{-1}}{2} \left[I_{ij\dots\beta\dots n} - I_{ij\dots\beta\cancel{1}\dots n} + \left(r_{\beta-1}^2 - m_{\beta-1}^2 - r_\beta^2 + m_\beta^2 \right) I_{ij\dots n} \right] \quad (2.51)$$

For a rank-2 tensor the strategy is similar, the basis used to decompose the integral will now contain all the independent rank-2 tensors that we can build, which are the 4-dimensional metric $g_{\mu\nu}$ and all products of the $(n-1)$ external momenta two-by-two, of which we have $(n-1)^2$:

$$I_{ij\dots n}^{\mu\nu} = g^{\mu\nu} C_n^{00} + \sum_{\alpha,\beta=1}^{n-1} p_\alpha^\mu p_\beta^\nu C_n^{\alpha\beta} \quad , \quad C_n^{\alpha\beta} = C_n^{\beta\alpha} \quad (2.52)$$

Let us mention that we include only the 4-dimensional part of the metric, as opposed to the full D -dimensional one, for consistency with the $(n-1)$ external momenta, who live in the 4-dimensional sector exclusively.

We now contract this with all the independent momenta, obtaining $(n-1)$ equations:

$$p_{\gamma\mu} I_{ij\dots n}^{\mu\nu} = p_\gamma^\nu C_n^{00} + \sum_{\alpha=1}^{n-1} \sum_{\beta=1}^{n-1} \mathbb{G}_{\gamma\alpha}^{(n-1)} p_\beta^\nu C_n^{\alpha\beta} \quad (2.53)$$

where $\mathbb{G}_{\beta\gamma}^{(n-1)}$ is the $(n-1) \times (n-1)$ Gram matrix of external momenta.

The left-hand side is an integral with numerator $\bar{q}^\mu (\bar{q} \cdot p_\gamma)$, which can be expanded similarly to 2.49, obtaining:

$$p_{\gamma\mu} I_{ij\dots n}^{\mu\nu} = \int d^D \bar{q} \frac{(\bar{q} \cdot p_\gamma) \bar{q}^\nu}{\bar{D}_i \bar{D}_j \dots \bar{D}_n} = \frac{1}{2} \left[I_{ij\dots\cancel{\gamma}\dots n}^\nu - I_{ij\dots\cancel{\gamma}\dots n}^\nu + (r_{\gamma-1}^2 - m_{\gamma-1}^2 - r_\gamma^2 + m_\gamma^2) I_{ij\dots n}^\nu \right] \quad (2.54)$$

which is a decomposition into rank-1 tensor integrals. Those can all be reduced using the previous results, bearing in mind to plug in the correct particle momenta and, if needed, shift the loop momentum variable; in the case of a rank-2 bubble, the decomposition will include rank-1 tadpoles, which vanish by symmetry arguments.

After fully decomposing all tensor integrals down to the scalar MIs in each equation, one separates all terms proportional to each p_β^ν on the l.h.s to bring it in the same form of 2.53.

Then, in every equation, one collects all terms multiplying p_β^ν for each value of the index β separately.

The result is $(n-1)$ systems of equations in the variables $C_n^{\alpha\beta}$ where beta is now fixed. It could be shown by explicit calculation that each of these systems can be assembled in matrix form:

$$\mathbb{G}_{\gamma\alpha}^{(n-1)} \begin{pmatrix} C_n^{\alpha=1\beta} \\ C_n^{\alpha=2\beta} \\ \vdots \\ C_n^{\alpha=n-1\beta} \end{pmatrix} = \begin{pmatrix} R_{\gamma=1}^\beta \\ R_{\gamma=2}^\beta \\ \vdots \\ R_{\gamma=n-1}^\beta \end{pmatrix} \quad , \quad \beta = 1, 2 \dots n-1 \quad (2.55)$$

where R_γ^β is the collection of all terms proportional to p_β^ν within $p_{\gamma\mu} I_{ij\dots n}^{\mu\nu}$.

We point out that these systems are not fully determined since the term $R_{\gamma=\beta}^\beta$ in each system contains C_n^{00} . This last form factor is extracted by contracting 2.52 with the 4-dimensional metric.

Expanding the l.h.s, we have the contraction of the 4-dimensional metric with $\bar{q}^\mu \bar{q}^\nu$, which yields the projection of the loop momentum squared on the 4-dimensional coordinates, i.e. q^2 .

The numerator of the integrand is decomposed as follows, using 2.22:

$$I_{ij\dots n}^{\mu\nu} g_{\mu\nu} = \int d^D \bar{q} \frac{q^2}{\bar{D}_i \bar{D}_j \dots \bar{D}_n} = \int d^D \bar{q} \frac{\bar{D}_\gamma + m_\gamma^2 + \mu^2}{\bar{D}_i \bar{D}_j \dots \bar{D}_n} = [I_{ij\dots n}^\mu + m_\gamma^2 I_{ij\dots n}^\mu + I_{ij\dots n}^\mu [\mu^2]] \quad (2.56)$$

where $I_{ij\dots n}^\mu [\mu^2]$ denotes the n-point loop integral with μ^2 at the numerator.

For the r.h.s:

$$g_{\mu\nu} I_{ij\dots n}^{\mu\nu} = 4 C_n^{00} + \sum_{\alpha, \beta=1}^{n-1} \mathbb{G}_{\alpha\beta}^{(n-1)} C_n^{\alpha\beta} = \sum_{\beta=1}^{n-1} R_\beta^\beta \quad (2.57)$$

where we plugged in each of the $\gamma = \beta$ equations of 2.55.

From 2.57 C_n^{00} can be extracted (recalling that each of the R_β^β terms contains it) and plugged into 2.55, which are then solved to extract all coefficients in terms of scalar products and MIs.

It could be shown that, in general, the form factors belonging to the 4-dimensional metric will contain an integral of the form $I_{ij\dots n}^{\mu\nu\dots} [\mu^2]$, which we showed explicitly for C_n^{00} . These terms are known as *rational terms* since they constitute the leftover part of the simplification of a 4-dimensional numerator against a D -dimensional denominator i.e. a ratio of two incommensurable quantities. We will say more about them shortly.

The PV procedure is readily generalised to reduce integrals of arbitrary rank (although still $\leq n$), and the final result is a decomposition onto the independent tensor objects available, each multiplied by a coefficient $C_n^{\alpha\beta\dots}$ containing scalar Master Integrals $I_{ij\dots}$. Table 2.1 of [1] displays the full chain of decomposition of each of the $C_n^{\alpha\beta\dots}$ coefficients down to the individual MIs. The $C_n^{\alpha\beta\dots}$ quantities written here are denoted therein as: $A_{\alpha\beta\dots}$ for $n = 1$, $B_{\alpha\beta\dots}$ for $n = 2$ etc. and their $A_0, B_0 \dots$ functions correspond to the MIs $I_i, I_{ij} \dots$.

It is then easy to morph this result into an expansion onto the MIs themselves, with coefficients containing the tensor objects. The expansion takes the form:

$$\begin{aligned} \mathcal{M}_n &= \int d^D \bar{q} \mathcal{M}(q) = \\ &= \sum_{i << l} \int d^D \bar{q} \frac{c_{4,0}^{ijkl}}{\bar{D}_i \bar{D}_j \bar{D}_k \bar{D}_l} + \sum_{i << k} \int d^D \bar{q} \frac{c_{3,0}^{ijk}}{\bar{D}_i \bar{D}_j \bar{D}_k} + \sum_{i < j} \int d^D \bar{q} \frac{c_{2,0}^{ij}}{\bar{D}_i \bar{D}_j} + \sum_i \int d^D \bar{q} \frac{c_{1,0}^i}{\bar{D}_i} + \mathcal{R} \end{aligned} \quad (2.58)$$

where $i \ll l$ simply fixes the ordering of whatever denominators are relevant to one given term in the master integral series. We also notice the term \mathcal{R} which encompasses the rational terms i.e. all the integrals not reducible into scalar MIs.

Equation 2.58 can be represented pictorially, where a indicates a particular configuration of denominators i, j, \dots for brevity:

$$\mathcal{M}_n^{1-loop} = \text{Sun} = \sum_a c_4^a \text{Box} + \sum_a c_3^a \text{Triangle} + \sum_a c_2^a \text{Bubble} + \sum_a c_1^a \text{Bubble} + \mathcal{R} \quad (2.59)$$

The scalar integrals with four, three, two and one internal lines are known respectively as *box*, *triangle*, *bubble* and *tadpole*, in analogy with the shape of their respective diagrams. We now write them down using the notation used by automatic code packages such as FEYNCALC[50, 51]:

$$\begin{aligned}
 A_0(m_1^2) &= \frac{-i(2\mu\pi)^{4-D}}{\pi^2} \int d^D \bar{q} \frac{1}{q^2 - m_1^2} \\
 B_0(p_1^2, m_1^2, m_2^2) &= \frac{-i(2\mu\pi)^{4-D}}{\pi^2} \int d^D \bar{q} \frac{1}{(q^2 - m_1^2) \left((q+p_1)^2 - m_2^2 \right)} \\
 C_0(p_1^2, p_{12}, p_2^2, m_1^2, m_2^2, m_3^2) &= \frac{-i(2\mu\pi)^{4-D}}{\pi^2} \int d^D \bar{q} \frac{1}{(q^2 - m_1^2) \left((q+p_1)^2 - m_2^2 \right) \left((q+p_2)^2 - m_3^2 \right)} \\
 D_0(p_1^2, p_{12}, p_{23}, p_2^2, p_3^2, p_{13}, m_1^2, m_2^2, m_3^2, m_4^2) &= \\
 \frac{-i(2\mu\pi)^{4-D}}{\pi^2} \int d^D \bar{q} \frac{1}{(q^2 - m_1^2) \left((q+p_1)^2 - m_2^2 \right) \left((q+p_2)^2 - m_3^2 \right) \left((q+p_3)^2 - m_4^2 \right)} & \quad (2.60)
 \end{aligned}$$

where $p_{ij} := (p_i - p_j)^2$. These scalar integrals have been classified and computed explicitly by 't Hooft and Veltman [123]. There exist simpler version of these functions where several arguments are either identical or zero outright, their explicit expressions end up being equally simpler.

Let us briefly comment on the rational terms. The MI-basis of tadpoles, bubbles, triangles and boxes, is a complete integral basis in 4 dimensions, and the presence of rational terms in D -dimensions means that this basis is no longer complete in the case of dimensionally-regulated space-time. In [45] these terms were investigated and classified into two categories: the \mathcal{R}_1 terms arise from the extra dimensionality of the denominators and \mathcal{R}_2 from the dimensionality of the numerators¹³. These rational terms were, originally, handled separately from the main calculations, either computed directly or reconstructed from tree-level amplitudes.

2.2.2 D-dimensional amplitude decomposition

The more modern approach is to adopt a more general view of Dimensional Regularisation: instead of interpreting the D -dimensional space-time as a "small extension" of a four-dimensional space-time (i.e. $D = 4 - 2\epsilon$), it could instead be envisaged as a *5-dimensional* space, with the familiar 4 dimensions augmented by an extra degree of freedom that encompasses the remaining sector.

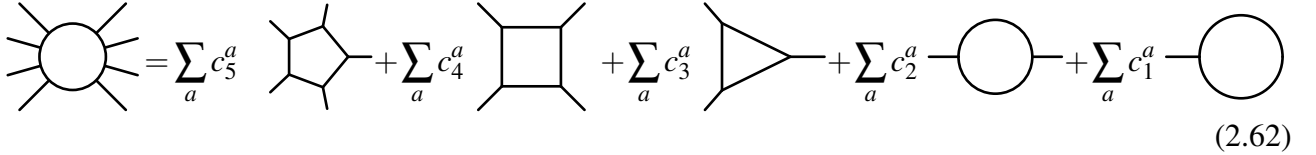
In this way one can identify this fifth degree of freedom with μ^2 itself, and this immediately enables one to interpret integrals of the form $I_{ij\dots n}^{\mu\nu\dots} \left[(\mu^2)^\alpha \right]$ as distinct Master Integrals of their own right: the former rational terms are thus automatically captured and accounted for, without any need for ad-hoc techniques to deal with them separately.

At the very beginning of section 2.2 we remarked that in four space-time dimensions the number of degrees of freedom restricted the MI basis to include up to 4-point integrals. By the same token,

¹³This classification of the rational terms was formalised in within the context of *Integrand Decomposition*, which will be detailed in the following chapter.

in this peculiar view of D -dimensional space the basis should be extended to include 5-dimensional Master Integrals, which we will henceforth call *pentagons*. We shall then amend 2.58 and write down a D -dimensional Feynman amplitude parametrisation as follows [30, 40, 44]:

$$\begin{aligned} \mathcal{M}_n &= \int d^D q A(\bar{q}) = \\ &= \sum_{i < < m} \bar{C}_{ijklm} I_{ijklm} + \sum_{i < < l} \bar{C}_{ijkl} I_{ijkl} + \sum_{i < < k} \bar{C}_{ijk} I_{ijk} + \sum_{i < < j} \bar{C}_{ij} I_{ij} + \sum_i \bar{C}_i I_i \end{aligned} \quad (2.61)$$



$$\text{Sun} = \sum_a c_5^a \text{Pentagon} + \sum_a c_4^a \text{Square} + \sum_a c_3^a \text{Triangle} + \sum_a c_2^a \text{Circle} + \sum_a c_1^a \text{Circle} \quad (2.62)$$

where $ijk\dots$ are ordered partitions of the n external momenta grouped in sets of five, four, three etc. depending on the particular integral in question.

According to our scheme, external momenta are strictly four-dimensional, therefore the D -dimensionality of the MI coefficients occurs through \bar{q}^2 and, by extension, through μ^2 alone and powers thereof. The rank restriction mentioned previously still holds; for this reason bubbles and triangles will contain at most contributions of μ^2 while boxes will comprise μ^2 and μ^4 , while tadpoles need to be purely 4-dimensional.

The newly-introduced pentagon integral should, intuitively, bring a scalar contribution as well as μ^2 and μ^4 terms. However, in [124] it was shown that the integrals $I_{ijklm}[1]$, $I_{ijklm}[\mu^2]$, $I_{ijklm}[\mu^4]$ differ from each other by \bar{q} -independent factors that depend in the kinematic variables of the pentagon in question and at most four-point integrals. Therefore any, but only one, of those three should be selected as the representative pentagon Master Integral. For this discussion we shall pick the scalar one for consistency with [30, 40], but in chapter 4.1.2 we will say more about this and make a different choice.

These considerations enable us to write down 2.61 in terms of a new MI-basis:

$$\begin{aligned} \mathcal{M}_n &= \int d^D q A(\bar{q}) = \\ &= \sum_{i < < m} \bar{C}_{ijklm} I_{ijklm} + \sum_{i < < l} \left\{ C_{ijkl}^{[0]} I_{ijkl}[1] + C_{ijkl}^{[2]} I_{ijkl}[\mu^2] + C_{ijkl}^{[4]} I_{ijkl}[\mu^4] \right\} + \\ &\sum_{i < < k} \left\{ C_{ijk}^{[0]} I_{ijk}[1] + C_{ijk}^{[2]} I_{ijk}[\mu^2] \right\} + \sum_{i < < j} \left\{ C_{ij}^{[0]} I_{ij}[1] + C_{ij}^{[2]} I_{ij}[\mu^2] \right\} + \sum_i C_i I_i \end{aligned} \quad (2.63)$$

The integrals contributing factors of μ^2 at the numerator can be dealt with by writing them as scalar integrals in dimensions *higher* than D itself, via the so-called *dimensional shift identities* described in appendix A of [26]:

$$I_n^D[\mu^{2\alpha}] = I_n^{D+2\alpha}[1] \frac{1}{2\alpha} \prod_{k=0}^{\alpha-1} (D+4-k) \quad (2.64)$$

Moreover it was realised long ago [125] that the scalar pentagon integral in $D = 4$ dimensions can be written as a linear combination of five $D = 4$ box integrals. In [126] this result was found true also in

$D = 4 - 2\varepsilon$ up to order ε . For these reasons the pentagon term is usually omitted outright.

We thus arrive at the following parametrisation of the decomposed amplitude:

$$\begin{aligned}
 \mathcal{M}_n &= \int d^D q \mathcal{M}(\bar{q}) = \\
 &= \sum_{i < < l} \left\{ \tilde{C}_{ijkl} I_{ijkl}^D + \frac{D-4}{2} C_{ijkl}^{[2]} I_{ijkl}^{D+2} + \frac{(D-4)(D-2)}{4} C_{ijkl}^{[4]} I_{ijkl}^{D+4} \right\} + \\
 &\sum_{i < < k} \left\{ C_{ijk}^{[0]} I_{ijk}^D + \frac{D-4}{2} C_{ijk}^{[2]} I_{ijk}^{D+2} \right\} + \sum_{i < < j} \left\{ C_{ij}^{[0]} I_{ij}^D + \frac{D-4}{2} C_{ij}^{[2]} I_{ij}^{D+2} \right\} + \sum_i C_i I_i^D
 \end{aligned} \tag{2.65}$$

where \tilde{C}_{ijklm} and \tilde{C}_{ijkl} are modifications on the respective coefficients brought about by the shift identities, an explicit expression can be found in equations 3.11 and 3.12 of [30]. In this expression we identify several higher-dimensional contributions that disappear in the $D = 4$ limit due to the vanishing of their numerical coefficients. These correspond to none other than the *rational terms* that are missed in the strictly four-dimensional calculation.

2.3 Master Integral Identities

In general, a Master Integral (MI) decomposition is not unique, and there exists more than one set of MIs capable of representing the original amplitude.

Whenever a Feynman amplitude is to be decomposed it becomes desirable to have the result as simple and compact as possible, in particular the final set of MIs should be the smallest and the easiest to evaluate that one can reach given the amplitude.

This is hard to accomplish *a priori*, but can be made easier by some remarkable properties of Feynman Integrals in Dimensional Regularisation. These integrals are a slightly more general version of 2.46:

$$I_{ij\dots n}(x_1 \dots x_{\mathcal{K}}) = \int d^D \bar{q} \frac{S_1 \dots S_q}{\bar{D}_i \bar{D}_j \dots \bar{D}_n} \tag{2.66}$$

where:

- the set of quantities $\{S_i\}$ represents the *Irreducible scalar products* (ISP) of the particular topology, that is, the particular scalar kinematic quantities that cannot be written in terms of the denominators that define the sector and simplified against them¹⁴. We say there are q distinct terms, counting in also all the powers they can be raised to compatibly with rank restrictions;
- The variables $\mathbf{x} := \{x_1 \dots x_{\mathcal{K}}\}$ are the kinematic invariants that parametrise the integral as a whole (such as the particles' masses or the Mandelstam invariants s, t), they depend in turn on the external momenta of the Feynman amplitude p_i ;

2.3.1 Lorentz invariance identities

Scalar MIs such as those reached with Passarino-Veltman decomposition will be invariant under Lorentz transformations, such as the following rotation of the external four-momenta:

¹⁴In chapter 4 we show how a generic collection of scalar products can be parametrised and simplified against the denominators, leaving behind the ISPs.

$$p_i^\mu \rightarrow p_i^\mu + \delta p_i^\mu = p_i^\mu + \delta \omega^{\mu\nu} p_{i\nu} \quad (2.67)$$

where $\delta \omega^{\mu\nu}$ is the anti-symmetric infinitesimal Lorentz transformation tensor. Let us now impose the invariance of a scalar integral such as 2.66 and manipulate the left-hand side:

$$I_{ij\dots n}(p_i + \delta p_i) = I_{ij\dots n}(p_i)$$

$$I_{ij\dots n}(p_i + \delta p_i) = I_{ij\dots n}(p_i) + \sum_j \delta \omega^{\mu\nu} \left(p_j^\nu \frac{\partial}{\partial p_j^\mu} \right) I_{ij\dots n}(p_i) \equiv I_{ij\dots n}(p_i)$$

this, plus the anti-symmetry of the tensor $\delta \omega^{\mu\nu}$, results in the following identity:

$$\sum_j \left(p_j^\nu \frac{\partial}{\partial p_j^\mu} - p_j^\mu \frac{\partial}{\partial p_j^\nu} \right) I_{ij\dots n}(p_i) = 0 \quad (2.68)$$

Contracting this relation with all the possible anti-symmetric tensors $p_i^\mu p_j^\nu$ constructed from the $n - 1$ independent external momenta, it is possible to obtain $(n - 1)(n - 2)$ *Lorentz-invariance identities* (LI).

Let us show this in the case of four-point scalar box integrals, where one has only three independent momenta:

$$\begin{aligned} (p_1^\mu p_2^\nu - p_2^\mu p_1^\nu) \sum_j \left(p_j^\nu \frac{\partial}{\partial p_j^\mu} - p_j^\mu \frac{\partial}{\partial p_j^\nu} \right) I_{ij\dots n}(p_i) & \begin{array}{c} p_2 \quad p_3 \\ \diagdown \quad \diagup \\ \text{---} \quad \text{---} \\ \diagup \quad \diagdown \\ p_1 \quad p_4 \end{array} = 0 \\ (p_1^\mu p_3^\nu - p_3^\mu p_1^\nu) \sum_j \left(p_j^\nu \frac{\partial}{\partial p_j^\mu} - p_j^\mu \frac{\partial}{\partial p_j^\nu} \right) I_{ij\dots n}(p_i) & \begin{array}{c} p_2 \quad p_3 \\ \diagdown \quad \diagup \\ \text{---} \quad \text{---} \\ \diagup \quad \diagdown \\ p_1 \quad p_4 \end{array} = 0 \\ (p_2^\mu p_3^\nu - p_3^\mu p_2^\nu) \sum_j \left(p_j^\nu \frac{\partial}{\partial p_j^\mu} - p_j^\mu \frac{\partial}{\partial p_j^\nu} \right) I_{ij\dots n}(p_i) & \begin{array}{c} p_2 \quad p_3 \\ \diagdown \quad \diagup \\ \text{---} \quad \text{---} \\ \diagup \quad \diagdown \\ p_1 \quad p_4 \end{array} = 0 \end{aligned} \quad (2.69)$$

differentiating the scalar integrals with respect to the external momenta will raise the power of the denominators in question and create new terms at the numerator, which depend on the momenta and may be tensors. Some of these terms can be re-written in terms of the denominators and simplified, leaving behind ISP terms that give in turn new scalar integrals: the result is an identity between integrals of different topologies.

2.3.2 Integration-by-parts identities

These identities, first recognised in the eighties [127], are a consequence of the validity of Gauss's integral theorem in D dimensions. An integral of the type 2.66 is regularised and the dimensional parameter D is continuous, therefore one can assume safely that it is convergent at the boundary of the domain of the loop momentum.

If this is true then the *integrand* has to vanish at the very same boundary, at least rapidly enough to ensure the overall integral converges. As a consequence, when integrating 2.46 by parts, no boundary

term can be generated.

Gauss's theorem expresses these facts as the vanishing of the following divergence integral:

$$I_{ij\dots n} = \int d^D \bar{q} \frac{\partial}{\partial q^\mu} \left[\frac{v_i^\mu}{\bar{D}_i \bar{D}_j \dots \bar{D}_n} \right] \quad (2.70)$$

where $\frac{\partial}{\partial q^\mu}$ could in fact be a derivative with respect to any loop momentum if several were present, and v_i^μ could be any of the independent four-momenta under advisement: $\{q_1, \dots, q_l, p_1, \dots, p_{n-1}\}$. This operation will once again alter the power of the denominators and generate scalar product terms at the numerator, which can be written in terms of the denominators themselves and simplified. The resulting *Integration-by-parts Identity* (IBP) is then a relation between different scalar integrals, that may correspond to some integral present in the MI decomposition or be completely novel; regardless, a total of $l(l+n-1)$ such identities can be generated for each scalar integral at hand.

A few examples

Let us first consider a scalar tadpole integral, the simplest Feynman integral conceivable. We drop the bar notation for clarity:

$$\int d^D q \frac{1}{(q^2 - m^2)} = \int d^D q \frac{1}{D_0} \quad (2.71)$$

The only independent momentum available is q^μ itself, using $\partial_\mu D_0 = 2q_\mu$ we obtain:

$$0 = \int d^D q \frac{\partial}{\partial q^\mu} \left[\frac{q^\mu}{D_0} \right] = \int d^D q \left[\frac{D}{D_0} - \frac{2q^2}{D_0^2} \right] = \int d^D q \left[\frac{D-2}{D_0} + \frac{2m^2}{D_0^2} \right] \quad (2.72)$$

which entails an IBP identity between the two tadpole integrals:

$$\int d^D q \frac{1}{D_0^2} = -\frac{D-2}{2m^2} \int d^D q \frac{1}{D_0} \quad (2.73)$$

$$\text{---} \bigcirc \text{---} = -\frac{D-2}{2m^2} \text{---} \bigcirc \text{---}$$

we represented the IBP diagrammatically by defining a dotted internal line as meaning a squared denominator, and by representing a massive propagator with a thick line.

Let us now consider a scalar bubble:

$$\int d^D q \frac{1}{(q^2) \left((q-p)^2 - m^2 \right)} = \int d^D q \frac{1}{D_1 D_2} \quad (2.74)$$

This case is more involved as there are two denominators to be differentiated and two independent vectors q^μ, p^μ . Choosing $v^\mu = q^\mu$ and skipping through the calculations one gets:

$$0 = \int d^D q \frac{D-3}{D_1 D_2} - \int d^D q \frac{1}{D_2} = \int d^D q \frac{D-3}{D_1 D_2} - \int d^D q \frac{1}{D_0} \quad (2.75)$$

where the last integral was written in terms of the tadpole of the previous example by applying a loop momentum shift: $q \rightarrow q + p$.

Using the previous IBP we define a new identity, and write it down diagrammatically:

$$\int d^D q \frac{1}{D_1 D_2} = -\frac{D-2}{D-3} \frac{1}{2m^2} \int d^D q \frac{1}{D_0} \quad (2.76)$$

$$\text{---} \bigcirc \text{---} = -\frac{D-2}{D-3} \frac{1}{2m^2} \text{---} \bigcirc \text{---}$$

These examples make it clear how it is possible not only to reduce a set of Master Integrals into a subset of *truly independent* MIs, but how some of these integrals are of a simpler topology than the starting ones, which simplifies the overall result.

In a more realistic case, with several integrals up to boxes, the identities become ever more complex and involve many integrals at once. The generation of IBP identities suitable to be applied to any given case can be done automatically using the *Laporta algorithm* [18] which has been implemented in several software suites which generate the IBP and LI identities, identify the integrals which yield the simplest and most compact end result and calculate the substitution rules by solving the system of identities for those integrals. Two examples of implementation of the Laporta algorithm are KIRA [19] and REDUZE [20].

2.4 Evaluating Master Integrals with Differential Equations

After the decomposition onto Master Integrals has been obtained and optimised through the aforementioned identities, the final step is to tackle the problem of their calculation. In a similar way to what we did to derive IBPs, it is possible to generate sets of *Differential Equations* satisfied by the MIs that can be solved to obtain an expression for the integral itself. This concept first appeared in [21] and later extended to more general Differential Equation in any set of Mandelstam variables in [22].

Let us start once again from an integral of the form 2.66 and write down the following:

$$p_j^\mu \frac{\partial}{\partial p_k^\mu} I_{ij\dots n}(\mathbf{x}) \quad (2.77)$$

where p_i^μ is one of the $n-1$ independent external momenta. The integral is expressed in terms of the invariants \mathbf{x} , using the chain rule this becomes:

$$p_j^\mu \sum_{x \in \mathbf{x}} \frac{\partial x}{\partial p_k^\mu} \partial_x I_{ij\dots n}(\mathbf{x}) = \sum_{x \in \mathbf{x}} \left(p_j^\mu \cdot \frac{\partial x}{\partial p_k^\mu} \right) \partial_x I_{ij\dots n}(\mathbf{x}) \quad (2.78)$$

The quantity in parentheses can be written out explicitly knowing the ISPs of the topology, and the result is a differential equation for the integral I:

$$\sum_{x \in \mathbf{x}} \left(p_j^\mu \cdot \frac{\partial x}{\partial p_k^\mu} \right) \partial_x I_{ij\dots n}(\mathbf{x}) = p_j^\mu \frac{\partial}{\partial p_k^\mu} I_{ij\dots n}(\mathbf{x}) \quad (2.79)$$

If $I(\mathbf{x})$ is a Master Integral, its differentiation with respect to the external momenta will produce several different integrals all belonging to the same topology (since the powers of the denominators can only rise or stay the same). These integrals can all be related to the MIs of that particular topology by means of known IBP and LI identities.

The result is a system of first-order inhomogeneous differential equations between the Master Integrals and their sub-topologies, of the form:

$$\partial_x I_j(\mathbf{x}) = \sum_k A_k I_k(\mathbf{x}) + \sum_m B_m I'_m(\mathbf{x}) \quad (2.80)$$

where $\partial_x \equiv \frac{\partial}{\partial x}$ for $x \in \mathbf{x}$, I' are the MIs of the sub-topologies of I and A_k, B_k are rational coefficients. If we re-define I as a vector that includes all independent MIs and related sub-topologies (let us say their number is \mathcal{N}), we can re-write the system compactly as a matrix system of differential equations:

$$\partial_x I(\mathbf{x}, D) = \mathbb{M}_x(\mathbf{x}, D) I(\mathbf{x}, D) \quad (2.81)$$

where each \mathbb{M}_x is a $\mathcal{N} \times \mathcal{N}$ matrix.

Let us clarify a few points. First, the matrices $\mathbb{M}_l(\mathbf{x}, \varepsilon)$ are in general *block-triangular*: IBP and LI identities between MIs, as we saw, can send an integral into integrals of the same topology or, at most, a sub-topology (This is because differentiation will never be able to generate a new denominator term). The differential equations for a 1-pt MI will thus involve only 1-pt integrals, while 2-pt integrals may be related to 1- and 2-pt integrals and so on, until the largest MI of the topology. The matrix is thus organised in blocks for each distinct sector, and each block is triangular to reflect the structuring of the sub-topologies. It is worth mentioning that they still have rational entries at this stage.

Then, in 2.81 we made explicit the D -dependence of the MIs since this system is exact in generic D space-time dimensions. Ideally this is the condition in which one would solve the system, but in practical applications one works with $D = 4 - 2\varepsilon$, in order to be able to take the limit $D \rightarrow 4$. The system is thus re-written in terms of the ε parameter:

$$\partial_x I(\mathbf{x}, \varepsilon) = \mathbb{M}_x(\mathbf{x}, \varepsilon) I(\mathbf{x}, \varepsilon) \quad (2.82)$$

enabling one to expand the basis of MIs in powers of ε :

$$I_j(\mathbf{x}, \varepsilon) = \sum_k I_j^k(\mathbf{x}) \varepsilon^k \quad (2.83)$$

The DE system is now in the series coefficients $I_j^k(\mathbf{x})$, and its solution is made simpler since the ε -dependence is decoupled. Additionally one can stop before obtaining the full series since one is often only interested in the $D \rightarrow 4$ limit. Moreover, this would be in general a *Laurent series* but it can be turned into a simpler *Taylor series* by choosing appropriate normalisations for the MIs that ensure good convergence properties of the series coefficients.

There exist automatic codes that are able to generate systems of Differential Equations given an input list of Master Integrals. Amongst these a great tool is the software suite REDUZE [20] which (as mentioned) is also capable of reducing a set of scalar integrals onto a Master Integral basis via the generation and use of IBP relations, and then to set up the system of DEs to be solved separately.

2.4.1 Differential equations in canonical form

Finding a solution to the system is strongly dependent on the form of the matrices involved and their dependency on both the kinematic variables and ε . First, one can always simplify the ε part by expanding the MIs in power series and considering the Differential Equation order-by-order. Then, in case of triangular systems, it is possible to determine each MI starting from the equation with just a single matrix element and using methods such as *Euler's variation of constants*, and then proceeding in a *bottom-up* fashion re-cycling the previous solutions.

In the more general case of a non-triangular system of DEs the way forward is to find a suitable transformation matrix capable of transforming the system in a triangular one. In other words, the goal is to find a matrix $\mathbb{B}(x, \varepsilon)$ defined as:

$$I(x, \varepsilon) = \mathbb{B}(x, \varepsilon) \tilde{I}(x, \varepsilon) \quad (2.84)$$

which, defining $\tilde{\mathbb{M}} = \mathbb{B}^{-1}(x, \varepsilon) [\mathbb{M}(x, \varepsilon) \mathbb{B}(x, \varepsilon) - \partial_x \mathbb{B}(x, \varepsilon)]$, yields a new triangular system:

$$\partial_x \tilde{I}(x, \varepsilon) = \tilde{\mathbb{M}}(x, \varepsilon) \tilde{I}(x, \varepsilon) + S(x, \varepsilon) \quad (2.85)$$

Once again this change of basis exploits the fact that, while the number of MIs and the sectors are generally determined by the problem, the actual set of MIs is not unique.

It is possible to simplify even further the process of finding a solution by imposing a few more restrictions on the form of the DE system. In particular we wish to obtain a system of DEs in the so-called *ε -factorised form* [23]:

$$\partial_x I(x, \varepsilon) = \varepsilon \mathbb{M}_x(x) I(x, \varepsilon) + S(x, \varepsilon) \quad (2.86)$$

The immediate advantage of this factorisation is that, expanding in powers of ε , the DEs only couple the k th order coefficient to the $(k-1)$ -th:

$$\partial_x I^k(x) = \mathbb{M}_x(x) I^{k-1}(x) \quad (2.87)$$

therefore at any stage the DEs become homogeneous, in the $D \rightarrow 4$ limit (i.e. $\varepsilon \rightarrow 0$) they decouple altogether and the solutions are *constants*, that depend on the boundary condition:

$$\partial_x I^0(x) = 0 \implies I^0(x) \equiv I^0(x_0) \quad (2.88)$$

In the case of multiple invariants \mathbf{x} the ε -factorised DEs can be combined into a total differential equation:

$$dI(\mathbf{x}, \varepsilon) = \varepsilon d\mathbb{A}(\mathbf{x}) I(\mathbf{x}, \varepsilon) \quad (2.89)$$

with $\partial_x \mathbb{A}(\mathbf{x}) = \mathbb{M}_x(\mathbf{x})$. Expanding once again in powers of ε :

$$dI^k(\mathbf{x}) = d\mathbb{A}(\mathbf{x})I^{k-1}(\mathbf{x}) \quad (2.90)$$

which is formally trivial to solve and can be written as an *iterated integral* along a path γ in \mathbf{x} space:

$$I^k(\mathbf{x}) = \int d\mathbb{M}^{k-1}(\mathbf{x}) = \int \underbrace{d\mathbb{M} \dots d\mathbb{M}}_{k \text{ times}} I^0(\mathbf{x}_0) \quad (2.91)$$

If we re-package the ε -expansion using these expressions for the coefficients the solution becomes:

$$I(\mathbf{x}, \varepsilon) = \exp \left[\varepsilon \int d\mathbb{A} \right] I(\mathbf{x}_0, \varepsilon) \quad (2.92)$$

This template of solution is so far quite formal. To move towards a practical, iterative method of finding a general solution is it convenient to assume that the matrix $d\mathbb{A}(\mathbf{x})$ only possesses, in any of its entries, *simple poles* in the variables \mathbf{x} , and to this end the kinematic variables may be re-defined, shifted or rescaled.

The poles will be of the form $\frac{1}{\eta_i}$ where η_i is any combination of the kinematic variables that yields a simple pole. These quantities will form the kernel of the iterated integration, as we shall see, and if the simple-poles condition is satisfied then the matrix $d\mathbb{M}(\mathbf{x})$ is in the so-called *dlog* form since, upon integration, the simple poles give rise to logarithms:

$$\mathbb{A}(\mathbf{x}) = \sum_{i=1}^k \mathbb{M}_i \log \eta_i(\mathbf{x}) \quad (2.93)$$

In this expression the new matrices \mathbb{M}_i are constant and related to each η_i , known as *letters* of an *alphabet* that defined the Differential Equation.

To summarise, one usually seeks DE systems that satisfy two requirements:

- The ε dependency can be factorised from the dependence on \mathbf{x} within the system's matrices $d\mathbb{M}(\mathbf{x})$;
- The factorised matrices $d\mathbb{M}(\mathbf{x})$ only have simple poles, and can then be cast in dlog form

In this case one say that the system is in so-called *Canonical form* [23] and its solution can be computed relatively easily through a *Dyson series* of iterated integrals, as we will see.

The first major hurdle is then to find the basis transformation \mathbb{B} applied to the MI basis that can bring the system in canonical form. There exist several ways to accomplish this, such as the *Magnus exponential method* [128] which can be applied to a special class of DE systems and which we describe next.

2.4.2 The Magnus exponential method

Let us consider a system of Master Integral DEs in a single kinematic variable x and seek to bring it in canonical form. Let us assume for the moment that the matrix \mathbb{M} in 2.82 is *linear* in ε , allowing one to write the system in the following simple form:

$$\partial_x I(x, \varepsilon) = [\mathbb{M}^0(x) + \varepsilon \mathbb{M}^1(x)] I(x, \varepsilon) \quad (2.94)$$

Let us now perform the change of basis 2.84 and choose $\mathbb{B}(x)$ such that it constitutes a *matrix solution* of the DE system at $\varepsilon = 0$:

$$\partial_x \mathbb{B}(x) = \mathbb{M}^0(x) \mathbb{B}(x) \quad (2.95)$$

The change of basis has the effect of absorbing the ε -independent term, rendering the DE system at once simpler and ε -factorised:

$$\partial_x \tilde{I}(x, \varepsilon) = \varepsilon [\mathbb{B}^{-1}(x) \mathbb{M}^1(x) \mathbb{B}(x)] \tilde{I}(x, \varepsilon) := \varepsilon \tilde{\mathbb{M}}^1(x) \tilde{I}(x, \varepsilon) \quad (2.96)$$

The problem is then to solve 2.95 for \mathbb{B} , which is difficult in general. In [128] the solution was written as a *Magnus exponential* [24]:

$$\mathbb{B}(x) = e^{\Omega[\mathbb{M}^0](x)} = \mathbb{1} + \Omega[\mathbb{M}^0](x) + \frac{1}{2!} \Omega[\mathbb{M}^0](x) \Omega[\mathbb{M}^0](x) + \dots \quad (2.97)$$

the linear operator Ω is itself given as the infinite sum:

$$\Omega[\mathbb{M}^0](x) = \sum_{i=0}^{+\infty} \Omega_i[\mathbb{M}^0](x) \quad (2.98)$$

where each summand is an iterated integral of nested commutators of the kernel \mathbb{M}^0 , the first three terms being:

$$\begin{aligned} \Omega_1[\mathbb{M}^0](x) &= \int_{x_0}^x d\tau_1 \mathbb{M}^0(\tau_1) \\ \Omega_2[\mathbb{M}^0](x) &= \frac{1}{2} \int_{x_0}^x d\tau_1 \int_{x_0}^{\tau_1} d\tau_2 [\mathbb{M}^0(\tau_1), \mathbb{M}^0(\tau_2)] \\ \Omega_3[\mathbb{M}^0](x) &= \frac{1}{6} \int_{x_0}^x d\tau_1 \int_{x_0}^{\tau_1} d\tau_2 \int_{x_0}^{\tau_2} d\tau_3 [\mathbb{M}^0(\tau_1), [\mathbb{M}^0(\tau_2), \mathbb{M}^0(\tau_3)]] + [\mathbb{M}^0(\tau_3), [\mathbb{M}^0(\tau_2), \mathbb{M}^0(\tau_1)]] \end{aligned}$$

This representation is useful since, usually, the nested commutators vanish after a number of steps and thus the iteration is truncated.

The Magnus exponential can be put to practical use with the following procedure:

1. First we re-label the system's matrix:

$$\mathbb{M}(x, \varepsilon) \equiv \mathbb{M}_{(0)}(x, \varepsilon) = \mathbb{M}_{(0)}^0(x) + \varepsilon \mathbb{M}_{(0)}^1(x) \quad (2.99)$$

and we split $\mathbb{M}_{(0)}^0(x)$ in its diagonal and off-diagonal parts:

$$\mathbb{M}_{(0)}^0 = \mathbb{D}_{(0)}^0 + \mathbb{N}_{(0)}^0 \quad (2.100)$$

2. we define a first change-of-basis matrix \mathbb{B}_1 using just the diagonal part of the system matrix:

$$\mathbb{B}_1 = e^{\Omega[\mathbb{D}_{(0)}^0]} = e^{\int_{x_0}^x d\tau_1 \mathbb{D}_{(0)}^0(\tau_1)} \quad (2.101)$$

since diagonal matrices commute with their integral the nested commutators all vanish and only the first term survives. The transformed system matrix $\mathbb{M}_{(1)}$ is then:

$$\mathbb{M}_{(1)} := \mathbb{B}_1^{-1} [\mathbb{M}_{(0)} \mathbb{B}_1 - \partial_x \mathbb{B}_1] \quad (2.102)$$

This transformation absorbs away the diagonal part $\mathbb{D}_{(1)}^0$, since a diagonal matrix commutes with its integral:

$$\mathbb{D}_{(1)}^0 = \mathbb{B}_1^{-1} [\mathbb{D}_{(0)}^0 \mathbb{B}_1 - \partial_x \mathbb{B}_1] = \mathbb{B}_1^{-1} \mathbb{B}_1 [\mathbb{D}_{(0)}^0 - \mathbb{D}_{(0)}^0] = 0 \quad (2.103)$$

thus the ε -free part of $\mathbb{M}_{(1)}^0$ is fully non-diagonal i.e.:

$$\mathbb{M}_{(1)}^0 \equiv \mathbb{N}_{(1)}^0 \quad (2.104)$$

3. We rotate away this term with a second Magnus transformation:

$$\begin{aligned} \mathbb{B}_2 &= e^{\Omega[\mathbb{N}_{(1)}^0]} = e^{\int_{x_0}^x d\tau_1 \mathbb{N}_{(1)}^0(\tau_1)} \\ \mathbb{M}_{(2)} &:= \mathbb{B}_2^{-1} [\mathbb{M}_{(1)} \mathbb{B}_2 - \partial_x \mathbb{B}_2] \longrightarrow \mathbb{M}_{(2)}^0 = 0 \rightarrow \mathbb{M}_{(2)}^0 = \mathbb{B}_2^{-1} [\mathbb{N}_{(1)}^0 \mathbb{B}_2 - \mathbb{B}_2 \mathbb{N}_{(1)}^0] \end{aligned} \quad (2.105)$$

This might not actually be doable in a single rotation as the kernel $\mathbb{N}_{(1)}^0$ does not commute with its own integral, but the leftover commutator may itself be rotated away, leaving behind nested commutators and so on until the leftover commutators vanish (which they generally do after a number of steps).

Therefore the matrix transformation that casts the system in the ε -factorised form 2.96 is $\mathbb{B} = \mathbb{B}_1 \mathbb{B}_2$.

To handle the case of multiple kinematic variables $\mathbf{x} = \{x_i\}$, $i = 1 \dots \mathcal{K}$, step 2 is done once on the first system with matrix $\mathbb{M}_{x_1(0)}$ and then repeated for each of the \mathcal{K} systems, compounding the Magnus transformations at each step. The same is done for step 3, and the final transformation \mathbb{B} is then the product of $2\mathcal{K}$ Magnus exponentials.

The Magnus exponential can bring an ε -linear system in ε -factorised form, but says nothing about how to find the linear system in the first place. No general method to achieve this form is available, in practice this is done by trial and error using knowledge acquired through experience (i.e. that certain classes of Master Integrals instead of others will yield this form), using IBP and LI identities to reach a convenient MI basis and even rescaling some MIs by ε . Regardless of the methods employed, finding an ε -linear system has proven possible in most known cases, and much easier than finding an ε -factorised system right away without resorting to the Magnus method.

Still in [128] a strategy was laid out to apply the Magnus exponential method to DE systems which are *polynomial* in ε .

2.4.3 General solution via Iterated Integrals

Let us write down a generic canonical system of Differential Equations:

$$dI(\mathbf{x}, \varepsilon) = \varepsilon d\mathbb{A}(\mathbf{x})I(\mathbf{x}, \varepsilon) \quad (2.106)$$

We saw how the formal solution to this system can be written as a matrix exponential:

$$I(\mathbf{x}, \varepsilon) = \exp \left[\varepsilon \int_{\gamma} d\mathbb{A} \right] I(\mathbf{x}_0, \varepsilon) \quad (2.107)$$

This solution can be expanded as a *Dyson series*, which we write down for a single variable x :

$$I(x, \varepsilon) = \left\{ \mathbb{1} + \varepsilon \int^x dt_1 d\mathbb{A}(t_1) + \varepsilon^2 \int^x dt_1 d\mathbb{A}(t_1) \int_1^t dt_2 d\mathbb{A}(t_2) + \dots \right\} I(\mathbf{x}, \varepsilon) \quad (2.108)$$

where $I(x_0, \varepsilon)$ is a vector of boundary conditions to be fixed.

It is easy to prove that this is a solution by plugging it into equation 2.106 and examining it order-by-order in ε :

$$\begin{aligned} \varepsilon \partial_x \int^x dt_1 d\mathbb{A}(t_1) &= \varepsilon d\mathbb{A}(x) = \varepsilon d\mathbb{A}(x) \times \mathbb{1} \\ \varepsilon^2 \partial_x \int^x dt_1 d\mathbb{A}(t_1) \int_1^t dt_2 d\mathbb{A}(t_2) &= \varepsilon^2 d\mathbb{A}(x) \int^x dt_1 d\mathbb{A}(t_1) = \varepsilon d\mathbb{A}(x) \times \varepsilon \int^x dt_1 d\mathbb{A}(t_1) \end{aligned} \quad (2.109)$$

where we simplified the boundary conditions for simplicity.

Let us now assume two kinematic variables $\mathbf{x} = \{x, y\}$, we will then have two system matrices $\mathbb{M}_{x,y} = \mathbb{M}_{x,y}(x, y)$. For this reason, a general solution as a series in ε cannot be written straight away for both variables as they are coupled at nearly all orders. The only viable way is to construct a solution order-by-order in ε^k :

$$I(x, y, \varepsilon) = \{ B^0 + \varepsilon B^1(x, y) + \varepsilon^2 B^2(x, y) + \dots \} I(\mathbf{x}, \varepsilon) \quad (2.110)$$

- **k=0** The presence of ε factorised means that the solution at this order is simply a constant, we define it $B^0 := \mathbb{1}$.
- **k=1** We first integrate the \mathbb{M}_x system in x , which produces a function of y as a constant term:

$$B^1(x, y) = \int^x dt \mathbb{M}_x(t, y) + C^1(y) \quad (2.111)$$

and just like before one can verify that this satisfied the DE for x at this order in ε . We now plug it into the y equation and pick order ε :

$$\varepsilon \partial_y \left[\int^x dt \mathbb{M}_x(t, y) + C^1(y) \right] = \varepsilon \mathbb{M}_y(x, y) \times B^0 (= \mathbb{1}) \quad (2.112)$$

from which one determines the C function by integrating:

$$\partial_y C^1(y) = \mathbb{M}_y(x, y) - \partial_y \int^x dt \mathbb{M}_x(t, y) \quad (2.113)$$

- **generic k** By plugging in the general solution and extracting the k -th power of ε one finds:

$$\partial_{x,y} B^k(x, y) = \mathbb{M}_{x,y} B^{k-1}(x, y) \quad (2.114)$$

once again we integrate first in the x variable:

$$B^k(x, y) = \int^x dt \mathbb{M}_x(t, y) B^{k-1}(t, y) + C^k(y) \quad (2.115)$$

and, similarly as before, we plug this in the y equation at order k and extract the constant term

$$\partial_y C^k(y) = \mathbb{M}_y(x, y) B^{k-1}(x, y) - \partial_y \int^x dt \mathbb{M}_x(t, y) B^{k-1}(t, y) \quad (2.116)$$

By iterating these steps one can formally find the solution at any desired order in ε , although it is customary to stop after only a few orders since, for the sake of physical calculations, one is usually interested in the limit $\varepsilon \rightarrow 0$.

Generalised Polylogarithms (GPLs)

This procedure entails repeated integrations of the matrices \mathbb{M}_x in all their variables. At this point we recall that systems in canonical basis are cast in dlog-form:

$$\mathbb{A}(\mathbf{x}) = \sum_{i=1}^k \mathbb{A}_i \log \eta_i(\mathbf{x}) \quad \Leftrightarrow \quad \mathbb{M}(\mathbf{x}) = d\mathbb{A}(\mathbf{x}) = \sum_{i=1}^k \mathbb{M}_i \frac{1}{\eta_i(\mathbf{x})} \quad (2.117)$$

The *letters of the alphabet* $\eta_i(\mathbf{x})$ encapsulate all the difficulty in performing the iterated integrals. For the sake of this discussion we assume that the alphabet is *rational*:

$$\eta_i(\mathbf{x}) = \prod_{x_j \in \mathbf{x}} (x_j - \omega_j) \quad (2.118)$$

where each letter is factored with respect to each kinematic variable and a weight ω , that can depend on all \mathbf{x} variables except x_j .

In this case the iterated integration structure can be expressed using *Goncharov (or Generalised) PolyLogarithms (GPLs)* [25], defined as follows:

$$G(\{\omega_1, \omega_2, \dots, \omega_n\}, x_j) = \int^x dt \frac{1}{t - \omega_1} G(\{\omega_2, \dots, \omega_n\}, t) \quad (2.119)$$

$$G(\{0_n\}, x_j) = \frac{1}{n!} \log^n(x_j) \quad (2.120)$$

where the number of weights n is the *weight of the GPL* and corresponds to the number of iterated integrations over x that define it.

When one is dealing with a system of DEs cast as in [**dlog form**], it is easy to implement the strategy described in the previous section, as integrating the system's matrices simply involves acting on the letters $\eta_i(\mathbf{x})$ appearing therein while the matrices \mathbb{M}_i keep track of where they contribute in the system. In the iterated solution, at order $k > 1$ in ε , after the first integration in x_1 one will need to compute all the "constant terms" in the variables $x_i \neq x_1$ by differentiation, and thus one will require the derivative of a GPL with respect to one of its weights. Without detailing the derivation we give the result [129]:

$$\begin{aligned} \frac{\partial}{\partial x_i} G(\{\vec{\omega}(x_i)\}, x_j) &= \left(-\frac{\partial \omega_k}{\partial x_i} \right) \times \\ &\times \left[\left(\frac{1}{\omega_k - \omega_{k-1}} \right) (G(\{\omega_1, \dots, \cancel{\omega}_k, \dots, \omega_n\}, x_j)) - G(\{\omega_1, \dots, \omega_{k-1}, \dots, \omega_n\}, x_j) \right. \\ &\left. + \left(\frac{1}{\omega_{k+1} - \omega_k} \right) (G(\{\omega_1, \dots, \cancel{\omega}_k, \dots, \omega_n\}, x_j) - G(\{\omega_1, \dots, \omega_{k+1}, \dots, \omega_n\}, x_j)) \right] \end{aligned} \quad (2.121)$$

this formula is of course extendible to the case of multiple weights depending on x_i .

Boundary conditions

The general solution, up to order ε^k , is only partially complete without the vector of *boundary conditions* $I(\mathbf{x}_0, \varepsilon)$, which contains the value of each Master Integral at the base integration kinematic point \mathbf{x}_0 . Usually the vector is itself written as a power series in ε :

$$I(\mathbf{x}_0, \varepsilon) = \sum_{k=0} I_0^k \varepsilon^k \quad (2.122)$$

where the highest order should be consistent with the order in ε chosen for the general solution; this leaves each of the values I_0^k to be determined, usually one MI at a time. The simplest way to do this is to determine the value of the full solution at special kinematic points and fix the constants accordingly, perhaps via direct integration if possible. An alternative approach is to impose a "physical" regularity condition for the solution at special kinematic points. Since often we deal with canonical systems built via a Magnus rotation, some kinematic factors yielding unphysical singularities may be introduced in the canonical solution, while they were not featured in the original set of MIs. Imposing that the canonical solution is also regular at those *pseudo-thresholds* can provide a way to fix the boundary conditions (that contribute to the canonical solution, not to the original one).

This is not always viable as, sometimes, the Magnus exponential introduces proper *thresholds*, that is, singularities of the DE coefficients that are also physical singularities of the original integral. In this case a way forward may be to exploit the differential equation for the MI under advisement: if one of the coefficients in the DE provides a pseudo-threshold (a kinematic point where we know the integral is regular while the coefficient diverges) this can be removed by re-scaling the canonical MI by the inverse of this coefficient. The regularity of the re-scaled integral at the pseudo-threshold can then be used to fix the boundary conditions order-by-order in ε .

We illustrated a few practical techniques often used but this is by no means an exhaustive treatment on the determination of Boundary conditions. This should serve to convey that, despite fixing a single value of the solution is in principle far easier than computing the full solution, the process is a tricky and delicate one and, consequently, a single unified method is not currently available.

Chapter 3

Unitarity methods for one-loop amplitudes

This chapter is dedicated to discussing a set of properties that Feynman amplitudes satisfy which all descent from the so-called *Optical Theorem*. These properties give rise to some powerful techniques for calculating Feynman amplitudes, which can be used to obtain scalar-integral decompositions in an efficient and algorithmic way.

3.1 Unitarity and the Optical Theorem

In Quantum Mechanics the key object which governs the transitions between particle states and their temporal evolution is the $S(t)$ operator.

We shall focus on the *unitarity* property of this operator, which is heuristically related to the notion that the probabilities of all possible outcomes of the evolution should add up to one.

More specifically, let us define with $|i\rangle$ the state of particles initially present. The particles in this state will interact and the state as a whole will evolve according to the rules of the theory at hand. We are interested in the probability that this state evolves in a particular final state $|f\rangle$ as a result of the interactions. To compute this we define the evolved state $|OUT(t)\rangle = S(t)|i\rangle$, project this onto the final state and square:

$$P(i, f) = |\langle f|OUT(t)\rangle|^2 = |\langle f|S(t)|i\rangle|^2 = \langle i|S^\dagger|f\rangle \langle f|S|i\rangle$$

Let us now consider $\{|f\rangle\}$, the subset of our Fock space encompassing all possible outcomes of the interaction. Logically, summing $|f\rangle$ over this set entails considering all possible outcomes at once and thus the probability must be one. Therefore:

$$1 = \sum_{|f\rangle \in \{|f\rangle\}} \langle i|S^\dagger|f\rangle \langle f|S|i\rangle = \langle i|S^\dagger S|i\rangle$$

where we used the completeness of the set of final states.

Assuming $\langle i|i\rangle = 1$ i.e. that the initial state is properly normalised, this entails $S^\dagger S = 1$ i.e. the S operator is unitary. This can also be derived by expressing S as a time-evolution operator: $S(t) = e^{-iHt}$, and recalling that H is observable and thus hermitian.

In Quantum Field Theory the S operator is replaced with the S -matrix which cannot be expressed as simply as in quantum mechanics, and is instead computed in perturbation theory as a Taylor-like series of terms.

We will therefore write:

$$S = \mathbb{1} + iT \quad (3.1)$$

The identity matrix represents the trivial evolution of a state into itself at a later point in space-time, i.e. no interaction. T is known as *transfer matrix* and represents instead all the non-trivial contributions to the evolution of a state into another. Unitarity gives us the following result:

$$\mathbb{1} = S^+ S = \mathbb{1} + i(T - T^+) + T^+ T \quad \implies \quad i(T^+ - T) = T^+ T \quad (3.2)$$

To understand the significance of this result we consider once again initial and final states $|i\rangle, |f\rangle$ and compute the non-trivial transition matrix element between these. The l.h.s gives:

$$i\langle f | (T^+ - T) | i \rangle = i(\langle i | T | f \rangle)^* - i\langle f | T | i \rangle$$

while on the r.h.s we insert a complete set of intermediate states $|x\rangle$:

$$\begin{aligned} \mathbb{1} &= \sum_x \int d\Pi_x |x\rangle \langle x| \\ d\Pi_x &= \prod_{j \in f} \frac{d^3 p_j}{(2\pi)^3} \frac{1}{2E_j} \end{aligned}$$

obtaining:

$$T^+ T = \sum_x \int d\Pi_x \langle f | T^+ | x \rangle \langle x | T | i \rangle \quad (3.3)$$

We now write out the transfer matrix element in momentum space in terms of the so-called *Feynman amplitude*:

$$\langle b | T | a \rangle = (2\pi)^4 \delta^{(4)}(p_b - p_a) \mathcal{M}(a \rightarrow b)$$

and use it to re-write both sides of 3.2:

$$(2\pi)^4 \delta^{(4)}(p_f - p_i) (\mathcal{M}(f \rightarrow i)^* - \mathcal{M}(i \rightarrow f)) = \quad (3.4)$$

$$= \sum_x \int d\Pi_x (2\pi)^8 \delta^{(4)}(p_f - p_x) \delta^{(4)}(p_x - p_i) \mathcal{M}(f \rightarrow x)^* \mathcal{M}(i \rightarrow x) \quad (3.5)$$

We turned equation 3.2, which was an identity between transfer matrix elements, into a relation between Feynman amplitudes which is known as the (*generalised*) *Optical Theorem*:

$$2\text{Im}[\mathcal{M}(i \rightarrow f)] = \sum_x \int d\Pi_x (2\pi)^4 \delta^{(4)}(p_x - p_i) \mathcal{M}(f \rightarrow x)^* \mathcal{M}(i \rightarrow x) \quad (3.6)$$

which can be represented pictorially:

$$2\text{Im} \left[\langle i | \text{---} \text{---} \text{---} \text{---} \text{---} | f \rangle \right] = \sum_x \int d\Pi_x (2\pi)^4 \delta^{(4)}(p_x - p_i) \left[\langle i | \text{---} \text{---} \text{---} \text{---} \text{---} | x \rangle \right] \left[\langle x | \text{---} \text{---} \text{---} \text{---} \text{---} | f \rangle \right] \quad (3.7)$$

In greater detail, we related the imaginary part of a Feynman amplitude to a product of tree-level amplitudes, each corresponding to a diagram involving intermediate particle states. Remarkably, this is also a relation between amplitudes at different orders of perturbation theory, as the order of the l.h.s. of 3.6 must be higher than the intermediate amplitudes comprising the r.h.s by simple power-counting.

This, as well as the theorem as a whole, holds true at all orders of perturbation theory.

It is easy to notice that, in order for 3.6 to be physically sensible, we need the intermediate lines $|x\rangle$ to actually behave as external lines, i.e. we need the corresponding Feynman propagators to be *on-shell*. On a related note, let us take a look at the structure of a Feynman propagator:

$$\frac{1}{(p_k^2 - m_k^2 + i\varepsilon)} = \frac{p_k^2 - m_k^2 - i\varepsilon}{((p_k^2 - m_k^2)^2 + \varepsilon^2)}$$

$$\text{Im} \left[\frac{1}{(p_k^2 - m_k^2 + i\varepsilon)} \right] = \frac{-\varepsilon}{((p_k^2 - m_k^2)^2 + \varepsilon^2)}$$

As $\varepsilon \rightarrow 0$, the imaginary part vanishes except when $p^2 = m^2$, i.e. when the propagator lies exactly on-shell. This is obviously similar to the behaviour of $\delta(p_k^2 - m_k^2)$.

A 1-loop amplitude can be constructed as a complex analytical function of a complex variable s , taken as the square of the centre-of-mass energy of a process. As we saw, the imaginary part of such a function entails a constraint on its internal lines, corresponding to the energy threshold s_0 for the on-shell production of the lightest intermediate particles, in analogy to a decay process. Should the threshold not be met, i.e. $s < s_0$, then none of the intermediate states can be put on-shell and therefore the amplitude is fully real.

The Feynman amplitude, by construction, can be analytically continued everywhere on the complex plane of s via the *Schwarz reflection principle* for a complex function of a complex variable:

$$A^*(s) = A(s^*)$$

which entails in turn, for $s \in \mathbb{R}$, $s \geq s_0$:

$$2i\text{Im}[A(s)] = A(s) - A^*(s) = A(s) - A(s^*)$$

And, immediately:

$$\begin{aligned} \text{Re}[A(s + i\epsilon)] &= \text{Re}[A(s + i\epsilon)] \\ \text{Im}[A(s + i\epsilon)] &= -\text{Im}[A(s - i\epsilon)] \end{aligned}$$

Therefore, from the threshold s_0 and above, we have a discontinuity between the upper and lower halves of the plane, defining thus a so-called *branch cut* of the amplitude.

The key take-aways from this discussion, which are important for the remainder of the chapter, are:

- that the discontinuity across the branches of an amplitude can be identified with imaginary part of the amplitude itself;
- that, by the Optical theorem, the imaginary part of an amplitude can be obtained by considering all possible ways in which the amplitude can be "severed" into two tree-level-like amplitudes;
- that the severing, or *cutting* of an amplitude corresponds to placing internal lines on-shell;

3.2 Unitary cuts

In [1] Cutkosky presented a re-formulation of equation 3.6 which explicitly shows the on-shellness of the internal lines, as well as paving the way to make practical use of the generalised optical theorem.

Let us focus on the r.h.s. of 3.6, and consider the case of the intermediate state $|x\rangle$ being in fact a multi-particle state, without loss of generality. The term $d\Pi_x \delta^{(4)}(p_x - p_i)$ can be re-written as:

$$d\Pi_x \delta^{(4)}(p_x - p_i) = \frac{d^3 p_1 \dots d^3 p_l}{(2\pi)^{3l} 2E_1 \dots 2E_l} \delta^{(4)}\left(\sum_{j=1}^l p_j - p_i\right) = \frac{d^3 p_1 \dots d^3 p_{l-1}}{(2\pi)^{3l} 2E_1 \dots 2E_l} \delta\left(\sum_{j=1}^l p_j^0 - E_i\right) \quad (3.8)$$

where the δ^3 was used to collapse one of the 3-momentum integrations, leaving behind a δ over the energy components of the 4-momenta. As previously stated, all particles in the intermediate state $|x\rangle$ are on-shell, therefore one could insert terms like $\delta(p_j^0 - E_j)$, $j = 0, \dots, l - 1$ without changing the overall integral:

$$d\Pi_x \delta^{(4)}(p_x - p_i) = \frac{d^3 p_1 \dots d^3 p_{l-1}}{(2\pi)^{3l}} \frac{\delta(p_1^0 - E_1)}{2E_1} \dots \frac{\delta(p_{l-1}^0 - E_{l-1})}{2E_{l-1}} \frac{\delta\left(\sum_{j=1}^l p_j^0 - E_i\right)}{2E_l} \quad (3.9)$$

We intentionally gathered these new deltas over the $2E_j$ terms since these can be re-written using the remarkable property of Dirac deltas:

$$\sum_{x_j / f(x_j)=0} \frac{\delta(x - x_j)}{f'(x_j)} = \delta(f(x)) \quad (3.10)$$

where the function $f(E_j)$ would be $E_j^2 - (p_j^2 - m_j^2)$ in the rest frame of the particle, with an added $\Theta(p_j^0)$ in order to pick the positive-energy solution.

By taking overall momentum conservation into account, the same substitution can be applied to the last delta as well, obtaining:

$$\begin{aligned} d\Pi_x \delta^{(4)}(p_x - p_i) &= \frac{d^3 p_1 \dots d^3 p_{l-1}}{(2\pi)^{3l}} (p_1^2 - m_1^2) \Theta(p_1^0) \dots (p_l^2 - m_l^2) \Theta(p_l^0) \\ &= \frac{d^3 p_1 \dots d^3 p_{l-1}}{(2\pi)^{3l}} \sum_{j \in |x\rangle} (p_j^2 - m_j^2) \Theta(p_j^0) \end{aligned} \quad (3.11)$$

Thus we obtain a sum of delta functions of inverse propagators $(p_j^2 - m_j^2)$, which runs over all the intermediate particles within $|x\rangle$. This rewriting of the optical theorem highlights how the previously-mentioned on-shellness of the internal particles is automatically encoded in the formalism, and not a mere observation.

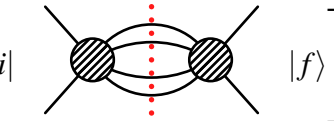
This also suggests that placing internal lines on-shell can be used as a tool to extract the imaginary part of any loop amplitude. This important operation is known as *cutting* the corresponding line, and the Cutkosky procedure provides a way to do this in practice [1]:

- Find all the possible ways to *completely* sever a loop amplitude in two, by placing internal lines on-shell without violating momentum conservation.
- Perform the cut by means of the *Cutkosky replacement rule*:

$$\frac{1}{(p_j^2 - m_j^2 + i\varepsilon)} \longrightarrow (-2\pi i) \delta(p_j^2 - m_j^2) \Theta(p_j^0) = (-2\pi i) \delta^{(+)}(p_j^2 - m_j^2) \quad (3.12)$$

- Extract the imaginary part of the loop amplitude by summing over all cut diagrams as per the generalised optical theorem

This procedure is represented pictorially in equation 3.13, where the cuts are indicated by a dashed line crossing the propagators being cut. The two portions would be tree-level diagrams in case of a 1-loop amplitude, but generally they would be more elaborate and containing loops. In 3.13 the two blobs represent the sum of all possible diagrams connecting the initial (final, respectively) external lines with the internal ones being cut, on a cut-by-cut basis.

$$2Im[\mathcal{M}_{loop}] = \sum_{cuts} \left[\langle i | \text{diagram} | f \rangle \right] \quad (3.13)$$


Two comments are in order. First, the Cutkosky rule is valid only for the cutting of scalar lines. In general, one needs to write the particle's propagator in the "Klein-Gordon" form i.e. by highlighting the $\frac{1}{(p_j^2 - m_j^2)}$ term. Whatever tensor structure (encoding spin or polarisation configurations) was spoiled in the process will appear at the numerator of the propagator, and will be present as a multiplicative factor in the replacement rule.

Second, due to the presence of $\Theta(p_j^0)$, the cuts depend on the direction of momentum flow through the cut line, they are thus directional.

3.3 The Feynman Tree Theorem

So far we have used the term "loop amplitude" rather loosely: it turns out that the procedure described is applicable to a 1-loop amplitude being cut into a sum of tree-level ones.

The unitarity procedure can, however, be taken a step further and used to relate tree-level amplitude to generic amplitudes at *any* loop level. The following discussion follows chapter 2 of [130].

A bit of polology

Let us consider the following integral:

$$\int dx \frac{f(x)}{x - x_0} \quad (3.14)$$

It is not immediately clear how to deal with the divergence at the pole $x = x_0$. One possible procedure entails the analytical continuation of the variable x to the complex plane. Complex integrals are performed as contour integrals, in this case the contour would be shaped like a semi-circle where the base corresponds to the integral over the real x -axis, while the circle part is taken at $|x| = +\infty$. Since this contour intersects the pole x_0 , one could deform the contour to avoid it, but it is easier to shift the pole by a small amount ε along the imaginary axis:

$$\int dx \frac{f(x)}{x - x_0 \pm i\varepsilon} \quad (3.15)$$

Figure 3.1 is a representation of the two possibilities:

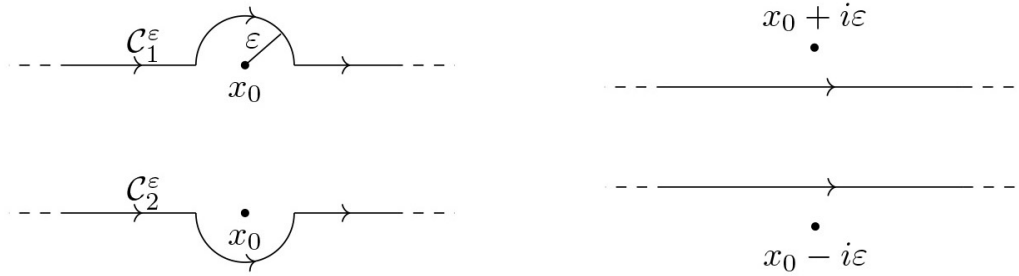


Figure 3.1: Different prescription for regulating complex integrals. Left is the deformation of the integration contour on the plane. Right is the pole shift along the imaginary axis.

The $i\varepsilon$ prescription is the one adopted to regulate the mass pole for Feynman propagators in the coordinate representation.

Depending on which half of the complex plane the circle at infinity lies in, shifting the pole up or down will entail a difference. From Cauchy's Residue theorem this is exactly the residue of the integrand, which in this case is the value of f at the pole x_0 :

$$\int dx \frac{f(x)}{x - x_0 + i\varepsilon} = \int dx \frac{f(x)}{x - x_0 - i\varepsilon} + 2\pi i f(x_0) \quad (3.16)$$

which can be written as:

$$\begin{aligned} \int dx f(x) \left[\frac{1}{x-x_0+i\epsilon} \right] &= \int dx f(x) \left[\frac{1}{x-x_0-i\epsilon} + 2\pi i \delta(x-x_0) \right] \\ \Rightarrow \frac{1}{x-x_0+i\epsilon} &= \frac{1}{x-x_0-i\epsilon} + 2\pi i \delta(x-x_0) \end{aligned} \quad (3.17)$$

This last equation provides a way to switch between one method of regulating simple poles to another, by means of the residue theorem.

We now move on to considering Feynman propagators, themselves possessing simple poles lying at the mass of the particle:

$$\Pi_F(p) = \frac{i}{q^2 - m^2 + i\epsilon} = \frac{i}{(p^0)^2 - \omega_q^2 + i\epsilon} = \frac{i}{(p^0 - \omega_p + i\epsilon)(p^0 + \omega_p - i\epsilon)} \quad (3.18)$$

where we put ourselves in the particle's rest frame. Let us also define the *advanced* Feynman propagator:

$$\Pi_A(p) = \frac{i}{(p^0 - \omega_q + i\epsilon)(p^0 + \omega_p + i\epsilon)} \quad (3.19)$$

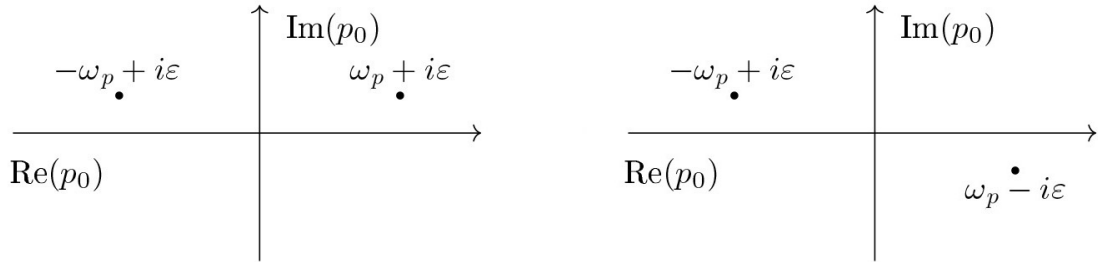


Figure 3.2: Pole placement for the Feynman propagator (right) and the advanced propagator (left)

It should now come natural to write down a relation between the two propagators like equation 3.17:

$$\begin{aligned} \Pi_A(q) &= \frac{i}{(p^0 + \omega_p + i\epsilon)(p^0 - \omega_q + i\epsilon)} = \frac{i}{(p^0 + \omega_p + i\epsilon)} \left[\frac{1}{(p^0 - \omega_p - i\epsilon)} + 2\pi i \delta(p^0 - \omega_p) \right] = \\ &= \Pi_F(p) - 2\pi \frac{\delta(p^0 - \omega_p)}{2\omega_p} = \Pi_F(p) - 2\pi \delta(q^2 - m^2) \Theta(p^0) \end{aligned} \quad (3.20)$$

where in the second line we took $p^0 = \omega_p$ and then used 3.10 once again. We thus arrive at:

$$\Pi_A(p) = \Pi_F(p) - 2\pi \delta^{(+)}(p^2 - m^2) \quad (3.21)$$

Let us now consider the following integral:

$$\int \frac{d^4 q}{(2\pi)^4} \Pi_A(p-q) \Pi_A(p) = 0 \quad (3.22)$$

This integral is computed by analytical-continuation in the complex plane of q^0 , and we recall that it is up to us to choose how to define the integration contour. The two advanced propagators, as we have seen, both have poles lying entirely in the upper half of the complex plane. If we then choose to close the contour in the *bottom* half of the plane, which we always can, then this integral trivially vanishes. However, by plugging in 3.21:

$$\begin{aligned} & \int \frac{d^4 q}{(2\pi)^4} \Pi_A(p-q) \Pi_A(p) \\ = & \int \frac{d^4 q}{(2\pi)^4} \left[\Pi_F(p-q) - 2\pi\delta^{(+)}\left((p-q)^2 - m^2\right) \right] \left[\Pi_F(p) - 2\pi\delta^{(+)}(p^2 - m^2) \right] \\ = & \int \frac{d^4 q}{(2\pi)^4} \left[\Pi_F(p-q) \Pi_F(p) - 2\pi\delta^{(+)}\left((p-q)^2 - m^2\right) \Pi_F(p) - \right. \\ & \left. - 2\pi\delta^{(+)}(p^2 - m^2) \Pi_F(p-q) + (2\pi)^2 \delta^{(+)}\left((p-q)^2 - m^2\right) \delta^{(+)}(p^2 - m^2) \right] = 0 \end{aligned} \quad (3.23)$$

from which:

$$\begin{aligned} & \int \frac{d^4 q}{(2\pi)^4} \Pi_F(p-q) \Pi_F(p) = \\ & \int \frac{d^4 q}{(2\pi)^4} \left[2\pi\delta^{(+)}\left((p-q)^2 - m^2\right) \Pi_F(p) + 2\pi\delta^{(+)}(p^2 - m^2) \Pi_F(p-q) - \right. \\ & \left. - (2\pi)^2 \delta^{(+)}\left((p-q)^2 - m^2\right) \delta^{(+)}(p^2 - m^2) \right] \end{aligned} \quad (3.24)$$

These are scalar integrals containing Feynman denominators, and therefore can be interpreted as fully-fledged Feynman amplitudes. Moreover, in light of the Cutkosky rule, we can give a diagrammatic representation of this equation:

$$\text{circle} = \underbrace{\text{circle with 2 red dots}}_{\text{single cut}} + \underbrace{\text{circle with 3 red dots}}_{\text{double cut}} \quad (3.25)$$

Recalling that the complete cut of the amplitude, labelled "double cut" in 3.25, corresponded only to the imaginary part of the whole loop amplitude, equation 3.25 provides then a way to compute the *whole* amplitude in terms of cut amplitudes [28].

This is a remarkable result, especially since it generalises without issues to any amplitude of any complexity and loop order ¹⁵. The only difference would be the increased complexity, as more complex

¹⁵This comes because no matter how many advanced propagators we use to begin the argument, they would all have their poles in the upper half of the complex plane, and thus nothing would change logic-wise.

amplitudes can be cut multiple times and there are many ways to cut such amplitude once, twice etc. This result is known as *Feynman Tree Theorem*, let us briefly delve into the meaning behind this name. We have previously shown that a cut one-loop amplitude can be expressed as a sum of tree-level amplitudes, integrated over the phase-space of all¹⁶ the momenta flowing through the lines being cut. Heuristically, one could say that a l -loop amplitude can then be analogously expressed as a sum of at most $(l - 1)$ -loop amplitudes. These can then be further decomposed until only tree-level amplitudes make up the full expression, plus the phase space integrals.

A few final comments are in order:

- First, cutting an amplitude as per the Feynman Tree theorem may lead to a slightly different result than simply applying the Cutkosky rule, namely the arguments of the Θ -functions may differ. One should always recall that, while the Cutkosky replacement comes from the general principle of unitarity, the Tree theorem stems from the manipulation of a regularisation prescription and the result thus depends on the steps taken to obtain it.
- Let us now perform a single cut on a four-point box integral:


(3.26)

The application of a Cutkosky replacement on the cut denominator entails, of course, that said denominator disappears from the amplitude. Effectively a cut operation turns a box topology into a triangle diagram, which is one of its sub-topologies. This is effectively a *pinching* operation that "brings together" the two external legs adjacent to the cut propagator, as represented by the double-line flowing into the triangle vertex.

This also means that this new external line carries the sum of the four-momenta of the two former external lines; this is a direct consequence of the presence of the Dirac delta, plus momentum conservation which is preserved by the cut.

3.4 Multiple cuts and Generalised Unitarity

So far we have dealt with (one)-loop amplitudes in two different ways:

1. by decomposing the tensor integrals appearing therein onto a suitable basis of simpler integrals *à la* Passarino-Veltman;
2. by writing down a complicated loop amplitude as a sum of simpler amplitudes by cutting progressively more and more internal lines using the Cutkosky rule, as per the Feynman tree theorem;

The two techniques can be combined as the tree theorem is applicable even in the case of a 1-loop amplitude \mathcal{M}^{1-loop} which has already been manipulated with a reduction prescription such as Passarino-Veltman. Such amplitude will be expressed as a sum of MIs like equation 2.59 where the coefficients are rational functions of momentum variables.

Performing unitary cuts on a MI-decomposition then reduces to cutting the MIs themselves, leaving

¹⁶It is worth noting that these phase-space integrals arise exactly because the internal lines now behave like they were external, just like any ordinary tree-level amplitude. They are thus totally unrelated to the integration over the *loop momentum*, which is technically encompassed within the definition of the amplitude itself.

the coefficients alone. At each stage j propagators are cut, and the corresponding integrals that contain them will receive a Dirac δ from the Cutkosky rules, until all denominators in every integral have been cut.

There is one seemingly simple feature which will prove immensely useful shortly: by performing multiple unitary cuts of *some* internal Feynman propagators not all integrals appearing in the decomposition can survive. Naïvely, this happens because the insertion of Dirac δ s brought about by the Cutkosky rules kill off the integrals which do not have the correct denominators. This entails that the more cuts we perform, the more decomposition terms we rid ourselves from and the simpler each cut integral becomes.

Let us see this in action in a simple four-dimensional example: let a 1-loop amplitude be decomposed in the fashion of equation 2.59, which we re-iterate here:

$$\mathcal{M}_n^{1-loop} = \text{Sun} = \sum_a c_4^a \text{Box} + \sum_a c_3^a \text{Triangle} + \sum_a c_2^a \text{Bubble} + \sum_a c_1^a \text{Circle} \quad (3.27)$$

where we neglected the rational terms for simplicity. Let us now perform multiple cuts over this expression. We first cut a generic ξ denominator, then another one η , then ζ and finally χ :

$$\begin{aligned} \text{Sun} &= \sum_{\xi} c_4^{\xi} \text{Box} + \sum_{\xi} c_3^{\xi} \text{Triangle} + \sum_{\xi} c_2^{\xi} \text{Bubble} + c_1^{\xi} \text{Circle} \\ \text{Sun} &= \sum_{\xi\eta} c_4^{\xi\eta} \text{Box} + \sum_{\xi\eta} c_3^{\xi\eta} \text{Triangle} + c_2^{\xi\eta} \text{Bubble} \\ \text{Sun} &= \sum_{\xi\eta\zeta} c_4^{\xi\eta\zeta} \text{Box} + c_3^{\xi\eta\zeta} \text{Triangle} \\ \text{Sun} &= c_4^{\xi\eta\zeta\chi} \text{Box} \end{aligned} \quad (3.28)$$

It is evident that by cutting more internal lines fewer and fewer terms contribute to the full cut amplitude. At each stage the sums run over the cuts, and gather all the integrals of a certain topology which possess the precise denominators being cut. By what we argued, if one performs a j -cut then only *one single* j -point integral will survive.

In this sense, multiple unitary cuts act as *projectors*, since cutting an amplitude projects it onto the diagrams that are compatible with the multiple cut, while the rest are killed off by the cuts themselves. Cuts used in this way are known as *generalised* unitary cuts, and give rise to the scheme of *Generalised Unitarity* which takes advantage of this property to extract iteratively all coefficients.

One first performs a quadruple cut, all integrals with ≤ 3 denominators will vanish automatically, while only the box with exactly the denominators being cut survives, and it is then possible to extract its coefficient. By cycling through and cutting all combinations of four denominators one extracts all the box coefficients. One then moves down to the triple-cut level and, since all the box coefficients are known, it is possible to extract all triangles in the same way, and so on.

The Generalised Unitarity prescription thus creates a triangular system where in each equation a different coefficient is extracted, recycling the knowledge of all the previous ones, as shown in figure 3.29.

$$\begin{aligned}
 & \text{Circle} = c_4^{\xi\eta\zeta\chi} \text{Box} \xrightarrow{\text{extract}} c_4^{\xi\eta\zeta\chi} \\
 & \text{Circle} = \sum_{\xi\eta\zeta} c_4^{\xi\eta\zeta} \text{Box} + c_3^{\xi\eta\zeta} \text{Triangle} \xrightarrow{\text{extract}} c_3^{\xi\eta\zeta} \\
 & \text{Circle} = \sum_{\xi\eta} c_4^{\xi\eta} \text{Box} + \sum_{\xi\eta} c_3^{\xi\eta} \text{Triangle} + c_2^{\xi\eta} \text{Circle} \xrightarrow{\text{extract}} c_2^{\xi\eta} \\
 & \text{Circle} = \sum_{\xi} c_4^{\xi} \text{Box} + \sum_{\xi} c_3^{\xi} \text{Triangle} + \sum_{\xi} c_2^{\xi} \text{Circle} + c_1^{\xi} \text{Circle} \xrightarrow{\text{extract}} c_1^{\xi}
 \end{aligned}
 \tag{3.29}$$

This is just an outline of the method. To understand more precisely the tasks at hand at each step of the process, let us take a closer look at a quadruple cut of a scalar box integral:

$$I_4 = \int d^4 q \frac{1}{D_1 D_2 D_3 D_4} \tag{3.30}$$

We take the external particles as massless for simplicity, and we temporarily forgo the application of dimensional regularisation.

First, one parametrises the loop momentum q^μ using a four-momentum basis $\mathcal{E} = \{e_1, e_2, e_3, e_4\}$ as follows:

$$q^\mu = \sum_{i=1}^4 x_i e_i^\mu \quad (3.31)$$

For the basis we impose the following requirements:

$$\begin{aligned} e_i^2 &= 0 \\ (e_1 \cdot e_3) &= (e_1 \cdot e_4) = 0 \\ (e_2 \cdot e_3) &= (e_2 \cdot e_4) = 0 \\ (e_1 \cdot e_2) &= -(e_3 \cdot e_4) \end{aligned}$$

We shall use such a basis again later on, and we defer its explicit derivation to appendix A. Suffice it to say for the moment that the vectors $e_{1,2}$ are linear combinations of two of the independent external momenta, for instance $p_{1,2}$, which belong to the external legs bordering the inverse propagator D_i . Vectors $e_{3,4}$ are then constructed to be orthogonal to the previous two, in order to satisfy the criteria. As required by the Cutkosky rules, all four propagators need to be placed on-shell simultaneously by imposing $D_i = 0$, $i = 1 \dots 4$. Since all propagators contain the loop momentum, the on-shell conditions are actually four equations that constrain the four x_i parameters in the q^μ expansion. To find the solution, one first re-parametrises the inverse propagators in terms of the new variables:

$$\begin{aligned} D_1 &= q^2 = 2(x_1 x_2 - x_3 x_4) p_1 \cdot p_4 \\ D_2 &= (q + p_1)^2 = 2(x_1 x_2 - x_3 x_4 + x_2) p_1 \cdot p_4 \\ D_3 &= (q + p_1 + p_2)^2 = (q + P_{12})^2 = 2(x_1 x_2 - x_3 x_4) p_1 \cdot p_4 + 2(x_1 p_1 \cdot P_{12} + x_2 p_4 \cdot P_{12} + x_3 e_3 \cdot P_{12} + x_4 e_4 \cdot P_{12}) \\ D_4 &= (q - p_4)^2 = 2(x_1 x_2 - x_3 x_4 - x_1) p_1 \cdot p_4 \end{aligned}$$

where $P_{12} = (p_1 + p_2)$.

the same change of variables is performed upon the integration measure, yielding:

$$d^4 q = (p_1 \cdot p_4)^2 dx_1 dx_2 dx_3 dx_4 \quad (3.32)$$

It is possible to pack the four x_i variables into a single vector \vec{x} , and by the same token define the vector function $D = (D_1, D_2, D_3, D_4) = D(\vec{x}) : \mathbb{R}^4 \rightarrow \mathbb{R}^4$.

Then one can use the result:

$$\delta^{4(+)}(D(\vec{x})) = \sum_{\vec{x}_0 \in \text{Sol.}} \frac{1}{\left| \text{Det} \frac{\partial D_i}{\partial x_j} \right|_{\vec{x}=\vec{x}_0}} \delta^4(\vec{x} - \vec{x}_0) \quad (3.33)$$

which evidently comprises all four Cutkosky replacements at once. The presence of $\delta^4(\vec{x} - \vec{x}_0)$ makes the cut integral trivial to compute:

$$\begin{aligned} \text{Cut}_4 [I_4] &= (p_1 \cdot p_4)^2 \sum_{\vec{x}_0 \in \text{Sol.}} \frac{1}{\left| \text{Det} J_{ij} \right|_{\vec{x}=\vec{x}_0}} \\ \text{Det} J_{ij} &= \text{Det} \frac{\partial D_i}{\partial x_j} = 16(p_1 \cdot p_4) [x_3 e_3 \cdot P_{12} - x_4 e_4 \cdot P_{12}] \end{aligned} \quad (3.34)$$

One then needs to find all solutions to the cut conditions, compute the determinant on those and sum all results. One could prove that, for this simple case, there exist two such solutions. It is important to mention that, in general, the solution corresponds to a complex loop momentum.

To determine the box coefficient c_4 , however, one needs to compute the quadruple cut of A_n^{1-loop} present on the l.h.s. of the first line of 3.29. It is possible to re-cycle the first line of 3.34, since a quadruple cut of a one-loop diagram reduces it to the product of four tree-level amplitudes with all particles on-shell. I.e.

$$Cut_4 \left[\mathcal{M}_n^{1-loop} \right] = \text{Diagram} = \int d^4 \vec{x} (p_1 \cdot p_4)^2 \mathcal{M}_1^{tree} \mathcal{M}_2^{tree} \mathcal{M}_3^{tree} \mathcal{M}_4^{tree} \delta^{4(+)}(D(\vec{x}))$$

We recall that the internal denominators are not part of the tree-level amplitudes, as their external lines are treated as on-shell particles, thus the tree-level amplitudes are separate from the delta functions. This integral yields:

$$Cut_4 [I_4] = (p_1 \cdot p_4)^2 \sum_{\vec{x}_0 \in Sol.} \frac{A_1^{tree} A_2^{tree} A_3^{tree} A_4^{tree}}{|Det J_{ij}|} \Big|_{\vec{x}=\vec{x}_0} \quad (3.35)$$

$$Det J_{ij} = Det \frac{\partial D_i}{\partial x_j}$$

The coefficient can then be extracted immediately:

$$c_4 = \frac{Cut_4 \left[\mathcal{M}_n^{1-loop} \right]}{Cut_4 [I_4]} \quad (3.36)$$

since many factors in the expressions of both cut quantities match, the final expression is simply dependent on the tree-level amplitudes, evaluated at all solutions of the cut conditions.

Since we are cutting at amplitude level this term may encompass an arbitrary number of diagrams to be cut, depending on the theory at hand. Luckily, in some cases, symmetry relations originating from either the kinematics or the group properties of the theory may simplify the computation of the cut integrals to just a few distinct calculations.

The subsequent steps are more involved for several reasons: first, the cut conditions are no longer sufficient to fully constrain the loop momentum, and thus after the application of the cutting rules some of loop momentum parameters are left over as variables, which need to be integrated upon.

Moreover it is not immediately trivial how to separate the contribution from the higher-point coefficients extracted previously from the amplitude under examination. For instance, in the case of a triple cut, one expects a triangle contribution (in fact, a *single* triangle per every cut configuration) plus box contributions that share the propagators being cut, which correspond to triangles with a vertex

split open into a new internal line. This is true for all the lower cuts, and at each step separating the pure triangle, bubble and tadpole contributions from the rest is the only way to isolate the coefficient. Finally, this is repeated for every possible permutation of four, three, two or one denominators being cut, and every coefficient is extracted.

In [35] the different contributions to the triangle were separated by treating the integration over the leftover parameter t as a complex integral along some contour in the complex plane; by employing partial-fractioning techniques the integrand is split into terms containing the residues of the poles at finite t and terms at $t = +\infty$, as it was realised that the former contributed to all the boxes and therefore the latter had to correspond to the triangle.

Generalised D -dimensional Unitarity

Restricting the integral decomposition to four dimensions, as we saw in section 2.2.2, means that rational terms will be missed from the expansion, therefore it is desirable to perform the full decomposition and cutting procedure in D -dimensions. On the other hand, the various diagrams that comprise an amplitude produce tree-level amplitudes that ought to be computed to determine the coefficients. Historically, Generalised Unitarity was employed to perform NLO calculations in Quantum Chromodynamics (QCD) in preparation for the high-energy experiments to be carried out at the Large Hadron Collider. Within this framework the most compact and efficient way to compute tree-level Feynman amplitudes is to use the Spinor-Helicity formalism (described in chapter 6.2), which does not extend well to D -dimensions [35]

To generalise the method from $D = 4$ dimensions to generic D , one first needs some method to extract the μ dependence from the coefficients, as evidenced in 2.63. The D -dimensional loop momentum can be written as:

$$\bar{q}^2 = q^2 - \mu^2 = 0 \tag{3.37}$$

$$\implies q^2 = \mu^2 \tag{3.38}$$

i.e. treating the D -dimensional loop momentum as massless is formally equivalent to replacing the momentum with a four-momentum with mass μ^2 . This effectively corresponds to assigning a uniform mass to all internal lines. This procedure was used in [26, 27] within the framework of Generalised Unitarity.

Next, the cut conditions are solved using the fictitious μ^2 mass parameter in the same fashion as the four-dimensional case, and the cut integrals are performed splitting the D -dimensional measure as in 2.23. The μ^2 variable itself is treated as complex, and since the denominators themselves are now μ -dependent one can study the pole structure of the integrand and extract contributions coming from the rational terms, using the same techniques employed for the loop variables for the lower-cut integrals.

Methods such as these were employed in the handling of quadruple [29, 30], triple [30–32], double [33, 34] and single [35–37] cut integrals for Generalised Unitarity within the framework of Dimensional Regularisation.

Chapter 4

Integrand-level Decomposition methods

Computing cut integrals and separating the contributions to the cut amplitude from boxes, triangles, bubbles and tadpoles to extract the decomposition coefficients, as prescribed by Generalised Unitarity, proved a difficult task, requiring the development of advanced theoretical techniques and lengthy calculations.

The fact that the integral coefficients are rational functions of kinematic invariants and the external momenta spurred new research towards purely algebraic procedures that can bypass any integration.

This chapter is devoted to introducing techniques applied at the *integrand* level, in 4-dimensions at first, that enable the reconstruction of the cut-constructible terms of a generic amplitude in an efficient way. This method is based on two key ideas [41]:

- studying the most general *polynomial* structure of the integrand in the kinematic and loop variables;
- studying the pole structure of the integrand itself when evaluated numerically at a phase-space point corresponding to one of the cut solutions (that place all propagators on-shell);

These novel techniques are still built upon the key result developed in section 2.2: that any n-point 1-loop integral with a tensor structure can be decomposed onto a basis of scalar Master Integrals:

$$\mathcal{M}_n^{1-loop} \int d^4q \mathcal{M}(q) = \sum_{i < < l} \int d^4q \frac{c_{4,0}^{ijkl}}{D_i D_j D_k D_l} + \sum_{i < < k} \int d^4q \frac{c_{3,0}^{ijk}}{D_i D_j D_k} + \sum_{i < j} \frac{c_{2,0}^{ij}}{D_i D_j} + \sum_i \int d^4q \frac{c_{1,0}^i}{D_i} \quad (4.1)$$

which can be rewritten more compactly using the compact notation for the master integrals of equation 2.46:

$$\int d^4q A(q) = \sum_{i < < l} c_{4,0}^{ijkl} I_{ijkl} + \sum_{i < < k} c_0^{ijk} I_{ijk} + \sum_{i < j} c_{2,0}^{ij} I_{ij} + \sum_i c_{1,0}^i I_i \quad (4.2)$$

we recall that this expression is valid in $D = 4$ dimensions.

4.1 The OPP decomposition method

One of the first *Integrand Decomposition Methods* was formulated by Ossola, Papadopoulos and Pittau in [38, 39] and later expanded in [40, 44]; this technique is known today as the OPP method.

In this description of the procedure we shall follow the formalism of [4, 42].

The first step is to obtain an *integrand*-level equivalent of equation 4.2. If we naïvely drop the integral sign we neglect all the integration constants coming from each of the scalar integrals, therefore spoiling the equality:

$$\mathcal{M}_n(q) \neq \sum_{i < < l} \frac{c_{4,0}^{ijkl}}{D_i D_j D_k D_l} + \sum_{i < < k} \frac{c_0^{ijk}}{D_i D_j D_k} + \sum_{i < j} \frac{c_{2,0}^{ij}}{D_i D_j} + \sum_i \frac{c_{1,0}^i}{D_i}$$

We could, however, introduce ad-hoc functions $f_{ijk\dots}^s(q)$ which restore the integrand-level equality:

$$\mathcal{M}_n(q) = \sum_{i < < l} \frac{c_{4,0}^{ijkl} + f_{ijkl}^s}{D_i D_j D_k D_l} + \sum_{i < < k} \frac{c_0^{ijk} + f_{ijk}^s}{D_i D_j D_k} + \sum_{i < j} \frac{c_{2,0}^{ij} + f_{ij}^s}{D_i D_j} + \sum_i \frac{c_{1,0}^i + f_i^s}{D_i}$$

these functions define the so-called *spurious terms*, which should vanish upon integrating over the loop momentum to recover 2.58:

$$\frac{f_{ijk\dots}^s(q)}{D_i D_j D_k \dots} \implies \int d^4 q \frac{f_{ijk\dots}^s(q)}{D_i D_j D_k \dots} = 0$$

we can package all terms at each numerator into a single quantity $\Delta_{ijk\dots}(q)$:

$$\mathcal{M}_n(q) = \sum_{i < < l} \frac{\Delta_{ijkl}}{D_i D_j D_k D_l} + \sum_{i < < k} \frac{\Delta_{ijk}}{D_i D_j D_k} + \sum_{i < j} \frac{\Delta_{ij}}{D_i D_j} + \sum_i \frac{\Delta_i}{D_i} \quad (4.3)$$

We have thus promoted the loop-integral expression for an n-point amplitude into an integrand-level one. As evident, this expansion is in fact a multi-particle pole expansion of the amplitude's integrand, as placing any of the virtual particles on their mass-shell means computing the amplitude right on a pole of the integrand function.

If we now multiply 4.3 by all the propagators $D_i D_j D_k \dots$ we obtain:

$$N_n(q) := \sum_{i < < l} \Delta_{ijkl} \prod_{\eta \neq i,j,k,l} D_\eta + \sum_{i < < k} \Delta_{ijk} \prod_{\eta \neq i,j,k} D_\eta + \sum_{i < j} \Delta_{ij} \prod_{\eta \neq i,j} D_\eta + \sum_i \Delta_i \prod_{\eta \neq i} D_\eta \quad (4.4)$$

From this we can see that, by putting the internal propagators on-shell by applying unitary cuts, the $\Delta_{ijk\dots}$ quantities are none other than the residues of the complex integrand function computed at the poles defined by the cuts themselves.

The OPP method is essentially a machinery to extract all the Δ s recursively. We first perform a four-fold cut on the box diagram and set $D_{i,j,k,l} = D_l \equiv 0$; only the term corresponding to the box residue survives:

$$N_n(q) = \sum_{i < < l} \Delta_{ijkl} \prod_{\eta \neq i,j,k,l} D_\eta$$

$$\Delta_{ijkl} = \text{Res}_{(ijkl)} \left[\frac{N_n(q)}{D_1 \dots D_n} \right]$$

And it is now apparent how Δ_{ijkl} is the residue of the diagram after placing the i, j, k, l propagators on-shell. This way it's possible to extract all the box residues, the number of which depends on how

many box diagrams appear in the original decomposition. Next we place only $D_{i,j,k} = 0$, two terms now survive, but knowing all the Δ_{ijkl} s from the previous cuts we isolate the next residue:

$$N_n(q) - \sum_{i < < l} \Delta_{ijkl} \prod_{\eta \neq i,j,k,l} D_\eta = \sum_{i < < k} \Delta_{ijk} \prod_{\eta \neq i,j,k} D_\eta$$

$$\Delta_{ijk} = \text{Res}_{(ijkl)} \left[\frac{N_n(q)}{D_1 \dots D_n} - \sum_{i < < l} \frac{\Delta_{ijkl}}{D_i D_j D_k D_l} \right]$$

By cutting twice and then only once, and subtracting all the previous steps, we isolate the last residues:

$$N_n(q) - \sum_{i < < l} \Delta_{ijkl} \prod_{\eta \neq i,j,k,l} D_\eta - \sum_{i < < k} \Delta_{ijk} \prod_{\eta \neq i,j,k} D_\eta = \sum_{i < j} \Delta_{ij} \prod_{\eta \neq i,j} D_\eta$$

$$\Delta_{ij} = \text{Res}_{(ijkl)} \left[\frac{N_n(q)}{D_1 \dots D_n} - \sum_{i < < l} \frac{\Delta_{ijkl}}{D_i D_j D_k D_l} - \sum_{i < < k} \frac{\Delta_{ijk}}{D_i D_j D_k} \right]$$

$$N_n(q) - \sum_{i < < l} \Delta_{ijkl} \prod_{\eta \neq i,j,k,l} D_\eta - \sum_{i < < k} \Delta_{ijk} \prod_{\eta \neq i,j,k} D_\eta - \sum_{i < j} \Delta_{ij} \prod_{\eta \neq i,j} D_\eta = \sum_i \Delta_i \prod_{\eta \neq i} D_\eta$$

$$\Delta_i = \text{Res}_{(ijkl)} \left[\frac{N_n(q)}{D_1 \dots D_n} - \sum_{i < < l} \frac{\Delta_{ijkl}}{D_i D_j D_k D_l} - \sum_{i < < k} \frac{\Delta_{ijk}}{D_i D_j D_k} - \sum_{i < j} \frac{\Delta_{ij}}{D_i D_j} \right]$$

The final system of equations that yield the residues is triangular:

$$\begin{aligned} \Delta_{ijkl} &= \text{Res}_{(ijkl)} \left[\frac{N_n(\bar{q})}{D_1 \dots D_n} \right] \\ \Delta_{ijk} &= \text{Res}_{(ijk)} \left[\frac{N_n(\bar{q})}{D_1 \dots D_n} - \sum_{i < < l} \frac{\Delta_{ijkl}}{D_i D_j D_k D_l} \right] \\ \Delta_{ij} &= \text{Res}_{(ij)} \left[\frac{N_n(\bar{q})}{D_1 \dots D_n} - \sum_{i < < l} \frac{\Delta_{ijkl}}{D_i D_j D_k D_l} - \sum_{i < < k} \frac{\Delta_{ijk}}{D_i D_j D_k} \right] \\ \Delta_i &= \text{Res}_{(i)} \left[\frac{N_n(\bar{q})}{D_1 \dots D_n} - \sum_{i < < l} \frac{\Delta_{ijkl}}{D_i D_j D_k D_l} - \sum_{i < < k} \frac{\Delta_{ijk}}{D_i D_j D_k} - \sum_{i < j} \frac{\Delta_{ij}}{D_i D_j} \right] \end{aligned} \quad (4.5)$$

and it shouldn't be surprising that it looks formally very similar to the one found at *amplitude level* in 3.29: generalised Unitarity is at the very core of both prescriptions. We will say more about how the coefficients are obtained in practice using these equations later on in this chapter.

4.1.1 Parametric expansion of the residues

First, we require an explicit way to compute the Δ s. This is done by parametrising the residues in terms of scalar products of loop-momenta and the independent external momenta with each other and constant terms such as the masses [4, 42, 49]. However, not all quantities constructed from such scalar products can appear in the parametrisation.

If any of the residues in 4.3 contains a term proportional to one of the inverse propagators in the same term (e.g. if Δ_{ijk} contained a term $\propto D_{i,j,k}$) then the inverse propagator would simplify with itself at the denominator, and the resulting term should actually contribute to the constant term in the parametrisation of the residue with one fewer denominator. We say that any object re-expressible in terms of some D_i is not an *Irreducible Scalar Product (ISP)* useful for the parametrisation.

By a similar token q^2 cannot appear in the parametrisation, for it can be written as:

$$q^2 = D_i + m_i^2 - r_i^2 - 2q \cdot r_i$$

and therefore the q^2 contribution splits into a contribution to another scalar product, a constant term and a constant term for the residue with one fewer denominator.

Moreover, the scalar products $(q \cdot p_i)$ are also decomposed as:

$$q \cdot p_i = q \cdot (r_i - r_{i-1}) \propto D_i - D_{i-1} + \text{const}$$

The way to find the valid ISPs is to parametrise the loop momentum q^μ in a convenient way, specifically onto a basis of four massless vectors $\{e_i^\mu\}$ constructed ad-hoc for each cut:

$$(q + p_i)^\mu = \frac{1}{(e_1 \cdot e_2)} (x_1 e_1^\mu + x_2 e_2^\mu + x_3 e_3^\mu + x_4 e_4^\mu) \quad (4.6)$$

The basis is very similar to the one employed in section 3.4 which, once again, is constructed in appendix A. We will just re-iterate the properties of such a basis:

$$\begin{aligned} e_i^2 &= 0 \\ (e_1 \cdot e_3) &= (e_1 \cdot e_4) = 0 \\ (e_2 \cdot e_3) &= (e_2 \cdot e_4) = 0 \\ (e_1 \cdot e_2) &= -(e_3 \cdot e_4) \end{aligned}$$

The ISPs will then be all the scalar products $(q \cdot e_i)$ and powers thereof, for all the e_i s *not* constructed from independent external momenta. Each power of an ISP entails a factor q^μ and since, once again, the rank of the numerator of the integrand should satisfy $r \leq n$, so should the powers of the ISPs in the parametric expansion.

The exact identity of the ISPs varies on a cut-by-cut basis and we will take a look at them separately.

Let us also notice that, thanks to the properties of the chosen basis:

$$(q \cdot e_1) = x_2 \quad (4.7)$$

$$(q \cdot e_2) = x_1 \quad (4.8)$$

$$(q \cdot e_3) = -x_4 \quad (4.9)$$

$$(q \cdot e_4) = -x_3 \quad (4.10)$$

showing that the x_i quantities are directly related to the ISPs themselves via projection. A parametrisation onto ISPs therefore is equivalent to a parametrisation onto polynomials of the x_i , as we can

write down formally:

$$N_n(q) = N_n(x_1, x_2, x_3, x_4) = \sum_{j_1, j_2, j_3, j_4} c_{j_1 j_2 j_3 j_4} x_1^{j_1} x_2^{j_2} x_3^{j_3} x_4^{j_4} \quad (4.11)$$

$$j_1 + j_2 + j_3 + j_4 \leq r_{max}$$

where r_{max} is the maximum allowed rank given the number of denominators of the integrand being reduced.

In appendix B we derive explicitly the most general parametrisation of the residues for the four, three, two and one-point loop integrals on the solution of their respective maximal cuts, using the aforementioned loop parametrisation and rank restrictions:

$$\begin{aligned} \Delta_{ijkl} &= c_{4,0} + c_{4,1}x_4 \\ \Delta_{ijk} &= c_{3,0} + c_{3,1}x_4 + c_{3,2}x_4^2 + c_{3,3}x_4^3 + c_{3,4}x_3 + c_{3,5}x_3^2 + c_{3,6}x_3^3 \\ \Delta_{ij} &= c_{2,0} + c_{2,1}x_1 + c_{2,2}x_1^2 - c_{2,3}x_4 + c_{2,4}x_4^2 - c_{2,5}x_3 + c_{2,6}x_3^2 - c_{2,7}x_1x_4 - c_{2,8}x_1x_3 \\ \Delta_i &= c_{1,0} + c_{1,1}x_1 - c_{1,2}x_2 - c_{1,3}x_3 - c_{1,4}x_4 \end{aligned} \quad (4.12)$$

Switching once again to integral level, only the $c_{j,0}$ coefficients survive within the residues, and thus we recover the scalar integral decomposition 4.2

Sampling the residues

Once the explicit form of the residues in term of the loop momentum parameters, we can trace the steps of the OPP procedure described above. At each step the residues are isolated by cutting a set number of propagators to be on shell, this operation creates a system of cutting equations whose solution constrains the x_i coefficients.

Once this is done, the cut integrand is evaluated several times, as many times as there are coefficients to be fixed, at different phase space points that are compatible with the solutions to the cutting equations. In the case of the box residue the cutting conditions are enough to fully constrain all four parameters, and as mentioned in the previous chapter there exist two solutions provided that we complexify the loop momentum. This enables us to sample twice the residue, and to use these two values to invert the parametric form of the box residue to extract the two coefficients $c_{4,0}$ and $c_{4,1}$. This procedure is known as *fit on the cut*.

Of course, in the case of lower cuts, there are not enough cutting equations to fully constrain the variables, one can only find relations between them. On the one hand this is convenient as the number of sampling to perform grows with the number of coefficients to be fixed, but this then calls for a systematic approach to choosing the sample points. An efficient way is the so-called *discrete Fourier Transform (DFT)* method, applied to the OPP algorithm in [41].

4.1.2 Extension to D dimensions

As we have seen for Passarino-Veltman decomposition, the OPP method can produce integrands which yield divergent integrals, and thus are regulated by switching to the D -dimensional picture.

This produces rational terms \mathcal{R}_1 and \mathcal{R}_2 as a result, which are missed in the four-dimensional derivation just like it occurs in Generalised Unitarity, these terms must then be written down by some other method to obtain a complete result. The \mathcal{R}_2 terms can be derived by introducing appropriate Feynman rules, while the \mathcal{R}_1 terms can be extracted by highlighting the μ^2 dependence in the OPP coefficients

with a mass shift: $m_i^2 \rightarrow m_i^2 - \mu^2$ [45]. These methods are also well-suited to be automatised, and have been implemented along with the OPP method in the public code CUTOOLS [3].

In [40, 43] the OPP method was re-formulated and extended into a full D -dimensional integrand decomposition method, allowing to determine the complete set of contributions at once. The first difference from the 4-dimensional case is the presence of the additional degrees of freedom in the loop momentum \bar{q}^μ given by the μ component. The kinematic quantities that parametrise the cut residues will now be of the form $(\bar{q} \cdot p_i)$ but, since the external momenta p_i are 4-dimensional, they are not capable of picking out the extra component (since the metric of our D -dimensional space is block-diagonal).

Therefore μ^2 is a completely independent quantity, and constitutes a new variable to be inserted in the parametrisation. Moreover, μ can only enter the parametrisation through \bar{q}^2 and thus only even powers of μ will be allowed.

This new parameter implies, in turn, that now at most *five* propagators can be placed on-shell simultaneously; in just four dimensions this system would have been over-constrained and hence we never considered a pentagon diagram in the decomposition. Equation 4.3 then becomes:

$$\mathcal{M}_n(\bar{q}) = \sum_{i < < m} \frac{\bar{\Delta}_{ijklm}}{\bar{D}_i \bar{D}_j \bar{D}_k \bar{D}_l \bar{D}_m} + \sum_{i < < l} \frac{\bar{\Delta}_{ijkl}}{\bar{D}_i \bar{D}_j \bar{D}_k \bar{D}_l} + \sum_{i < < k} \frac{\bar{\Delta}_{ijk}}{\bar{D}_i \bar{D}_j \bar{D}_k} + \sum_{i < j} \frac{\bar{\Delta}_{ij}}{\bar{D}_i \bar{D}_j} + \sum_i \frac{\bar{\Delta}_i}{\bar{D}_i} \quad (4.13)$$

The parametrisation of the residues is carried out in D -dimensions just as we have shown explicitly for the four-dimensional case. The result turns out to be [4, 40, 131]:

$$\begin{aligned} \bar{\Delta}_{ijklm} &= c_{5,0} \mu^2 \\ \bar{\Delta}_{ijkl} &= c_{4,0} + c_{4,1} x_{4,v} + \mu^2 (c_{4,2} + c_{4,3} x_{4,v} + \mu^2 c_{4,4}) \\ \bar{\Delta}_{ijk} &= c_{3,0} + c_{3,1} x_4 + c_{3,2} x_4^2 + c_{3,3} x_4^3 + c_{3,4} x_3 + c_{3,5} x_3^2 + c_{3,6} x_3^3 + \mu^2 (c_{3,7} + c_{3,8} x_4 + c_{3,9} x_3) \\ \bar{\Delta}_{ij} &= c_{2,0} + c_{2,1} x_1 + c_{2,2} x_1^2 - c_{2,3} x_4 + c_{2,4} x_4^2 - c_{2,5} x_3 + c_{2,6} x_3^2 - c_{2,7} x_1 x_4 - c_{2,8} x_1 x_3 + c_{2,9} \mu^2 \\ \bar{\Delta}_i &= c_{1,0} + c_{1,1} x_1 - c_{1,2} x_2 - c_{1,3} x_3 - c_{1,4} x_4 \end{aligned} \quad (4.14)$$

First, the tadpole residue cannot have any μ^2 dependence by rank restrictions, and therefore is identical to the 4-dimensional case.

We then point the reader's attention to the pentagon residue: by recycling some of the results of our four-dimensional calculations one could easily see that the only candidates for ISPs at this level would be a constant term plus μ^2 and μ^4 terms. However it was mentioned in the previous discussion on D -dimensional integral decomposition that at *integral* level these three contributions differ only by boxes and \bar{q} -independent terms. Still in [124] it was shown that the equivalence of the pentagon MIs translates at *integrand* level to an equivalence in the parametrisation of the cut residue between a constant and any term $(\mu^2)^\alpha$, for they can be related by reducible terms.

It is then a good choice to keep μ^2 as the single representative of this class of ISPs since this way the pentagon residues vanishes trivially in the 4-dimensional limit.¹⁷

By integrating equation 4.13 with the residue parametrised as above, and discarding all the spurious terms one obtains [4]:

¹⁷The reason for this is related to the aforementioned fact that in the $D \rightarrow 4 - 2\epsilon$ limit the pentagon integral is related to box functions. As it turns out, this gives rise to cancellations between all the boxes appearing in the MI expansion, which may lead to instabilities when evaluating numerically the results [124]. Parametrising the pentagon residue with μ^2 ensures the pentagon vanishes in this limit, while still being an advantageous parametrisation for identifying the lower-point residues.

$$\begin{aligned}
 \mathcal{M}_n &= \int d^D q \mathcal{M}(\bar{q}) = \\
 &= \sum_{i < < l} \left\{ \tilde{c}_{4,0} I_{ijkl}^D - \frac{D-4}{2} c_{4,2} I_{ijkl}^{D+2} + \frac{(D-4)(D-2)}{4} c_{4,4} I_{ijkl}^{D+4} \right\} + \\
 \sum_{i < < k} \left\{ c_{3,0} I_{ijk}^D - \frac{D-4}{2} c_{3,7} I_{ijk}^{D+2} \right\} &+ \sum_{i < < j} \left\{ c_{2,0} I_{ij}^D + c_{2,1} J_{ij} + c_{2,2} K_{ij} - \frac{D-4}{2} c_{2,9} I_{ij}^{D+2} \right\} + \sum_i c_{1,0} I_i^D
 \end{aligned} \tag{4.15}$$

which is very similar to equation 2.65, with the exception of the additional bubble integrals J_{ij} , K_{ij} : these are added in manually to make the bubble-residue $\bar{\Delta}_{ij}$ more numerically-stable should the external kinematics cause a 2×2 Gram determinant to vanish [39].

We highlight that even with this monomial parametrisation the pentagon integral disappears, and that all higher-dimensional integrals (which are the result of *dimensional-shift identities*) all acquire coefficients $(D-4)$ which vanish in the $D \rightarrow 4$ limit.

Finally the OPP method of extracting the residues is performed in exactly the same fashion as the 4-dimensional case, with the exception of an additional step added to extract the pentagon residue. Let us lay out the procedure:

$$\begin{aligned}
 \bar{\Delta}_{ijklm} &= Res_{(ijklm)} \left[\frac{N_n(\bar{q})}{\bar{D}_1 \dots \bar{D}_n} \right] \\
 \bar{\Delta}_{ijkl} &= Res_{(ijkl)} \left[\frac{N_n(\bar{q})}{\bar{D}_1 \dots \bar{D}_n} - \sum_{i < < m} \frac{\Delta_{ijklm}}{\bar{D}_i \bar{D}_j \bar{D}_k \bar{D}_l \bar{D}_m} \right] \\
 \bar{\Delta}_{ijk} &= Res_{(ijk)} \left[\frac{N_n(\bar{q})}{\bar{D}_1 \dots \bar{D}_n} - \sum_{i < < m} \frac{\Delta_{ijklm}}{\bar{D}_i \bar{D}_j \bar{D}_k \bar{D}_l \bar{D}_m} - \sum_{i < < l} \frac{\Delta_{ijkl}}{\bar{D}_i \bar{D}_j \bar{D}_k \bar{D}_l} \right] \\
 \bar{\Delta}_{ij} &= Res_{(ij)} \left[\frac{N_n(\bar{q})}{\bar{D}_1 \dots \bar{D}_n} - \sum_{i < < m} \frac{\Delta_{ijklm}}{\bar{D}_i \bar{D}_j \bar{D}_k \bar{D}_l \bar{D}_m} - \sum_{i < < l} \frac{\Delta_{ijkl}}{\bar{D}_i \bar{D}_j \bar{D}_k \bar{D}_l} - \sum_{i < < k} \frac{\Delta_{ijk}}{\bar{D}_i \bar{D}_j \bar{D}_k} \right] \\
 \bar{\Delta}_i &= Res_{(i)} \left[\frac{N_n(\bar{q})}{\bar{D}_1 \dots \bar{D}_n} - \sum_{i < < m} \frac{\Delta_{ijklm}}{\bar{D}_i \bar{D}_j \bar{D}_k \bar{D}_l \bar{D}_m} - \sum_{i < < l} \frac{\Delta_{ijkl}}{\bar{D}_i \bar{D}_j \bar{D}_k \bar{D}_l} - \sum_{i < < k} \frac{\Delta_{ijk}}{\bar{D}_i \bar{D}_j \bar{D}_k} - \sum_{i < j} \frac{\Delta_{ij}}{\bar{D}_i \bar{D}_j} \right]
 \end{aligned} \tag{4.16}$$

and we recall that at every step one should compute the integrand at a phase space point \bar{q} that satisfies the cutting equations relevant to that step. The system of equations will be in the x_i parameters plus the value of μ^2 , which can only be fully constrained on the quintuple cut. Once again, the sampling of the residues should be done as many times as there are coefficients to be fixed.

This D -dimensional method was implemented in the code suite SAMURAI [4], which was later extended to include arbitrary-rank integrands (such as those potentially appearing in non-renormalisable Effective Quantum Field Theories) into the package XSAMURAI [131, 132].

4.2 Integrand decomposition via Polynomial Division

Amplitude reduction methods at the integrand level are advantageous since they turn an integral problem into an *algebraic* one, since the integrand is a rational function of polynomials of kinematic variables.

The reliance of this procedure on the algebraic manipulation of polynomials pointed toward a reformulation of the D -dimensional integrand decomposition procedure in the language of *algebraic geometry* [46, 47], which in turn enabled the generalisation of this class of methods beyond one-loop level [48, 133].

We remark that we now drop the barred notation for D -dimensional quantities as we shall no longer be working with four-dimensional Feynman integrals.

Let us re-write equation 4.3 in a compact form:

$$\mathcal{I}_{i_1 \dots i_m}(q) = \sum_{k=0}^s \sum_{j_1 \dots j_k} \frac{\Delta_{j_1 \dots j_k}}{D_{j_1} \dots D_{j_k}} \quad (4.17)$$

where s is generally less than the number of denominators m of the original amplitude, and as we say is typically equal to 4 or 5. This formula was derived from Lorentz Invariance of the amplitude (through Passarino-Veltman decomposition) and its multi-pole properties, as we saw.

From a purely algebraic perspective, this relation is simply the result of a *multivariate polynomial division* between the numerator of the integrand and all the subsets of denominators $\{D_{j_1} \dots D_{j_k}\}$ formed by the denominators of the amplitude; the terms $\Delta_{j_1 \dots j_k}$ can then be interpreted as the remainder of the division.

The remainder should therefore be *irreducible* with respect to the set of denominators $\{j_1 \dots j_k\}$ and not contain any terms which can be re-written (and simplified) in terms of the denominators themselves. Another desirable property is *universality* in the loop variables, which would make the whole procedure suitable for integrands of arbitrary complexity, arbitrary external legs and kinematics.

A simple example

Let f and g be two functions of the variable x . Let us perform the (univariate) division between them:

$$\frac{f(x)}{g(x)} = q(x) + \frac{r(x)}{g(x)}$$

where $q(x)$ is the division's quotient and $r(x)$ its remainder, and it necessarily holds true that $\text{Deg}[r] \leq \text{Deg}[g]$. The idea is then to write out f directly as the sum of a contribution proportional to g itself plus a remainder:

$$f(x) = q(x)g(x) + r(x) \quad (4.18)$$

doing this is entirely equivalent to performing the polynomial division. This can be immediately connected to the Cauchy Residue Theorem if we take $g(x) := (x - x_0)$:

$$\frac{f(x)}{(x - x_0)} = q(x) + \frac{r_0}{(x - x_0)}$$

where r_0 is the residue of f over the (simple) pole x_0 .

4.2.1 Integrand recurrence

For the remainder of this section we shall employ Dimensional Regularisation in the $D = 4 - 2\epsilon$ prescription detailed in section 2.1.1. We recall that with this prescription a Feynman integral can be parametrised in terms of the $l(l+9)/2$ variables \mathbf{z} of equation 2.28. We shall use these variables to parametrise the numerator, the remainders as well as the denominators.

For any set of denominators $\{D_{i_1} \dots D_{i_m}\}$ we define the *Ideal* $\mathcal{J}_{i_1 \dots i_m}$:

$$\mathcal{J}_{i_1 \dots i_m} = \langle D_{i_1} \dots D_{i_m} \rangle := \left\{ \sum_{k=1}^m h_k(\mathbf{z}) D_{i_k}(\mathbf{z}) \mid h_k(\mathbf{z}) \in P[\mathbf{z}] \right\} \quad (4.19)$$

i.e. the set of all possible polynomials in the variables \mathbf{z} (belonging to the polynomial ring $P[\mathbf{z}]$) that can be formed as a linear combination of denominators.

Let us now imagine to perform the multivariate polynomial division if the integrand's numerator against the denominators:

$$N_{i_1 \dots i_m}(\mathbf{z}) = \mathcal{Q}_{i_1 \dots i_m}(\mathbf{z}) + \Delta_{i_1 \dots i_m}(\mathbf{z}) \quad (4.20)$$

where $\Delta_{i_1 \dots i_m}(\mathbf{z})$ is the aforementioned remainder¹⁸ of the polynomial division between the numerator and the set of denominators, while $\mathcal{Q}_{i_1 \dots i_m}(\mathbf{z})$ is the quotient of said division, which necessarily belongs to the ideal as:

$$\mathcal{Q}_{i_1 \dots i_m}(\mathbf{z}) = \sum_{k=1}^m N_{i_1 \dots i_{k-1} i_{k+1} \dots i_m}(\mathbf{z}) D_{i_k}(\mathbf{z}) \quad (4.21)$$

Let us inset these definitions in the original expression for the integrand:

$$\begin{aligned} \mathcal{I}_{i_1 \dots i_m}(\mathbf{z}) &= \sum_{k=1}^m \frac{N_{i_1 \dots i_{k-1} i_{k+1} \dots i_m}(\mathbf{z}) D_{i_k}(\mathbf{z})}{D_{i_1} \dots D_{i_m}} + \frac{\Delta_{i_1 \dots i_m}(\mathbf{z})}{D_{i_1} \dots D_{i_m}} \\ &= \sum_{k=1}^m \mathcal{I}_{i_1 \dots i_{k-1} i_{k+1} \dots i_m}(\mathbf{z}) + \frac{\Delta_{i_1 \dots i_m}(\mathbf{z})}{D_{i_1} \dots D_{i_m}} \end{aligned} \quad (4.22)$$

It is now evident how D_{i_k} present in the quotient part of the numerator, by cancelling against the respective term at the denominator, generates a new integrand expression but with one fewer denominator, which corresponds to the integrand of a sub-diagram which can be further decomposed. This reduction procedure can be iterated until any further polynomial divisions are not possible. The result will comprise exclusively the remainder terms over the denominators, which is equivalent to a MI decomposition once we integrate over the \mathbf{z} variables.

4.2.2 Division modulo Gröbner bases

In describing the simple ideas behind this application of Polynomial division we glossed over some mathematical minutiae which we will briefly mention here.

1. In practice, division between polynomials is done by identifying the highest degree monomial in both the dividend and the divisor, dividing them to obtain the quotient, subtracting quotient times divisor to obtain the remainder and re-iterating over it until the remainder is lower in degree than the divisor.

A straightforward univariate example is $x^2 + 4x$ divided by $x - 1$:

¹⁸By no coincidence we use the same notation of the OPP residues, but we are not yet able to identify them as such.

$$\begin{aligned}\frac{x^2}{x} &= x & x^2 + 4x - x(x-1) &= 5x \\ \frac{5x}{x} &= 5 & 5x - 5(x-1) &= 5 \\ \implies x^2 + 4x &= (x-1)(x+5) + 5\end{aligned}$$

In the multivariate case there can be monomials of equal degree in different variables, and the result may not be unique if there is no consistent way to choose which monomials to divide first. The simplest choice is a *lexicographic ordering* of the variables, to resolve any ambiguities. With $x \succ y$ it is meant that x ought to be considered of higher order than y and thus should be given priority in ambiguous cases.

2. In the more complex case of a multivariate polynomial $p(x, y)$ divided by two polynomials $p_1(x, y)$ and $p_2(x, y)$ one also needs to specify the order of the divisors, and the results can change dramatically.

As an example, let $p(x, y) := x^2y^3 - 2x^2y$, $p_1(x, y) := xy^2 - 2x$ and $p_2(x, y) := y^3 - 1$. Let us define a lexicographic ordering $x \succ y$ and divide first by p_1 and then by p_2 :

$$\begin{aligned}\frac{x^2y^3}{xy^2} &= xy & x^2y^3 - 2x^2y - xy(xy^2 - 2x) &= 0 \\ \implies p(x, y) &= xy p_1(x, y)\end{aligned}$$

as we can see there is no remainder, and therefore $p(x, y)$ must belong to the ideal generated by p_1 and p_2 (this could have been immediately noticed). Let us now keep the lexicographic ordering but invert the polynomial divisor order:

$$\begin{aligned}\frac{x^2y^3}{y^3} &= x^2 & x^2y^3 - 2x^2y - x^2(y^3 - 1) &= -2x^2y + x^2 \\ \implies p(x, y) &= x^2 p_2(x, y) + x^2(y - 1)\end{aligned}$$

producing a completely different result, namely a remainder appears from the division of a polynomial which should belong to an ideal (and thus be exactly divisible).

This ambiguity is problematic for the decomposition of amplitude integrals, since a simple difference in ordering the denominators entails the non-uniqueness of the remainder; this in turn makes it impossible to unambiguously pick the terms belonging to the ideal \mathcal{J} which yield sub-topology integrands.

This last problem was solved by introducing the polynomial division *modulo a Gröbner basis* [46, 47].

Given an ideal \mathcal{J} on a ring of polynomials $P[\mathbf{z}]$, a Gröbner basis is a set of polynomials $\mathcal{G}(\mathbf{z}) = \{g_1(\mathbf{z}) \dots g_n(\mathbf{z})\}$ that generates \mathcal{J} and such that, given a monomial ordering for the variables within \mathbf{z} , the multivariate polynomial division of any $p(\mathbf{z}) \in P[\mathbf{z}]$ is unique.

$$\mathcal{J}_{i_1 \dots i_m} = \langle g_{i_1} \dots g_{i_m} \rangle := \left\{ \sum_{k=1}^n \tilde{h}_k(\mathbf{z}) g_{i_k}(\mathbf{z}) \mid \tilde{h}_k(\mathbf{z}) \in P[\mathbf{z}] \right\} \quad (4.23)$$

This definition does not detail how to practically compute a Gröbner basis given the Ideal; there exist automated algorithms that accomplish just that, but describing their workings is well beyond the scope

of this thesis.

We now perform the polynomial division of the numerator modulo this Gröbner basis, to obtain:

$$N_{i_1 \dots i_m}(\mathbf{z}) = \mathcal{Q}_{i_1 \dots i_m}(\mathbf{z}) + \Delta_{i_1 \dots i_m}(\mathbf{z}) \quad (4.24)$$

$$\mathcal{Q}_{i_1 \dots i_m}(\mathbf{z}) = \sum_{k=1}^n \Gamma_k(\mathbf{z}) g_k(\mathbf{z}) \quad (4.25)$$

where the quotient is written in terms of the new basis, and by its virtue the remainder Δ is now uniquely determined. Of course, since the elements of the Gröbner basis belong to the Ideal, one could write them on the basis of denominators and recover the the recurrence relation 4.22.

This enables the integrand to be completely decomposed as previously explained, but thanks to the use of a Gröbner basis the remainder terms are now both unique and irreducible (with respect to the denominators).

Now we are allowed to unambiguously associate each remainder $\Delta_{i_1 \dots j_k}$ with a set of denominators $\{D_{i_1}(\mathbf{z}) \dots D_{i_k}(\mathbf{z})\}$ and, using the language of Cauchy's theorem, refer to the remainder as the *residue* over a pole corresponding to the multiple cut $D_{i_1}(\mathbf{z}) = \dots = D_{i_k}(\mathbf{z}) = 0$.

After setting up the machinery to reduce integrands into residues and sub-topologies, one could naturally ponder whether there exist some condition under which the integrand produces no residue at all, and is instead completely reducible. The properties of Ideals over polynomial rings enable the formulation of the following principle [47]:

Theorem 1 (Reducibility Criterion). *If a multiple cut $D_{i_1}(\mathbf{z}) = \dots = D_{i_k}(\mathbf{z}) = 0$ has no solution, any integrand $= I_{i_1 \dots i_k}$ associated to it is completely reducible.*

By virtue of this result, each and every residue must be associated to a set of solutions to the cutting equations. Moreover, if this number of solutions is finite, then the cutting equations describe a so-called *maximum cut*; an example of this would be the quadruple cut of a box in four dimensions, discussed earlier in this chapter. In D -dimensions the maximum cut is the quintuple cut $D_1 \dots D_5 = 0$ which, as stated, admits a single solution.

The reducibility criterion serves as proof that in D -dimensions all one-loop amplitudes can be reduced to diagrams ranging from tadpoles up to at most pentagons, as solving a system of ≥ 6 cutting equations in only five variables $\mathbf{z} = \{x_1, x_2, x_3, x_4, \mu^2\}$ cannot have a solution.

Let us apply this method to a generic one-loop amplitude:

$$\mathcal{M}_{i_1 \dots i_r}^D = \int \frac{d^D q}{\pi^{D/2}} \frac{\mathcal{N}(q)}{D_{i_1} \dots D_{i_r}} \quad (4.26)$$

Adopting the $D = 4 - 2\epsilon$ prescription, the integrand can be parametrised in terms of the variables $\mathbf{z} = \{x_1, x_2, x_3, x_4, \mu^2\}$. The denominators are quadratic polynomials of \mathbf{z} in the form of equation 2.22, while the numerator shall be the most generic polynomial in these parameters:

$$\mathcal{N}(\mathbf{z}) = \sum_{\vec{j} \in J} a_{\vec{j}} x_1^{j_1} x_2^{j_2} x_3^{j_3} x_4^{j_4} (\mu^2)^{j_5} \quad (4.27)$$

$$J := \left\{ \vec{j} = (j_1, j_2, j_3, j_4, j_5) \mid j_1 + j_2 + j_3 + j_4 + 2j_5 \leq r \right\}$$

the sum runs over the 5-tuples of exponents that define the single monomials in the parametrisation of the numerator. The total degree in the parameters equals the overall degree in the loop momentum, which is constrained not to exceed the number of denominators since we are dealing with renormalisable Quantum field Theories.

One then defines a lexicographic ordering such as $x_1 \prec \dots \prec x_5 = \mu^2$, can use their Gröbner bases generator of choice and could perform the multivariate polynomial division modulo this basis.

The result matches exactly equation 4.14 [47], and we point out that polynomial division automatically produces the so-called *spurious terms* required to verify the integrand-level equality with the amplitude, but which vanish upon being integrated due to Lorentz symmetry. In other words, the parametrisation previously obtained (through term-by-term evaluation of all candidate Irreducible Scalar Products) is now performed automatically from the expression of the most general polynomial consistent with rank-restrictions.

Chapter 5

Adaptive Integrand Decomposition

The integrand decomposition method has been crucially important in the automation of loop calculations of processes at NLO, its four-dimensional and D -dimensional formulations have been implemented in several code packages such as CUTOOLS [3], SAMURAI [4], XSAMURAI [131, 132] and NINJA [5]. The re-formulation in the language of algebraic geometry has enabled the prospective extension of the method beyond one-loop order, mainly since the parametrisation and identification of residues can be applied to integrands of much greater complexity thanks to the properties of cut-associated Gröbner bases.

The full implementation of this method into a flexible, automated multi-loop package has, unfortunately, been hindered by a few technical caveats:

- The complexity of the calculation depends heavily on the choice of parametrisation \mathbf{z} and its lexicographic ordering, since they influence directly the form of the Gröebner basis and anything that depends on it. The most advantageous parametrisation is not immediately obvious case-by-case.
- Beyond one-loop the notion of a spurious term is not as well-defined as for the one-loop case: it becomes possible to have ISPs at integrand level which are not present in the original amplitude integral but still do not naïvely integrate to zero like spurious terms should.
- A unique MI basis generally does not exist, and the final expansion into MIs reached through a particular decomposition process is usually not the most compact possible. Given the expected complexity of the results beyond one-loop, this aspect becomes of crucial importance. The result could of course be simplified further by constructing and applying identities between the MIs themselves (the IBP and Lorentz-invariance identities described in section 2.3); these are however relations between integrals, and cannot be used to shorten the reduction calculations since they simply do not hold at integrand level.

The choice of loop parametrisation \mathbf{z} , once again, is important in determining how suited the final result is to a further simplification into the simplest basis of MIs.

5.1 Preliminaries

To address these issues, it was proven very advantageous to formulate the integrand decomposition method employing the $D = D_{\parallel} + D_{\perp}$ prescription for dimensional regularisation, described in section 2.1.2. The idea is to maximally-simplify the reduction algorithm by parametrising the loop variables with regard to the external kinematic variables on an integrand-by-integrand basis, which this prescription naturally implements.

This new approach has been formalised as the *Adaptive Integrand Decomposition method* [14–16], where adaptive refers to the ad hoc choice of variables based on the kinematics at hand .

As we discussed, the defining feature is the splitting between the so-called parallel space spanned by the subset of independent external momenta and the space orthogonal to the external momenta. This leads to parametrising the loop momenta in terms of $l(l+9)/2$ variables:

$$\mathbf{z} = \{x_{\parallel i}, x_{\perp i}, \lambda_{ij}\} \quad i, j = 1 \dots l \quad (5.1)$$

where both sets of x parameters parametrise the formerly four-dimensional part of the loop momenta while the λ_{ij} s describe the (-2ϵ) -dimensional part plus scalar products between $x_{\perp i}$ s.

As was seen, the denominators do not depend on x_{\perp} and their dependency on the orthogonal space enters exclusively through λ_{ij} . This is already an advantageous choice since reducing the number of variables that parametrise the denominators will simplify the polynomial ring generated by them and, by extension, the Ideal. Following this choice of variables, the integrand can be written as:

$$I_{i_1 \dots i_m}(x_{\parallel i}, x_{\perp i}, \lambda_{ij}) = \frac{\mathcal{N}_{i_1 \dots i_m}(x_{\parallel i}, x_{\perp i}, \lambda_{ij})}{D_{i_1}(x_{\parallel i}, \lambda_{ij}) \dots D_{i_m}(x_{\parallel i}, \lambda_{ij})} \quad (5.2)$$

This parametrisation of the integrand highlights the purely-polynomial dependence on the transverse components. This will enable them to be integrated away easily, as mentioned in section 2.1.2.

In section 4.1.1 we showed how the difference of two one-loop denominators is *linear* in the loop momentum, up to scalar products with external momenta. Having m denominators at our disposal, one can always build at least m independent difference equations and build a system, which can be solved to fix the parameters of the loop momentum itself.

This picture holds regardless of the parametrisation. It is, however, simplified by applying the $D = D_{\parallel} + D_{\perp}$ prescription, since¹⁹ the linearity in the loop momentum entails that this system is independent of $\lambda_{11} = \lambda^2$ (as well as the entirety of the perpendicular space). For this reason one can consider an $(m-1)$ -equations system and solve it to express x_{\parallel} in terms of differences of denominators. λ^2 can then be extracted directly from the expression of one of the denominators.

Beyond one-loop it is generally not possible to determine all x_{\parallel} variables as they outnumber the independent difference equations. One then distinguishes between those that can be expressed in terms of denominators and those that remain undetermined. The former are labelled as $x_{\parallel i}^{RSP}$ since, recalling that the x variables will parametrise all the scalar products between the external and loop momenta, they correspond to the *Reducible* scalar products; the latter are labelled as $x_{\parallel i}^{ISP}$ and represent the *physical Irreducible* scalar products, as we will see more clearly shortly.

Then, one sorts the denominators in partitions defined according to their dependency on the loop momenta or combinations thereof. A representative denominator is chosen for each partition and then the variables λ_{ij} are extracted from it.

To summarise, the advantage of applying the $D = D_{\parallel} + D_{\perp}$ prescription adapted to the external kinematic configuration is many-fold. Firstly, the number of variables parametrising the whole integrand is reduced since the polynomial Ideal generated by the denominators is independent of x_{\perp} , and the numerator depends on them only polynomially. For these reasons, these parameters can be treated as constants and dealt with separately. Second, fixing all the remaining parameters (which is equivalent to solving the cutting equations) is as simple as solving a linear system of difference equations.

¹⁹We momentarily focus on the one-loop case for simplicity.

The solutions of these linear equations enable us to define a set of substitution rules:

$$\begin{cases} x_{\parallel i}^{RSP} \longrightarrow P \left[D_{i_k}, x_{\parallel i}^{ISP} \right] \\ \lambda_{ij} \longrightarrow P \left[D_{i_k}, x_{\parallel i}^{ISP} \right] \end{cases} \quad (5.3)$$

which highlights how the variables $\{x_{\parallel i}^{RSP}, \lambda_{ij}\}$ are expressed as polynomials in the denominators and the irreducible parameters $x_{\parallel i}^{ISP}$.

If we plugged this set of substitutions into the numerator of the integrand at hand, the result would be a sum of terms polynomial in the variables $D_{i_k}, x_{\parallel i}^{ISP}$. Those terms that contain only ISP-variables would gather to form a residue-like term, while those containing products of denominators would simplify with the denominators down below and produce sub-topology-like terms, still dependent on $x_{\parallel i}^{ISP}$. The moniker "physical ISP" mentioned previously refers to this fact: that after applying the linear relations these parameters are the only irreducible ones, which are thus left over as part of the integrand expansion.

If one instead proceeded as described in section 4.2, by defining the lexicographic ordering $\lambda_{ij} \prec x_{\parallel i}$, computing the Gröbner bases and then running through the polynomial division recurrence algorithm, it could be shown that the polynomials in the Gröbner bases would be analogously linear in the $\{x_{\parallel i}^{RSP}, \lambda_{ij}\}$. Thus it can be shown that the end result of the polynomial division is identical to the one obtained via the linear relations 5.3.

The biggest advantage of the adaptive parametrisation is, therefore, that *one can outright avoid the computation of the Gröbner bases* and instead seek to build up the system of linear difference equations, solve it to obtain the substitution rules for the reducible parameters and, essentially, reduce the integrand without actually performing any polynomial division.

5.2 The Divide-Integrate-Divide (DID) procedure

The integrand decomposition method can be greatly simplified by taking advantage of the results discussed above, namely the existence of linear substitution rules that render the Gröbner bases obsolete and the possibility to integrate away the transverse components separately.

This new scheme is known as *Adaptive Integrand Decomposition* [14–16], which carries out the decomposition by iterating a three-step approach called *Divide-Integrate-Divide* (DID):

- **Division:** the first step is to write down the numerator in terms of the parameters $\{x_{\parallel i}, x_{\perp i}, \lambda_{ij}\}$ and to plug in the linear relations 5.3, obtaining:

$$\mathcal{N}_{i_1 \dots i_m}(x_{\parallel i}, x_{\perp i}, \lambda_{ij}) = \sum_{k=1}^m \mathcal{N}_{i_1 \dots i_{k-1} i_{k+1} \dots i_m}(x_{\parallel i}^{ISP}, x_{\perp i}) D_{i_k} + \Delta_{i_1 \dots i_m}(x_{\parallel i}^{ISP}, x_{\perp i}) \quad (5.4)$$

we highlight that the linear relations remove all dependence on the $\{x_{\parallel i}^{RSP}, \lambda_{ij}\}$ parameters, separating the sub-topology and cut-associated residue terms in the process, and also that the transverse parameters are left untouched. As we mentioned, it could be shown that this result is equivalent to computing the Gröbner basis \mathcal{G} , performing the multivariate polynomial division and re-writing the quotient in terms of the denominators through the expression of \mathcal{G} itself.

- **Integration:** at this stage the $x_{\perp i}$ parameters enter the decomposed numerator polynomially and, taking advantage of the properties of the $D = D_{\parallel} + D_{\perp}$ prescription, can be integrated away in a single step. The integration is performed on the residue only by mapping $x_{\perp i}$ into polynomials of the angular parameters Θ_{\perp} :

$$x_{\perp i} \longrightarrow P[\lambda_{ij}, \sin \Theta_{\perp}, \cos \Theta_{\perp}] \quad (5.5)$$

and then integrating over these. The result is a residue free of explicit transverse components and, by extension, spurious terms, at the expense of additional terms of the space-time dimensions D .

There is also some dependence on the transverse components implicit in the λ_{ij} which is re-introduces at this step, and which is taken care of next.

- **Second division:** The residues represented in this way have no explicit dependence on the $x_{\perp i}$, i.e. no spurious terms. They do, however, still depend on λ_{ij} as a result of the spurious integration step, and from equation 5.3 these variables do not constitute ISPs and are instead reducible further. By applying the linear relations a second time on the integrated residue, one obtains:

$$\Delta_{i_1 \dots i_m}^{int} \left(x_{\parallel}^{ISP}, \lambda_{ij} \right) = \sum_{k=1}^m \mathcal{N}_{i_1 \dots i_{k-1} i_{k+1} \dots i_m}^{int} \left(x_{\parallel}^{ISP} \right) D_{i_k} + \Delta'_{i_1 \dots i_m} \left(x_{\parallel}^{ISP} \right) \quad (5.6)$$

where $\Delta'_{i_1 \dots i_m} \left(x_{\parallel}^{ISP} \right)$ are completely free of both denominators, transverse components of left-over λ_{ij} s, and thus constitute the *true* residue terms.

All sub-topology terms, corresponding to the lower-cut integrands, are collected and the algorithm is re-iterated over them, at every instance removing all spurious terms and producing the residues associated with the cut.

The result is the full integrand decomposition into scalar integrands (written in the more general multi-loop case):

$$\mathcal{M}_{i_1 \dots i_r} = \sum_{k=0}^m \int \prod_{j=1}^l \frac{d^D q_j}{\pi^{D/2}} \sum_{j_1 \dots j_k} \frac{\Delta'_{j_1 \dots j_k} \left(x_{\parallel}^{ISP} \right)}{D_{j_1} \dots D_{j_k}} \quad (5.7)$$

where the first sum is over the multiple cuts (or, equivalently, the number of surviving inverse propagators) and the second sum encompasses all the possible ways to perform a $(m - k)$ -uple cut.

5.3 Adaptive Integrand Decomposition at one-loop

At this point we would like to interpret the workings of the Adaptive approach to integrand decomposition at one-loop with the previous approach discussed in chapter 4.1.2. Starting from an integrand like 5.2 parametrised in the $D = D_{\parallel} + D_{\perp}$ prescription we wish to see what happens to the n -point residues at each step of the DID algorithm, paying attention in particular to which variables are needed to capture their full polynomial properties.

Table 5.1 from [14, 16] details the result of each step. The first division yields a parametrisation analogous to 4.14, perhaps not so evidently since in the AID framework the distinction between μ^2 and the four-dimensional parameters is mixed amongst all variables. The second step removes all the spurious components from the variables, reducing all their non-vanishing contributions to powers of λ^2 . The pentagon residue vanishes at this stage as it should, this time since it is parametrised in terms of fully-spurious variables which are integrated away. This result matches closely 4.15 if one identifies the contributions from powers of λ^2 with the higher-dimensional integrals. The second division has the effect of sending all power-of- λ^2 contributions to rank zero numerators and lower-point integrals. The second division can then be interpreted as a backwards-implementation of the dimensional shift identities at *integrand level*.

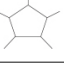





$\mathcal{I}_{i_1 \dots i_n}$	τ	$\Delta_{i_1 \dots i_n}$	$\Delta_{i_1 \dots i_n}^{\text{int}}$	$\Delta'_{i_1 \dots i_n}$
$\mathcal{I}_{i_1 i_2 i_3 i_4 i_5}$ 	$\{x_1, x_2, x_3, x_4, \mu^2\}$	1 {1}	— —	— —
$\mathcal{I}_{i_1 i_2 i_3 i_4}$ 	$\{x_1, x_2, x_3, \lambda^2\}$	5 {1, x_4, x_4^2, x_4^3, x_4^4 }	3 {1, λ^2, λ^4 }	1 {1}
$\mathcal{I}_{i_1 i_2 i_3}$ 	$\{x_1, x_2, \lambda^2\}$	10 {1, $x_3, x_4, x_3^2, x_3 x_4, x_4^2, x_3^3, x_3^2 x_4, x_3 x_4^2, x_4^3$ }	2 {1, λ^2 }	1 {1}
$\mathcal{I}_{i_1 i_2}$ 	$\{x_1, \lambda^2\}$	10 {1, $x_2, x_3, x_4, x_2^2, x_2 x_3, x_2 x_4, x_3^2, x_3 x_4, x_4^2$ }	2 {1, λ^2 }	1 {1}
$\mathcal{I}_{i_1 i_2}$ 	$\{x_1, x_2, \lambda^2\}$	10 {1, $x_1, x_3, x_4, x_1^2, x_1 x_3, x_1 x_4, x_3^2, x_3 x_4, x_4^2$ }	4 {1, x_1, x_1^2, λ^2 }	3 {1, x_1, x_1^2 }
\mathcal{I}_{i_1} 	$\{\lambda^2\}$	5 {1, x_1, x_2, x_3, x_4 }	1 {1}	— —

Figure 5.1: Residue parametrization for irreducible one-loop topologies. The first column indicates the residue under advisement, equivalently the integral it will belong to upon integration. The second column defines the set of variables $\tau \equiv \{x_{\parallel i}, \lambda_{ij}\}$ that parametrise the denominators. The third, fourth and fifth columns show the residue parametrisation after, respectively, the first division, the integration, and the second division. Also written out are the number of said variables at each step [14, 16].

A practical example

Let us see a simple application of the reduction procedure to a rank-2, three-point one-loop integral [15]:

$$I_{123} = \int \frac{d^D q}{\pi^{D/2}} \frac{(q \cdot p_1)(q \cdot p_2) + 4(q \cdot \varepsilon_{12})(q \cdot \varepsilon_{21})}{(q^2 - m^2) \left((q + p_1)^2 - m^2 \right) \left((q + p_1 + p_2)^2 - m^2 \right)} \quad (5.8)$$

where we can identify the three denominators as, respectively, D_1, D_2, D_3 , and for simplicity we let $p_{1,2}^\alpha$ be massless four-vectors. Also we define $(p_1 + p_2)^2 = 2p_1 \cdot p_2 := s_{12} \equiv s$.

ε_{ij}^α are transverse polarisation vectors taken to be orthogonal to both external momenta: $\varepsilon_{ij} \cdot p_k = 0$. These can be defined using the spinor-helicity formalism of chapter 6.2:

$$\varepsilon_{12}^\alpha := \frac{[2|1]}{\sqrt{2}} \varepsilon_+^\alpha(p_1, p_2) \quad (5.9)$$

$$\varepsilon_{21}^\alpha := \frac{\langle 2|1 \rangle}{\sqrt{2}} \varepsilon_-^\alpha(p_1, p_2) \quad (5.10)$$

Accordingly, they satisfy the following:

$$\begin{aligned} \varepsilon_{ij} \cdot \varepsilon_{ij} &= 0 \\ \varepsilon_{12} \cdot \varepsilon_{21} &= -\frac{[2|1]\langle 2|1 \rangle}{2} = \frac{s_{12}}{2} = \frac{s}{2} \end{aligned} \quad (5.11)$$

Let us first define the $D = D_{\parallel} + D_{\perp}$ prescription in this case. From the external kinematics it is clear that there are only 2 independent momenta, thus $D_{\parallel} = 2$. The loop momentum is then parametrised accordingly:

$$q^\alpha = q_{\parallel}^\alpha + \lambda^\alpha \quad (5.12)$$

$$q_{\parallel}^\alpha = x_1 p_1^\alpha + x_2 p_2^\alpha \quad (5.13)$$

$$\lambda^\alpha = x_3 e_3^\alpha + x_4 e_4^\alpha + \mu^\alpha \quad (5.14)$$

where the transverse vectors could be defined as $e_{3,4}^\alpha = \varepsilon_{12}^\alpha \pm \varepsilon_{21}^\alpha$. The integral is then parametrised according to the set of variables $\mathbf{z} = \{x_1, x_2, x_3, x_4, \lambda^2\}$:

$$\begin{aligned} I_{123} &= \int \frac{d^D q}{\pi^{D/2}} \frac{x_1 x_2 (p_1 \cdot p_2)^2 + 4 [(x_3 e_3 + x_4 e_4) \cdot \varepsilon_{12}] [(x_3 e_3 + x_4 e_4) \cdot \varepsilon_{21}]}{D_1 D_2 D_3} \\ &= \int \frac{d^D q}{\pi^{D/2}} \frac{x_1 x_2 (p_1 \cdot p_2)^2 + (\varepsilon_{12} \cdot \varepsilon_{21})^2 [x_3 - x_4] [x_3 + x_4]}{D_1 D_2 D_3} \\ &= s^2 \int \frac{d^D q}{\pi^{D/2}} \frac{x_1 x_2 + x_3^2 - x_4^2}{D_1 D_2 D_3} \end{aligned} \quad (5.15)$$

and so are the three denominators:

$$\begin{aligned} D_1 &= s x_1 x_2 + \lambda^2 - m^2 \\ D_2 &= s(x_1 + 1)x_2 + \lambda^2 - m^2 \\ D_3 &= s(x_1 + 1)(x_2 + 1) + \lambda^2 - m^2 \end{aligned} \quad (5.16)$$

where, thanks to the orthogonality of the parallel and orthogonal spaces, the denominators actually only depend on $\tau := \{x_1, x_2, \lambda^2\}$.

We now build difference equations between the denominators to obtain expressions linear in τ :

$$\begin{aligned} D_1 &= s x_1 x_2 + \lambda^2 - m^2 \\ D_2 - D_1 &= s x_2 \\ D_3 - D_1 &= s(x_1 + x_2 + 1) \end{aligned} \quad (5.17)$$

this is a system of equations linear in the three variables which is easily solved:

$$\begin{cases} x_1 \rightarrow \frac{D_3 - D_2 - s}{s} \\ x_2 \rightarrow \frac{D_2 - D_1}{s} \\ \lambda^2 \rightarrow \frac{(D_2 - D_1)(D_2 - D_3)}{s} + D_2 + m^2 \end{cases} \quad (5.18)$$

where the solutions have been written as substitution rules.

Let us now execute the DID algorithm:

- **Division:** We first plug into the integrand of 5.15 the substitutions 5.18 and perform the polynomial division:

$$\begin{aligned}
 s^2 \frac{x_1 x_2 + x_3^2 - x_4^2}{D_1 D_2 D_3} &\rightarrow \frac{(D_3 - D_2 - s)(D_2 - D_1) + s^2(x_3^2 - x_4^2)}{D_1 D_2 D_3} \\
 &= \frac{1}{D_1} - \frac{1}{D_2} - \frac{D_2 + s}{D_1 D_3} + \frac{1}{D_3} + \frac{s}{D_2 D_3} + \frac{s^2(x_3^2 - x_4^2)}{D_1 D_2 D_3} \\
 &= \frac{1}{D_1} - \frac{1}{D_2} + \frac{1}{D_3} - \frac{(q + p_1)^2 - m^2 + s}{D_1 D_3} + \frac{s}{D_2 D_3} + \frac{s^2(x_3^2 - x_4^2)}{D_1 D_2 D_3} \quad (5.19)
 \end{aligned}$$

- **Integration:** Integrating the last term in the integrand over the transverse coordinates x_3 and x_4 the spurious components vanish, but it can be shown that one non-vanishing contributions remains:

$$s^2 \int \frac{d^D q}{\pi^{D/2}} \frac{(x_3^2 - x_4^2)}{D_1 D_2 D_3} \rightarrow -\frac{2s}{D-2} \int \frac{d^D q}{\pi^{D/2}} \frac{\lambda^2}{D_1 D_2 D_3} \quad (5.20)$$

- **Second division:** We further decompose this last integrand by re-applying 5.18:

$$\begin{aligned}
 -\frac{2s}{D-2} \frac{\lambda^2}{D_1 D_2 D_3} &\rightarrow -\frac{2}{D-2} \frac{(D_2 - D_1)(D_2 - D_3) + s(D_2 + m^2)}{D_1 D_2 D_3} \\
 &= -\frac{2}{D-2} \left[-\frac{1}{D_3} - \frac{1}{D_1} + \frac{1}{D_2} + \frac{D_2 + s}{D_1 D_3} + \frac{s m^2}{D_1 D_2 D_3} \right] \\
 &= \frac{2}{D-2} \left[\frac{1}{D_1} - \frac{1}{D_2} + \frac{1}{D_3} - \frac{(q + p_1)^2 - m^2 + s}{D_1 D_3} - \frac{s m^2}{D_1 D_2 D_3} \right] \quad (5.21)
 \end{aligned}$$

We now put everything together and re-write the original integral, which we recall was rank-2, three-point:

$$\begin{aligned}
 I_{123} &= \int \frac{d^D q}{\pi^{D/2}} \left\{ \frac{D}{D-2} \left[\frac{1}{D_1} - \frac{1}{D_2} + \frac{1}{D_3} \right] - \frac{D(m^2 - s)}{D-2} \left[\frac{1}{D_1 D_3} \right] + s \left[\frac{1}{D_2 D_3} \right] - \frac{2s}{D-2} \left[\frac{1}{D_1 D_2 D_3} \right] \right\} \\
 &\quad - \frac{D}{D-2} \int \frac{d^D q}{\pi^{D/2}} \left[\frac{(q + p_1)^2}{D_1 D_3} \right] \quad (5.22)
 \end{aligned}$$

which is explicitly reduced into a series of scalar (rank-0) one-,two- and three-point integrals with rational coefficients, as well as a rank-2 *two-point* integral. It is evident how one iteration of the procedure has lowered the complexity of all contributions to the original integral.

This procedure was computed by applying the DID-algorithm "on the triple cut", by which it is meant that (all) three denominators were encompassed in the procedure. We recall that this is equivalent to performing the multivariate polynomial division of the numerator on the triple cut solution $D_1 = D_2 = D_3 = 0$. The full reduction to scalar integrals only now entails repeating this procedure from the top on the lower-point non-scalar integrals, of which there is only one in this case.

5.4 AIDA: ADAPTIVE INTEGRAND DECOMPOSITION ALGORITHM

AIDA [15] is a MATHEMATICA implementation of the Adaptive Integrand Decomposition and its DID algorithm, suitable for one and two-loop integrand decompositions, used to generate some of the main results of this thesis work. Here we shall give a brief outlook of its logic and operations.

Inputs

The algorithm expects as an input a list of square amplitudes, which correspond to cross-interferences of Feynman diagrams with common external kinematics. This is the usual case for many physical processes at the loop level where different types of diagrams participate.

Alternatively one may feed in a list of non-interfered amplitudes, so long as they do not contain uncontracted tensor indices. Consider for example the QED-regulated process of the photonic vacuum-polarisation at the 2-loop level:

$$\begin{array}{ccc}
 \mathcal{I}_1 & \mathcal{I}_2 & \mathcal{I}_3 \\
 \text{---} & \text{---} & \text{---} \\
 \text{---} & \text{---} & \text{---} \\
 \text{---} & \text{---} & \text{---} \\
 \text{---} & \text{---} & \text{---}
 \end{array} \quad (5.23)$$

Figure 5.2: The three diagrams that correct the photonic vacuum polarisation at two loops in QED.

In this case the amplitude would possess some naked Lorentz indices corresponding to the external photons. In order to generate a valid input for AIDA one can contract the amplitude with a suitably-chosen tensor such as a transverse polarisation operator.

The input amplitudes may be generated in several ways, such as using the MATHEMATICA packages FEYNARTS [134] and FEYNCALC [50, 51]

We will continue with this example to illustrate the operation of AIDA [15], where $l_k = \sum_{i=1}^l \alpha_{ki} q_i + \sum_{i=1}^{n-1} \beta_{ki} p_i$ is the momentum that flows in the k -th propagator. The input is thus the list:

$$\mathcal{I} = \left\{ \mathcal{I}_1, \mathcal{I}_2, \mathcal{I}_3 \right\} \quad (5.24)$$

where every amplitude is represented in terms of the numerator, the loop propagators and their powers, as follows:

```

Int [1]
{Num[1], {{q1, m2}, {p + q1, m2}, {-p + q2, m2}, {q2, m2}, {q1 + q2, 0}},
{1, 1, 1, 1, 1}}
Int [2]
{Num[2], {{q1, m2}, {-p + q1, m2}, {q2, m2}, {p - q1 + q2, 0}}, {1, 2, 1, 1}}
Int [3]
{Num[3], {{q1, m2}, {-p + q1, m2}, {q2, m2}, {p - q1 + q2, 0}}, {1, 2, 1, 1}}
    
```

where the powers of two, of course, come since in the second and third diagrams a fermionic propagator is repeated twice.

Grouping

The first operation performed by the algorithm is known as *grouping*, as it entails gathering together amplitudes that can be reduced simultaneously later on.

The grouping re-arranges the input list as follows:

$$\mathcal{I} = \bigcup_k \mathcal{G}_k, \quad \mathcal{G}_k = \left\{ \mathcal{I}_1^{\mathcal{G}_k}, \mathcal{I}_2^{\mathcal{G}_k}, \dots, \mathcal{I}_m^{\mathcal{G}_k} \right\} \quad (5.25)$$

The grouping is performed by identifying all amplitudes that can be obtained by pinching one or more internal lines of other amplitudes. The largest amplitude, from which all other amplitudes in the group are obtained by repeated pinching, is referred as the *parent integrand*. In the notation above, the parent integrand corresponds to $\mathcal{I}_1^{\mathcal{G}_k}$ and is represented internally as:

$$\mathcal{I}_1^{\mathcal{G}_k} = \left\{ \mathcal{N}_1^{\mathcal{G}_k}, \left\{ D_1, \dots, D_j \right\}, \left\{ \max_{\mathcal{G}_k}(a_1), \dots, \max_{\mathcal{G}_k}(a_j) \right\} \right\} \quad (5.26)$$

evidently encompassing all denominators present in the sub-topologies of \mathcal{G}_k . One should note that the parent integrand may not actually correspond to one of the original amplitudes, but instead could be defined from scratch specifically to yield the other amplitudes by pinching its internal lines. In this case, its numerator would be initialised to zero.

In order to bring two amplitudes in a single group in a practical sense it may be necessary to re-define the loop momentum by a shift. At one loop the momentum q is shifted by a combination of the external momenta flowing in through the external lines, but beyond 1-loop the shifting may also involve the other loop momenta.

Let us illustrate the process taking as an example the amplitudes of figure 5.2. It is immediately evident that \mathcal{I}_2 and \mathcal{I}_3 differ only by the direction of momentum flow and thus are virtually the same amplitude. Therefore AIDA would merge the two numerators and define a new integrand \mathcal{I}_{23} with the same set of loop denominators.

Then the algorithm would try to shift the loop momenta of this combined integrand to write its denominators in terms of those of \mathcal{I}_1 . This can be done with the shift:

$$\begin{cases} q_1 \rightarrow -q_1 \\ q_2 \rightarrow q_2 - p \end{cases}$$

\mathcal{I}_1 , however, cannot be the parent integrand since one of the denominators of \mathcal{I}_{23} is squared. The parent integrand $\mathcal{I}_1^{\mathcal{G}}$ is then defined from scratch, and the resulting group is:

$$\mathcal{G} = \left\{ \mathcal{I}_1^{\mathcal{G}}, \mathcal{I}_2^{\mathcal{G}} = \mathcal{I}_1, \mathcal{I}_3^{\mathcal{G}} = \mathcal{I}_{23} \right\} \quad (5.27)$$

with:

```
IntG[1]
{0, {{q1, m2}, {p + q1, m2}, {-p + q2, m2}, {q2, m2}, {q1 + q2, 0}}, {1, 2, 1, 1, 1}}
IntG[2]
{Num[1], {{q1, m2}, {p + q1, m2}, {-p + q2, m2}, {q2, m2}, {q1 + q2, 0}}, {1, 1, 1, 1, 1}}
IntG[3]
{Num[2] + Num[3],
{{q1, m2}, {p + q1, m2}, {-p + q2, m2}, {q2, m2}, {q1 + q2, 0}},
{1, 2, 1, 0, 1}}
```

Next, the algorithm analyses the structure of the amplitudes, group-by-group, to extract all the information required to build the adaptive parametrisation.

First, for every parent integrand, the list of denominators is arranged into a so-called *graph*, which is a list of vertices connected by denominators.

A *sub-graph* is generated by merging two adjacent vertices, which corresponds to cutting the propagator in-between; the algorithm seeks all possible ways to do this, which corresponds to completely defining the cut structure of the integrand. Using the graph formalism enables AIDA to immediately reconstruct the momentum flow after each cut.

Every sub-graph and all of their information are encoded in a *topology* as such:

$$T_{1\dots m} = \left\{ \mathcal{N}^{\square\updownarrow}, \{q_1, q_2\}, \{p_1, \dots, p_m\}, \left\{ \{D_1, \dots, D_{m_1}\}, \{D_{m+1}, \dots, D_{m_1+m_2}\}, \{D_{m_1+m_2}, \dots, D_m\} \right\} \right\} \quad (5.28)$$

This object contains information on the loop momenta (2, in this example), the external kinematics and all the denominators, grouped together based on which loop momenta they depend on: $q_1, q_2, q_1 \pm q_2$. The numerator is left as a place holder variable for the moment.

For each topology, the algorithm constructs a $D = D_{\parallel} + D_{\perp}$ parametrisation using the stored information on the topology's external momenta. This is then used to parametrise all denominators, and subsequently to construct and solve the system of linear relations expressing $\{x_{\parallel i}^{RSP}, \lambda_{ij}\}$ in terms of loop denominators, to be used later on. We recall that this corresponds precisely to computing the solution to the cut conditions that produce the topology in question.

At this step, the algorithm associates each integrand to one of the topologies via the definition of a *cut*:

$$\begin{aligned} Cut_{1\dots m}^{a_1\dots a_m} = & \left\{ \mathcal{N}_{1\dots m}^{a_1\dots a_m} \right. \\ & \left. \left\{ \{1, \dots, m_1\} \{m_1 + 1, \dots, m_1 + m_2\}, \{m_1 + m_2, \dots, m\} \right\}, \right. \\ & \left. \left\{ a_1, \dots, a_{m_1}, a_{m_1+1}, \dots, a_{m_1+m_2}, a_{m_1+m_2+1}, \dots, a_m \right\} \right\} \end{aligned} \quad (5.29)$$

where the denominator indices and the related exponents are taken from the associated topology, and where the numerator is given by the specific integrand. All topologies not paired with an integrand are initialised with zero numerator.

A generic cut can always receive a contribution to its numerator from the reduction of a larger topology during the execution of the DID procedure. Therefore the final step in the initialisation phase is to determine which cuts may contribute to which other cuts and sort them accordingly. The cuts are then organised into *Jobs*, where the first job contains only the cut associated with the parent integrand, which could theoretically contribute to all subsequent cuts, while all the other jobs contain a set of cuts which depend on the previous calculations but that would never contribute to each other. This enables AIDA to be parallelised.

The job structure generated for the previous example is as follows:

```

Job[1]
{Cut[{{1, 2}, {3, 4}, {5}}, {1, 2, 1, 1, 1}]}
Job[2]
{Cut[{{1, 2}, {3, 4}, {5}}, {1, 1, 1, 1, 1}]}
Job[3]
{Cut[{{2}, {3, 4}, {5}}, {0, 2, 1, 1, 1}], Cut[{{1, 2}, {4}, {5}}, {1, 2, 0, 1, 1}],
Cut[{{1, 2}, {3}, {5}}, {1, 2, 1, 0, 1}], Cut[{{1, 2}, {3, 4}}, {1, 2, 1, 1, 0}]}
Job[4]
{Cut[{{2}, {3, 4}, {5}}, {0, 1, 1, 1, 1}],
Cut[{{1}, {3, 4}, {5}}, {1, 0, 1, 1, 1}], Cut[{{1, 2}, {4}, {5}}, {1, 1, 0, 1, 1}],
Cut[{{1, 2}, {3}, {5}}, {1, 1, 1, 0, 1}], Cut[{{1, 2}, {3, 4}}, {1, 1, 1, 1, 0}]}
Job[5]
{Cut[{{2}, {4}, {5}}, {0, 2, 0, 1, 1}], Cut[{{2}, {3}, {5}}, {0, 2, 1, 0, 1}],
Cut[{{2}, {3, 4}}, {0, 2, 1, 1, 0}], Cut[{{1, 2}, {5}}, {1, 2, 0, 0, 1}],
Cut[{{1, 2}, {4}}, {1, 2, 0, 1, 0}], Cut[{{1, 2}, {3}}, {1, 2, 1, 0, 0}]}
Job[6]
{Cut[{{3, 4}, {5}}, {0, 0, 1, 1, 1}], Cut[{{2}, {4}, {5}}, {0, 1, 0, 1, 1}],
Cut[{{2}, {3}, {5}}, {0, 1, 1, 0, 1}], Cut[{{2}, {3, 4}}, {0, 1, 1, 1, 0}],
Cut[{{1}, {4}, {5}}, {1, 0, 0, 1, 1}], Cut[{{1}, {3}, {5}}, {1, 0, 1, 0, 1}],
Cut[{{1}, {3, 4}}, {1, 0, 1, 1, 0}], Cut[{{1, 2}, {5}}, {1, 1, 0, 0, 1}],
Cut[{{1, 2}, {4}}, {1, 1, 0, 1, 0}], Cut[{{1, 2}, {3}}, {1, 1, 1, 0, 0}]}
Job[7]
{Cut[{{2}, {5}}, {0, 2, 0, 0, 1}],
Cut[{{2}, {4}}, {0, 2, 0, 1, 0}], Cut[{{2}, {3}}, {0, 2, 1, 0, 0}]}
Job[8]
{Cut[{{4}, {5}}, {0, 0, 0, 1, 1}], Cut[{{3}, {5}}, {0, 0, 1, 0, 1}],
Cut[{{2}, {5}}, {0, 1, 0, 0, 1}], Cut[{{2}, {4}}, {0, 1, 0, 1, 0}],
Cut[{{2}, {3}}, {0, 1, 1, 0, 0}], Cut[{{1}, {5}}, {1, 0, 0, 0, 1}],
Cut[{{1}, {4}}, {1, 0, 0, 1, 0}], Cut[{{1}, {3}}, {1, 0, 1, 0, 0}]}

```

The cuts that are initialised to the input amplitudes are:

```

Cut[{{1, 2}, {3, 4}, {5}}, {1, 2, 1, 1, 1}]
Cut[{{1, 2}, {3, 4}, {5}}, {1, 1, 1, 1, 1}]
Cut[{{1, 2}, {3}, {5}}, {1, 2, 1, 0, 1}]

```

DID algorithm execution

Finally the algorithm proceeds to apply the DID procedure to each job, one by one starting from the top. The numerator of each job is gathered together with all existing contributions to that particular topology that might have appeared from the reduction of previous jobs.

The algorithm builds the adaptive parametrisation, solves the cut and finds the substitution rules. These are then plugged into the amplitude belonging to the parent topology, thus performing the first division. A set of substitution routines perform the transverse-space integration, simply looking for the relevant kinematic configuration in a table of known results as mentioned. The division routine is called once again and, finally, the results are distributed to the relevant places. All the quotients are passed over to the relevant lower-cut integrands as numerators, while the leftover term is returned as the residue of the cut $\Delta_1 \dots m^{a_1 \dots a_m}$.

This procedure is applied to each cut of the job at hand (possibly in parallel), and every job is handled one after the other until all that is left are the non-vanishing residues associated to every integral.

It is important to mention that the final list of integrals will often contain "spurious integrals" that are either vanishing or can be related to one another upon shifting the loop momentum variable. If the integral vanishes then the residue ought to be discarded, while if two integrals are really identical their residues are merged. This situation arises because of the symmetries of the quantities involved in the Integrand decomposition method. Therefore, from the standpoint of Integrand decomposition, all the integrals that survive this simplification step should be regarded as independent.

For instance, the result of running the DID algorithm over the above list of jobs produces the following list of residues:

```

Δ[{{1, 2}, {3, 4}, {5}}, {1, 1, 1, 1, 1}]
Δ[{{1, 2}, {3}, {5}}, {1, 2, 1, 0, 1}]
Δ[{{2}, {3, 4}, {5}}, {0, 1, 1, 1, 1}]
Δ[{{1}, {3, 4}, {5}}, {1, 0, 1, 1, 1}]
Δ[{{1, 2}, {4}, {5}}, {1, 1, 0, 1, 1}]
Δ[{{1, 2}, {3}, {5}}, {1, 1, 1, 0, 1}]
Δ[{{1, 2}, {3, 4}}, {1, 1, 1, 1, 0}]
Δ[{{2}, {3}, {5}}, {0, 2, 1, 0, 1}]
Δ[{{1, 2}, {5}}, {1, 2, 0, 0, 1}]
Δ[{{1, 2}, {3}}, {1, 2, 1, 0, 0}]
Δ[{{3, 4}, {5}}, {0, 0, 1, 1, 1}]
Δ[{{2}, {4}, {5}}, {0, 1, 0, 1, 1}]
Δ[{{2}, {3}, {5}}, {0, 1, 1, 0, 1}]
Δ[{{2}, {3, 4}}, {0, 1, 1, 1, 0}]
Δ[{{1}, {4}, {5}}, {1, 0, 0, 1, 1}]
Δ[{{1}, {3}, {5}}, {1, 0, 1, 0, 1}]
Δ[{{1}, {3, 4}}, {1, 0, 1, 1, 0}]
Δ[{{1, 2}, {5}}, {1, 1, 0, 0, 1}]
Δ[{{1, 2}, {4}}, {1, 1, 0, 1, 0}]
Δ[{{1, 2}, {3}}, {1, 1, 1, 0, 0}]
Δ[{{2}, {5}}, {0, 2, 0, 0, 1}]
Δ[{{2}, {3}}, {0, 2, 1, 0, 0}]
Δ[{{2}, {5}}, {0, 1, 0, 0, 1}]
Δ[{{2}, {3}}, {0, 1, 1, 0, 0}]
Δ[{{1}, {5}}, {1, 0, 0, 0, 1}]
Δ[{{1}, {3}}, {1, 0, 1, 0, 0}]
Δ[{{1}, {3, 4}}, {1, 0, 1, 1, 0}]
Δ[{{1, 2}, {5}}, {1, 1, 0, 0, 1}]
Δ[{{1, 2}, {4}}, {1, 1, 0, 1, 0}]
Δ[{{1, 2}, {3}}, {1, 1, 1, 0, 0}]
Δ[{{2}, {5}}, {0, 2, 0, 0, 1}]
Δ[{{2}, {3}}, {0, 2, 1, 0, 0}]
Δ[{{2}, {5}}, {0, 1, 0, 0, 1}]
Δ[{{2}, {3}}, {0, 1, 1, 0, 0}]
Δ[{{1}, {5}}, {1, 0, 0, 0, 1}]
Δ[{{1}, {3}}, {1, 0, 1, 0, 0}]

```

where the associated integral can easily be read off. It turns out that this list can be reduced to the following list of independent residues:

```

Δ[{{1, 2}, {3, 4}, {5}}, {1, 1, 1, 1, 1}]
Δ[{{1, 2}, {3}, {5}}, {1, 2, 1, 0, 1}]
Δ[{{1, 2}, {3}, {5}}, {1, 1, 1, 0, 1}]
Δ[{{1, 2}, {3, 4}}, {1, 1, 1, 1, 0}]
Δ[{{2}, {3}, {5}}, {0, 2, 1, 0, 1}]
Δ[{{1, 2}, {3}}, {1, 2, 1, 0, 0}]
Δ[{{1}, {3}, {5}}, {1, 0, 1, 0, 1}]
Δ[{{2}, {3}, {5}}, {0, 1, 1, 0, 1}]
Δ[{{1, 2}, {3}}, {1, 1, 1, 0, 0}]
Δ[{{2}, {3}}, {0, 2, 1, 0, 0}]

```

We mention that AIDA also offer the possibility of running a simplified decomposition algorithm: instead of solving the cutting equations for all possible cuts, obtaining the substitution rules and running the DID algorithm job-by-job it only solves the largest cut present, constructs a single table of substitutions based on it and only performs the first division on each numerator. Based on what we said in section 5.3 this will entail more spurious integrals present in the final decomposition that will need to be simplified either by dimensional-shift relations or by the Integration-by-parts (IBP) and Lorentz-invariance identities of section 2.3, but in return the computational cost is much reduced.

In conclusion we stress once more that nothing in the Integrand decomposition method guarantees that the final list of integrals is the minimal Master integral basis, since relations between integrals exist solely at *integral-level*, and their workings cannot be captured and accounted for by integrand-level reduction methods. Therefore, as a final simplification step, one should feed the output to dedicated codes that generate and apply IBP and Lorentz-invariance identities between the Master Integrals. To this end, AIDA is engineered in a flexible way, its results are adaptable to be fed to the automated IBP codes such as KIRA and REDUZE through the use of interfaces within the MATHEMATICA framework.

Chapter 6

N-point kinematics

A physical quantity is said to possess *n-point kinematics* if it is a function of n external momenta that sum up to zero by momentum conservation. Feynman amplitudes, loop integrals and the integrands that appear in the aforementioned decomposition procedures naturally possess n -point kinematics. The kinematics determine the independent variables upon which physical quantities depend. This chapter is devoted to introducing some possible ways to parametrise quantities in n -point kinematics.

6.1 Mandelstam variables

In $D = 4$ the dependence on the external momenta most often comes in the form of contractions with $g_{\mu\nu}$, i.e. scalar products. These, in turn, are labelled either by kinematic invariants such as masses or by the so-called Mandelstam variables:

$$\begin{aligned} m_i^2 &:= p_i^2 \\ s_{ij} &:= (p_i + p_j)^2 \end{aligned} \tag{6.1}$$

Not all these variables are independent. Given n external momenta, if momentum conservation is to be enforced, the independent external momenta should not be n , but $(n - 1)$ instead. It follows that the distinct pairings of different momenta p_i and p_j that we could construct are $(n - 1)(n - 2)/2$. Meanwhile we also have the on-shell conditions $p_i^2 = m_i^2$. For the $(n - 1)$ independent momenta this amounts to a simple change of variable. Given that the leftover momentum is written in terms of the others by momentum conservation, its on-shell condition acts as a constraint on the independent momenta.

By this logic, the actual independent Mandelstam variables are:

$$\frac{(n - 1)(n - 2)}{2} - 1 = \frac{n(n - 3)}{2} \tag{6.2}$$

From $n = 6$ and above, one ought to have at least five independent momenta and one momentum-conservation relation. However, in four dimensional space-time, the number of linearly-independent vectors is at most four. Consequently any 5×5 Gram matrix $\mathbb{G}_{\alpha\beta}$ that can be constructed by choosing any 5 external momenta has vanishing determinant.

Given n total momenta, let us choose 4 independent ones and set them aside. The distinct ways to pair up the remaining $(n - 4)$ are then $(n - 4)(n - 5)/2$. This is also the number of vanishing Gram

determinants, and thus the number of constraints that reduce the number of independent Mandelstam variables.

After discarding the extra Mandelstams, the final number of independent variables is:

$$\frac{n(n-3)}{2} - \frac{(n-4)(n-5)}{2} = \frac{(6n-20)}{2} = 3n-10 \quad (6.3)$$

Let us compare the two formulas for varying n in a table:

n	$n(n-3)/2$	$3n-10$
3	0	-
4	2	2
5	5	5
6	9	8
7	14	11
8	20	14

this makes clear how, from 6-point kinematics on, momentum-conservation plus the on-shellness condition are no longer enough to determine the minimal set of Mandelstam variables.

For the familiar four-point kinematics the two independent Mandelstams can be defined as: $s := (p_1 + p_2)^2$, $t := (p_1 + p_4)^2$ in the case of incoming external momenta. A third Mandelstam variable $u := (p_1 + p_3)^2$ could be defined, but is related to the others by the relation:

$$s + t + u = \sum_{i=1}^4 m_i^2 \quad (6.4)$$

Beyond four-point amplitudes, one usually speaks of *generalised* Mandelstam variables. In the case of five-point kinematics a common choice for the five parameters is the following set of cyclic Mandelstam variables [135–138] :

$$s_{12}, s_{23}, s_{34}, s_{45}, s_{51} \quad (6.5)$$

$$s_{ij} := (p_i + p_j)^2 = 2p_i p_j$$

where the last relation is valid in the massless case. The non-cyclic Mandelstams can be related to these by the following relations [136]:

$$s_{i,i+2} = s_{i+3,i+4} - s_{i,i+1} - s_{i+1,i+2} \quad (6.6)$$

6.2 Spinor-Helicity Formalism

The Spinor-Helicity formalism is an alternative representation for massless four-momenta. It is based on writing down the kinematics on the so-called helicity basis, built upon the massless Dirac equation. This formalism is often advantageous compared to the ordinary momentum representation since helicity is a conserved quantity along fermionic lines, and since it enables to exploit gauge-invariance effectively by choosing an appropriate representation for polarisation states.

In this appendix we shall present the basic definitions and identities [2, 136, 139] of which we shall make use later on in this chapter, as well as elsewhere in this thesis.

Helicity

The helicity operator is defined as the projection of a particle's spin operator onto the direction of motion, defined by normalising the particle's four-momentum:

$$\hat{p}^\mu := \frac{p^\mu}{|p|} \quad (6.7)$$

$$h(\hat{p}) := \frac{1}{2} \Sigma \cdot \hat{p} \quad (6.8)$$

as an operator, it commutes with the Hamiltonian and is thus well-defined.

Chirality

Let us now consider the Dirac equation in momentum space for both a fermion and its anti-particle of four-momentum p_i^μ :

$$\left(\not{p}_i + m_i \right) u(p_i) = 0 \quad (6.9)$$

$$\left(\not{p}_i - m_i \right) v(p_i) = 0 \quad (6.10)$$

It is evident how, in the massless limit $m_i \rightarrow 0$ there is no difference between the particle and antiparticle solutions, which can thus be identified.

We introduce the two *Chiral projectors* $P_\pm := \frac{1}{2} (\mathbb{1} + \gamma^5)$, these are used to write down the two solutions of the massless Dirac equation, as well as the conjugate ones:

$$\begin{aligned} u_\pm(p_i) &:= P_\pm u(p_i) & \bar{u}_\pm(p_i) &:= \bar{u}(p_i) P_\mp \\ v_\pm(p_i) &:= P_\mp v(p_i) & \bar{v}_\pm(p_i) &:= \bar{v}(p_i) P_\pm \end{aligned}$$

These are known as left- and right- handed chiral spinors.

6.2.1 Massless fermion representation

The spinor-helicity formalism exploits the wave equation for chiral massless fermions to construct an alternative representation for momenta and spinor products. We now define the angle and square brackets, which indicate different chirality states:

$$\begin{aligned} |i\rangle &:= u_+(p_i) = v_-(p_i) & \langle i| &:= \bar{u}_-(p_i) = \bar{v}_+(p_i) \\ [i] &:= u_-(p_i) = v_+(p_i) & [i| &:= \bar{u}_+(p_i) = \bar{v}_-(p_i) \end{aligned}$$

and the massless Dirac equation becomes:

$$\begin{aligned} \not{p}_i |i\rangle &= 0 & \langle i| \not{p}_i &= 0 \\ \not{p}_i [i] &= 0 & [i| \not{p}_i &= 0 \end{aligned} \quad (6.11)$$

Inner products of spinors are written as:

$$\langle i|j\rangle := \bar{u}_-(p_i)u_+(p_j) \quad [i|j] := \bar{u}_+(p_i)u_-(p_j)$$

and satisfy the following symmetry relations:

$$\begin{aligned} \langle i|i\rangle &= [i|i] = 0 & \langle i|j\rangle &= -\langle j|i\rangle \\ \langle i|j\rangle &= [i|j] = 0 & [i|j] &= -[j|i] \end{aligned}$$

By using the Gordon identity, one can express the four-momentum p_i^μ in terms of spinors:

$$p_i^\mu = \frac{1}{2} \langle i|\gamma^\mu|i\rangle = \frac{1}{2} [i|\gamma^\mu|i] \quad (6.12)$$

and, in turn, the outer product between spinors:

$$|i\rangle [i| = \frac{1}{2} (\mathbb{1} + \gamma^5) \not{p}_i \quad [i| \langle i| = \frac{1}{2} (\mathbb{1} - \gamma^5) \not{p}_i$$

The spinor outer product satisfies useful relations such as:

- charge conjugation:

$$[i|\gamma^\mu|j\rangle = \langle j|\gamma^\mu|i] \quad (6.13)$$

- the Fierz identity:

$$[i|\gamma^\mu|j\rangle [k|\gamma_\mu|l] = 2 [i|k] \langle l|j\rangle \quad (6.14)$$

- the Schouten identity:

$$\begin{aligned} \langle i|j\rangle \langle k|l\rangle + \langle i|k\rangle \langle j|l\rangle + \langle i|l\rangle \langle j|k\rangle &= 0 \\ [i|j] [k|l] + [i|k] [j|l] + [i|l] [j|k] &= 0 \end{aligned} \quad (6.15)$$

Let us now set to work on an explicit representation for the angle and square brackets. Both of them are solutions to the massless Dirac equation and, therefore, can be represented either as a single four-component Dirac spinor or in terms of 2-component Weyl spinors:

$$\begin{aligned} |i\rangle &= u_+(p_i) = \lambda_\alpha(p_i), \quad \alpha = 1, 2 \\ \langle i| &= \bar{u}_-(p_i) = \lambda^\alpha(p_i), \quad \alpha = 1, 2 \\ |i] &= u_-(p_i) = \bar{\lambda}^{\dot{\alpha}}(p_i), \quad \dot{\alpha} = 1, 2 \\ [i| &= \bar{u}_+(p_i) = \bar{\lambda}_{\dot{\alpha}}(p_i), \quad \dot{\alpha} = 1, 2 \end{aligned} \quad (6.16)$$

the usual convention for undotted indices is to regard upper indices as row indices and lower indices as column ones, and doing the inverse for dotted indices.

The indices are raised and lowered as customary in 2-component notation:

$$\begin{aligned}\lambda^\alpha &= \varepsilon^{\alpha\beta} \lambda_\beta & \lambda_\alpha &= \varepsilon_{\alpha\beta} \lambda^\beta \\ \bar{\lambda}^{\dot{\alpha}} &= \varepsilon^{\dot{\alpha}\dot{\beta}} \bar{\lambda}_{\dot{\beta}} & \bar{\lambda}_{\dot{\alpha}} &= \varepsilon_{\dot{\alpha}\dot{\beta}} \bar{\lambda}^{\dot{\beta}}\end{aligned}$$

with:

$$\varepsilon^{\alpha\beta} = \varepsilon^{\dot{\alpha}\dot{\beta}} = \begin{pmatrix} 0 & 1 \\ -1 & 0 \end{pmatrix} \quad \varepsilon_{\alpha\beta} = \varepsilon_{\dot{\alpha}\dot{\beta}} = \begin{pmatrix} 0 & -1 \\ 1 & 0 \end{pmatrix}$$

and the inner products of spinors can be expanded in components:

$$\begin{aligned}\langle i|j\rangle &= \lambda^\alpha \eta_\alpha = \varepsilon^{\alpha\beta} \lambda_\beta \eta_\alpha = \eta_1 \lambda_2 - \lambda_1 \eta_2 \\ [i|j] &= \bar{\lambda}_{\dot{\alpha}} \bar{\eta}^{\dot{\alpha}} = \varepsilon_{\dot{\alpha}\dot{\beta}} \bar{\lambda}^{\dot{\beta}} \bar{\eta}^{\dot{\alpha}} = \bar{\lambda}^1 \bar{\eta}^2 - \bar{\eta}^1 \bar{\lambda}^2\end{aligned} \quad (6.17)$$

In the Weyl representation the Dirac γ -matrices are decomposed in terms of the Pauli matrices $\sigma_{\alpha\beta}^\mu$:

$$\sigma_{\alpha\beta}^0 = \begin{pmatrix} 1 & 0 \\ 0 & 1 \end{pmatrix}, \quad \sigma_{\alpha\beta}^1 = \begin{pmatrix} 0 & 1 \\ 1 & 0 \end{pmatrix}, \quad \sigma_{\alpha\beta}^2 = \begin{pmatrix} 0 & -i \\ i & 0 \end{pmatrix}, \quad \sigma_{\alpha\beta}^3 = \begin{pmatrix} 1 & 0 \\ 0 & -1 \end{pmatrix} \quad (6.18)$$

we can contract these with a four-vector p^μ and obtain:

$$p_\mu \sigma_{\alpha\beta}^\mu = \begin{pmatrix} p^0 - p^3 & -(p^1 - ip^2) \\ -(p^1 + ip^2) & p^0 + p^3 \end{pmatrix} \quad (6.19)$$

If we compute the determinant of this matrix we find:

$$\text{Det} [p_\mu \sigma_{\alpha\beta}^\mu] = p_\mu p^\mu = p^2 \quad (6.20)$$

Since the momenta are massless, the determinant vanishes and thus the matrix is rank-1. It can therefore be written as the outer product of two Weyl spinors:

$$p_\mu \sigma_{\alpha\beta}^\mu = \lambda_\alpha \bar{\lambda}_\beta \quad (6.21)$$

and this yields an explicit expression for both the chiral and anti-chiral spinors, i.e. angle and square brackets:

$$|i\rangle = \lambda_\alpha(p_i) = \begin{pmatrix} \sqrt{p_i^0 + p_i^3} \\ \frac{p_i^1 + ip_i^2}{\sqrt{p_i^0 + p_i^3}} \end{pmatrix} \quad [i] = \bar{\lambda}_{\dot{\alpha}}(p_i) = \left(\sqrt{p_i^0 + p_i^3}, \frac{p_i^1 - ip_i^2}{\sqrt{p_i^0 + p_i^3}} \right) \quad (6.22)$$

Proving this is straightforward, keeping in mind $p_i^2 = 0$.

One could contract 6.19 with $(\bar{\sigma}^\nu)^{\dot{\alpha}\beta} = \varepsilon^{\dot{\alpha}\dot{\gamma}} \varepsilon^{\beta\delta} \sigma_{\delta\dot{\gamma}}^\nu$ and, with some 2-component algebra, obtain a representation for the momentum p_i^μ in terms of spinors:

$$\bar{\lambda}_{\dot{\alpha}}(p_i) (\bar{\sigma}^{\mu})^{\dot{\alpha}\beta} \lambda_{\beta}(p_i) = 2p_i^{\mu} \quad (6.23)$$

which is basically the Gordon identity in 2-component notation.

Given the Fierz Identity for Pauli matrices: $\sigma_{\alpha\dot{\beta}}^{\mu} (\bar{\sigma}^{\mu})^{\dot{\alpha}\beta} = \delta_{\alpha}^{\dot{\alpha}} \delta_{\dot{\beta}}^{\beta}$ we can express kinematic invariants in terms of spinors:

$$\begin{aligned} s_{ij} = 2p_i \cdot p_j &= \frac{1}{2} \bar{\lambda}_{\dot{\alpha}}(p_i) (\bar{\sigma}^{\mu})^{\dot{\alpha}\alpha} \lambda_{\alpha}(p_i) \bar{\lambda}_{\dot{\beta}}(p_j) (\bar{\sigma}^{\mu})^{\dot{\beta}\beta} \lambda_{\beta}(p_j) \\ &= \lambda_{\alpha}(p_i) \lambda^{\alpha}(p_j) \bar{\lambda}_{\dot{\alpha}}(p_j) \bar{\lambda}^{\dot{\alpha}}(p_i) \\ &\implies s_{ij} = \langle i|j\rangle [j|i] \end{aligned} \quad (6.24)$$

where $s_{ij} := (p_i + p_j)^2$ is a generalised Mandelstam variable.

One final comment is in order: any four-momentum p_i^{μ} can be re-constructed just from the knowledge of the two spinors of opposite helicity $|i\rangle, |i]$ by virtue of equation 6.12, although the resulting four-vector is in general complex.

Moreover, the spinor-helicity formalism encodes the on-shell condition ($p_i^2 = 0$) naturally by construction.

6.2.2 Massless vector boson representation

Using the same formalism one can construct a representation for massless chiral vector bosons, namely for their polarisation vectors:

$$\begin{aligned} \varepsilon_{+}^{\mu}(p_i, q) &:= -\frac{\langle i|\gamma^{\mu}|q\rangle}{\sqrt{2}\langle qi\rangle} & \varepsilon_{-}^{\mu}(p_i, q) &:= \frac{[i|\gamma^{\mu}|q\rangle}{\sqrt{2}\langle qi\rangle} \\ \varepsilon_{+}^{*\mu}(p_i, q) &:= \frac{\langle q|\gamma^{\mu}|i\rangle}{\sqrt{2}\langle qi\rangle} & \varepsilon_{-}^{*\mu}(p_i, q) &:= -\frac{[q|\gamma^{\mu}|i\rangle}{\sqrt{2}\langle qi\rangle} \end{aligned}$$

The four-vector q_i^{μ} is an auxiliary reference vector.

In this representation, the polarisation vectors behave as they should:

$$(\varepsilon_{\pm}) = \varepsilon_{\mp} \quad \varepsilon_{\pm} \cdot \varepsilon_{\pm} = 0 \quad \varepsilon_{\pm} \cdot \varepsilon_{\mp} = -1 \quad (6.25)$$

$$\varepsilon_{+}^{\mu} \varepsilon_{+}^{\nu} + \varepsilon_{-}^{\mu} \varepsilon_{-}^{\nu} = -g^{\mu\nu} + \frac{p_i^{\mu} q^{\nu} + p_i^{\nu} q^{\mu}}{p_i \cdot q} \quad (6.26)$$

One could prove that, given two choices for such a vector a^{μ}, b^{μ} the difference between two polarisation vectors constructed using them is proportional to p_i^{μ} itself.

On the grounds of the invariance of Feynman amplitudes under the gauge transformation $\varepsilon^{\mu}(p_i) \rightarrow \varepsilon^{\mu}(p_i) + \alpha_i p_i^{\mu}$, one can claim that the choice of reference vectors used in the helicity representation is completely arbitrary.

Moreover, these definitions are fit for representing transverse polarisation vectors since, by virtue of 6.11, they are orthogonal to the momentum:

$$\varepsilon_{\pm}(p_i, q) \cdot p_i = 0 \quad (6.27)$$

6.2.3 Little-group scaling

One final noteworthy feature of the spinor-helicity formalism is the invariance of equation 6.12 under the following re-scaling transformation of the spinors:

$$\begin{aligned} |i\rangle &\longrightarrow t_i |i\rangle \\ |i] &\longrightarrow t_i^{-1} |i] \end{aligned} \tag{6.28}$$

This re-scaling is a transformation that leaves invariant the four-momentum of an on-shell particle: in the language of group theory such transformations are known as *Little group transformations*.

The parameter t_i is in fact a complex phase $e^{i\theta_i}$, this is because the little-group scaling needs to preserve the reality of the four-momentum p^μ and therefore the relation $|i]^\dagger = |i\rangle$.

Similarly, relation 6.21 is defined up to complex-phase transformation of the spinors therein. This re-scaling is of course just the little group action upon massless particles which, by definition, leaves momenta invariant.

The formalism of spinor-helicity has been implemented in the MATHEMATICA package S@M [140], enabling the use of complex-spinor algebra and the manipulation and numerical evaluation of spinorial objects.

6.3 Momentum twistors

As we showed previously, quantities that possess n -point kinematics such as scattering amplitudes depend on $(3n - 10)$ parameters, where this number is the by-product of general requirements such as on-shellness, momentum conservation and the dimension of space-time (through the vanishing of Gram determinants).

The Mandelstam variables, however, are nothing more than a labelling standard for these parameters, written in terms of external momenta. The influence of the aforementioned formal properties is only reflected in the number of independent Mandelstams.

A more sophisticated formalism, encoding naturally these generic features, would go a long way towards optimising the handling and computation of scattering amplitudes.

In the case of Adaptive Integrand Decomposition this is immediately obvious, as the application of the $D = D_{\parallel} + D_{\perp}$ regularisation prescription depends explicitly on the external kinematics. Moreover, the new variables parametrising the kinematics will turn out to be ratios of momentum-related quantities. The simple fact that these new parameters are rational objects is highly-desirable for the sake of numerical stability of the AID algorithm.

In this section we shall detail the construction of this novel formalism, following [135, 141–143].

6.3.1 Dual variables

Our starting point is to study momentum conservation by adopting a "geometrical" perspective. Let us consider 6 four-momenta $(p_1^\mu, \dots, p_6^\mu)$ under the condition $p_1 + \dots + p_6 = 0$. By plotting the vectors sequentially, the conservation condition entails that these form a closed loop:

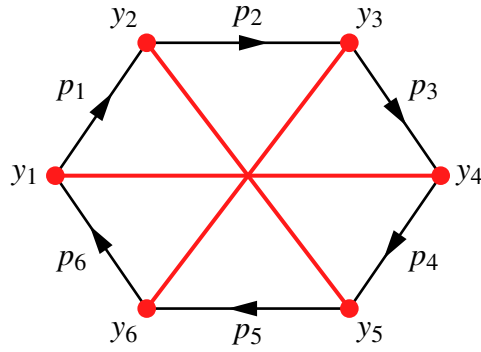


Figure 6.1: Relationship between the momentum four-vectors, arranged in a closed loop to represent momentum conservation, and the dual coordinates.

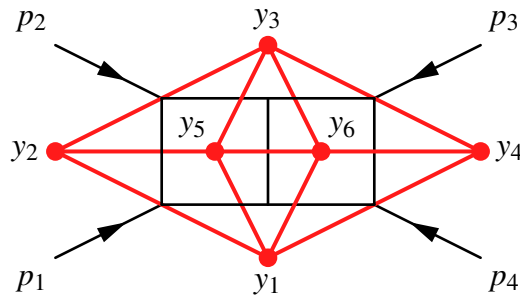
This contour can be described either by its edges (the four-momenta) or just as well by the vertices (y_1, \dots, y_6) . These coordinates can be interpreted as being *dual* to the momenta: by defining a *dual space* the momentum contour lying in p^μ -space generates an analogous lattice in this new space, represented by the coordinates $(y_1^\mu, \dots, y_6^\mu)$.

They are related to the original momenta by the relation:

$$p_i^\mu = (y_i - y_{i+1})^\mu \quad (6.29)$$

These coordinates are not ordinary space-time coordinates, in particular they possess mass-dimension 1. Momentum conservation in p -space is expressed in dual space with the periodicity condition on these coordinates: $y_{n+1} \equiv y_1$. The dual coordinates thus embed momentum conservation naturally.

Let us now consider the more involved case of a four-point two-loop Feynman diagram:



We defined six dual coordinates, corresponding to the four external momenta (p_1, \dots, p_4) and the two loop momenta q, k .

Let us write down the Feynman integral corresponding to this topology, i.e. neglecting the numerator:

$$\int \frac{d^D k d^D l}{\pi^{D/2}} \frac{1}{k^2 (k + p_1)^2 (k + p_1 + p_2)^2 l^2 (l - k)^2 (l + p_1 + p_2)^2 (l - p_4)^2} \quad (6.30)$$

The dual-coordinate representation of this integral is obtained by writing the four external momenta and the loop momenta, respectively, as:

$$\begin{aligned} p_i^\mu &= (y_i - y_{i+1})^\mu \\ k^\mu &= (y_5 - y_1)^\mu \\ l^\mu &= (y_6 - y_1)^\mu \end{aligned} \quad (6.31)$$

and by defining the dual-space counterparts of the Mandelstam variables, which correspond to distances in dual space:

$$y_{ij}^2 := (y_i - y_j)^2 \equiv (p_i + p_{i+1} + \dots + p_{j-1})^2 \quad (6.32)$$

$$\int \frac{d^D x_5 d^D x_6}{\pi^{D/2}} \frac{1}{(y_5 - y_1)^2 (y_5 - y_1 + y_1 - y_2)^2 (y_5 - y_1 + y_1 - y_2 + y_2 - y_3)^2} \times \quad (6.33)$$

$$\times \frac{1}{(y_6 - y_1)^2 (y_6 - y_1 + y_1 - y_2 + y_2 - y_3)^2 (y_6 - y_1 + y_1 - y_4)^2} \quad (6.34)$$

$$= \int \frac{d^D x_5 d^D x_6}{\pi^{D/2}} \frac{1}{y_{51}^2 y_{52}^2 y_{53}^2 y_{61}^2 y_{65}^2 y_{63}^2 y_{64}^2} \quad (6.35)$$

where, in performing the change of variables, we exploited the shift-invariance of the measures. This shows how a Feynman integral parametrised in terms of dual variables depends only on the distances y_{ij}^2 .

Let us highlight a point related to the final remark of section 6.2.1. From figure 6.1, starting from a set of n dual coordinates (y_1, \dots, y_n) the set of n momenta can be immediately extracted since $p_i^\mu = (y_i - y_{i+1})^\mu$.

The reverse is not true, since in fact figure 6.1 conceals an important feature of the dual coordinates:

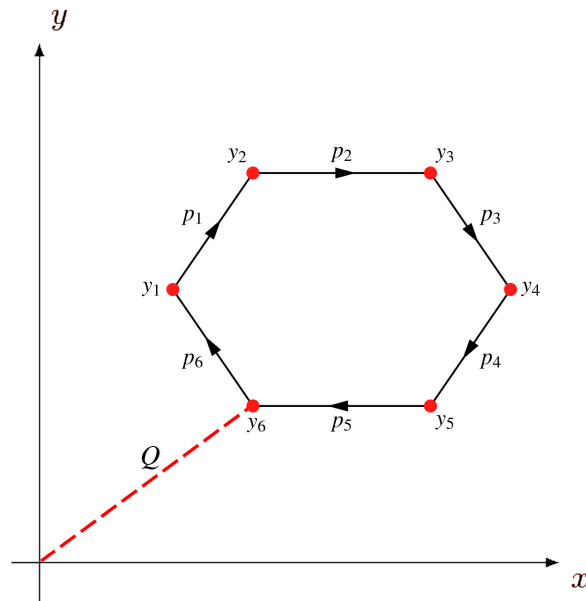


Figure 6.2: Similar to figure 6.1, except now the definition of the dual coordinates depends directly on an arbitrary vector Q .

Figure 6.2 makes it clear how the knowledge of n four-momenta is by itself not sufficient to define the dual coordinates unambiguously: their ultimate position in dual space will inevitably be defined up to translations by a vector Q . The key point is that Q is arbitrary, and so there is an inherent freedom in defining the dual coordinates. Regardless of the ambiguity, the parametrisation is a good one as long as it yields back the correct set of four-momenta.

6.3.2 Twistor parametrisation

Our goal now is to give a spinorial representation of the dual coordinates. We proceed by contracting the relation $p_i^\mu = (y_i - y_{i+1})^\mu$ with Dirac γ -matrices²⁰, introducing a massless spinor $|i\rangle$ and using the Dirac equation:

$$\not{p}_i |i\rangle = (\not{y}_i - \not{y}_{i+1}) |i\rangle = 0 \quad (6.36)$$

and defining the new spinor variable through the so-called *incidence relation*

$$|\xi_i] := \not{y}_i |i\rangle = \not{y}_{i+1} |i\rangle \quad (6.37)$$

The newly-introduced spinors can be written in two-component notation:

$$\begin{aligned} |i\rangle &= \lambda_\alpha (p_i) \equiv (\lambda_i)_\alpha \\ |\xi_i] &= \xi_i^{\dot{\beta}} = -(y_i)_\mu (\bar{\sigma}^\mu)^{\dot{\beta}\alpha} (\lambda_i)_\alpha \end{aligned} \quad (6.38)$$

Let us now write down an identity and manipulate it with a little two-component algebra:

$$\begin{aligned} y_i^\nu &= (y_i)_\mu \eta^{\mu\nu} = (y_i)_\mu \eta^{\mu\nu} \frac{2\langle i|i-1\rangle}{2\langle i|i-1\rangle} \\ &= (y_i)_\mu \frac{2\eta^{\mu\nu} (\lambda_i)^\alpha (\lambda_{i-1})_\alpha}{2\langle i|i-1\rangle} = (y_i)_\mu \frac{(\lambda_i)^\alpha [2\eta^{\mu\nu} \delta_\alpha^\beta] (\lambda_{i-1})_\beta}{2\langle i|i-1\rangle} = (y_i)_\mu \frac{(\lambda_i)^\alpha [\sigma^\mu \bar{\sigma}^\nu + \sigma^\nu \bar{\sigma}^\mu]_\alpha^\beta (\lambda_{i-1})_\beta}{2\langle i|i-1\rangle} \\ &= (y_i)_\mu \frac{(\lambda_i)^\alpha (\sigma^\mu)_{\alpha\dot{\gamma}} (\bar{\sigma}^\nu)^{\dot{\gamma}\beta} (\lambda_{i-1})_\beta + (\lambda_i)^\alpha (\sigma^\nu)_{\alpha\dot{\gamma}} (\bar{\sigma}^\mu)^{\dot{\gamma}\beta} (\lambda_{i-1})_\beta}{2\langle i|i-1\rangle} \\ &= (y_i)_\mu \frac{(\lambda_i)^\alpha \varepsilon_{\alpha\delta} \varepsilon_{\dot{\gamma}\dot{\eta}} (\bar{\sigma}^\mu)^{\dot{\eta}\delta} \varepsilon^{\beta\rho} \varepsilon^{\dot{\gamma}\dot{\chi}} (\sigma^\nu)_{\rho\dot{\chi}} (\lambda_{i-1})_\beta + (\lambda_i)^\alpha (\sigma^\nu)_{\alpha\dot{\gamma}} (\bar{\sigma}^\mu)^{\dot{\gamma}\beta} (\lambda_{i-1})_\beta}{2\langle i|i-1\rangle} \\ &= (y_i)_\mu \frac{- (\lambda_i)^\alpha \varepsilon_{\alpha\delta} (\bar{\sigma}^\mu)^{\dot{\eta}\delta} \varepsilon^{\beta\rho} \delta_{\dot{\eta}}^{\dot{\chi}} (\sigma^\nu)_{\rho\dot{\chi}} (\lambda_{i-1})_\beta + (\lambda_i)^\alpha (\sigma^\nu)_{\alpha\dot{\gamma}} (\bar{\sigma}^\mu)^{\dot{\gamma}\beta} (\lambda_{i-1})_\beta}{2\langle i|i-1\rangle} \\ &= (y_i)_\mu \frac{+ (\lambda_{i-1})^\rho \varepsilon^{\beta\rho} (\sigma^\nu)_{\rho\dot{\eta}} (\bar{\sigma}^\mu)^{\dot{\eta}\delta} (\lambda_i)^\alpha \varepsilon_{\alpha\delta} + (\lambda_i)^\alpha (\sigma^\nu)_{\alpha\dot{\gamma}} (\bar{\sigma}^\mu)^{\dot{\gamma}\beta} (\lambda_{i-1})_\beta}{2\langle i|i-1\rangle} \\ &= (y_i)_\mu \frac{- (\lambda_{i-1})^\rho (\sigma^\nu)_{\rho\dot{\eta}} (\bar{\sigma}^\mu)^{\dot{\eta}\delta} (\lambda_i)_\delta + (\lambda_i)^\alpha (\sigma^\nu)_{\alpha\dot{\gamma}} (\bar{\sigma}^\mu)^{\dot{\gamma}\beta} (\lambda_{i-1})_\beta}{2\langle i|i-1\rangle} \\ &= \frac{(\lambda_{i-1})^\rho (\sigma^\nu)_{\rho\dot{\eta}} \left[- (y_i)_\mu (\bar{\sigma}^\mu)^{\dot{\eta}\delta} (\lambda_i)_\delta \right] - (\lambda_i)^\alpha (\sigma^\nu)_{\alpha\dot{\gamma}} \left[- (y_i)_\mu (\bar{\sigma}^\mu)^{\dot{\gamma}\beta} (\lambda_{i-1})_\beta \right]}{2\langle i|i-1\rangle} \\ &\implies y_i^\nu = \frac{\langle i|\sigma^\nu|\xi_{i-1}] - \langle i-1|\sigma^\nu|\xi_i]}{2\langle i-1|i\rangle} \end{aligned} \quad (6.39)$$

²⁰since we are dealing with massless two-component spinors we really mean Pauli σ -matrices, as mentioned in the previous section.

The last expression defines a map between coordinates, useful to perform changes of variables:

$$\{y_i\} \rightarrow \{Z_i\} := \left\{ \begin{pmatrix} (\lambda_i)_\alpha \\ (\xi_i)_\beta \end{pmatrix} \right\} = \left\{ \begin{pmatrix} |i\rangle \\ |\xi_i] \end{pmatrix} \right\} \quad (6.40)$$

The new four-component variables Z_i are known as *Momentum twistors*.

The twistors enjoy special properties owing to their definition. First, they manifest Poincaré symmetry by construction. Then, from the incidence relation, under the little-group scaling of the spinors 6.28 they transform linearly:

$$Z_i = \begin{pmatrix} |i\rangle \\ |\xi_i] \end{pmatrix} \longrightarrow \begin{pmatrix} t_i |i\rangle \\ t_i |\xi_i] \end{pmatrix} = t_i Z_i \quad (6.41)$$

Tracing these steps backwards, we can say that a linear re-scaling of the twistors Z_i leaves the incidence relation invariant and, by extension, the relation between twistors and momenta.

For this reason the twistors are defined *projectively* [141] up to the phase t_i , and thus they enjoy a $U(1)$ symmetry (where the parameter is t_i itself). Being there n spinors to re-scale there will actually be $n \times U(1)$ symmetry groups.

The n four-momenta will obey momentum conservation (since the twistor variables inherit the properties of the dual variables), and the spinor-helicity formalism will ensure the on-shell condition. By a similar token, the momentum twistors show the same ambiguity/freedom in the definition of their components of the dual variables. For this reason writing down n twistors really corresponds to determining $4n$ components, which are collectively called *twistor variables*.

The $4n$ twistor variables are not all independent because of the symmetry relations they must obey: 10 constraints are generated by Poincaré symmetry, as well as n constraints from the n $U(1)$ phase rotations.

The final degrees-of-freedom count is then:

$$4n - 10 - n = 3n - 10 \quad (6.42)$$

which is precisely the same number of free-parameters necessary to describe n -point kinematics ($n \geq 4$), in the case of massless external momenta.

These twistor variables can however be chosen in many ways, giving rise to different parametrisations.

Starting from n momentum twistors (Z_1, \dots, Z_n) one can re-construct the associated n four-momenta from the knowledge of $|i\rangle$ and the following definition:

$$[i] = \frac{\langle i+1|i\rangle [\xi_{i-1}] + \langle i|i-1\rangle [\xi_{i+1}] + \langle i-1|i+1\rangle [\xi_i]}{\langle i-i|i\rangle \langle i|i+1\rangle} \quad (6.43)$$

and finally taking advantage of the Gordon identity 6.12 to define each momentum.

4-point twistor parametrisation

Four momentum twistors (Z_1, Z_2, Z_3, Z_4) are completely defined by $3 \times 4 - 10 = 2$ twistor variables, which we label (z_1, z_2) . One possible parametrisation [139] can be chosen as:

$$(Z_1 Z_2 Z_3 Z_4) = \begin{pmatrix} |1\rangle & |2\rangle & |3\rangle & |4\rangle \\ |\xi_1] & |\xi_2] & |\xi_3] & |\xi_4] \end{pmatrix} = \begin{pmatrix} 1 & 0 & \frac{1}{z_1} & \frac{1+z_2}{z_1 z_2} \\ 0 & 1 & 1 & 1 \\ 0 & 0 & -1 & -1 \\ 0 & 0 & 0 & 1 \end{pmatrix} \quad (6.44)$$

This parametrisation fixes the square brackets $|i]$ as:

$$(|1] \ |2] \ |3] \ |4]) = \begin{pmatrix} -1 & -z_1 & z_1 & 0 \\ 1 & 1 & z_1 z_2 & -z_1 z_2 \end{pmatrix} \quad (6.45)$$

from 6.17, yields the following replacement rules for spinor products:

$$\left\{ \begin{aligned} \langle 1|2\rangle &\rightarrow -1, [2|1] \rightarrow -z[1], \langle 1|3\rangle \rightarrow -1, [3|1] \rightarrow z_1(1+z_2), \\ \langle 1|4\rangle &\rightarrow -1, [4|1] \rightarrow -z_1 z[2], \langle 2|3\rangle \rightarrow \frac{1}{z_1}, [3|2] \rightarrow z_1^2 z[2], \\ \langle 2|4\rangle &\rightarrow \frac{1+z_2}{z_1 z_2}, [4|2] \rightarrow -z_1^2 z[2], \langle 3|4\rangle \rightarrow \frac{1}{z_1 z_2}, [4|3] \rightarrow z_1^2 z_2 \end{aligned} \right\} \quad (6.46)$$

By recalling $s_{ij} = \langle i|j\rangle [j|i]$ one writes the generalised Mandelstam variables in terms of twistors:

$$\begin{aligned} s &\equiv s_{12} = \langle 1|2\rangle [2|1] = z_1 \\ t &\equiv s_{14} = \langle 1|4\rangle [4|1] = z_1 z_2 \end{aligned} \quad (6.47)$$

and from this it is possible to parametrise the twistors in terms of the Mandelstam variables:

$$\begin{aligned} z_1 &\equiv s \\ z_2 &\equiv \frac{t}{s} \end{aligned} \quad (6.48)$$

This result is not surprising: at the four-point level the situation is straightforward enough that using two Mandelstam variables is apparently just as good as employing the more sophisticated twistor technology. Parametrising with twistors, however, encodes naturally all the kinematic properties that would need to be checked forcibly if one chooses the Mandelstam picture.

As stated, this is not the only possible parametrisation at 4-point. An alternative one [135, 136] provides an even more straightforward connection between the twistor variables and the Mandelstams.

5-point twistor parametrisation

Five-point momentum twistors $(Z_1, Z_2, Z_3, Z_4, Z_5)$ are completely defined by $3 \times 5 - 10 = 5$ twistor variables, which we label (z_1, \dots, z_5) . One possible twistor parametrisation is [139]:

$$(Z_1 Z_2 Z_3 Z_4 Z_5) = \left(\begin{array}{c|c|c|c|c} |1\rangle & |2\rangle & |3\rangle & |4\rangle & |5\rangle \\ \hline |\xi_1] & |\xi_2] & |\xi_3] & |\xi_4] & |\xi_5] \end{array} \right) = \begin{pmatrix} 1 & 0 & \frac{1}{z_1} & \frac{1+z_2}{z_1 z_2} & \frac{1+z_3(1+z_2)}{z_1 z_2 z_3} \\ 0 & 1 & 1 & 1 & 1 \\ 0 & 0 & 0 & \frac{z_4}{z_2} & 1 \\ 0 & 0 & 1 & 1 & 1 - \frac{z_5}{z_4} \end{pmatrix} \quad (6.49)$$

This parametrisation fixes the square brackets $|i]$ as:

$$\left(\begin{array}{c|c|c|c|c} |1] & |2] & |3] & |4] & |5] \\ \hline \frac{z_5}{z_4} - 1 & -z_1 & z_1 & \frac{z_1 z_2 z_3 z_5}{z_4} & -\frac{z_1 z_2 z_3 z_5}{z_4} \\ 1 & 0 & z_1 z_4 & z_1 (z_2 z_3 - z_4 (1 + z_3)) & z_1 z_3 (z_4 - z_2) \end{array} \right) \quad (6.50)$$

and the spinor products:

$$\left\{ \begin{array}{l} \langle 1|2\rangle \rightarrow -1, [2|1] \rightarrow -z[1], \langle 1|3\rangle \rightarrow -1, [3|1] \rightarrow z_1(1 + z_4 - z_5), \\ \langle 1|4\rangle \rightarrow -1, [4|1] \rightarrow -z[1](-z_2 z[3] + (1 + z_3)(z_4 - z_5)), \\ \langle 1|5\rangle \rightarrow -1, [5|1] \rightarrow -z_1 z[3](z_2 - z_4 + z_5), \langle 2|3\rangle \rightarrow \frac{1}{z_1}, [3|2] \rightarrow z_1^2 z[4], \\ \langle 2|4\rangle \rightarrow \frac{(1 + z_2)}{(z_1 z_2)}, [4|2] \rightarrow z_1^2 (z_2 z_3 - (1 + z_3)z[4]), \\ \langle 2|5\rangle \rightarrow \frac{(1 + z_3 + z_2 z_3)}{(z_1 z_2 z[3])}, [5|2] \rightarrow -z[1]^2 z_3 (z_2 - z_4), \\ \langle 3|4\rangle \rightarrow \frac{1}{(z_1 z_2)}, [4|3] \rightarrow z_1^2 ((1 + z_3)z_4 + z_2 z[3](-1 + z_5)), \\ \langle 3|5\rangle \rightarrow \frac{(1 + z_3)}{(z_1 z_2 z[3])}, [5|3] \rightarrow -z[1]^2 z_3 (z_4 + z_2(-1 + z_5)), \\ \langle 4|5\rangle \rightarrow \frac{1}{(z_1 z_2 z[3])}, [5|4] \rightarrow z_1^2 z_2 z_3 z_5 \end{array} \right\} \quad (6.51)$$

The five independent Mandelstam variables chosen previously in this chapter are:

$$\begin{aligned} s_{12} &= \langle 1|2\rangle [2|1] = z_1 \\ s_{23} &= \langle 2|3\rangle [3|2] = z_1 z_4 \\ s_{34} &= \langle 3|4\rangle [4|3] = \frac{z_1 (z_4 (1 + z_3) + z_2 z_3 (-1 + z_5))}{z_2} \\ s_{45} &= \langle 4|5\rangle [5|4] = z_1 z_5 \\ s_{51} &= \langle 5|1\rangle [1|5] = z_1 z_3 (z_2 - z_4 + z_5) \end{aligned} \quad (6.52)$$

Alternative twistor parametrisations of five-point kinematics are possible, such as those presented in [136, 144].

A generic template for $n \geq 5$ can be defined [139, 145]. These twistor parametrisations, along with all the tools required to write kinematics and scalar products in their terms, have been implemented in a MATHEMATICA package T@M [146] which relies on the aforementioned S@M for the spinor-helicity technology.

Chapter 7

The NNLO real-virtual corrections to muon-electron scattering

In the final sections of chapter 1 it has been made clear how the Quantum Electrodynamics corrections to muon-electron scattering $\mu^\pm e^- \rightarrow \mu^\pm e^-$ are of crucial importance to the *MuonE* experiment, and that these corrections must be evaluated up to NNLO in perturbation theory to be consistent with the desired experimental accuracy.

A full NNLO estimate of μe scattering is still missing, since the process has generally been the subject of little attention from the theoretical standpoint. Historically the focus was on the QED NLO differential cross-section [109–111] (a full differential Monte Carlo result was obtained in [112]) and on the inclusion of the Electroweak sector [147–149]. Some of the two-loop NNLO corrections to Bhabha scattering in QED [113–117] can be applied to muon-electron scattering, as can some of the diagrams participating in heavy-to-light quark decay [118] and $t\bar{t}$ -production [119].

The first steps towards the full NNLO QED corrections were the calculations of planar and non-planar two-loop Feynman diagrams [10–12], which constitute the fully-virtual radiative corrections at this order in perturbation theory. For these calculations Integration-by-parts-identities [18, 150] were employed to identify 65 Master Integrals which were computed using the *Differential equations* method [128, 151]. As mentioned, these calculations were carried out in the massless-electron approximation $m_e = 0$ [10].

This thesis will focus on the NNLO real-virtual corrections, that is, $\mu e \rightarrow \mu e$ at one-loop with a real photon radiated in the final states²¹. The various kinds of diagrams that participate are represented in 7.34. The square amplitudes to be computed correspond to these diagrams interfered with the four tree-level real-radiation diagrams of 7.18.

In preparation for the task of computing the NNLO corrections, some preliminary work was done at LO and NLO orders to acquire familiarity in carrying out automatic computations in Quantum Field Theory and to re-obtain some known results.

We will study muon-electron scattering with the following labelling convention for the particles' momenta:

$$\mu^-(p_4) + e^-(p_1) \longrightarrow \mu^-(p_3) + e^-(p_2) \quad (7.1)$$

in this convention all momenta are defined positively as incoming.

²¹These are distinct from the fully real corrections with no loops but two photons radiated from a tree-level diagram.

We will mention here that all the Feynman diagrams relevant to a process at a given loop order and their relative Feynman square amplitudes have been computed using the MATHEMATICA packages FEYNARTS [134] and FEYNCALC [50, 51] in combination.

7.1 Calculations with FEYNCALC

FEYNCALC is a useful tool to generate Feynman amplitudes and perform calculations with them. It supports basic one-loop calculation capabilities through its implementation of Passarino-Veltman (PV) decomposition and the evaluation of the scalar function generated. For consistency with higher-order calculations, all the square amplitude including the tree-level one have been calculated in D space-time dimensions, and furthermore we keep track of the electron's mass m_e in addition to the muon's m_μ .

7.1.1 Leading Order

At leading order (LO) the only amplitude present (labelled with \mathcal{M}_0) is represented by the tree-level muon-electron scattering diagram:

$$\begin{array}{c}
 \mu^- \quad p_4 \quad \mu^- \quad p_3 \\
 \swarrow \quad \searrow \\
 \gamma \\
 \swarrow \quad \searrow \\
 e^- \quad p_1 \quad e^- \quad p_2
 \end{array}
 \quad := i\mathcal{M}_0 \quad (7.2)$$

With this particular labelling of particles the usual Mandelstam variables are written as:

$$s := (p_1 + p_4)^2 \quad t := (p_1 + p_2)^2 \quad u := (p_1 + p_3)^2 \quad (7.3)$$

this definition is of course compatible with 6.4.

The Leading order contribution is then the contraction of the leading-order amplitude with itself, with a $\frac{1}{4}$ factor to account for the average over the initial spin states of the e^- and μ :

$$\chi_0 := \frac{1}{4} \mathcal{M}_0 \mathcal{M}_0^* = \frac{e^4 \left[(D-2)t^2 + 4(m_e^2 + m_\mu^2 - s)^2 + 4st \right]}{t^2} \quad (7.4)$$

We also write down the $D \rightarrow 4$ limit of this quantity, useful for future reference. This simply corresponds to setting D to 4 since there are no divergent terms:

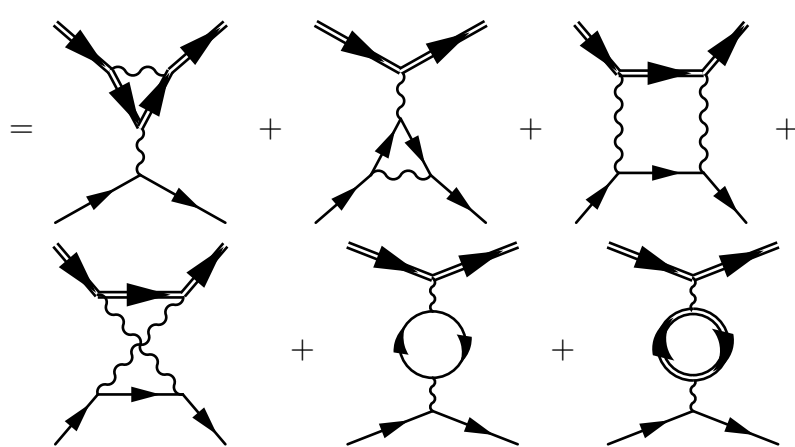
$$\chi'_0 := \frac{1}{4} \mathcal{M}_0 \mathcal{M}_0^* \Big|_{D \rightarrow 4} = \frac{e^4 \left[2t^2 + 4(m_e^2 + m_\mu^2 - s)^2 + 4st \right]}{t^2} \quad (7.5)$$

Setting $m_e = m_\mu = 0$ replicates the well-known formula:

$$\chi'_{0, m_e=m_\mu=0} = 2e^4 \frac{(s^2 + u^2)}{t^2} \quad (7.6)$$

7.1.2 Next-to-leading Order

At Next-to-leading order (NLO) the virtual corrections comprise six amplitudes: two vertex corrections (VC_μ, VC_e), two boxes (one planar Box and one crossed Box_x) and two vacuum-polarisations (VP_e, VP_μ). In figure 7.7 we listed these contributions and drawn their respective Feynman diagram and also introduced the label \mathcal{M}_1 for their collective amplitude.

$$i\mathcal{M}_1 = i\mathcal{M}_1^{VC\mu} + i\mathcal{M}_1^{VCe} + i\mathcal{M}_1^{Box} + i\mathcal{M}_1^{Box_x} + i\mathcal{M}_1^{VPe} + i\mathcal{M}_1^{VP\mu}$$

(7.7)

One then calculates the interference between these amplitudes and the tree-level amplitude, and since interferences are basically cross-products there should be a $\times 2$ factor in addition to $\frac{1}{4}$. Appendix C reports the lengthy results, evaluated using the built-in FEYN CALC Passarino-Veltman functions. To compress slightly the resulting expressions, we applied the following identity between PV functions (which is really an *Integration-by-parts identity*):

$$B_0(0, m_l, m_l) \rightarrow \frac{(D-2)A_0(m_l)}{2m_l} \quad (7.8)$$

Therein one can notice that the VP contributions correspond to the LO contribution times a factor that accounts for the bubble insertion, and that this insertion is identical in form between the muon and electron VP, differing only in the mass variable.

Additionally, a test of the renormalisability of Quantum Electrodynamics has been performed using FEYN CALC. The goal was, more specifically, to introduce counterterm diagrams and verify the cancellation of all ultra-violet (UV) divergences present at this level. Such divergences are given by the vacuum-polarisation diagrams (VP) and the vertex-correction diagrams (VC, also called "triangle diagrams").

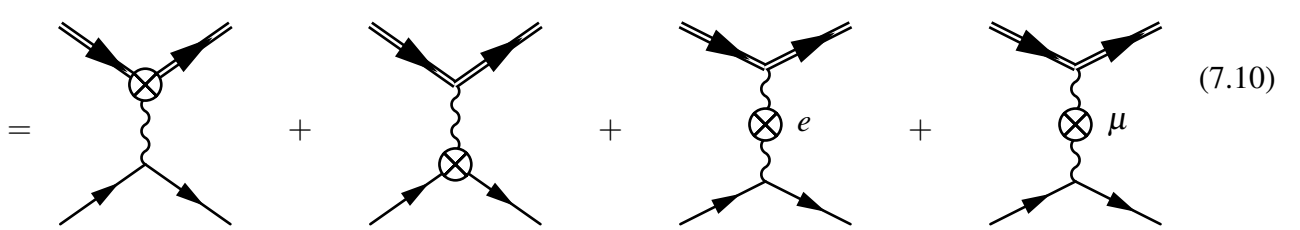
This can be seen by feeding the results of appendix C to the FEYN CALC function `PaXEvaluateUV`, which evaluates the PV scalar integrals and keeps only the ultraviolet-divergent contribution, expressing it in terms of the divergent object $\Delta_{UV} \sim \frac{1}{\epsilon_{UV}}$ and the numerical factors γ and $\log(4\pi)$ ²²:

²²These come from the explicit evaluation of Feynman loop integrals using Dimensional regularisation, as detailed in many textbooks. They are kept for compatibility with various different renormalisation schemes, as some define the counterterms ad-hoc to cancel the term proportional to Δ_{UV} only while others also cancel out everything proportional to these numerical factors.

$$\begin{aligned}
 \left[2 \times \frac{1}{4} \mathcal{M}_1^{VC\mu} \mathcal{M}_0^* \right] |_{UV} &= 2e^2 (\Delta_{UV} + \gamma - \log(4\pi)) \chi'_0, \\
 \left[2 \times \frac{1}{4} \mathcal{M}_1^{VCe} \mathcal{M}_0^* \right] |_{UV} &= 2e^2 (\Delta_{UV} + \gamma - \log(4\pi)) \chi'_0, \\
 \left[2 \times \frac{1}{4} \mathcal{M}_1^{Box} \mathcal{M}_0^* \right] |_{UV} &= 0 \\
 \left[2 \times \frac{1}{4} \mathcal{M}_1^{Boxx} \mathcal{M}_0^* \right] |_{UV} &= 0 \\
 \left[2 \times \frac{1}{4} \mathcal{M}_1^{VPe} \mathcal{M}_0^* \right] |_{UV} &= -\frac{8}{3} e^2 (\Delta_{UV} + \gamma - \log(4\pi)) \chi'_0, \\
 \left[2 \times \frac{1}{4} \mathcal{M}_1^{VP\mu} \mathcal{M}_0^* \right] |_{UV} &= -\frac{8}{3} e^2 (\Delta_{UV} + \gamma - \log(4\pi)) \chi'_0
 \end{aligned} \tag{7.9}$$

Both the VP and the VC ultra-violet can be expressed in terms of the LO contribution in the $D \rightarrow 4$ limit. The two boxes do not bring any UV divergences but they do have an infra-red (IR) pole, as do the triangle corrections (since, by power-counting, it turns out they are *log-divergent*). We will say more on this shortly.

To cancel these divergences we introduce counterterm amplitudes, labelled by \mathcal{N} . They are represented by the following Feynman diagrams:

$$i\mathcal{N}_1 = i\mathcal{N}_1^{VC\mu} + i\mathcal{N}_1^{VCe} + i\mathcal{N}_1^{VPe} + i\mathcal{N}_1^{VP\mu}$$


$$= \text{[Diagram 1]} + \text{[Diagram 2]} + \text{[Diagram 3]} + \text{[Diagram 4]} \tag{7.10}$$

the last two diagram look identical, and we made explicit that one is a counter to the electron VP diagram and the other is for the muon.

The interference amplitudes for these diagrams are computed in exactly the same way as any ordinary Feynman diagram, provided one treats the counterterm insertions as brand-new interaction vertices and applies the correct Feynman rule. Using the rules listed in appendix D we get:

$$\begin{aligned}
 2 \times \frac{1}{4} \mathcal{N}_1^{VC\mu} \mathcal{M}_0^* &= [2 (\sqrt{Z_A} Z_e Z_\psi - 1) \chi_0] |_{l=\mu} \\
 2 \times \frac{1}{4} \mathcal{N}_1^{VCe} \mathcal{M}_0^* &= [2 (\sqrt{Z_A} Z_e Z_\psi - 1) \chi_0] |_{l=e} \\
 2 \times \frac{1}{4} \mathcal{N}_1^{VPe} \mathcal{M}_0^* &= [2 (Z_A - 1) \chi_0] |_{l=e} \\
 2 \times \frac{1}{4} \mathcal{N}_1^{VP\mu} \mathcal{M}_0^* &= [2 (Z_A - 1) \chi_0] |_{l=\mu}
 \end{aligned} \tag{7.11}$$

The label l indicates which mass parameters should be fed into the expression for the counterterms. All four interferences are basically a counterterm insertion on top of the LO contribution, this shouldn't come as a surprise.

Cancellation of UV divergence for Vacuum-Polarisation

All the counterterm square amplitude was taken and the renormalisation parameters Z_i rewritten as detailed in appendix D: $Z_i = 1 + \alpha \delta_i$ where α is a dummy parameter that we set to 1²³ and where the δ are replaced with their explicit expressions, specifying the lepton l as e or μ given the diagram with which they were paired.

The subtraction between the vacuum-polarisation diagram and the related counterterm diagram was evaluated with `PaXEvaluateUV`, and it was verified that the result yielded zero, indicating that no UV-divergent objects survive as expected.

The subtraction was then re-evaluated with `PaXEvaluate` to obtain explicitly the finite part of the PV functions, which constitutes the contribution to the cross-section of the renormalised VP diagrams. We list the resulting expression valid for both $l = e, \mu$, with the tree-level square amplitude χ_0 factored out:

$$2 \times \frac{1}{4} \left(\mathcal{M}_1^{VPl} \mathcal{M}_0^* - \mathcal{N}_1^{VPl} \mathcal{M}_0^* \right) = - \frac{8e^2 \left(t(12m_l^2 + 5t) + 3\sqrt{t(t - 4m_l^2)}(2m_l^2 + t) \log \left(\frac{\sqrt{t(t - 4m_l^2)} + 2m_l^2 - t}{2m_l^2} \right) \right)}{9t^2} \chi_0 \quad (7.12)$$

These expressions have been cross-checked with the results obtained by M.Vitti [107]. While we used the built-in `PaXEvaluate` function of `FEYNCalc` to compute explicitly the scalar integrals, his results have been evaluated first by using the IBP-identity 7.8 and then using the explicit expressions for the PV functions given in appendix B of [107].

To compare the results we defined a phase-space point PS_{point} for the mass parameters and the Mandelstam variables:

$$PS_{point} := \left\{ t = \frac{1}{\sqrt{13}}, s = \frac{1}{\sqrt{17}}, m_e^2 = \frac{1}{206}, m_\mu^2 = 1 \right\} \quad (7.13)$$

The comparison was then performed, and perfect agreement was found.

Cancellation of UV divergence for Vertex-correction

By looking at the Feynman rule D.4 for the vertex correction, one has several renormalisation constants multiplied together. However one should only keep terms linear in the counterterms δ_i at this order. This is the reason for writing the renormalisation constants as $Z_i = 1 + \alpha \delta_i$: one can expand the counterterm amplitude in powers of the parameter α and keep the first order terms, thus picking out the single powers of δ_i . This issue is of course not present for the VP counterterm amplitude.

The procedure is thus to expand in α , keep the first order terms, set $\alpha = 1$ and plug in the counterterm definitions. Once this is done the amplitude can be computed with `PaXEvaluateUV` as before.

Strangely, the result found was not zero as expected, but instead:

²³ α should be interpreted as a parameter identifying a single power of a counterterm, and not the fine-structure constant of QED. Its role becomes clear when evaluating the triangle corrections.

$$\left[2 \times \frac{1}{4} \left(\mathcal{M}_1^{VCl} \mathcal{M}_0^* - \mathcal{N}_1^{VCl} \mathcal{M}_0^* \right) \right] \Big|_{UV} = -4e^2 \chi_0 \quad (7.14)$$

for both triangle amplitudes $l = e, \mu$.

However it was found that the subtraction would yield zero if the vertex counterterm amplitude was rescaled by $\frac{1}{3}$ prior to subtracting it. We attributed this to a mislabelling of the poles by FEYNCalc upon computing the δ_e counterterm: by computing the Feynman amplitude for the divergent vertex loop D.4, extracting the F_1 form-factor coefficient, obtaining its PV decomposition and evaluating its divergent parts respectively with PaXEvaluateUV and PaXEvaluateIR we get:

$$\begin{cases} \left[2 \times \frac{1}{4} \mathcal{M}_1^{VCl} \mathcal{M}_0^* \right] \Big|_{F1,UV} = -\frac{e^2}{16\epsilon_{UV}} \\ \left[2 \times \frac{1}{4} \mathcal{M}_1^{VCl} \mathcal{M}_0^* \right] \Big|_{F1,IR} = -\frac{e^2}{8\epsilon_{IR}} \end{cases} \quad (7.15)$$

and we see that the IR-divergent term is twice the UV-divergent one. Since the δ_e counterterm is obtained by extracting the F_1 term from the whole triangle loop, tensor-decomposing it and enforcing the cancellation with the counterterm amplitude, it is possible that the final expression for the counterterm encompasses part of the IR poles in addition to the UV ones, and this corresponds to $\frac{2}{3}$ of the vertex counterterm so defined.

Once again we evaluated the subtracted vertex square amplitudes and compared our results with obtained by M.Vitti [107]. For this we removed the artificial factor $\frac{1}{3}$ from the counterterm, hoping that any leftover IR pole would find a correspondent in the expressions of [107].

For the divergent C_0 triangle PV integrals we used explicit expressions from [152], however we couldn't just plug in the given expressions since in there the calculations for the IR-divergent PV functions were done using a fictitious photon mass $\lambda \rightarrow 0$ as a regulator, while we sought to work in Dimensional Regularisation as much as possible.

Luckily, equation 4.13 of [153] provides a way to relate this kind of regulator to the regulator produced by the Dimensional regularisation prescription:

$$\log(\lambda^2) \rightarrow \frac{r_\Gamma}{\epsilon} + \log(\mu^2) + \mathcal{O}(\epsilon) \quad (7.16)$$

and where r_Γ is a constant that enters the normalisation of the scalar integrals, in this case it is set to 1.

The subtraction was once again evaluated at the same numerical phase-space point:

$$2 \times \frac{1}{4} \left(\mathcal{M}_1^{VCl} \mathcal{M}_0^* - \mathcal{N}_1^{VCl} \mathcal{M}_0^* \right) = (0.904713 \log(\mu) - 0.0552893) e^6 \quad (7.17)$$

this shows cancellation of all divergent poles, but some numerical factors are left over, possibly due to discrepancies between the expressions for the PV integrals employed.

Let us briefly touch on the IR divergences. These can come either from the $q \rightarrow 0$ limit of Feynman loop integrals with the correct power-counting, but they can come also from the integration over the external particles' momenta in the case of a so-called *soft* particle. This is exactly the case of real radiation processes where a photon could be emitted at very low energy and not be detected, but still affect the overall amplitude.

For $\mu - e$ -scattering at NLO, the IR poles coming from loop integrals are due to box and triangle diagrams, as mentioned, while those from real corrections are given by the cross-products of the

amplitudes in 7.18 with each other, complex-conjugated (which results in 16 square amplitudes). We highlight that these are five-point processes as a result of the presence of the extra photon.

$$i\mathcal{M}_1^{real} = \text{[Diagram 1]} + \text{[Diagram 2]} + \text{[Diagram 3]} + \text{[Diagram 4]} \quad (7.18)$$

The cancellation of all IR divergences entails evaluating both the infra-red limit of the PV functions as well as the phase-space integrals of the real-correction square amplitudes, in the soft photon limit. This task requires different mathematical techniques to the ones employed for loop integrals, and thus goes beyond the scope of this thesis.

7.2 Calculations with AIDA

The MATHEMATICA package AIDA is a sophisticated tool to decompose loop amplitudes onto a basis of scalar Master Integrals (MIs), by employing the Adaptive Integrand Decomposition algorithm iteratively, as detailed in chapter 5. This package was used as the main tool to compute the NNLO real-virtual amplitudes, in particular their MI-decomposition.

All interference amplitudes to be fed into AIDA are computed using FEYN CALC.

7.2.1 Next-to-leading Order

In preparation for tackling the task of reducing the real-virtual NNLO amplitudes of $\mu - e$ scattering, we first applied AIDA to compute the MI expansion of the NLO amplitudes 7.7 interfered with the tree-level amplitude, thus approaching the results of the previous section from a different angle. This was done to acquire familiarity with its usage and the mathematical techniques it employs.

7.2.1.1 Massive Electron case

Grouping

In section 5.4 the grouping procedure was detailed, mentioning in particular that the topologies are grouped together based on the external legs and whether topologies can be obtained as a *pinching* of a larger parent topology. These notions are relative to the loop and not the whole amplitude, as external leg factors and non-loop propagators do not influence the loop integral.

In the case of the NLO amplitudes, the relevant information on the topologies is given by the loop diagrams 7.7 since they are interfered with non-loop amplitudes.

The grouping step gave four groups as output. Two correspond to the planar and crossed box amplitudes, independent of one another, while the other two encompass the vertex-correction and vacuum-polarisation diagrams, for the electron and muon loop separately.

These corrections are grouped together since the VP loop can be seen as a pinching of the vertex loop. Let us show this for the electronic vertex loop, although it is true regardless of the particle running in the loop since, as far as AIDA is concerned, they only differ by the labelling of a mass parameter:

$$\begin{array}{c}
 \begin{array}{c}
 \downarrow p_3 + p_4 \\
 \diagup D_4 \quad \diagdown D_2 \\
 \quad \quad \quad \vdots \\
 \quad \quad \quad D_1 \\
 \diagdown \quad \diagup \\
 p_1 \quad p_2
 \end{array}
 \quad \longrightarrow \quad
 \begin{array}{c}
 \downarrow p_3 + p_4 \\
 \bigcirc D_2 \quad D_4 \\
 \diagdown \quad \diagup \\
 p_1 + p_2
 \end{array}
 \end{array}
 \quad (7.19)$$

As evident from the diagram above, along one leg the momentum flowing into the loop is a sum $p_3 + p_4$. This is an example of a parent diagram where the loop has fewer external legs than the amplitude as a whole. As we shall see, the twistor parametrisation is built from the four-momenta external to the *amplitude* while the substitution rules for the DID algorithm are constructed from the momenta external to the *loop*. When these two do not match, as in the case above, the substitution rules will be unable to re-write and simplify many terms at the numerator, which are then carried over and needlessly increase the computational cost of the calculation.

Since an automated interface between amplitude-generation suites like FEYN CALC and the AIDA package has not yet been developed it is necessary to intervene manually to avoid these issues. Referring to the example above, the solution is to interpret the parent triangle as a single cut of a *box integral* as shown in 3.26, and doing this in reverse enables the integral to be interpreted correctly by AIDA.

The fix is then to identify the missing denominator D_3 and multiply and divide the triangle amplitude by it, in order not to change the overall amplitude but still technically turn it into a box loop:

$$\begin{array}{c}
 \begin{array}{c}
 \downarrow p_3 + p_4 \\
 \diagup D_4 \quad \diagdown D_2 \\
 \quad \quad \quad \vdots \\
 \quad \quad \quad D_1 \\
 \diagdown \quad \diagup \\
 p_1 \quad p_2
 \end{array}
 \quad \longrightarrow \quad
 \begin{array}{c}
 p_4 \quad p_3 \\
 \diagdown \quad \diagup \\
 D_3 \\
 \diagdown \quad \diagup \\
 D_4 \quad D_2 \\
 \diagdown \quad \diagup \\
 p_1 \quad p_2 \\
 \quad \quad \quad \times D_3
 \end{array}
 \end{array}
 \quad (7.20)$$

Twistor parametrisation

As mentioned in chapter 6.3, the AID procedure employs the *Momentum Twistor* formalism to re-write the external momenta and, at the same time, encode all the important properties of the external kinematics.

First we should identify exactly how many variables are required to describe the kinematics at hand. Having four external momenta we shall require $3 \times 4 - 10 = 2$ kinematic variables, but we should also account for the two masses which define the on-shellness of said momenta.

We therefore need four independent parameters.

Attempting to parametrise this four-point massive kinematics using twistors immediately highlights one complication: the twistor formalism requires strictly massless external momenta, while in this occasion we seek to keep all particles as massive.

The issue can be resolved by writing the massive momenta in terms of two massless ones: a massless momentum has two free components, therefore two of them can span the four free components of a massive momentum.

We will therefore have:

$$\begin{aligned}
 p_1 &= l_1 + l_2 \\
 p_2 &= l_3 + l_4 \\
 p_3 &= l_5 + l_6 \\
 p_4 &= l_7 + l_8
 \end{aligned}
 \tag{7.21}$$

where we defined eight massless momenta, labelled $l_1 - l_8$. This replacement has a pictorial interpretation as the "opening up" of the massive external legs (represented by thick lines), originating a diagram that can be seen as the cut of an opt diagram:

$$\tag{7.22}$$

This turns the issue of parametrising four massive momenta into parametrising eight massless ones. This is readily done using the tools within the MATHEMATICA package T@M, and a map from the eight massless momenta to $3 \times 8 - 10 = 14$ distinct twistor variables is generated.

The task now is to narrow down these 14 twistor variables to only 4 independent ones, as required by the actual kinematics. This is done by setting up a system of 10 constraints on the massless momenta $l_1 - l_8$, to find expressions for 8 twistor variables in terms of the remaining six.

Two such constraints arise naturally from requiring that $p_1^2 = p_2^2$ and $p_3^2 = p_4^2$ since they represent the same particles. These entail two constraints on the massless momenta, once the re-definitions above are plugged in.

We then impose the on-shellness of these momenta, i.e. $p_1^2 = m_e^2$ and $p_3^2 = m_\mu^2$: although this does not actually add any new information (as the momenta already did not square to zero), it is a re-labelling in terms of two mass scales which is appropriate given that two of the parameters defining the external kinematics are the masses themselves.

We can impose more constraints by choosing a pair of massless momenta i, j , define their spinors of both chiralities and write down the following expressions in spinor-helicity formalism:

$$\begin{cases} \langle l_i | l_j \rangle = 0 \\ [l_i | l_j] = 0 \end{cases}
 \tag{7.23}$$

which are essentially orthogonality relations. We can impose these two constraints on any pair of external momenta i, j so long as:

- $i \neq j$, as the contrary follows trivially from the spinor-helicity relations and thus doesn't add any information;
- i, j do not parametrise the same massive momentum (e.g. $\langle l_1 | l_2 \rangle$ would be invalid), as this would spoil the independence of all the components of the massive momentum itself²⁴;
- $i \in \{1, 2, 3, 4\}$ and $j \in \{5, 6, 7, 8\}$ or the other way around, in order to ensure that the incoming massive momenta are independent of each other (and same for the outgoing ones);

²⁴At least more than is already done by the on-shellness relations.

We therefore require four pairs of such constraints, to build the necessary eight remaining constraints. The twelve constraints are then gathered, written in terms of the twistor variables and the system is solved, which yields the expression of twelve twistor variables in terms of two independent ones plus the two masses.

One final aspect to keep in mind is that these expressions ought to be strictly rational functions of the independent twistors and the masses, and should not contain any square roots within.

This is for the sake of numerical stability and consistency: square-root functions are essentially Taylor expansions and therefore introduce some noise when evaluated numerically, this might mean that objects that ought to cancel out exactly might instead give a very small value (such as 10^{-15}).

We set up a procedural search for a twistor parametrisation that would satisfy all these requirements, by cycling through all the allowed pairings of momenta i, j and discarding all those that could not yield a solvable system. The final parametrisations were checked by hand, and in the end we selected $\{\{2,6\}, \{3,7\}, \{4,6\}, \{4,8\}\}$, which gave the most compact expression of the constrained parameters in terms of the four independent variables $\{z_3, z_7, m_e^2, m_\mu^2\}$.

It would perhaps be desirable to re-label the remaining two twistor variables in terms of more familiar quantities such as the Mandelstams s, t , but we were unable to add their definitions without finding square roots in the final parametrisation.

Integrand reduction and Master Integrals

After expressing all the momenta and scalar products in the amplitudes in terms of the independent twistor variables, the four topologies were reduced using the DID algorithm. For the first two groups the largest MIs found corresponded to the parent boxes themselves, while for the latter two the largest MIs corresponded to the scalar triangles defining the loop itself. The results were then fed to the reduction code KIRA which applied IBP and LI identities to simplify the list of Master Integrals output by AIDA.

The Master Integrals will be listed group-by-group, and represented by "abstract" Feynman diagrams which only serve to depict the topology of the denominators and the momenta flowing through them in relation to the external kinematics. Internal lines are drawn as a thin line when they represent a massless propagator, a thick line for the electron's mass and a double line for the muon's mass. Each family is defined by their set of denominators, which we specify using KIRA's notation:

[Propagator momentum, Propagator mass].

For clarity we chose not to attach the denominator labels to the integral lines in each diagram, but given the external kinematics and the type of line it is easy to assign the correct labelling in a given diagram.

G1

1 - [k_1 , 0]

2 - [$k_1 + p_4$, μ^2]

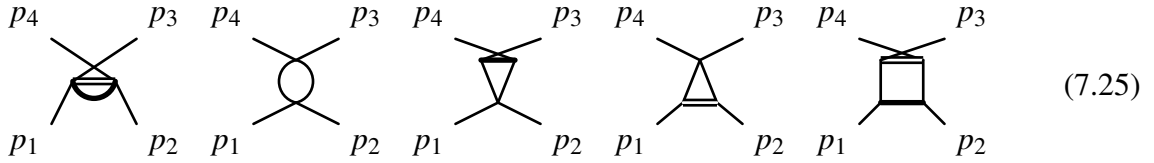
3 - [$k_1 + p_3 + p_4$, 0]

4 - [$k_1 + p_2 + p_3 + p_4$, m_e^2]

(7.24)

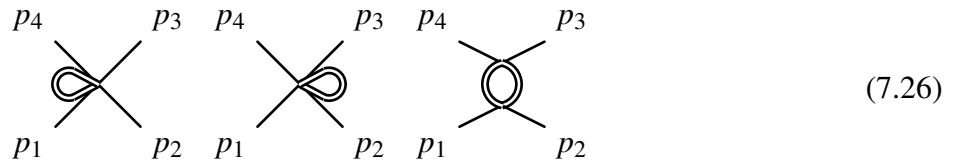
G2

- 1 - [k_1 , m_e^2]
- 2 - [$k_1 + p_2$, 0]
- 3 - [$k_1 + p_2 + p_4$, m_μ^2]
- 4 - [$k_1 + p_2 + p_3 + p_4$, 0]



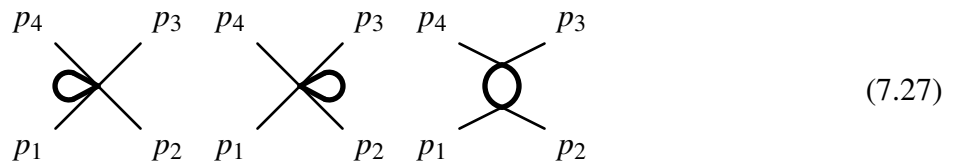
G3

- 1 - [k_1 , 0]
- 2 - [$k_1 + p_3$, m_μ^2]
- 3 - [$k_1 + p_2 + p_3$, m_μ^2]
- 4 - [$k_1 + p_1 + p_2 + p_3$, m_μ^2]



G4

- 1 - [k_1 , 0]
- 2 - [$k_1 + p_2$, m_e^2]
- 3 - [$k_1 + p_2 + p_3$, m_e^2]
- 4 - [$k_1 + p_2 + p_3 + p_4$, m_e^2]



7.2.1.2 Massless electron limit

We now use AIDA to obtain a scalar integral decomposition of the NLO amplitudes in the massless electron limit. Immediately it should be noted that this calculation needs to be done from scratch, as the simple act of setting the electron's mass to zero is incompatible with the previous twistor parametrisation and, additionally, it produces numerical divergences.

Grouping

the number of distinct groups identified by AIDA is now only three as opposed to the previous four: in the $m_e \rightarrow 0$ limit the electron's vertex and vacuum-polarization diagrams turn out to be obtainable as cuts of the planar box, and therefore they can be incorporated as sub-topologies of the the first group.

Twistor parametrisation

The twistor parametrisation is simplified in this case. We require the usual $3 \times 4 - 10 = 2$ parameters plus a single mass scale, bringing the total to three. Moreover we only need to parametrise the two massive four-momenta for the muon in terms of massless ones, as the electron momenta $p_{3,4}$. The momentum definitions are as follows:

$$\begin{aligned} p_1 &= l_1 \\ p_2 &= l_2 \\ p_3 &= l_3 + l_4 \\ p_4 &= l_5 + l_6 \end{aligned} \tag{7.28}$$

We generate a 6-pt twistor parametrisation, writing the six l_i momenta in terms of $3 \times 6 - 10 = 8$ variables. Subsequently we introduce five constraints to narrow down the variables: the lone relation $p_3^2 = p_4^2$ (the other one previously present is already satisfied) and two pairs of spinor orthogonality relations $\{\{4, 2\}, \{6, 2\}\}$.

This time it was possible to re-write the three twistor variables in terms of kinematic quantities, using the on-shellness condition for p_3^2 and the definitions of the Mandelstam variables s, t :

$$\begin{cases} p_3^2 = m_\mu^2 \\ (p_1 + p_4)^2 = s \\ (p_3 - p_4)^2 = t \end{cases} \tag{7.29}$$

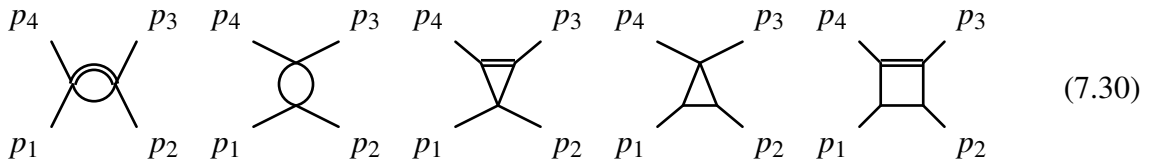
The final set of independent variables is then $\{m_\mu^2, s, t\}$. We remark that these variables are still applied following the underlying twistor parametrisation, whose advantages are still being exploited to the fullest while making the result more familiar-looking.

Integrand reduction and Master Integrals

Just like before the parametrised amplitudes were fed to AIDA and the reduction performed, and the final list of scalar integrals was then simplified using KIRA. The first family involves much the same Master Integrals compared to the previous results, with the difference that they now possess a single mass scale within, while the second and third families are described by fewer integrals this time.

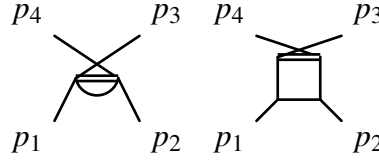
G1

- 1 - [k_1 , 0]
- 2 - [$k_1 + p_4$, μ^2]
- 3 - [$k_1 + p_3 + p_4$, 0]
- 4 - [$k_1 + p_2 + p_3 + p_4$, 0]



G2

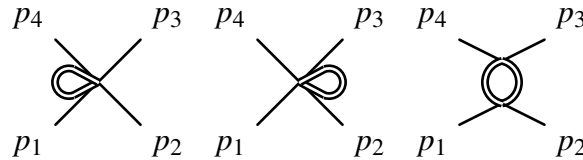
- 1 - [k_1 , 0]
- 2 - [$k_1 + p_2$, 0]
- 3 - [$k_1 + p_2 + p_4$, μ_2]
- 4 - [$k_1 + p_2 + p_3 + p_4$, 0]



(7.31)

G3

- 1 - [k_1 , 0]
- 2 - [$k_1 + p_3$, μ_2]
- 3 - [$k_1 + p_2 + p_3$, μ_2]
- 4 - [$k_1 + p_1 + p_2 + p_3$, μ_2]

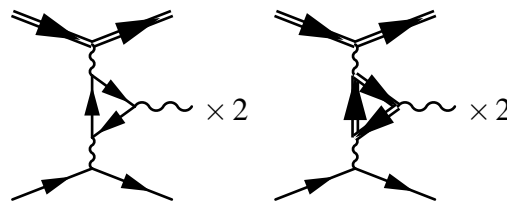


(7.32)

7.2.2 Next-to-next-to-leading Order

We tackle for the first time the process $\mu^- e^- \rightarrow \mu^- e^- \gamma$, where the momentum labelling convention will stay unchanged with the exception of introducing a massless momentum p_5 to describe the real photon.

The real-virtual corrections to $\mu - e$ scattering at NNLO comprise 44 diagrams. The four depicted in 7.33 are essentially VP corrections with the real photon coming from one of the two loop propagators, both cases are represented by the same diagram:



(7.33)

All of these diagrams have a fermion loop with odd-numbered internal lines and, as it turns out, each one differs from its similar only by the direction of charge flow within the loop. By Furry's theorem they cancel each other out at amplitude level, and thus they can then be immediately discarded.

The NNLO amplitude \mathcal{M}_2 is composed by 40 non-cancelling diagrams, in 7.34 we write out the full NNLO amplitude but we explicitly draw only half of the diagrams, in particular those where the real photon is radiated from one of the muon legs:

$$i\mathcal{M}_2 = \text{[15 diagrams]} \times 2 + (\text{crossing}) \tag{7.34}$$

Once again, for most cases the photon may be radiated from more than one location, resulting in a similar but distinct diagram; we represented this by the $\times 2$ label for brevity .

The remaining 20 diagrams, represented by (*crossing*), need not be evaluated explicitly since they can be related to the diagrams above by performing the label swaps ($m_\mu \leftrightarrow m_e, p_1 \leftrightarrow p_4, p_2 \leftrightarrow p_3$). This is a *crossing symmetry* transformation that can relate two distinct topologies of Feynman amplitudes, this is made even more apparent by flipping the resulting diagram vertically to keep the configuration of external particles and momenta visually consistent throughout.

We show this explicitly with an example:

$$\text{[Diagram 1]} \xrightarrow{\text{crossing symmetry}} \text{[Diagram 2]} \xrightarrow{\text{flip vertically}} \text{[Diagram 3]} \tag{7.35}$$

The crossing symmetry can be applied before or after the amplitude reduction with AIDA to the same effect, we thus take advantage of this to halve the number of amplitudes to be reduced.

7.2.2.1 Massive electron case

Grouping

AIDA gathered the 20 amplitudes 7.34 into five groups, two of which have the planar and crossed pentagons as their respective parent topologies, two which have boxes as parent and the last one with a parent triangle amplitude.

The latter three groups have a parent topology with less than five legs coming into the loop, and thus need to be handled in much the same way as done for the NLO amplitudes, only this time they are written as cuts of *pentagons* in accordance with the external kinematics.

Twistor parametrisation

The same considerations for the twistor parametrisation given earlier apply in this case, only this time the external leg number is 5 so we require $3 \times 5 - 10 = 5$ parameters plus the two masses, bringing the total to 7.

Having four massive and one massless momenta, one introduces 9 massless momenta and generates a 9-point twistor parametrisation using T@M, with $3 \times 9 - 10 = 17$ free twistor variables. Much like before, one can reduce this number to 7 using the two constraints $p_1^2 = p_2^2$, $p_3^2 = p_4^2$ and four pairs of spinor orthogonality relations, plus two on-shellness relations so that two of the independent parameters will be the masses m_e^2 and m_μ^2 .

We were, unfortunately, unable to generate any good parametrisation in this way since all of the systems of equations tested would either have no solution or never converge to an explicit solution.

We devised an alternative method to construct a valid parametrisation from scratch, by expressing the massive momenta in the following way:

$$\begin{aligned}
 p_1 &= (1-x)l_1 + xl_2 \\
 p_2 &= xl_1 + (1-x)l_2 \\
 p_3 &= (1-y)l_3 + yl_4 \\
 p_4 &= yl_3 + (1-y)l_4 \\
 p_5 &= l_5
 \end{aligned} \tag{7.36}$$

The momenta are expressed in terms of five massless momenta $l_1 \dots l_5$. Each massive momentum is expressed in terms of two massless ones, in a combination determined by the mixing parameters x, y . The way the mixing is defined ensures that all momenta are independent of each other, and that the electron and muon momenta respectively square to the same values as they should.

This parametrisation thus "hard-codes" all the features we require and naturally contains seven variables: five twistor variables and the two mixing parameters. We only need to re-express two of these in terms of the two masses, without the need to add any ad-hoc constraints.

The final variables extracted are $\{z_2, z_4, z_5, x, y, m_e^2, m_\mu^2\}$, and once again we did not express anything in terms of the Generalised Mandelstams in order to avoid square roots.

Integrand reduction and Master Integrals

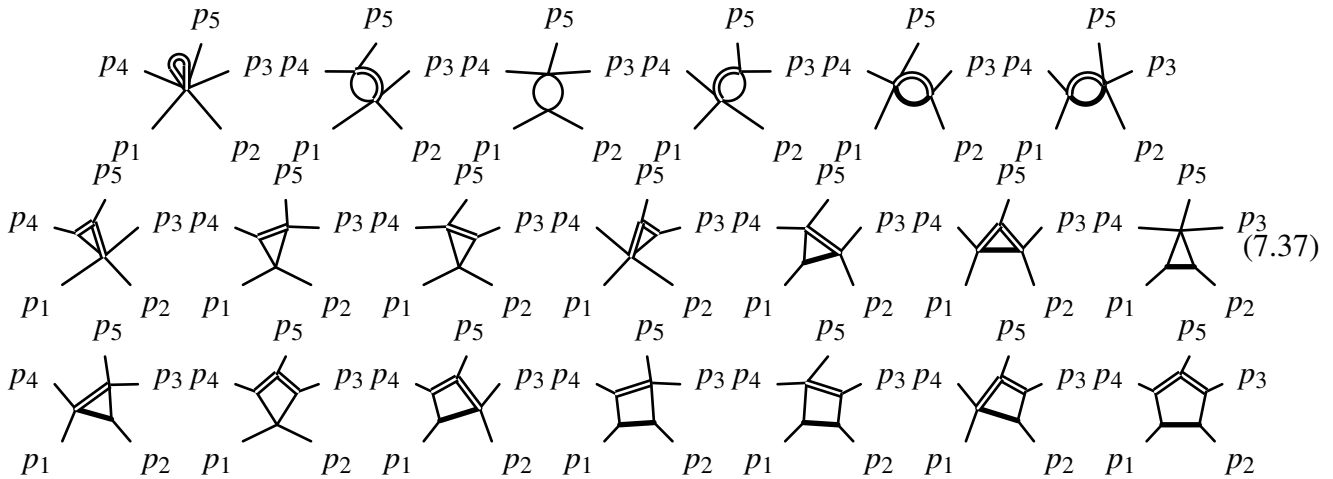
The integrand reduction was performed not with the full DID algorithm, but instead with the simplified version of AIDA which only computes the cut solutions to the quintuple cut (the largest one present in this case) and plugs them in without integrating in transverse space. This choice was imposed by computational hardware constraints.

As shown in chapter 5.3 this entails a proliferation of scalar integrals present in the resulting decomposition, beyond what is necessary to capture the 5-point amplitude. This lengthy list of Scalar Integrals was reduced using the IBP reduction code KIRA to the lists reported here, which are Master Integrals in D -dimension.

Most prominently the integral decomposition features two scalar pentagons, one planar and one crossed, belonging to two different topologies. We stress that the pentagon is only a master integral in D dimensions and its contribution vanishes either in the limit $D \rightarrow 4 - 2\epsilon$ or upon the integration over the transverse space. This can be fixed by means of a dimensional-shift identity able to map the pentagon onto scalar boxes up to order ϵ , which would be used to distribute the pentagon residue onto the box contributions.

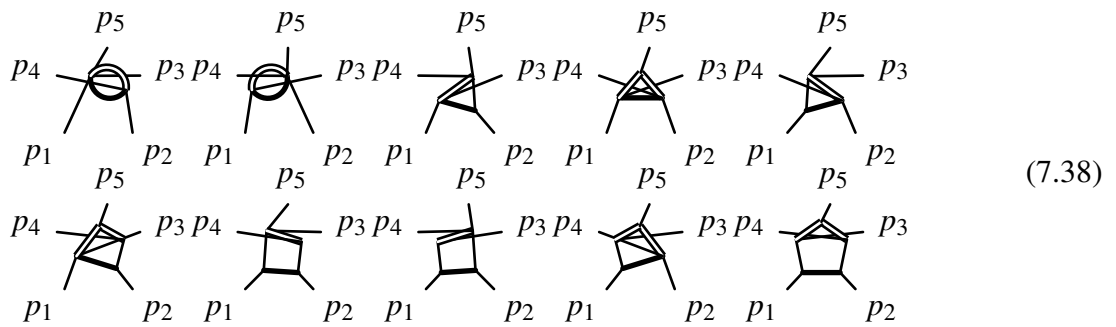
G1

- 1 - [k_1 , 0]
- 2 - [$k_1 + p_4$, μ_2]
- 3 - [$k_1 + p_4 + p_5$, μ_2]
- 4 - [$k_1 + p_3 + p_4 + p_5$, 0]
- 5 - [$k_1 + p_2 + p_3 + p_4 + p_5$, m_e^2]



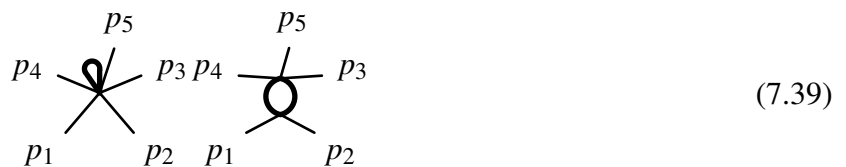
G2

- 1 - [k_1 , m_e^2]
- 2 - [$k_1 + p_2$, 0]
- 3 - [$k_1 + p_2 + p_4$, μ_2]
- 4 - [$k_1 + p_2 + p_4 + p_5$, μ_2]
- 5 - [$k_1 + p_2 + p_3 + p_4 + p_5$, 0]



G3

- 1 - [k_1 , 0]
- 2 - [$k_1 + p_2$, m_e^2]
- 3 - [$k_1 + p_2 + p_3$, 0]
- 4 - [$k_1 + p_2 + p_3 + p_4$, m_e^2]
- 5 - [$k_1 + p_2 + p_3 + p_4 + p_5$, m_e^2]



G4

- 1 - [k_1 , 0]
- 2 - [$k_1 + p_1 + p_2 + p_3 + p_5$, μ_2]
- 3 - [$k_1 + p_3$, μ_2]
- 4 - [$k_1 + p_1 + p_2 + p_3$, μ_2]
- 5 - [$k_1 + p_2 + p_3$, 0]

(7.40)

G5

- 1 - [k_1 , 0]
- 2 - [$k_1 + p_1 + p_2 + p_3 + p_5$, μ_2]
- 3 - [$k_1 + p_3$, μ_2]
- 4 - [$k_1 + p_3 + p_5$, μ_2]
- 5 - [$k_1 + p_2 + p_3 + p_5$, 0]

(7.41)

7.2.2.2 Numerical reduction of the Massive electron case

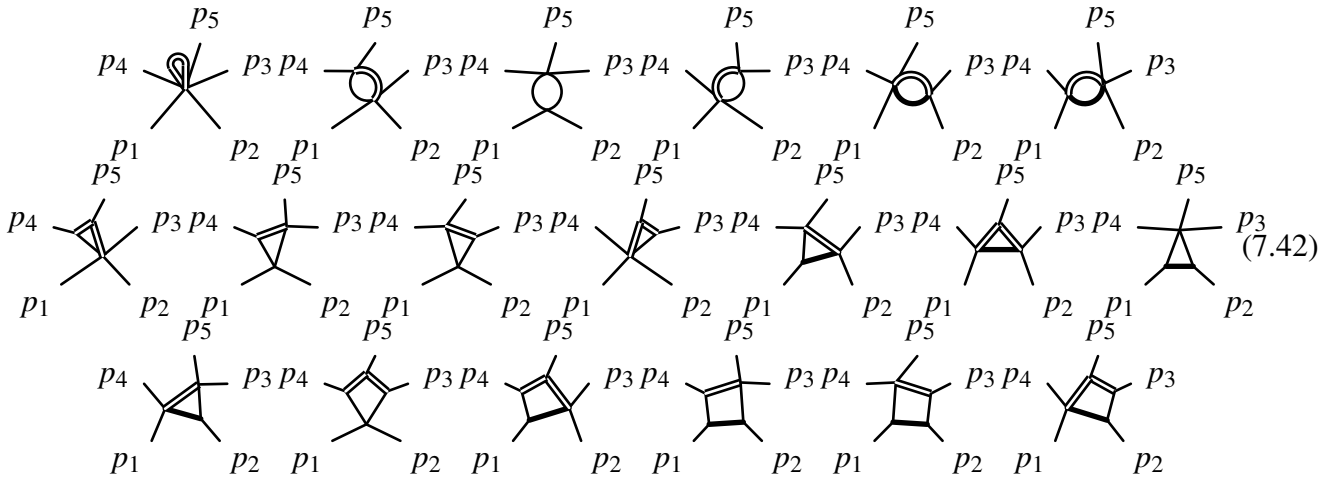
We sought to verify how many of the above integrals would not have been present had we carried out an *AIDA* reduction with the full DID algorithm. We were able to do this by running a numerical decomposition: after the (unchanged) momentum twistor parametrisation was fixed we assigned numerical values to the three twistor variables and the x, y parameters, keeping the masses explicit. The numbers were chosen as fractions of prime numbers to ensure numerical independence between them and thus have little physical meaning, but this is not important for the sake of determining the final Master Integrals and the application of IBP identities.

The *AIDA* decomposition features much fewer scalar integrals and, as expected, the pentagons were missing altogether. We still fed the results to *KIRA* as we expected not all these scalar integrals to be Master Integrals, and indeed a few disappeared.

The final lists of Master Integrals end up being identical to the simplified analytical case detailed previously minus the two pentagons, showing that the simplifications done in *AIDA* can be amended using IBPs and dimensional-shift relations.

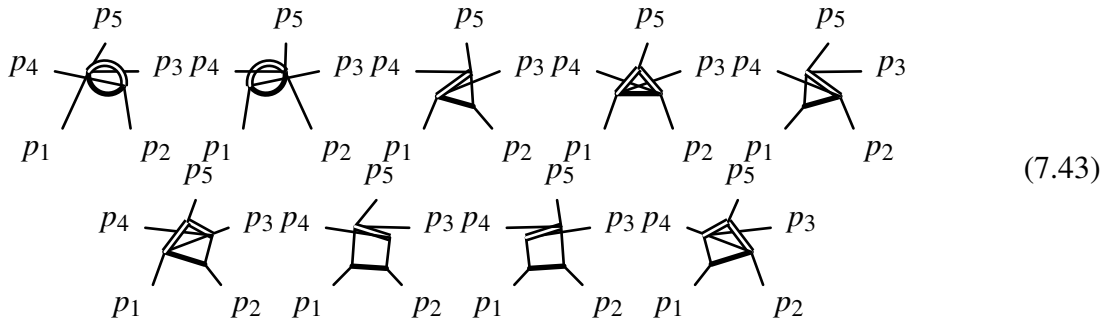
G1

- 1 - [k_1 , 0]
- 2 - [$k_1 + p_4$, μ_2]
- 3 - [$k_1 + p_4 + p_5$, μ_2]
- 4 - [$k_1 + p_3 + p_4 + p_5$, 0]
- 5 - [$k_1 + p_2 + p_3 + p_4 + p_5$, μ_2]



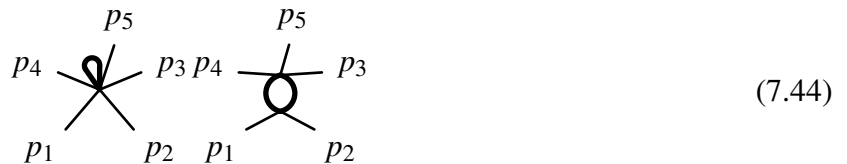
G2

- 1 - [k_1 , me_2]
- 2 - [$k_1 + p_2$, 0]
- 3 - [$k_1 + p_2 + p_4$, mu_2]
- 4 - [$k_1 + p_2 + p_4 + p_5$, mu_2]
- 5 - [$k_1 + p_2 + p_3 + p_4 + p_5$, 0]



G3

- 1 - [k_1 , 0]
- 2 - [$k_1 + p_2$, me_2]
- 3 - [$k_1 + p_2 + p_3$, 0]
- 4 - [$k_1 + p_2 + p_3 + p_4$, me_2]
- 5 - [$k_1 + p_2 + p_3 + p_4 + p_5$, me_2]



G4

- 1 - [k_1 , 0]
- 2 - [$k_1 + p_1 + p_2 + p_3 + p_5$, mu_2]
- 3 - [$k_1 + p_3$, mu_2]
- 4 - [$k_1 + p_1 + p_2 + p_3$, mu_2]
- 5 - [$k_1 + p_2 + p_3$, 0]

G5

- 1 - [k_1 , 0]
- 2 - [$k_1 + p_1 + p_2 + p_3 + p_5$, μ_2]
- 3 - [$k_1 + p_3$, μ_2]
- 4 - [$k_1 + p_3 + p_5$, μ_2]
- 5 - [$k_1 + p_2 + p_3 + p_5$, 0]

7.2.2.3 Massless electron limit

Grouping

We then considered the $m_e \rightarrow 0$ limit of the 20 amplitudes 7.34. In this limit the absence of the electron mass entails that some multiple cuts end up giving essentially the same result: for this reason AIDA identified only four topology groups as the former group G3 is fully encompassed within group G1 below.

Twistor parametrisation

To parametrise this case we require $3 \times 5 - 10 = 5$ parameters plus a single mass, bringing the total to 6. The momentum twistor parametrisation was constructed using the double-massive one as a template. We introduced five massless momenta $l_1 \dots l_5$ and a single mixing parameter y , given that we only have two massive momenta to write down, and parametrised the external kinematics as follows:

$$\begin{aligned}
 p_1 &= l_1 \\
 p_2 &= l_2 \\
 p_3 &= (1-y)l_3 + yl_4 \\
 p_4 &= yl_3 + (1-y)l_4 \\
 p_5 &= l_5
 \end{aligned}
 \tag{7.47}$$

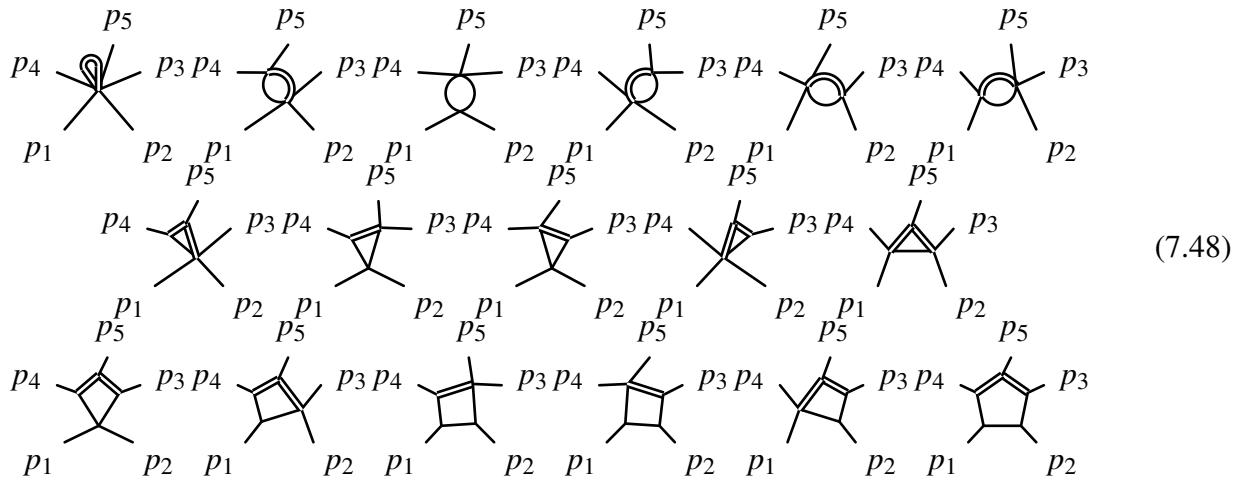
This is essentially equivalent to setting $x = 0$ in the parametrisation used for the massive case, therefore all the desired features present previously translate naturally.

The final 6 variables used are $\{z_1, z_2, z_3, z_5, y, m_\mu^2\}$, the extra twistor variable present is due to the lack of the on-shellness condition for the electron. Once again we did not express anything in terms of the Generalised Mandelstams in order to avoid square roots.

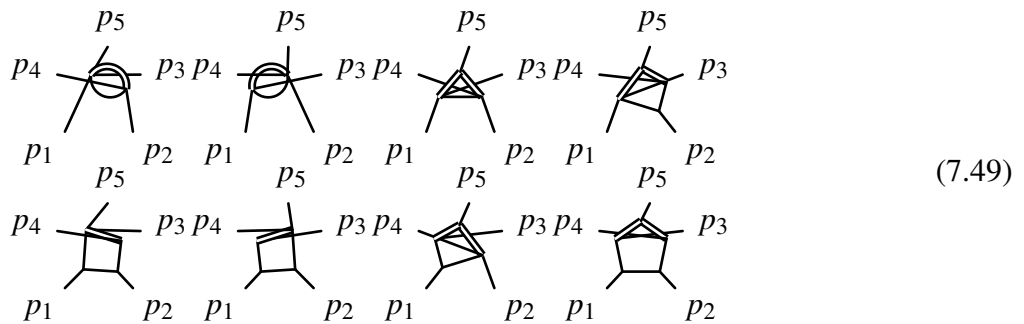
Integrand reduction and Master Integrals

Once again the AIDA reduction was performed using the simplified version of the algorithm, and the scalar integral decomposition was once more simplified with KIRA. In addition to the missing integral family we also find that the first two families feature fewer Master Integrals compared to the analytical massive case.

G1
 1 - [k_1 , 0]
 2 - [$k_1 + p_4$, μ^2]
 3 - [$k_1 + p_4 + p_5$, μ^2]
 4 - [$k_1 + p_3 + p_4 + p_5$, 0]
 5 - [$k_1 + p_2 + p_3 + p_4 + p_5$, 0]



G2
 1 - [k_1 , 0]
 2 - [$k_1 + p_2$, 0]
 3 - [$k_1 + p_2 + p_4$, μ^2]
 4 - [$k_1 + p_2 + p_4 + p_5$, μ^2]
 5 - [$k_1 + p_2 + p_3 + p_4 + p_5$, 0]



G3

- 1 - [k_1 , 0]
- 2 - [$k_1 + p_1 + p_2 + p_3 + p_5$, μ_2]
- 3 - [$k_1 + p_3$, μ_2]
- 4 - [$k_1 + p_1 + p_2 + p_3$, μ_2]
- 5 - [$k_1 + p_2 + p_3$, 0]

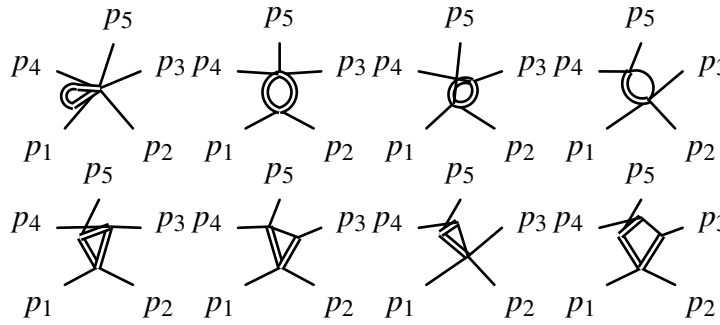


Diagram (7.50) shows eight Feynman diagrams arranged in two rows of four. Each diagram has five external lines labeled p_1, p_2, p_3, p_4, p_5 . The top row diagrams feature a loop with a self-energy correction on the p_5 line. The bottom row diagrams feature a loop with a self-energy correction on the p_3 line. The diagrams are labeled (7.50) on the right.

G4

- 1 - [k_1 , 0]
- 2 - [$k_1 + p_1 + p_2 + p_3 + p_5$, μ_2]
- 3 - [$k_1 + p_3$, μ_2]
- 4 - [$k_1 + p_3 + p_5$, μ_2]
- 5 - [$k_1 + p_2 + p_3 + p_5$, 0]

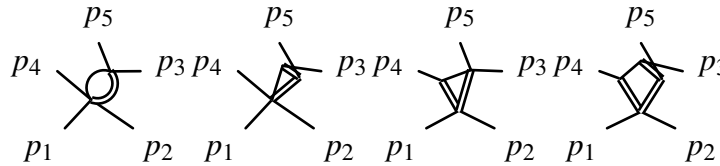


Diagram (7.51) shows four Feynman diagrams in a single row. Each diagram has five external lines labeled p_1, p_2, p_3, p_4, p_5 . The diagrams feature a loop with a self-energy correction on the p_5 line. The diagrams are labeled (7.51) on the right.

Chapter 8

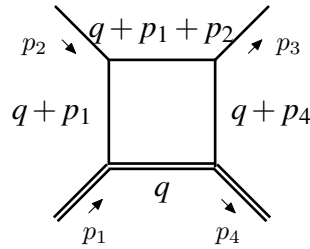
Evaluation of massive one-loop 4-point Master Integrals with Differential Equations

In this chapter we illustrate in practice the methods detailed in chapter 2.4, from the generation of a canonical system of Differential Equations for Master Integrals to writing down the general solution with boundary conditions. The goal is to evaluate the Master Integrals for one-loop 4-point diagrams for μ^-e^- -scattering in the massless electron limit²⁵. The complete lists of Master integrals were shown in section 7.2.1.2.

For consistency with the results shown in section 5 of [10] and chapter 2.8 of [52] we will modify the external momentum labelling to the following:

$$\mu^-(p_1) + e^-(p_2) \longrightarrow \mu^-(p_4) + e^-(p_3) \quad (8.1)$$

explicitly shown for the massive box below:



with the following definitions for the Mandelstam variables:

$$\begin{cases} s = (p_1 + p_2)^2 \\ t = (p_2 - p_3)^2 \end{cases} \quad (8.2)$$

Moreover it will prove convenient to introduce a peculiar normalisation for the Feynman integral measure:

$$\widetilde{d^D q} := -\frac{i16\pi^2}{\Gamma(1+\varepsilon)} \left(\frac{m_\mu^2}{4\pi\mu^2} \right)^\varepsilon \frac{d^D q}{(2\pi)^D} \quad (8.3)$$

²⁵Handling the presence of a second mass scale complicates matters considerably.

where μ is the scale parameter in dimensional regularisation.

First we examine the first family of integrals 7.2.1.2, which we recall describes the decomposed QED box-loop diagram originally present. Despite this being a perfectly good basis of Master Integrals to that aim, experience tells that this basis is ill-suited to be solved with the Differential Equations method. Much preferable is to use IBP relations on 7.2.1.2 to rotate the decomposition onto the following basis of Master Integrals $\{\mathcal{T}_1, \dots, \mathcal{T}_5\}$:

$$(8.4)$$

where dots indicate a denominator raised to the power 2. The automatic code REDUZE is capable of performing IBP-reduction onto a set of integrals and write the end result onto a basis specified by the user, as in this case.

One might wonder whether we ought not to encompass in the calculation the Master Integrals appearing in the families 7.2.1.2 and 7.2.1.2. In fact, however, the entire third family of Master Integrals can be obtained from these by means of IBP relations, while the two crossed diagrams of the second family can be obtained from these still by applying a *crossing relation* generated by REDUZE itself: essentially re-defining the Mandelstam invariant t is all that is needed to obtain those crossed amplitudes.

8.1 System of Differential Equations in canonical form

The systems of differential equations are set up in the independent kinematic invariants of the problem which, as shown in the previous chapter, can be taken as $\{m_\mu^2, s, t\}$. Once again we used REDUZE to generate the three systems of Differential Equations relating the Master Integrals $\vec{\mathcal{T}} = \{\mathcal{T}_1, \dots, \mathcal{T}_5\}$. In fact only two systems are needed to solve the problem: Feynman integrals are *homogeneous functions* of their kinematic invariants, with an ε -dependent exponent determined by power-counting:

$$\mathcal{T}(\lambda s, \lambda t, \lambda m_\mu^2) = \lambda^{\alpha(\varepsilon)} \mathcal{T}(s, t, m_\mu^2) \quad (8.5)$$

thus Euler's homogeneous functions theorem provides a relation between the systems of differential equations, decreasing the number of independent systems by one:

$$(s\partial_s + t\partial_t + m_\mu^2\partial_{m_\mu^2}) \mathcal{T}(s, t, m_\mu^2, \varepsilon) = \alpha(\varepsilon) \mathcal{T}(s, t, m_\mu^2, \varepsilon) \quad (8.6)$$

We are then going to solve the two systems:

$$\partial_s \vec{\mathcal{T}}(s, t, \varepsilon) = \mathbb{M}_s(s, t) \vec{\mathcal{T}}(s, t, \varepsilon) \quad \partial_t \vec{\mathcal{T}}(s, t, \varepsilon) = \mathbb{M}_t(s, t) \vec{\mathcal{T}}(s, t, \varepsilon) \quad (8.7)$$

where the matrices are generated as ε -linear form the start:

$$\mathbb{M}_s = \begin{pmatrix} 0 & 0 & 0 & 0 & 0 \\ -\frac{\varepsilon}{(m_\mu^2-s)s} & \left(\frac{1}{s} - \frac{2}{s-m_\mu^2}\right)\varepsilon - \frac{1}{s} & 0 & 0 & 0 \\ 0 & 0 & 0 & 0 & 0 \\ 0 & 0 & 0 & 0 & 0 \\ \frac{m_\mu^2+s}{(m_\mu^2-s)^4+st(m_\mu^2-s)^2} & -\frac{2s(m_\mu^2+s)}{(m_\mu^2-s)^4+st(m_\mu^2-s)^2} & -\frac{-2m_\mu^2+2s+t}{(m_\mu^2-s)^3+st(m_\mu^2-s)} & \frac{(4m_\mu^2-t)\varepsilon}{(m_\mu^2-s)^3+st(m_\mu^2-s)} & \frac{(2m_\mu^2t+2st)\varepsilon}{2((m_\mu^2-s)^3+st(m_\mu^2-s))} + \frac{1}{m_\mu^2-s} \end{pmatrix}$$

$$\mathbb{M}_t = \begin{pmatrix} 0 & 0 & 0 & 0 & 0 \\ 0 & 0 & 0 & 0 & 0 \\ 0 & 0 & -\frac{\varepsilon}{t} - \frac{1}{t} & 0 & 0 \\ \frac{1}{t(t-4m_\mu^2)} & 0 & \frac{1}{t-4m_\mu^2} & \frac{t-2m_\mu^2}{(4m_\mu^2-t)t} - \frac{4m_\mu^2\varepsilon}{(4m_\mu^2-t)t} & 0 \\ \frac{s}{(m_\mu^2-s)t((m_\mu^2-s)^2+st)} & -\frac{2s^2}{(m_\mu^2-s)t((m_\mu^2-s)^2+st)} & \frac{m_\mu^2-s}{t((m_\mu^2-s)^2+st)} & \frac{(m_\mu^2+s)\varepsilon}{t((m_\mu^2-s)^2+st)} & \left(\frac{s}{(m_\mu^2-s)^2+st} - \frac{1}{t}\right)\varepsilon - \frac{1}{t} \end{pmatrix}$$

These matrices are first brought in canonical form using two *Magnus exponential* rotation matrices, and at the same time the Master Integrals are rescaled by appropriate powers of ε to remove their ε -poles. The Magnus rotations also change the basis of master integrals from $\{\mathcal{T}_1, \dots, \mathcal{T}_5\}$ to $\{\mathcal{I}_1, \dots, \mathcal{I}_5\}$:

$$\{\mathcal{I}_1, \mathcal{I}_2, \mathcal{I}_3, \mathcal{I}_4, \mathcal{I}_5\} \equiv \left\{ \varepsilon\mathcal{T}_1, -s\varepsilon\mathcal{T}_2, -t\varepsilon\mathcal{T}_3, -\frac{t\varepsilon^2\sqrt{4m_\mu^2-t}}{\sqrt{-t}}\mathcal{T}_4, t\varepsilon^2(s-m_\mu^2)\mathcal{T}_5 \right\} \quad (8.8)$$

At this point it is also convenient to perform a change of variables, from $\{s, t\}$ to the dimensionless $\{x, y\}$:

$$\begin{cases} s \longrightarrow -xm_\mu^2 \\ t \longrightarrow -\frac{(1-y)^2}{y}m_\mu^2 \end{cases} \quad (8.9)$$

The two systems of differential equations are then manifestly ε -factorisable:

$$\partial_x \vec{\mathcal{I}}(x, y, \varepsilon) = \varepsilon \mathbb{M}_x(x, y) \vec{\mathcal{I}}(x, y, \varepsilon) \quad \partial_t \vec{\mathcal{I}}(x, y, \varepsilon) = \varepsilon \mathbb{M}_y(x, y) \vec{\mathcal{I}}(x, y, \varepsilon) \quad (8.10)$$

$$\begin{aligned}
 \mathbb{M}_x &= \begin{pmatrix} 0 & 0 & 0 & 0 & 0 \\ -1 & -2 & 0 & 0 & 0 \\ 0 & 0 & 0 & 0 & 0 \\ 0 & 0 & 0 & 0 & 0 \\ 2 & 4 & 0 & 0 & -2 \end{pmatrix} \frac{1}{1+x} + \begin{pmatrix} 0 & 0 & 0 & 0 & 0 \\ 0 & 1 & 0 & 0 & 0 \\ 0 & 0 & 0 & 0 & 0 \\ 0 & 0 & 0 & 0 & 0 \\ 0 & 0 & 0 & 0 & 0 \end{pmatrix} \frac{1}{x} \\
 &+ \begin{pmatrix} 0 & 0 & 0 & 0 & 0 \\ 0 & 0 & 0 & 0 & 0 \\ 0 & 0 & 0 & 0 & 0 \\ 0 & 0 & 0 & 0 & 0 \\ -1 & -2 & -1 & -1 & 1 \end{pmatrix} \frac{1}{x+y} + \begin{pmatrix} 0 & 0 & 0 & 0 & 0 \\ 0 & 0 & 0 & 0 & 0 \\ 0 & 0 & 0 & 0 & 0 \\ 0 & 0 & 0 & 0 & 0 \\ -1 & -2 & -1 & 1 & 1 \end{pmatrix} \frac{y}{1+xy} \\
 \mathbb{M}_y &= \begin{pmatrix} 0 & 0 & 0 & 0 & 0 \\ 0 & 0 & 0 & 0 & 0 \\ 0 & 0 & -2 & 0 & 0 \\ 0 & 0 & 0 & -2 & 0 \\ 0 & 0 & 2 & 0 & -2 \end{pmatrix} \frac{1}{-1+y} + \begin{pmatrix} 0 & 0 & 0 & 0 & 0 \\ 0 & 0 & 0 & 0 & 0 \\ 0 & 0 & 0 & 0 & 0 \\ 0 & 0 & 0 & 2 & 0 \\ 0 & 0 & 0 & 0 & 0 \end{pmatrix} \frac{1}{1+y} + \begin{pmatrix} 0 & 0 & 0 & 0 & 0 \\ 0 & 0 & 0 & 0 & 0 \\ 0 & 0 & 1 & 0 & 0 \\ 1 & 0 & -1 & 0 & 0 \\ 1 & 2 & 0 & 0 & 0 \end{pmatrix} \frac{1}{y} \\
 &+ \begin{pmatrix} 0 & 0 & 0 & 0 & 0 \\ 0 & 0 & 0 & 0 & 0 \\ 0 & 0 & 0 & 0 & 0 \\ 0 & 0 & 0 & 0 & 0 \\ -1 & -2 & -1 & -1 & 1 \end{pmatrix} \frac{1}{x+y} + \begin{pmatrix} 0 & 0 & 0 & 0 & 0 \\ 0 & 0 & 0 & 0 & 0 \\ 0 & 0 & 0 & 0 & 0 \\ 0 & 0 & 0 & 0 & 0 \\ -1 & -2 & -1 & 1 & 1 \end{pmatrix} \frac{x}{1+xy}
 \end{aligned}$$

where we wrote the $\mathbb{M}_{x,y}$ matrices in *dlog* form, identifying the matrices \mathbb{M}_i belonging to each *letter* $\eta_i(x,y)$. One can notice how matrices which happen to be identical across \mathbb{M}_x and \mathbb{M}_y , also multiply the partial derivative of the same *dlog* ($\eta_i(x,y)$), only with respect to different variables.

Since the system is canonical and all letters are clearly rational, the solution may be given as detailed in chapter 2.4.3, namely as a Dyson series evaluated with Generalised Polylogarithms. The iterated integrals have been computed manually up to order ε^2 . The general solution then is of the form:

$$\vec{\mathcal{I}}(x, y, \varepsilon) = (\mathbb{1} + \varepsilon \mathbb{B}^1(x, y) + \varepsilon^2 \mathbb{B}^2(x, y)) \vec{\mathcal{I}}^0(\varepsilon) \quad (8.11)$$

where each component of the vector of boundary conditions is written as:

$$\mathcal{I}_k^0(\varepsilon) = \sum_{j=0}^2 \varepsilon^j \xi(k, j) \quad (8.12)$$

In appendix E we write out explicitly the matrix product of the general solution with the boundary conditions, keeping terms up to order 4 in ε .

8.2 Boundary conditions

Keeping these results in mind, the goal is now to derive physically-sensible relations and use them to fix the boundary-condition coefficients $\xi(k, j)$. To do this one will require a tool to evaluate GPLs numerically, we used the MATHEMATICA notebook attached to [154].

We examine one Master-Integral at a time:

- For \mathcal{I}_1 we take advantage of the fact that it is computable analytically with Feynman parameters and, using the specific normalisation given in 8.3, it is simply 1. Looking at E.3, to enforce this condition it is sufficient to choose:

$$\begin{cases} \xi_{10} = 1 \\ \xi_{11} = 0 \\ \xi_{12} = 0 \end{cases} \quad (8.13)$$

- For the one-mass bubble \mathcal{I}_2 we can recall the relation $\mathcal{I}_2 = -s\mathcal{T}_2$ up to the ε -rescaling. In the limit $s \rightarrow 0$ \mathcal{T}_2 is evidently regular and thus \mathcal{I}_2 vanishes trivially by its definition. This limit corresponds to $x \rightarrow 0$, which also shrinks the integration bounds of all Polylogarithms, making them vanish. Looking at E.4, to enforce the vanishing of \mathcal{I}_2 when $x \rightarrow 0$ it is enough to set all boundary coefficients to zero:

$$\begin{cases} \xi_{20} = 0 \\ \xi_{21} = 0 \\ \xi_{22} = 0 \end{cases} \quad (8.14)$$

- The t -channel scalar bubble \mathcal{I}_3 is also computable analytically with Feynman parameters giving, using our normalisation convention:

$$-t(1 - \varepsilon^2 \zeta_2) \quad (8.15)$$

where ζ_2 is the *Riemann Zeta function* evaluated at $s = 2$, which is $\zeta_2 = \frac{\pi^2}{6}$. To fix the boundary conditions we then need to take E.5 and fix the coefficients so that it matches the above result *order-by-order in ε* . The result is simply:

$$\begin{cases} \xi_{30} = 1 \\ \xi_{31} = 0 \\ \xi_{32} = -\frac{\pi^2}{6} \end{cases} \quad (8.16)$$

- For $\mathcal{I}_4 \sim -\frac{t\sqrt{4m_\mu^2-t}}{\sqrt{-t}}\mathcal{T}_4$ we can use the regularity of \mathcal{T}_4 at $t \rightarrow 4m_\mu^2$, which kills off the square root factor. This limit corresponds to $y \rightarrow -1$ and x generic, and at this phase-space point the boundary conditions need to ensure that \mathcal{I}_4 vanishes order-by-order in ε . Looking at the expressions E.6 (after having set all previous conditions) the required definitions are:

$$\begin{cases} \xi_{40} = 0 \\ \xi_{41} = 0 \\ \xi_{42} = G(\{0,0\}, -1) - 2G(\{0,1\}, -1) = -\frac{2\pi^2}{3} \end{cases} \quad (8.17)$$

- For $\mathcal{I}_5 \sim t(s - m_\mu^2)\mathcal{T}_5$ it would be natural to try and set a condition for either $t \rightarrow 0$ or $s \rightarrow m_\mu^2$ but, as it turns out, the box integral \mathcal{T}_5 is not regular in either of these *thresholds*. Let us take a look at the differential equations in *dlog* form; let us then choose a letter η , pick

the differential equations proportional to $d \log(\eta)$ and multiply both sides by the letter itself: if the limit $\eta \rightarrow 0$ corresponds to a regularity point for \mathcal{T}_5 and *all the other integrals appearing therein* we have found a *pseudo-threshold* for the original equation, then the differential $\eta d\mathcal{I}_5$ would vanish safely and we could construct a boundary condition from the right-hand side of the DE.

We shall choose $\eta = x + y$ in the limit $x = -\frac{1}{2}, y = \frac{1}{2}$ since this corresponds to the phase-space point $s = -t = \frac{m_\mu^2}{2}$, regular for each of the \mathcal{T}_i . We then extract the differential equation for \mathcal{I}_5 corresponding to this letter:

$$[(x+y)d\mathcal{I}_5]_{x=-\frac{1}{2},y=\frac{1}{2}} = 0 = [-\mathcal{I}_1 - 2\mathcal{I}_2 - \mathcal{I}_3 - \mathcal{I}_4 + \mathcal{I}_5]_{x=-\frac{1}{2},y=\frac{1}{2}} \quad (8.18)$$

On the right the only unknowns are the BC coefficients of \mathcal{I}_5 , and we set them so that the entire right-hand side vanishes order-by-order in ε :

$$\begin{cases} \xi_{50} = 2 \\ \xi_{51} = 0 \\ \xi_{52} = 2G\left(\{-1\}, -\frac{1}{2}\right)G(\{0\}, -1) - 4G\left(\{-1\}, -\frac{1}{2}\right)G(\{1\}, -1) + 4G\left(\{-1, -1\}, -\frac{1}{2}\right) \\ \quad - 2G\left(\{0, -1\}, -\frac{1}{2}\right) - 2G(\{1, 0\}, -1) + 4G(\{1, 1\}, -1) - \frac{5\pi^2}{6} = -\frac{5\pi^2}{6} \end{cases} \quad (8.19)$$

Let us write the final solution:

$$\begin{cases} \mathcal{I}_1 = 1 \\ \mathcal{I}_2 = -\varepsilon G(\{-1\}, x) + \varepsilon^2(2G(\{-1, -1\}, x) - G(\{0, -1\}, x)) \\ \mathcal{I}_3 = 1 + \varepsilon^2 \zeta_2 \\ \mathcal{I}_4 = \varepsilon^2 \left(-\frac{2\pi^2}{3} - G(\{0, 0\}, y) + 2G(\{0, 1\}, y) \right) \\ \mathcal{I}_5 = 2 + \varepsilon(-2G(\{-1\}, x) + G(\{0\}, y) - 2G(\{1\}, y)) \\ \quad + \varepsilon^2 \left(-\frac{5\pi^2}{6} - 2G(\{-1\}, x)G(\{0\}, y) + 4G(\{-1\}, x)G(\{1\}, y) \right) \end{cases} \quad (8.20)$$

This result matches perfectly the preliminary results in [52]. To take this one step further and reproduce the final results of both [52] and [10] the above expressions need to be simplified using algebraic identities between the Polylogarithm functions known as *Shuffle Algebra*.

Conclusions

In this thesis we reviewed the Standard Model contributions to the muon's anomalous magnetic moment, focussing on the theoretical framework behind the Leading Hadronic corrections and its possible determination through $\mu^\pm e^- \rightarrow \mu^\pm e^-$ scattering. In this context, our goal was to advance the state-of-the-art results in muon-electron scattering at Next-To-Next-To-Leading Order by evaluating the real-virtual corrections at one-loop given by the process $\mu^- e^- \rightarrow \mu^- e^- \gamma$ in Quantum-Electrodynamics.

We thus introduced the powerful Unitarity-based methods used to compute loop Feynman amplitudes able to produce a decomposition onto Scalar Integrals by means of unitary cuts, with attention to the extension to the Dimensional Regularisation framework. We showed that simple but general underlying principles govern the kinds of integrals that can appear in the decomposition, and that the form of these Master Integrals is *universal* at one loop, regardless of the complexity of the Feynman amplitude at hand.

Thereafter we outlined the remarkable properties that Feynman integrals satisfy, namely the IBP relations that are able to map integrals onto one another and identify the minimal basis of Master Integrals, and the Differential Equations method which allows the determination of each Master Integral as the solution of a coupled system of differential equations in the kinematic invariants.

We continued our discussion on decomposition methods by describing Integrand-level schemes such as the *OPP method* which obtain decompositions by performing polynomial divisions, and their connection to advanced mathematical techniques such as Algebraic Geometry. The generality of these ideas is key to applying these methods beyond the one-loop level

We described in detail the *Adaptive Integrand Decomposition* technique and its implementation, the AIDA package. This unitarity-based method enhances the previous integrand methods by using the external momenta as a basis to parametrise the loop momentum, and the remarkable simplification that follow enable the automatic identification and removal of spurious terms at one-loop and beyond. Given the importance of the external momenta to this algorithm, we introduced the powerful mathematical languages of *spinor-helicity* and *momentum twistors*, which allow an efficient parametrisation of the kinematics with the optimal number of variables and encode naturally four-momentum conservation.

We then put all the aforementioned theoretical tools to work on muon-electron scattering. First we re-evaluated the known Leading-Order and Next-To-Leading Order virtual contributions, verifying the ultra-violet pole cancellations at one-loop crucial to the renormalisability of QED.

We then evaluated the Master Integrals for the one-loop Next-To-Leading Order contributions with the AIDA package, for which we developed approaches to interface the package with amplitude-generation code suites such as FEYNCALC, as well as novel twistor parametrisations for four-point massive kinematics in both the single mass case and for two masses. In the massless electron approximation we evaluated the five planar Master Integrals with the Differential Equations method with Magnus exponentials, obtaining the final expressions in terms of Goncharov Polylogarithms up to order 2 in ϵ .

We then applied all the expertise learned in these applications and took the first steps in the eval-

uation of the amplitudes for $\mu^- e^{\rightarrow} \mu^- e^- \gamma$ at one-loop, which constitute part of the Next-To-Next-To-Leading Order contributions to muon-electron scattering. This calculation is among the first fully-analytical five-point, one-loop amplitude decompositions with two mass scales, a testament to the power of the Adaptive Integrand Decomposition technique. Once again we developed twistor parametrisation for both the single and double mass cases and, applying IBP relations, identified the Master integrals. For these runs we used the simplified version of the Adaptive Integrand Decomposition algorithm due to computational constraints and therefore expected the final set of integrals not to correspond to the minimal basis, not in the least for the presence of scalar pentagon integrals. By means of a numerical reduction with the full algorithm we identified the actual set of Master Integrals and confirmed that the pentagon is the only spurious integral present in the fully-analytical result. Future work will no doubt be oriented on the completion of our preliminary work, mainly towards the evaluation of the Master Integrals identified by us with methods such as Differential Equations. Despite the fact that for the five-point amplitudes studied the Master Integral ought to comprise at most four-point functions, the effect of the radiated real photon is to change the momentum flow along the internal propagators, and may entail that results for the four-point Master Integrals may not be recycled so easily.

This work is a further step in the direction of the complete analytical evaluation of $\mu^- e^{\rightarrow} \mu^- e^-$ scattering at Next-To-Next-To-Leading Order. This process may lead to the most accurate and inclusive estimate of the anomalous magnetic moment of the muon to date, one of the gold standards currently available to probe the effects of Beyond-the-Standard-Model physics.

Finally, the importance of the quest for ever-higher precision calculations in Quantum Field Theory cannot be overstated, for it is only with continual advancements on the theory side that experimental data can be properly understood, a fundamental step in the validation of any theory in high-energy physics.

Acknowledgements

I wish to express my immense gratitude to all those who made this thesis work possible.

I thank my supervisor, professor Pierpaolo Mastrolia, for offering me this opportunity in the first place, for introducing me to the breadth of knowledge that lays the foundations of this work, for lending his expertise and guidance at every step of the way, for introducing me to his entire research group, for displaying inspiring passion and commitment to research and, most importantly, for striving to always dedicate time to this thesis project.

I thank my co-supervisor, professor Massimo Passera, for providing an exciting phenomenological background to this thesis work, for guiding my way in the field of Muon physics and clarifying all my doubts on the theory behind the anomalous magnetic moment of the Muon and its measurement.

I thank my co-supervisor, doctor William Javier Torres Bobadilla, for following me in my first steps with automatic amplitude-evaluation codes, for introducing me to AIDA, for his great support in developing Momentum Twistor parametrisation, for his unwavering assistance with technical hurdles and for always having a prompt answer to any issue whatsoever.

I thank Luca Mattiazzi for teaching me the usage of KIRA and REDUZE, for his massive help with IBP-identities and Magnus exponentials, for all the stimulating discussions and for always finding time to be available to help.

I thank Federico Gasparotto for guiding me into the field of Differential Equations and their solution, and for all the time lent to fix my calculations.

I thank Tiziano Peraro for his pivotal suggestion regarding Momentum Twistor parametrisations.

I thank Giovanni Ossola for taking time to clarify doubts regarding integrand decomposition and the OPP method.

I thank Hjalte Frellesvig, Manoj K. Mandal and Stefano Laporta for helpful remarks and insightful discussions in-between work.

I thank Jonathan Ronca for his help with the virtual machines and their software, and for the helpful discussion during his short stay.

I thank the Padova section of INFN for allowing me to use their computing hardware, without which my work would not have been possible, and for providing software licences.

I would also like to show gratitude to the University of Padova and Imperial College London for awarding me a once-in-a-lifetime opportunity to study in London for nine months, be immersed in a stimulating environment and making lasting acquaintances.

I thank all the people who have stood by my side and contributed to making my journey brighter and more pleasing. Friends of many years and sometimes even decades, too many to list individually, who offer moments to cherish and make it all fun and interesting.

Finally I thank immensely my family, for supporting me in thought and action every day for so many years, for providing me with opportunities to achieve what I sought in life. I am truly grateful.

Appendix A

Construction of a massless basis for loop momenta

In multiple situations throughout this thesis we find it convenient to parametrise q^μ , the strictly four-dimensional part of a D -dimensional loop momentum \bar{q}^μ in terms of massless vectors e_i^μ :

$$q^\mu = \sum_{i=1}^4 x_i e_i^\mu \quad (\text{A.1})$$

where the massless vectors can be chosen to satisfy certain criteria:

$$\begin{aligned} e_i^2 &= 0 \\ (e_1 \cdot e_3) &= (e_1 \cdot e_4) = 0 \\ (e_2 \cdot e_3) &= (e_2 \cdot e_4) = 0 \\ (e_1 \cdot e_2) &= -(e_3 \cdot e_4) \end{aligned}$$

Such a basis can be constructed as detailed in [38, 131, 155], and here we shall walk through the steps of its construction.

First, we prove that two massless four-momenta e_{12}^μ can always be obtained from two massive ones. The task at hand is, given two massive vectors K_{12}^μ , to write them as a linear combination of the two massless ones as:

$$\begin{pmatrix} K_1 \\ K_2 \end{pmatrix} = \begin{pmatrix} a & b \\ c & d \end{pmatrix} \begin{pmatrix} e_1 \\ e_2 \end{pmatrix} \quad (\text{A.2})$$

This equation must be inverted, recalling that the inverse of a non-singular matrix is the *adjugate* matrix divided by the determinant:

$$\begin{pmatrix} e_1 \\ e_2 \end{pmatrix} = \frac{1}{(ad - bc)} \begin{pmatrix} d & -b \\ -c & a \end{pmatrix} \begin{pmatrix} K_1 \\ K_2 \end{pmatrix} \quad (\text{A.3})$$

we plug these expressions for e_{12}^μ in their masslessness condition:

$$0 = e_1^2 = \left(\frac{dK_1 - bK_2}{(ad - bc)} \right)^2 \Rightarrow d^2 K_1^2 + b^2 K_2^2 - 2bd K_1 \cdot K_2 = 0 \quad (\text{A.4})$$

$$0 = e_2^2 = \left(\frac{-cK_1 + aK_2}{(ad - bc)} \right)^2 \Rightarrow c^2 K_1^2 + a^2 K_2^2 - 2ac K_1 \cdot K_2 = 0 \quad (\text{A.5})$$

We solve the first equation for d :

$$d = \frac{2bK_1 \cdot K_2 \pm \sqrt{4b^2 (K_1 \cdot K_2)^2 - 4b^2 K_1^2 K_2^2}}{2K_1^2} = \frac{b}{K_1^2} \left[K_1 \cdot K_2 \pm \sqrt{4b^2 (K_1 \cdot K_2)^2 - 4b^2 K_1^2 K_2^2} \right] := \frac{b}{K_1^2} \gamma_{\pm}$$

Analogously we solve the second one and obtain:

$$c = \frac{a}{K_1^2} \gamma_{\pm}$$

the non-singular determinant condition forces us to choose different signs for the γ s, we therefore pick:

$$d = \frac{b}{K_1^2} \gamma_+ \quad (\text{A.6})$$

$$c = \frac{a}{K_1^2} \gamma_- \quad (\text{A.7})$$

It is possible to check explicitly that the following relations are true:

$$\gamma_+ + \gamma_- = 2K_1 \cdot K_2 \quad (\text{A.8})$$

$$\gamma_+ \gamma_- = K_1^2 K_2^2 \quad (\text{A.9})$$

using these and the expressions for c and d lets us re-write the determinant:

$$ad - bc = ad \left(1 - \frac{bc}{ad} \right) = ad \left(1 - \frac{\gamma_-}{\gamma_+} \right) = ad \left(1 - \frac{K_1^2 K_2^2}{\gamma_+^2} \right) := ad\beta \quad (\text{A.10})$$

We define for subsequent simplicity $r_{1,2} := \frac{K_{1,2}^2}{\gamma_+}$. Using all these relations we write the massless vectors:

$$e_1^\mu = \frac{1}{ad\beta} (dK_1^\mu - bK_2^\mu) = \frac{1}{a\beta} (K_1^\mu - r_1 K_2^\mu) \quad (\text{A.11})$$

$$e_2^\mu = \frac{1}{ad\beta} (-cK_1^\mu + aK_2^\mu) = \frac{1}{d\beta} (K_2^\mu - r_2 K_1^\mu) \quad (\text{A.12})$$

Both a and d are arbitrary parameters, so we set them to 1, obtaining the final expression for e_{12}^μ :

$$e_1^\mu = \frac{1}{\beta} (K_1^\mu - r_1 K_2^\mu) \quad (\text{A.13})$$

$$e_2^\mu = \frac{1}{\beta} (K_2^\mu - r_2 K_1^\mu) \quad (\text{A.14})$$

Finally we simplify the scalar product between them using $\beta = 1 - r_1 r_2$:

$$e_1 \cdot e_2 = \frac{1}{\beta^2} (K_1 \cdot k_2 - r_1 K_2^2 - r_2 K_1^2 + r_1 r_2 K_1 \cdot K_2) = \frac{1}{\beta^2} \left(\left(\frac{\gamma_+ + \gamma_-}{2} \right) \left(1 + \frac{\gamma_-}{\gamma_+} \right) - 2\gamma_- \right) \quad (\text{A.15})$$

$$= \frac{\gamma_+}{2\beta^2} \left(1 - 2\frac{\gamma_-}{\gamma_+} + \frac{\gamma_-^2}{\gamma_+^2} \right) = \frac{\gamma_+}{2\beta^2} (1 - r_1 r_2)^2 \quad (\text{A.16})$$

$$= \frac{\gamma_+}{2} \quad (\text{A.17})$$

To complete the basis we need a way to define the other two vectors. We wish to represent massless momentum vectors and therefore we can re-cycle the spinor-helicity representation of polarisation vectors:

$$e_3^\mu = \frac{1}{2} \langle e_1 | \gamma^\mu | e_2 \rangle \quad (\text{A.18})$$

$$e_4^\mu = \frac{1}{2} \langle e_2 | \gamma^\mu | e_1 \rangle \quad (\text{A.19})$$

which are orthogonal to both $e_{1,2}$ as required.

As evident, the entire basis is defined according to two massive vectors. In the context of parametrising a loop momentum within a Feynman amplitude, the natural choice for these vectors is to pick two massive vectors from the external kinematics of the diagram as done in section 4.1.1.

If the kinematics contains less than two independent momenta this is not possible, and K_{12} can only be chosen arbitrarily.

Appendix B

Parametric expansion of Integrand Decomposition residues on the cut solutions

In this appendix we derive explicitly the parametrisation of the Δ s appearing in the integrand decomposition relation 4.4 in terms of *Irreducible Scalar Product (ISP)* in the four-dimensional case.

Let us recap some results derived in chapter 4.1: any term proportional or expressible in terms of the denominators $D_{i,j,k}$ will not constitute an ISP, and it was immediately shown how q^2 and the scalar products $q \cdot p_i$ cannot appear in the parametrisation by this token.

To find the ISPs we shall parametrise the loop momentum q^μ as follows:

$$(q + p_i)^\mu = \frac{1}{(e_1 \cdot e_2)} (x_1 e_1^\mu + x_2 e_2^\mu + x_3 e_3^\mu + x_4 e_4^\mu) \quad (\text{B.1})$$

the loop momentum is expanded onto a basis of four massless vectors $\{e_i^\mu\}$ which satisfies the following:

$$\begin{aligned} e_i^2 &= 0 \\ (e_1 \cdot e_3) &= (e_1 \cdot e_4) = 0 \\ (e_2 \cdot e_3) &= (e_2 \cdot e_4) = 0 \\ (e_1 \cdot e_2) &= -(e_3 \cdot e_4) \end{aligned}$$

such a basis can be constructed as detailed in appendix A.

Thanks to the properties of the chosen basis:

$$(q \cdot e_1) = x_2 \quad (\text{B.2})$$

$$(q \cdot e_2) = x_1 \quad (\text{B.3})$$

$$(q \cdot e_3) = -x_4 \quad (\text{B.4})$$

$$(q \cdot e_4) = -x_3 \quad (\text{B.5})$$

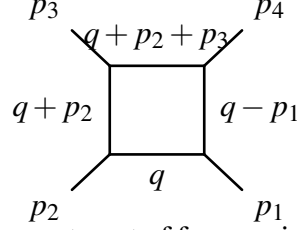
A parametrisation onto ISPs therefore is equivalent to a parametrisation onto polynomials of the x_i :

$$\begin{aligned} N_n(q) = N_n(x_1, x_2, x_3, x_4) &= \sum_{j_1, j_2, j_3, j_4} c_{j_1 j_2 j_3 j_4} x_1^{j_1} x_2^{j_2} x_3^{j_3} x_4^{j_4} \\ j_1 + j_2 + j_3 + j_4 &\leq r_{max} \end{aligned} \quad (\text{B.6})$$

where r_{max} is the maximum allowed rank given the number of denominators of the integrand being reduced.

We shall now consider four, three, two and one-point integrand in succession and derive the most general parametrisation of their residues, taking advantage of the cut conditions that need to be satisfied as per the OPP method, and we will also identify the ISPs.

The four-point residue



In a box diagram only three external momenta out of four are independent, we choose $p_4 = -(p_1 + p_2 + p_3)$. Moreover we choose $p_{1,2}$ to construct $e_{1,2}$.

As for the remaining two massless vectors, it is convenient in this case to combine them as follows [49] to define two new *auxiliary vectors*

$$v^\mu = (p_3 \cdot e_4) e_3^\mu + (p_3 \cdot e_3) e_4^\mu \quad (\text{B.7})$$

$$v_\perp^\mu = (p_3 \cdot e_4) e_3^\mu - (p_3 \cdot e_3) e_4^\mu \quad (\text{B.8})$$

where v^μ can be shown to be a combination of $p_{1,2,3}$ and v_\perp^μ is orthogonal to all of them.

We have:

$$\begin{aligned} v^2 &= -2(p_3 \cdot e_3)(p_3 \cdot e_4)(e_1 \cdot e_2) \\ v_\perp^2 &= 2(p_3 \cdot e_3)(p_3 \cdot e_4)(e_1 \cdot e_2) \\ (v \cdot v_\perp) &= 0 \end{aligned}$$

We now express $e_{3,4}$ in terms of the new vectors:

$$\begin{aligned} e_3^\mu &= \frac{v^\mu + v_\perp^\mu}{2(p_3 \cdot e_4)} \\ e_4^\mu &= \frac{v^\mu - v_\perp^\mu}{2(p_3 \cdot e_3)} \end{aligned}$$

Before rewriting q^μ in this new basis, let us list the cut conditions under which the residue is to be parametrised:

$$\begin{aligned} q^2 = 0 & & (x_1 x_2 - x_3 x_4) \frac{1}{(e_1 \cdot e_2)} = 0 \\ (q - p_1)^2 = 0 & \implies & -(q \cdot p_1) = 0 \\ (q + p_2)^2 = 0 & & (q \cdot p_2) = 0 \\ (q + p_2 + p_3)^2 = 0 & & (q \cdot p_3) + (p_2 \cdot p_3) = 0 \end{aligned}$$

where we used the general properties of the $\{e_i^\mu\}$ basis.

From the first we deduce $x_1 x_2 = x_3 x_4$ and from the second and third:

$$q \cdot e_{1,2} = 0 \quad \implies \quad x_{1,2} = 0$$

And therefore $x_1 x_2 = x_3 x_4 = 0$.

We now rewrite B.1:

$$(q + p_i)^\mu = \frac{1}{(e_1 \cdot e_2)} \left(x_1 e_1^\mu + x_2 e_2^\mu + \left[\frac{x_3}{2(p_3 \cdot e_4)} + \frac{x_4}{2(p_3 \cdot e_3)} \right] v^\mu + \left[\frac{x_3}{2(p_3 \cdot e_4)} - \frac{x_4}{2(p_3 \cdot e_3)} \right] v_\perp^\mu \right) \quad (\text{B.9})$$

Given that the first two quantities $x_{1,2}$ in fact vanish, we immediately infer that $(q \cdot e_{1,2})$ cannot appear in the parametrisation and are not ISPs. Let us therefore project the loop momentum onto the auxiliary vectors:

$$\begin{aligned} (q \cdot v^\mu) &= [x_3 (p_3 \cdot e_3) + x_4 (p_3 \cdot e_4)] \\ (q \cdot v_\perp^\mu) &= [-x_3 (p_3 \cdot e_3) + x_4 (p_3 \cdot e_4)] \end{aligned}$$

Only $(q \cdot v_\perp^\mu)$ is an ISP, as the other auxiliary vector is a combination of the external momenta. To examine any potential other ISP, let us square these two:

$$\begin{aligned} (q \cdot v^\mu)^2 &= \left[x_3^2 (p_3 \cdot e_3)^2 + x_4^2 (p_3 \cdot e_4)^2 + 2x_3 x_4 (p_3 \cdot e_3) (p_3 \cdot e_4) \right] \\ (q \cdot v_\perp^\mu)^2 &= \left[x_3^2 (p_3 \cdot e_3)^2 + x_4^2 (p_3 \cdot e_4)^2 - 2x_3 x_4 (p_3 \cdot e_3) (p_3 \cdot e_4) \right] \\ \implies (q \cdot v_\perp^\mu)^2 &= (q \cdot v^\mu)^2 \end{aligned}$$

where we used $x_3 x_4 = 0$. This proves that any higher power of $(q \cdot v_\perp^\mu)$ can be written as reducible scalar products, and therefore is not an ISP.

If we define new parameters associated to the new vectors we introduced:

$$\begin{aligned} (q \cdot v^\mu) &:= x_{3,v} \\ (q \cdot v_\perp^\mu) &:= x_{4,v} \end{aligned}$$

then we can finally write down the parametrised box residue in a simple form:

$$\Delta_{ijkl} = c_{4,0} + c_{4,1} (q \cdot v_\perp) = c_{4,0} + c_{4,1} x_{4,v} \quad (\text{B.10})$$

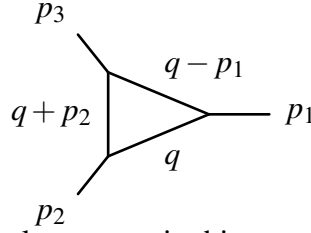
This expression plugs into 4.3. Let us then integrate the box-residue term of 4.3 over the loop momentum (as one would do to retread back to the integral level) to see that the ISP term generates a spurious term.

$$\int d^D q \frac{\Delta_{ijkl}}{D_i D_j D_k D_l} = c_{0,0} I_{ijkl} + c_{3,0} v_{\perp}^{\mu} I_{ijkl}^{\mu} = c_{4,0} I_{ijkl} + c_{4,1} v_{\perp}^{\mu} [A_4 p_1^{\mu} + B_4 p_2^{\mu} + C_4 p_3^{\mu}]$$

$$= c_0 I_{ijkl}$$

where we tensor-decomposed I_{ijkl}^{μ} and recalled that v_{\perp}^{μ} is by definition orthogonal to all independent external momenta.

The three-point residue



There are only two independent external momenta in this case. We begin by listing the cut conditions:

$$\begin{aligned} q^2 &= 0 \\ (q - p_1)^2 &= 0 \\ (q + p_2)^2 &= 0 \end{aligned} \quad \Longrightarrow \quad \begin{aligned} x_1 x_2 &= x_3 x_4 \\ -(q \cdot p_1) &= 0 \\ (q \cdot p_2) &= 0 \end{aligned}$$

and, once again, $x_{1,2} = 0$ and thus $x_3 x_4 = 0$.

Since $e_{3,4}$ are all independent of the two external momenta used to construct $e_{1,2}$, we immediately have two ISPs:

$$\begin{aligned} (q \cdot e_3) &= -x_4 \\ (q \cdot e_4) &= -x_3 \end{aligned}$$

The cross-product $(q \cdot e_3)(q \cdot e_4)$ is proportional to $x_3 x_4$ and therefore trivially not an ISP.

The ISPs are then $(q \cdot e_{3,4})$ and all their powers, except for the cross-products. The expanded residue is:

$$\begin{aligned} \Delta_{ijk} &= c_{3,0} + c_{3,1} (q \cdot e_4) + c_{3,2} (q \cdot e_4)^2 + c_{3,3} (q \cdot e_4)^3 + c_{3,4} (q \cdot e_3) + c_{3,5} (q \cdot e_3)^2 + c_{3,6} (q \cdot e_3)^3 \\ &= c_{3,0} + c_{3,1} x_4 + c_{3,2} x_4^2 + c_{3,3} x_4^3 + c_{3,4} x_3 + c_{3,5} x_3^2 + c_{3,6} x_3^3 \end{aligned}$$

Let us integrate over the loop momentum:

$$\int d^D q \frac{\Delta_{ijk}}{D_i D_j D_k} =$$

$$= c_0 I_{ijk} + [c_{3,4} e_3^{\mu} + c_{3,0} e_4^{\mu}] I_{ijk}^{\mu} + [c_{3,5} e_3^{\mu} e_3^{\nu} + c_{3,2} e_4^{\mu} e_4^{\nu}] I_{ijk}^{\mu\nu} + [c_{3,6} e_3^{\mu} e_3^{\nu} e_3^{\rho} + c_{3,3} e_4^{\mu} e_4^{\nu} e_4^{\rho}] I_{ijk}^{\mu\nu\rho}$$

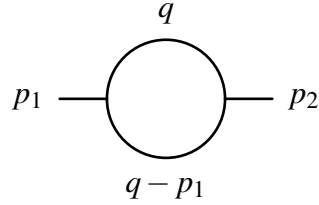
and list the (formal) tensor decomposition formulas that should be applied:

$$\begin{aligned}
 I_{ijk}^\mu &\simeq p_1^\mu + p_2^\mu \\
 I_{ijk}^{\mu\nu} &\simeq g^{\mu\nu} + \sum_{i,j=1}^2 p_i^\mu p_j^\nu \\
 I_{ijk}^{\mu\nu\rho} &\simeq \sum_{i=1}^2 (g^{\mu\nu} p_i^\rho + g^{\nu\rho} p_i^\mu + g^{\rho\mu} p_i^\nu) + \sum_{i,j,k=1}^2 p_i^\mu p_j^\nu p_k^\rho
 \end{aligned}$$

We thus have many contractions like $(e_{3,4} \cdot p_{1,2})$ which all vanish by orthogonality, as well as $g_{\mu\nu} e_{3,4}^\mu e_{3,4}^\nu$, which vanish by the massless condition.

Once again, the ISP terms are all spurious.

The two-point residue



Now only one external momentum is independent, therefore we need some arbitrary 4-vector K_2 to construct the massless basis. We choose this so that $(p_1 \cdot e_2) = 0$.

We list the cut conditions:

$$\begin{aligned}
 q^2 = 0 & & x_1 x_2 = x_3 x_4 \\
 (q - p_1)^2 = 0 & \implies & -(q \cdot p_1) = 0
 \end{aligned}$$

We have $x_2 = 0$ and therefore $x_1 x_2 = x_3 x_4 = 0$

We can construct $e_{1,2}$ so that one of $(q \cdot e_{1,2})$ is an ISP, but obviously not both. The cut conditions compel us to choose the latter and therefore the first ISPs are:

$$\begin{aligned}
 (q \cdot e_2) &= x_1 \\
 (q \cdot e_3) &= -x_4 \\
 (q \cdot e_4) &= -x_3
 \end{aligned}$$

Powers of these are also ISPs, up to degree 2.

Let us examine the cross products:

$$\begin{aligned}
 (q \cdot e_2)(q \cdot e_3) &= -x_1 x_4 \\
 (q \cdot e_2)(q \cdot e_4) &= -x_1 x_3 \\
 (q \cdot e_3)(q \cdot e_4) &= x_3 x_4
 \end{aligned}$$

By the cut conditions the last cross-product vanishes and is not an ISP.

The parametrised residue is then:

$$\begin{aligned}\Delta_{ij} &= c_{2,0} + c_{2,1} (q \cdot e_2) + c_{2,2} (q \cdot e_2)^2 + c_{2,3} (q \cdot e_3) + c_{2,4} (q \cdot e_3)^2 + \\ &\quad + c_{2,5} (q \cdot e_4) + c_{2,6} (q \cdot e_4)^2 - c_{2,7} (q \cdot e_2) (q \cdot e_3) - c_{2,8} (q \cdot e_2) (q \cdot e_4) \\ &= c_{2,0} + c_{2,1}x_1 + c_{2,2}x_1^2 - c_{2,3}x_4 + c_{2,4}x_4^2 - c_{2,5}x_3 + c_{2,6}x_3^2 - c_{2,7}x_1x_4 - c_{2,8}x_1x_3\end{aligned}$$

Integrating:

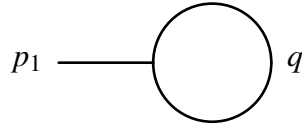
$$\begin{aligned}&\int d^D q \frac{\Delta_{ij}}{D_i D_j} = \\ &= c_{2,0} I_{ij} + [c_{2,1} e_2^\mu + c_{2,3} e_3^\mu + c_{2,5} e_4^\mu] I_{ij}^\mu + [c_{2,2} e_2^\mu e_2^\nu + c_{2,4} e_3^\mu e_3^\nu + c_{2,6} e_4^\mu e_4^\nu + c_{2,7} e_2^\mu e_3^\nu + c_{2,8} e_2^\mu e_4^\nu] I_{ij}^{\mu\nu}\end{aligned}$$

the tensor decompositions to be used are, in this case:

$$\begin{aligned}I_{ij}^\mu &\simeq p_1^\mu \\ I_{ij}^{\mu\nu} &\simeq g^{\mu\nu} + p_1^\mu p_1^\nu\end{aligned}$$

By the orthogonality and masslessness properties of the basis one sees how the ISP terms are all spurious.

The one-point residue



This time we are forced to construct the basis from scratch, having no independent external momenta available. We choose two arbitrary vectors to do so.

The only cut condition in this case is:

$$q^2 = 0 \quad \implies \quad x_1 x_2 = x_3 x_4$$

This is simply a constraint on these quantities, as in this case we have no further cut conditions that kill one of the x_i quantities.

Having not used any external momentum vector to build the basis we have the full complement of ISPs :

$$\begin{aligned}(q \cdot e_1) &= x_2 \\ (q \cdot e_2) &= x_1 \\ (q \cdot e_3) &= x_4 \\ (q \cdot e_4) &= x_3\end{aligned}$$

No higher powers of these are allowed since they would exceed the allowed rank. The parametrisation is then, simply:

$$\begin{aligned}\Delta_i &= c_{1,0} + c_{1,1}(q \cdot e_1) + c_{1,2}(q \cdot e_2) + c_{1,3}(q \cdot e_3) + c_{1,4}(q \cdot e_4) \\ &= c_{2,0} + c_{2,1}x_1 - c_{1,2}x_2 - c_{1,3}x_3 - c_{1,4}x_4\end{aligned}$$

By integrating we find:

$$\int d^D q \frac{\Delta_i}{D_i} = c_{1,0}I_i + [c_{1,1}e_1^\mu + c_{1,2}e_2^\mu + c_{1,3}e_3^\mu + c_{1,4}e_4^\mu] I_i^\mu$$

As I_i^μ vanishes trivially, we have proved that the ISPs are spurious.

Let us summarise the resulting parametrised residues:

$$\begin{aligned}\Delta_{ijkl} &= c_{4,0} + c_{4,1}x_{4,v} \\ \Delta_{ijk} &= c_{3,0} + c_{3,1}x_4 + c_{3,2}x_4^2 + c_{3,3}x_4^3 + c_{3,4}x_3 + c_{3,5}x_3^2 + c_{3,6}x_3^3 \\ \Delta_{ij} &= c_{2,0} + c_{2,1}x_1 + c_{2,2}x_1^2 - c_{2,3}x_4 + c_{2,4}x_4^2 - c_{2,5}x_3 + c_{2,6}x_3^2 - c_{2,7}x_1x_4 - c_{2,8}x_1x_3 \\ \Delta_i &= c_{1,0} + c_{1,1}x_1 - c_{1,2}x_2 - c_{1,3}x_3 - c_{1,4}x_4\end{aligned}\tag{B.11}$$

Appendix C

Complete NLO Virtual corrections to μ - e scattering

We report here in their entirety the the virtual NLO corrections to muon-electron scattering computed in FEYNCALC, which correspond to the interferences of the 1-loop amplitudes with the lone tree-level amplitude \mathcal{M}_0 . The square amplitudes have been decomposed using the FEYNCALC implementation of Passarino-Veltman reduction, which also uses the letters A, B, C, D to refer to one-,two-,three-,four-point PV-functions respectively.

$$\begin{aligned}
 2 \times \frac{1}{4} \mathcal{M}_1^{VPe} \mathcal{M}_0^* &= \text{[Diagram: 1-loop vertex correction to } \mu e \text{ scattering]} \quad (C.1) \\
 &= -\frac{4\pi^2 e^2}{(D-1)t} \chi_0 \left(c_1 B_0(t, m_e^2, m_e^2) + c_2 A_0(m_e^2) \right)
 \end{aligned}$$

where:

$$\begin{aligned}
 c_1 &= ((D-2)t + 4m_e^2) \\
 c_2 &= -2(D-2)
 \end{aligned}$$

$$\begin{aligned}
 2 \times \frac{1}{4} \mathcal{M}_1^{VP\mu} \mathcal{M}_0^* &= \text{[Diagram: 1-loop vertex correction to } \mu \mu \text{ scattering]} \quad (C.2) \\
 &= -\frac{4\pi^2 e^2}{(D-1)t} \chi_0 \left(c_1 B_0(t, m_\mu^2, m_\mu^2) + c_2 A_0(m_\mu^2) \right)
 \end{aligned}$$

where:

$$\begin{aligned}
 c_1 &= ((D-2)t + 4m_\mu^2) \\
 c_2 &= -2(D-2)
 \end{aligned}$$

$$2 \times \frac{1}{4} \mathcal{M}_1^{VC\mu} \mathcal{M}_0^* = \begin{array}{c} \text{Diagram 1} \\ \text{Diagram 2} \end{array} \quad (C.3)$$

$$= \frac{2\pi^2 e^6}{t^2(4m_\mu^2 - t)} \left(c_1 \mathbf{B}_0(m_\mu^2, 0, m_\mu^2) + c_2 \mathbf{B}_0(t, m_\mu^2, m_\mu^2) + c_3 \mathbf{C}_0(m_\mu^2, m_\mu^2, t, m_\mu^2, 0, m_\mu^2) + c_4 \mathbf{A}_0(m_\mu^2) \right)$$

where:

$$c_1 = 4 \left(-4t^2(s - (D-2)m_\mu^2) - (D-2)t^3 - 4t \left((m_e^2)^2 - 2s(m_e^2 + 2m_\mu^2) + (m_\mu^2)^2 + s^2 \right) + 8m_\mu^2(m_e^2 + m_\mu^2 - s)^2 \right)$$

$$c_2 = - \left(4t \left((D-7)(m_e^2)^2 - 2m_e^2((D-3)m_\mu^2 + (D-7)s) + (D-7)(m_\mu^2)^2 - 2(D-11)m_\mu^2 s + (D-7)s^2 \right) + 4(D-7)t^2(s - (D-2)m_\mu^2) + (D-7)(D-2)t^3 + 32m_\mu^2(m_e^2 + m_\mu^2 - s)^2 \right)$$

$$c_3 = 2 \left(8(m_\mu^2)^2 - 6m_\mu^2 t + t^2 \right) \left((D-2)t^2 + 4(m_e^2 + m_\mu^2 - s)^2 + 4st \right)$$

$$c_4 = 8(D-2) \left((m_e^2 + m_\mu^2 - s)^2 + t(s - m_e^2) \right)$$

$$2 \times \frac{1}{4} \mathcal{M}_1^{VCe} \mathcal{M}_0^* = \begin{array}{c} \text{Diagram 1} \\ \text{Diagram 2} \end{array} \quad (C.4)$$

$$= \frac{2\pi^2 e^6}{t^2(4m_e^2 - t)} \left(c_1 \mathbf{B}_0(m_e^2, 0, m_e^2) + c_2 \mathbf{B}_0(t, m_e^2, m_e^2) + c_3 \mathbf{C}_0(m_e^2, m_e^2, t, m_e^2, 0, m_e^2) + c_4 \mathbf{A}_0(m_e^2) \right)$$

where:

$$c_1 = 4 \left(-4t^2(s - (D-2)m_e^2) - (D-2)t^3 - 4t \left((m_e^2)^2 - 4m_e^2 s + (m_\mu^2 - s)^2 \right) + 8m_e^2(m_e^2 + m_\mu^2 - s)^2 \right)$$

$$c_2 = \left(4t \left((D-7)(m_e^2)^2 - 2m_e^2((D-3)m_\mu^2 + (D-11)s) + (D-7)(m_\mu^2 - s)^2 \right) + 4(D-7)t^2(s - (D-2)m_e^2) + (D-7)(D-2)t^3 + 32m_e^2(m_e^2 + m_\mu^2 - s)^2 \right)$$

$$c_3 = 2 \left(8(m_e^2)^2 - 6m_e^2 t + t^2 \right) \left((D-2)t^2 + 4(m_e^2 + m_\mu^2 - s)^2 + 4st \right)$$

$$c_4 = 8(D-2) \left((m_e^2 + m_\mu^2 - s)^2 + t(s - m_\mu^2) \right)$$

$$2 \times \frac{1}{4} \mathcal{M}_1^{Box} \mathcal{M}_0^* = \begin{array}{c} \text{---} \\ \text{---} \\ \text{---} \\ \text{---} \end{array} \begin{array}{c} \text{---} \\ \text{---} \\ \text{---} \\ \text{---} \end{array} \begin{array}{c} \text{---} \\ \text{---} \\ \text{---} \\ \text{---} \end{array} \begin{array}{c} \text{---} \\ \text{---} \\ \text{---} \\ \text{---} \end{array} \quad (C.5)$$

$$\begin{aligned} &= \frac{\pi^2 e^6}{t} \left(c_1 B_0(m_\mu^2, 0, m_\mu^2) + c_2 B_0(m_e^2, 0, m_e^2) + c_3 B_0(s, m_e^2, m_\mu^2) + c_4 B_0(t, 0, 0) \right. \\ &\quad + c_5 C_0(m_e^2, m_e^2, t, 0, m_e^2, 0) + c_6 C_0(m_\mu^2, m_\mu^2, t, 0, m_\mu^2, 0) \\ &\quad \left. + c_7 C_0(m_e^2, m_\mu^2, s, m_e^2, 0, m_\mu^2) + c_8 D_0(m_e^2, m_e^2, m_\mu^2, m_\mu^2, t, s, 0, m_e^2, 0, m_\mu^2) \right) \end{aligned}$$

where:

$$\begin{aligned} c_1 &= \frac{4m_\mu^2}{(4m_\mu^2 - t) \left((m_e^2)^2 - 2m_e^2(m_\mu^2 + s) + (m_\mu^2 - s)^2 \right)} \\ &\quad \left(4(D-2)(m_e^2 + m_\mu^2 - s) \left((m_e^2)^2 - 2m_e^2(m_\mu^2 + s) + (m_\mu^2 - s)^2 \right) - 2t \left((m_e^2 - m_\mu^2) \right. \right. \\ &\quad \left. \left((D-2)m_e^2 + (5D-14)m_\mu^2 \right) - 2(D-2)m_e^2 s + 4(D-3)m_\mu^2 s + (D-2)s^2 \right) \\ &\quad \left. + (3D-8)t^2(m_e^2 - m_\mu^2 + s) \right) \\ c_2 &= \frac{4m_e^2}{(4m_e^2 - t) \left((m_e^2)^2 - 2m_e^2(m_\mu^2 + s) + (m_\mu^2 - s)^2 \right)} \\ &\quad \left(2t \left((5D-14)(m_e^2)^2 - 4(D-3)m_e^2(m_\mu^2 + s) - (D-2)(m_\mu^2 - s)^2 \right) \right. \\ &\quad \left. + 4(D-2)(m_e^2 + m_\mu^2 - s) \left((m_e^2)^2 - 2m_e^2(m_\mu^2 + s) + (m_\mu^2 - s)^2 \right) - (3D-8)t^2(m_e^2 - m_\mu^2 - s) \right) \\ c_3 &= 2 \left(-\frac{(3D-8)t(m_e^2 - m_\mu^2 - s)(m_e^2 - m_\mu^2 + s)}{(m_e^2)^2 - 2m_e^2(m_\mu^2 + s) + (m_\mu^2 - s)^2} - 2(D-2)(m_e^2 + m_\mu^2 - s) \right) \\ c_4 &= \frac{2}{(t - 4m_e^2)(4m_\mu^2 - t)} \left(2t^2((D-2)s - (5D-14)(m_e^2 + m_\mu^2)) \right. \\ &\quad \left. + 32(D-2)m_e^2 m_\mu^2 (m_e^2 + m_\mu^2 - s) + 16(D-4)m_e^2 m_\mu^2 t + (3D-8)t^3 \right) \\ c_5 &= \frac{1}{4m_e^2 - t} \left(-8t \left((D-2)(m_e^2)^2 + (D-4)m_e^2 m_\mu^2 - (D-8)m_e^2 s - 2(m_\mu^2 - s)^2 \right) \right. \\ &\quad \left. + 8t^2(s - (D-3)m_e^2) + (3D-8)t^3 - 64m_e^2(m_\mu^2 - s)(m_e^2 + m_\mu^2 - s) \right) \\ c_6 &= \frac{1}{4m_\mu^2 - t} \left(8t \left(s((D-8)m_\mu^2 - 4m_e^2) + (m_e^2 + m_\mu^2)(2m_e^2 - (D-2)m_\mu^2) + 2s^2 \right) \right. \\ &\quad \left. + 8t^2(s - (D-3)m_\mu^2) + (3D-8)t^3 - 64m_\mu^2(m_e^2 - s)(m_e^2 + m_\mu^2 - s) \right) \\ c_7 &= -2(Dt + 8s)(m_e^2 + m_\mu^2 - s) \\ c_8 &= (-m_e^2 - m_\mu^2 + s) \left((3D-8)t^2 + 16(m_e^2 + m_\mu^2 - s)^2 + 8st \right) \end{aligned}$$

$$2 \times \frac{1}{4} \mathcal{M}_1^{Box} \mathcal{M}_0^* = \begin{array}{c} \text{---} \\ \text{---} \\ \text{---} \\ \text{---} \end{array} \begin{array}{c} \text{---} \\ \text{---} \\ \text{---} \\ \text{---} \end{array} \quad \begin{array}{c} \text{---} \\ \text{---} \\ \text{---} \\ \text{---} \end{array} \begin{array}{c} \text{---} \\ \text{---} \\ \text{---} \\ \text{---} \end{array} \quad (C.6)$$

$$= \frac{\pi^2 e^6}{t} \left(c_1 B_0(m_e^2, 0, m_e^2) + c_2 B_0(m_\mu^2, 0, m_\mu^2) + c_3 B_0(2m_e^2 + 2m_\mu^2 - s - t, m_e^2, m_\mu^2) \right. \\ \left. + c_4 B_0(t, 0, 0) + c_5 C_0(m_e^2, m_e^2, t, 0, m_e^2, 0) + c_6 C_0(m_e^2, m_\mu^2, 2m_e^2 + 2m_\mu^2 - s - t, m_e^2, 0, m_\mu^2) \right. \\ \left. + c_7 C_0(m_\mu^2, m_\mu^2, t, 0, m_\mu^2, 0) + c_8 D_0(m_e^2, m_e^2, m_\mu^2, m_\mu^2, t, 2m_e^2 + 2m_\mu^2 - s - t, 0, m_e^2, 0, m_\mu^2) \right)$$

where:

$$c_1 = \frac{4m_e^2}{(4m_e^2 - t) \left((m_e^2)^2 - 2m_e^2(m_\mu^2 + s + t) + (-m_\mu^2 + s + t)^2 \right)} \\ \left(2t \left((D-6)(m_e^2)^2 + 4m_e^2(3(D-3)m_\mu^2 + (D-1)s) - 5(D-2)(m_\mu^2 - s)^2 \right) + (D-4)t^3 \right. \\ \left. + 4(D-2)(m_e^2 + m_\mu^2 - s) \left((m_e^2)^2 - 2m_e^2(m_\mu^2 + s) + (m_\mu^2 - s)^2 \right) \right. \\ \left. + t^2((24 - 7D)m_e^2 - D(m_\mu^2 + 5s) + 8(m_\mu^2 + s)) \right) \\ c_2 = \frac{4m_\mu^2}{(4m_\mu^2 - t) \left((m_e^2)^2 - 2m_e^2(m_\mu^2 + s + t) + (-m_\mu^2 + s + t)^2 \right)} \\ \left(2t \left(-5(D-2)(m_e^2)^2 + 2m_e^2(6(D-3)m_\mu^2 + 5(D-2)s) + (m_\mu^2 - s)((D-6)m_\mu^2 + 5(D-2)s) \right) + (D-4)t^3 \right. \\ \left. + 4(D-2)(m_e^2 + m_\mu^2 - s) \left((m_e^2)^2 - 2m_e^2(m_\mu^2 + s) + (m_\mu^2 - s)^2 \right) + t^2((8 - D)m_e^2 + (24 - 7D)m_\mu^2 + (8 - 5D)s) \right) \\ c_3 = -\frac{2}{(m_e^2)^2 - 2m_e^2(m_\mu^2 + s + t) + (-m_\mu^2 + s + t)^2} \\ \left(t \left(3(D-4)(m_e^2)^2 + m_e^2((26D - 72)m_\mu^2 + 8s) + (m_\mu^2 - s)(3(D-4)m_\mu^2 + (3D-4)s) \right) + (D-4)t^3 \right. \\ \left. + 2(D-2)(m_e^2 + m_\mu^2 - s) \left((m_e^2)^2 - 2m_e^2(m_\mu^2 + s) + (m_\mu^2 - s)^2 \right) - 2t^2((3D-10)(m_e^2 + m_\mu^2) + 2s) \right) \\ c_4 = \frac{2}{(t - 4m_e^2)(4m_\mu^2 - t)} \left(2t^2((3D-10)(m_e^2 + m_\mu^2) + (D-2)s) + 32(D-2)m_e^2 m_\mu^2 (m_e^2 + m_\mu^2 - s) \right. \\ \left. + 16(8 - 3D)m_e^2 m_\mu^2 t + (4 - D)t^3 \right) \\ c_5 = -\frac{1}{4m_e^2 - t} \left(8t \left((D+18)(m_e^2)^2 + (D+12)m_e^2 m_\mu^2 - (D+16)m_e^2 s + 2(m_\mu^2 - s)^2 \right) \right. \\ \left. + 8t^2((2D+3)m_e^2 + 2m_\mu^2 - 3s) - 3Dt^3 + 64m_e^2(m_e^2 + m_\mu^2 - s)(2m_e^2 + m_\mu^2 - s) \right) \\ c_6 = -2(m_e^2 + m_\mu^2 - s - t)((D-8)t + 16m_e^2 + 16m_\mu^2 - 8s) \\ c_7 = \frac{1}{4m_\mu^2 - t} \left(-8t \left((D+12)m_e^2 m_\mu^2 + (D+18)(m_\mu^2)^2 - (D+16)m_\mu^2 s + 2(m_e^2)^2 - 4m_e^2 s + 2s^2 \right) \right. \\ \left. + 8t^2((2D+3)m_\mu^2 + 2m_e^2 - 3s) - 3Dt^3 + 64m_\mu^2(m_e^2 + m_\mu^2 - s)(m_e^2 + 2m_\mu^2 - s) \right) \\ c_8 = (-m_e^2 - m_\mu^2 + s + t) \left(3Dt^2 + 16(m_e^2 + m_\mu^2 - s)^2 - 16t(m_e^2 + m_\mu^2) + 24st \right)$$

Appendix D

Feynman rules for counterterm diagrams

The bare QED Langrangian can be written as:

$$\mathcal{L}_{QED} = \mathcal{L}_{REN} + \mathcal{L}_{CT} \quad (D.1)$$

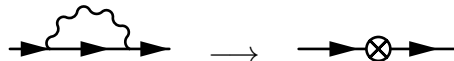
where²⁶:

$$\begin{aligned} \mathcal{L}_{REN} &= \bar{\Psi} (i\partial - m) \Psi - \frac{1}{4} F_{\mu\nu} F^{\mu\nu} - e \bar{\Psi} \gamma^\mu \Psi A_\mu \\ \mathcal{L}_{CT} &= (Z_\Psi - 1) \bar{\Psi} (i\partial - Z_m m) \Psi - (Z_A - 1) \frac{1}{4} F_{\mu\nu} F^{\mu\nu} - Z_e Z_\Psi Z_A^{1/2} e \bar{\Psi} \gamma^\mu \Psi A_\mu \end{aligned}$$

and where sometimes the renormalisation constants in front of the interaction term are compacted into z_1 . \mathcal{L}_{CT} is a lagrangian that produces so-called *counterterm diagrams* whose amplitudes are meant to be paired up with "regular" loop Feynman amplitudes in order to offset their unphysical divergences if present.

To deal with counterterm insertions in FEYNALC we used a custom interaction model, QEDW, developed for FEYNARTS and FEYNALC by William J. Torres Bobadilla. We draw here the counterterm Feynman diagrams associated to the divergent loop diagrams for a generic lepton l and we list the Feynman rules generated.

All the Feynman rules depend on three renormalisation factors Z_i , $i = e, m, A, \Psi$, associated to the four objects that need to be redefined in order for them to be "physical" expressions, as opposed to representing "bare" quantities that we are unable to measure.

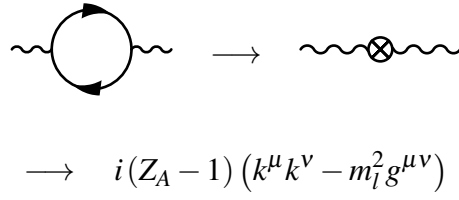


$$(D.2)$$

$$\longrightarrow -im_l (Z_m - 1) Z_\Psi$$

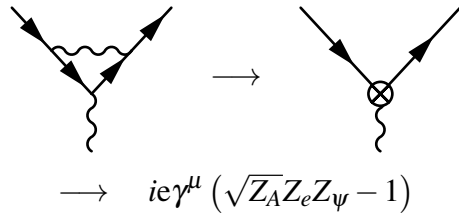
This expression is actually obtained by applying the massive Dirac equation for the lepton on the output given by FEYNALC.

²⁶For the purposes of this appendix we neglect the Gauge-Fixing term.



$$\begin{aligned} & \longrightarrow i(Z_A - 1)(k^\mu k^\nu - m_l^2 g^{\mu\nu}) \end{aligned} \quad (\text{D.3})$$

where k is the photon's four-momentum.



$$\longrightarrow ie\gamma^\mu(\sqrt{Z_A}Z_eZ_\psi - 1) \quad (\text{D.4})$$

and it is worth reminding that this counterterm is meant to be paired up only with the F_1 contribution to the whole triangle loop²⁷.

As it is often done in literature, these factors are re-written as $Z_i = 1 + \alpha\delta_i$ where the δ_i , $i = e, m, A, \psi$ are the *counterterms* proper, and where α should be interpreted as a parameter identifying a single power of a counterterm, and not the fine-structure constant of QED.

Once a renormalisation prescription has been set up, these terms receive an explicit expression. For the calculations in chapter 7 we shall use the following definitions derived in the on-shell renormalisation scheme, and have been simplified by applying once again 7.8:

$$\delta_e \longrightarrow \frac{\pi^2(D-2)e^2 A_0(m_l^2)}{3m_l^2} \quad (\text{D.5})$$

$$\delta_m \longrightarrow -\frac{\pi^2(D-2)(D-1)e^2 A_0(m_l^2)}{2(D-3)m_l^2} \quad (\text{D.6})$$

$$\delta_A \longrightarrow -\frac{2\pi^2(D-2)e^2 A_0(m_l^2)}{3m_l^2} \quad (\text{D.7})$$

$$\delta_\psi \longrightarrow -\frac{\pi^2(D-2)(D-1)e^2 A_0(m_l^2)}{2(D-3)m_l^2} \quad (\text{D.8})$$

the only PV function appearing is the tadpole A_0 , defined and normalised as reported at the end of chapter 2.2.1. These expressions are of course independent of the lepton particle under advisement, provided their electro-magnetic charge is always equal to e .

²⁷This can be seen in equation 1.47, if one neglects the Hadronic VP function insertion.

Appendix E

Detailed results for massive one-loop 4-point Master Integrals

In this appendix we write down explicitly the general solution to the systems of Differential Equations set up in chapter 8. As mentioned, the solutions have been computed running manually through the procedure detailed in chapter 2.4 up to second order in the ε expansion.

The general form of the solution is, once again:

$$\vec{\mathcal{I}}(x, y, \varepsilon) = (\mathbb{1} + \varepsilon \mathbb{B}^1(x, y) + \varepsilon^2 \mathbb{B}^2(x, y)) \vec{\mathcal{I}}^0(\varepsilon) \quad (\text{E.1})$$

where the B objects are 5×5 matrices whose entries contain Generalised Polylogarithms²⁸ up to weight 2, and where each component of the vector of boundary conditions $\vec{\mathcal{I}}^0$ is written as:

$$\mathcal{I}_k^0(\varepsilon) = \sum_{j=0}^2 \varepsilon^j \xi(k, j) \quad (\text{E.2})$$

Each integral is written as the matrix product of the B matrices with the boundary conditions vector, with explicit coefficient variables, expanded up to order ε^2 . These expressions will be useful in determining the $\xi(k, j)$ coefficients themselves.

$$\mathcal{I}_1 = \varepsilon \times \begin{array}{c} p_4 \quad p_3 \\ \diagdown \quad \diagup \\ \text{---} \text{---} \\ \diagup \quad \diagdown \\ p_1 \quad p_2 \end{array} = \xi(1, 0) + \varepsilon \xi(1, 1) + \varepsilon^2 \xi(1, 2) \quad (\text{E.3})$$

$$\mathcal{I}_2 = m_\mu^2 x \varepsilon \times \begin{array}{c} p_2 \quad p_3 \\ \diagdown \quad \diagup \\ \text{---} \text{---} \\ \diagup \quad \diagdown \\ p_1 \quad p_4 \end{array} = \xi(2, 0) + \varepsilon c_1 + \varepsilon^2 c_2 \quad (\text{E.4})$$

where:

$$\begin{aligned} c_1 &= \xi(1, 0)(-G(\{-1\}, x)) - 2\xi(2, 0)G(\{-1\}, x) + \xi(2, 0)G(\{0\}, x) + \xi(2, 1) \\ c_2 &= 2\xi(1, 0)G(\{-1, -1\}, x) - \xi(1, 0)G(\{0, -1\}, x) - \xi(1, 1)G(\{-1\}, x) \\ &\quad + 4\xi(2, 0)G(\{-1, -1\}, x) - 2\xi(2, 0)G(\{-1, 0\}, x) - 2\xi(2, 0)G(\{0, -1\}, x) \\ &\quad + \xi(2, 0)G(\{0, 0\}, x) - 2\xi(2, 1)G(\{-1\}, x) + \xi(2, 1)G(\{0\}, x) + \xi(2, 2) \end{aligned}$$

²⁸Their definition is given in relation 2.119.

$$\mathcal{I}_3 = \frac{m_\mu^2 (y-1)^2 \varepsilon}{y} \times \begin{array}{c} p_2 \quad p_3 \\ \diagdown \quad / \\ \bigcirc \\ / \quad \diagdown \\ p_1 \quad p_4 \end{array} = \xi(3,0) + \varepsilon c_1 + \varepsilon^2 c_2 \quad (\text{E.5})$$

where:

$$\begin{aligned} c_1 &= (\xi(3,0)G(\{0\},y) - 2\xi(3,0)G(\{1\},y) + \xi(3,1)) \\ c_2 &= 2(\xi(3,0)G(\{0,0\},y) - 2\xi(3,0)G(\{0,1\},y) - 2\xi(3,0)G(\{1,0\},y) + 4\xi(3,0)G(\{1,1\},y) \\ &\quad + \xi(3,1)G(\{0\},y) - 2\xi(3,1)G(\{1\},y) + \xi(3,2)) \end{aligned}$$

$$\mathcal{I}_4 = \frac{m_\mu^2 (y^2 - 1) \varepsilon^2}{y} \times \begin{array}{c} p_2 \quad p_3 \\ \diagdown \quad / \\ \triangle \\ / \quad \diagdown \\ p_1 \quad p_4 \end{array} = \xi(4,0) + \varepsilon c_1 + \varepsilon^2 c_2 \quad (\text{E.6})$$

where:

$$\begin{aligned} c_1 &= \xi(1,0)G(\{0\},y) - \xi(3,0)G(\{0\},y) + 2\xi(4,0)G(\{-1\},y) - 2\xi(4,0)G(\{1\},y) + \xi(4,1) \\ c_2 &= 2\xi(1,0)G(\{-1,0\},y) - 2\xi(1,0)G(\{1,0\},y) + \xi(1,1)G(\{0\},y) - 2\xi(3,0)G(\{-1,0\},y) \\ &\quad - \xi(3,0)G(\{0,0\},y) + 2\xi(3,0)G(\{0,1\},y) + 2\xi(3,0)G(\{1,0\},y) - \xi(3,1)G(\{0\},y) \\ &\quad + 4\xi(4,0)G(\{-1,-1\},y) - 4\xi(4,0)G(\{-1,1\},y) - 4\xi(4,0)G(\{1,-1\},y) + 4\xi(4,0)G(\{1,1\},y) \\ &\quad + 2\xi(4,1)G(\{-1\},y) - 2\xi(4,1)G(\{1\},y) + \xi(4,2) \end{aligned}$$

$$\mathcal{I}_5 = \frac{m_\mu^4 (x+1)(y-1)^2 \varepsilon^2}{y} \times \begin{array}{c} p_2 \quad p_3 \\ \diagdown \quad / \\ \square \\ / \quad \diagdown \\ p_1 \quad p_4 \end{array} = \xi(5,0) + \varepsilon c_1 + \varepsilon^2 c_2 \quad (\text{E.7})$$

where:

$$\begin{aligned} c_1 &= \xi(5,1) + \xi(1,0) \left(-G\left(\left\{-\frac{1}{y}\right\},x\right) - G(\{-y\},x) + 2G(\{-1\},x) \right) \\ &\quad + \xi(2,0) \left(-2G\left(\left\{-\frac{1}{y}\right\},x\right) - 2G(\{-y\},x) + 4G(\{-1\},x) \right) \\ &\quad - \xi(3,0) \left(G\left(\left\{-\frac{1}{y}\right\},x\right) + G(\{-y\},x) + G(\{0\},y) - 2G(\{1\},y) \right) \\ &\quad - \xi(4,0) \left(-G\left(\left\{-\frac{1}{y}\right\},x\right) + G(\{-y\},x) + G(\{0\},y) \right) \\ &\quad + \xi(5,0) \left(G\left(\left\{-\frac{1}{y}\right\},x\right) + G(\{-y\},x) - 2G(\{-1\},x) + G(\{0\},y) - 2G(\{1\},y) \right) \end{aligned}$$

$$\begin{aligned}
 c_2 = & +\xi(5,2) + \left(G(\{0\},y)G\left(\left\{-\frac{1}{y}\right\},x\right) - G(\{0\},y)G(\{-y\},x) - 8G(\{-1,-1\},x) + 2G\left(\left\{-1,-\frac{1}{y}\right\},x\right) \right. \\
 & + 2G(\{-1,-y\},x) - G(\{0,0\},y) + 4G\left(\left\{-\frac{1}{y},-1\right\},x\right) - G\left(\left\{-\frac{1}{y},-\frac{1}{y}\right\},x\right) \\
 & - G\left(\left\{-\frac{1}{y},-y\right\},x\right) + 4G(\{-y,-1\},x) - G\left(\left\{-y,-\frac{1}{y}\right\},x\right) - G(\{-y,-y\},x) \left. \right) \xi(1,0) \\
 & + \left(2G(\{-1\},x) - G\left(\left\{-\frac{1}{y}\right\},x\right) - G(\{-y\},x) \right) \xi(1,1) \\
 & - 2 \left(8G(\{-1,-1\},x) - 2G(\{-1,0\},x) - 2G\left(\left\{-1,-\frac{1}{y}\right\},x\right) - 2G(\{-1,-y\},x) \right. \\
 & - 4G\left(\left\{-\frac{1}{y},-1\right\},x\right) G\left(\left\{-\frac{1}{y},0\right\},x\right) + G\left(\left\{-\frac{1}{y},-\frac{1}{y}\right\},x\right) \\
 & + G\left(\left\{-\frac{1}{y},-y\right\},x\right) - 4G(\{-y,-1\},x) + G(\{-y,0\},x) + G\left(\left\{-y,-\frac{1}{y}\right\},x\right) + G(\{-y,-y\},x) \left. \right) \xi(2,0) \\
 & + \left(4G(\{-1\},x) - 2G\left(\left\{-\frac{1}{y}\right\},x\right) - 2G(\{-y\},x) \right) \xi(2,1) + (2G(\{-1\},x)G(\{0\},y) \\
 & - 3G\left(\left\{-\frac{1}{y}\right\},x\right) G(\{0\},y) - G(\{-y\},x)G(\{0\},y) - 4G(\{-1\},x)G(\{1\},y) + 4G(\{1\},y)G\left(\left\{-\frac{1}{y}\right\},x\right) \\
 & + 4G(\{1\},y)G(\{-y\},x) + 2G\left(\left\{-1,-\frac{1}{y}\right\},x\right) + 2G(\{-1,-y\},x) - G(\{0,0\},y) + 4G(\{0,1\},y) \\
 & + 4G(\{1,0\},y) - 8G(\{1,1\},y) - G\left(\left\{-\frac{1}{y},-\frac{1}{y}\right\},x\right) - G\left(\left\{-\frac{1}{y},-y\right\},x\right) - G\left(\left\{-y,-\frac{1}{y}\right\},x\right) \\
 & - G(\{-y,-y\},x) \left. \right) \xi(3,0) + \left(-G(\{0\},y) + 2G(\{1\},y) - G\left(\left\{-\frac{1}{y}\right\},x\right) - G(\{-y\},x) \right) \xi(3,1) \\
 & + \left(2G(\{-1\},x)G(\{0\},y) - G\left(\left\{-\frac{1}{y}\right\},x\right) G(\{0\},y) - G(\{-y\},x)G(\{0\},y) + 2G(\{-1\},y)G\left(\left\{-\frac{1}{y}\right\},x\right) \right. \\
 & - 2G(\{1\},y)G\left(\left\{-\frac{1}{y}\right\},x\right) - 2G(\{-1\},y)G(\{-y\},x) + 2G(\{1\},y)G(\{-y\},x) - 2G\left(\left\{-1,-\frac{1}{y}\right\},x\right) \\
 & + 2G(\{-1,-y\},x) - 2G(\{0,-1\},y) - G(\{0,0\},y) + 2G(\{0,1\},y) + 2G(\{1,0\},y) + G\left(\left\{-\frac{1}{y},-\frac{1}{y}\right\},x\right) \\
 & - G\left(\left\{-\frac{1}{y},-y\right\},x\right) + G\left(\left\{-y,-\frac{1}{y}\right\},x\right) - G(\{-y,-y\},x) \left. \right) \xi(4,0) + \left(-G(\{0\},y) + G\left(\left\{-\frac{1}{y}\right\},x\right) \right. \\
 & - G(\{-y\},x) \left. \right) \xi(4,1) + \left(-2G(\{-1\},x)G(\{0\},y) + G\left(\left\{-\frac{1}{y}\right\},x\right) G(\{0\},y) + G(\{-y\},x)G(\{0\},y) \right. \\
 & + 4G(\{-1\},x)G(\{1\},y) - 2G(\{1\},y)G\left(\left\{-\frac{1}{y}\right\},x\right) - 2G(\{1\},y)G(\{-y\},x) + 4G(\{-1,-1\},x) \\
 & - 2G\left(\left\{-1,-\frac{1}{y}\right\},x\right) - 2G(\{-1,-y\},x) + G(\{0,0\},y) - 2G(\{0,1\},y) - 2G(\{1,0\},y) + 4G(\{1,1\},y) \\
 & - 2G\left(\left\{-\frac{1}{y},-1\right\},x\right) + G\left(\left\{-\frac{1}{y},-\frac{1}{y}\right\},x\right) + G\left(\left\{-\frac{1}{y},-y\right\},x\right) - 2G(\{-y,-1\},x) + G\left(\left\{-y,-\frac{1}{y}\right\},x\right) \\
 & + G(\{-y,-y\},x) \left. \right) \xi(5,0) + \left(-2G(\{-1\},x) + G(\{0\},y) - 2G(\{1\},y) + G\left(\left\{-\frac{1}{y}\right\},x\right) + G(\{-y\},x) \right) \xi(5,1)
 \end{aligned}$$

Bibliography

- [1] R. Keith Ellis, Zoltan Kunszt, Kirill Melnikov, and Giulia Zanderighi. “One-loop calculations in quantum field theory: from Feynman diagrams to unitarity cuts” (2011). DOI: [10.1016/j.physrep.2012.01.008](https://doi.org/10.1016/j.physrep.2012.01.008). eprint: [arXiv:1105.4319](https://arxiv.org/abs/1105.4319).
- [2] Lance J. Dixon. “A brief introduction to modern amplitude methods” (2013). DOI: [10.5170/CERN-2014-008.31](https://doi.org/10.5170/CERN-2014-008.31). eprint: [arXiv:1310.5353](https://arxiv.org/abs/1310.5353).
- [3] Giovanni Ossola, Costas G. Papadopoulos, and Roberto Pittau. “CutTools: a program implementing the OPP reduction method to compute one-loop amplitudes” (2007). DOI: [10.1088/1126-6708/2008/03/042](https://doi.org/10.1088/1126-6708/2008/03/042). eprint: [arXiv:0711.3596](https://arxiv.org/abs/0711.3596).
- [4] P. Mastrolia, G. Ossola, T. Reiter, and F. Tramontano. “Scattering AMplitudes from Unitarity-based Reduction Algorithm at the Integrand-level” (2010). DOI: [10.1007/JHEP08\(2010\)080](https://doi.org/10.1007/JHEP08(2010)080). eprint: [arXiv:1006.0710](https://arxiv.org/abs/1006.0710).
- [5] Tiziano Peraro. “Ninja: Automated Integrand Reduction via Laurent Expansion for One-Loop Amplitudes” (2014). DOI: [10.1016/j.cpc.2014.06.017](https://doi.org/10.1016/j.cpc.2014.06.017). eprint: [arXiv:1403.1229](https://arxiv.org/abs/1403.1229).
- [6] Gavin Cullen, Hans van Deurzen, Nicolas Greiner, Gudrun Heinrich, Gionata Luisoni, Pierpaolo Mastrolia, Edoardo Mirabella, Giovanni Ossola, Tiziano Peraro, Johannes Schlenk, Johann Felix von Soden-Fraunhofen, and Francesco Tramontano. “GoSam-2.0: a tool for automated one-loop calculations within the Standard Model and beyond”. *The European Physical Journal C* 74.8 (2014), p. 3001. ISSN: 1434-6052. DOI: [10.1140/epjc/s10052-014-3001-5](https://doi.org/10.1140/epjc/s10052-014-3001-5). URL: <https://doi.org/10.1140/epjc/s10052-014-3001-5>.
- [7] Gavin P. Salam. *Perturbative QCD for the LHC*. 2011. eprint: [arXiv:1103.1318](https://arxiv.org/abs/1103.1318).
- [8] C. M. Carloni Calame, M. Passera, L. Trentadue, and G. Venanzoni. “A new approach to evaluate the leading hadronic corrections to the muon $g-2$ ” (2015). DOI: [10.1016/j.physletb.2015.05.020](https://doi.org/10.1016/j.physletb.2015.05.020). eprint: [arXiv:1504.02228](https://arxiv.org/abs/1504.02228).
- [9] G. Abbiendi, C. M. Carloni Calame, U. Marconi, C. Matteuzzi, G. Montagna, O. Nicrosini, M. Passera, F. Piccinini, R. Tenchini, L. Trentadue, and G. Venanzoni. “Measuring the leading hadronic contribution to the muon $g-2$ via μe scattering” (2016). DOI: [10.1140/epjc/s10052-017-4633-z](https://doi.org/10.1140/epjc/s10052-017-4633-z). eprint: [arXiv:1609.08987](https://arxiv.org/abs/1609.08987).
- [10] Pierpaolo Mastrolia, Massimo Passera, Amedeo Primo, and Ulrich Schubert. “Master integrals for the NNLO virtual corrections to μe scattering in QED: the planar graphs”. *JHEP* 11 (2017), p. 198. DOI: [10.1007/JHEP11\(2017\)198](https://doi.org/10.1007/JHEP11(2017)198). arXiv: [1709.07435](https://arxiv.org/abs/1709.07435) [[hep-ph](https://arxiv.org/abs/1709.07435)].
- [11] P. Mastrolia, M. Passera, A. Primo, U. Schubert, and W. J. Torres Bobadilla. “On μe -scattering at NNLO in QED”. *European Physical Journal Web of Conferences*. Vol. 179. 2018, p. 01014. DOI: [10.1051/epjconf/201817901014](https://doi.org/10.1051/epjconf/201817901014).

- [12] Stefano Di Vita, Stefano Laporta, Pierpaolo Mastrolia, Amedeo Primo, and Ulrich Schubert. “Master integrals for the NNLO virtual corrections to μe scattering in QED: the non-planar graphs” (2018). DOI: [10.1007/JHEP09\(2018\)016](https://doi.org/10.1007/JHEP09(2018)016). eprint: [arXiv:1806.08241](https://arxiv.org/abs/1806.08241).
- [13] G. 't Hooft and M. Veltman. “Regularization and renormalization of gauge fields”. *Nuclear Physics B* 44.1 (1972), pp. 189–213. ISSN: 0550-3213. DOI: [https://doi.org/10.1016/0550-3213\(72\)90279-9](https://doi.org/10.1016/0550-3213(72)90279-9). URL: <http://www.sciencedirect.com/science/article/pii/0550321372902799>.
- [14] Pierpaolo Mastrolia, Tiziano Peraro, and Amedeo Primo. “Adaptive Integrand Decomposition in parallel and orthogonal space” (2016). DOI: [10.1007/JHEP08\(2016\)164](https://doi.org/10.1007/JHEP08(2016)164). eprint: [arXiv:1605.03157](https://arxiv.org/abs/1605.03157).
- [15] Amedeo Primo. “Cutting Feynman Amplitudes: from Adaptive Integrand Decomposition to Differential Equations on Maximal Cuts”. PhD thesis. Università degli Studi di Padova, Dipartimento di Fisica e Astronomia “Galileo Galilei”, 2018.
- [16] Pierpaolo Mastrolia, Tiziano Peraro, Amedeo Primo, and William J. Torres Bobadilla. *Adaptive Integrand Decomposition*. 2016. eprint: [arXiv:1607.05156](https://arxiv.org/abs/1607.05156).
- [17] G. Passarino and M. J. G. Veltman. “One Loop Corrections for $e^+ e^-$ Annihilation Into $\mu^+ \mu^-$ in the Weinberg Model”. *Nucl. Phys. B* 160 (1979), pp. 151–207. DOI: [10.1016/0550-3213\(79\)90234-7](https://doi.org/10.1016/0550-3213(79)90234-7).
- [18] S. Laporta. “High-precision calculation of multi-loop Feynman integrals by difference equations” (2001). DOI: [10.1016/S0217-751X\(00\)00215-7](https://doi.org/10.1016/S0217-751X(00)00215-7). eprint: [arXiv:hep-ph/0102033](https://arxiv.org/abs/hep-ph/0102033).
- [19] Philipp Maierhoefer, Johann Usovitsch, and Peter Uwer. “Kira - A Feynman Integral Reduction Program” (2017). DOI: [10.1016/j.cpc.2018.04.012](https://doi.org/10.1016/j.cpc.2018.04.012). eprint: [arXiv:1705.05610](https://arxiv.org/abs/1705.05610).
- [20] A. von Manteuffel and C. Studerus. *Reduze 2 - Distributed Feynman Integral Reduction*. 2012. eprint: [arXiv:1201.4330](https://arxiv.org/abs/1201.4330).
- [21] A. V. Kotikov. “Differential equations method: New technique for massive Feynman diagrams calculation”. *Phys. Lett. B* 254 (1991), pp. 158–164. DOI: [10.1016/0370-2693\(91\)90413-K](https://doi.org/10.1016/0370-2693(91)90413-K).
- [22] Ettore Remiddi. *Differential Equations for Feynman Graph Amplitudes*. 1997. arXiv: [hep-th/9711188](https://arxiv.org/abs/hep-th/9711188) [[hep-th](https://arxiv.org/abs/hep-th/9711188)].
- [23] Johannes M. Henn. “Multiloop integrals in dimensional regularization made simple” (2013). DOI: [10.1103/PhysRevLett.110.251601](https://doi.org/10.1103/PhysRevLett.110.251601). eprint: [arXiv:1304.1806](https://arxiv.org/abs/1304.1806).
- [24] Wilhelm Magnus. “On the exponential solution of differential equations for a linear operator”. *Communications on Pure and Applied Mathematics* 7.4 (1954), pp. 649–673. DOI: [10.1002/cpa.3160070404](https://doi.org/10.1002/cpa.3160070404). eprint: <https://onlinelibrary.wiley.com/doi/pdf/10.1002/cpa.3160070404>. URL: <https://onlinelibrary.wiley.com/doi/abs/10.1002/cpa.3160070404>.
- [25] A. B. Goncharov. “Multiple polylogarithms, cyclotomy and modular complexes” (2011). eprint: [arXiv:1105.2076](https://arxiv.org/abs/1105.2076).
- [26] Z. Bern and A. G. Morgan. “Massive Loop Amplitudes from Unitarity” (1995). DOI: [10.1016/0550-3213\(96\)00078-8](https://doi.org/10.1016/0550-3213(96)00078-8). eprint: [arXiv:hep-ph/9511336](https://arxiv.org/abs/hep-ph/9511336).
- [27] Z. Bern, L. Dixon, D. C. Dunbar, and D. A. Kosower. “One-Loop Self-Dual and N=4 Super Yang-Mills” (1996). DOI: [10.1016/S0370-2693\(96\)01676-0](https://doi.org/10.1016/S0370-2693(96)01676-0). eprint: [arXiv:hep-th/9611127](https://arxiv.org/abs/hep-th/9611127).

- [28] M. Maniatis and C. M. Reyes. *Scattering amplitudes from a deconstruction of Feynman diagrams*. 2016. eprint: [arXiv:1605.04268](https://arxiv.org/abs/1605.04268).
- [29] Ruth Britto, Freddy Cachazo, and Bo Feng. “Generalized Unitarity and One-Loop Amplitudes in N=4 Super-Yang-Mills” (2004). DOI: [10.1016/j.nuclphysb.2005.07.014](https://doi.org/10.1016/j.nuclphysb.2005.07.014). eprint: [arXiv:hep-th/0412103](https://arxiv.org/abs/hep-th/0412103).
- [30] S. D. Badger. “Direct Extraction Of One Loop Rational Terms” (2008). DOI: [10.1088/1126-6708/2009/01/049](https://doi.org/10.1088/1126-6708/2009/01/049). eprint: [arXiv:0806.4600](https://arxiv.org/abs/0806.4600).
- [31] Pierpaolo Mastrolia. “On Triple-Cut of Scattering Amplitudes” (2006). DOI: [10.1016/j.physletb.2006.11.037](https://doi.org/10.1016/j.physletb.2006.11.037). eprint: [arXiv:hep-th/0611091](https://arxiv.org/abs/hep-th/0611091).
- [32] Darren Forde. “Direct extraction of one-loop integral coefficients” (2007). DOI: [10.1103/PhysRevD.75.125019](https://doi.org/10.1103/PhysRevD.75.125019). eprint: [arXiv:0704.1835](https://arxiv.org/abs/0704.1835).
- [33] Ruth Britto, Bo Feng, and Pierpaolo Mastrolia. “The Cut-Constructible Part of QCD Amplitudes” (2006). DOI: [10.1103/PhysRevD.73.105004](https://doi.org/10.1103/PhysRevD.73.105004). eprint: [arXiv:hep-ph/0602178](https://arxiv.org/abs/hep-ph/0602178).
- [34] Pierpaolo Mastrolia. “Double-Cut of Scattering Amplitudes and Stokes’ Theorem” (2009). DOI: [10.1016/j.physletb.2009.06.033](https://doi.org/10.1016/j.physletb.2009.06.033). eprint: [arXiv:0905.2909](https://arxiv.org/abs/0905.2909).
- [35] William B. Kilgore. *One-loop Integral Coefficients from Generalized Unitarity*. 2007. eprint: [arXiv:0711.5015](https://arxiv.org/abs/0711.5015).
- [36] Ruth Britto and Bo Feng. “Solving for tadpole coefficients in one-loop amplitudes” (2009). DOI: [10.1016/j.physletb.2009.10.038](https://doi.org/10.1016/j.physletb.2009.10.038). eprint: [arXiv:0904.2766](https://arxiv.org/abs/0904.2766).
- [37] Ruth Britto and Edoardo Mirabella. “Single Cut Integration” (2010). DOI: [10.1007/JHEP01\(2011\)135](https://doi.org/10.1007/JHEP01(2011)135). eprint: [arXiv:1011.2344](https://arxiv.org/abs/1011.2344).
- [38] Giovanni Ossola, Costas G. Papadopoulos, and Roberto Pittau. “Reducing full one-loop amplitudes to scalar integrals at the integrand level” (2006). DOI: [10.1016/j.nuclphysb.2006.11.012](https://doi.org/10.1016/j.nuclphysb.2006.11.012). eprint: [arXiv:hep-ph/0609007](https://arxiv.org/abs/hep-ph/0609007).
- [39] Giovanni Ossola, Costas G. Papadopoulos, and Roberto Pittau. “Numerical Evaluation of Six-Photon Amplitudes” (2007). DOI: [10.1088/1126-6708/2007/07/085](https://doi.org/10.1088/1126-6708/2007/07/085). eprint: [arXiv:0704.1271](https://arxiv.org/abs/0704.1271).
- [40] Walter T. Giele, Zoltan Kunszt, and Kirill Melnikov. “Full one-loop amplitudes from tree amplitudes” (2008). DOI: [10.1088/1126-6708/2008/04/049](https://doi.org/10.1088/1126-6708/2008/04/049). eprint: [arXiv:0801.2237](https://arxiv.org/abs/0801.2237).
- [41] P. Mastrolia, G. Ossola, C. G. Papadopoulos, and R. Pittau. “Optimizing the Reduction of One-Loop Amplitudes” (2008). DOI: [10.1088/1126-6708/2008/06/030](https://doi.org/10.1088/1126-6708/2008/06/030). eprint: [arXiv:0803.3964](https://arxiv.org/abs/0803.3964).
- [42] Pierpaolo Mastrolia, Edoardo Mirabella, and Tiziano Peraro. “Integrand reduction of one-loop scattering amplitudes through Laurent series expansion” (2012). DOI: [10.1007/JHEP06\(2012\)095](https://doi.org/10.1007/JHEP06(2012)095). eprint: [arXiv:1203.0291](https://arxiv.org/abs/1203.0291).
- [43] R. K. Ellis, W. T. Giele, and Z. Kunszt. “A Numerical Unitarity Formalism for Evaluating One-Loop Amplitudes” (2007). DOI: [10.1088/1126-6708/2008/03/003](https://doi.org/10.1088/1126-6708/2008/03/003). eprint: [arXiv:0708.2398](https://arxiv.org/abs/0708.2398).
- [44] R. K. Ellis, W. T. Giele, Z. Kunszt, and K. Melnikov. “Masses, fermions and generalized D-dimensional unitarity” (2008). DOI: [10.1016/j.nuclphysb.2009.07.023](https://doi.org/10.1016/j.nuclphysb.2009.07.023). eprint: [arXiv:0806.3467](https://arxiv.org/abs/0806.3467).

- [45] Giovanni Ossola, Costas G. Papadopoulos, and Roberto Pittau. “On the Rational Terms of the one-loop amplitudes” (2008). DOI: [10.1088/1126-6708/2008/05/004](https://doi.org/10.1088/1126-6708/2008/05/004). eprint: [arXiv:0802.1876](https://arxiv.org/abs/0802.1876).
- [46] Yang Zhang. “Integrand-Level Reduction of Loop Amplitudes by Computational Algebraic Geometry Methods” (2012). DOI: [10.1007/JHEP09\(2012\)042](https://doi.org/10.1007/JHEP09(2012)042). eprint: [arXiv:1205.5707](https://arxiv.org/abs/1205.5707).
- [47] Pierpaolo Mastrolia, Edoardo Mirabella, Giovanni Ossola, and Tiziano Peraro. “Scattering Amplitudes from Multivariate Polynomial Division” (2012). DOI: [10.1016/j.physletb.2012.09.053](https://doi.org/10.1016/j.physletb.2012.09.053). eprint: [arXiv:1205.7087](https://arxiv.org/abs/1205.7087).
- [48] Pierpaolo Mastrolia and Giovanni Ossola. “On the Integrand-Reduction Method for Two-Loop Scattering Amplitudes” (2011). DOI: [10.1007/JHEP11\(2011\)014](https://doi.org/10.1007/JHEP11(2011)014). eprint: [arXiv:1107.6041](https://arxiv.org/abs/1107.6041).
- [49] Pierpaolo Mastrolia, Edoardo Mirabella, Giovanni Ossola, and Tiziano Peraro. “Integrand Reduction for Two-Loop Scattering Amplitudes through Multivariate Polynomial Division” (2012). DOI: [10.1103/PhysRevD.87.085026](https://doi.org/10.1103/PhysRevD.87.085026). eprint: [arXiv:1209.4319](https://arxiv.org/abs/1209.4319).
- [50] R. Mertig, M. Bohm, and Ansgar Denner. “FEYN CALC: Computer algebraic calculation of Feynman amplitudes”. *Comput. Phys. Commun.* 64 (1991), pp. 345–359. DOI: [10.1016/0010-4655\(91\)90130-D](https://doi.org/10.1016/0010-4655(91)90130-D).
- [51] Vladyslav Shtabovenko, Rolf Mertig, and Frederik Orellana. “New Developments in FeynCalc 9.0” (2016). DOI: [10.1016/j.cpc.2016.06.008](https://doi.org/10.1016/j.cpc.2016.06.008). eprint: [arXiv:1601.01167](https://arxiv.org/abs/1601.01167).
- [52] Federico Gasparotto. “A modern approach to Feynman Integrals and Differential Equations”. MA thesis. Università degli Studi di Padova, Dipartimento di Fisica e Astronomia “Galileo Galilei”, 2018.
- [53] P. Kusch and H. M. Foley. “The Magnetic Moment of the Electron”. *Phys. Rev.* 74 (3 1948), pp. 250–263. DOI: [10.1103/PhysRev.74.250](https://doi.org/10.1103/PhysRev.74.250). URL: <https://link.aps.org/doi/10.1103/PhysRev.74.250>.
- [54] Julian Schwinger. “On Quantum-Electrodynamics and the Magnetic Moment of the Electron”. *Phys. Rev.* 73 (4 1948), pp. 416–417. DOI: [10.1103/PhysRev.73.416](https://doi.org/10.1103/PhysRev.73.416). URL: <https://link.aps.org/doi/10.1103/PhysRev.73.416>.
- [55] D. Hanneke, S. Fogwell, and G. Gabrielse. “New Measurement of the Electron Magnetic Moment and the Fine Structure Constant” (2008). DOI: [10.1103/PhysRevLett.100.120801](https://doi.org/10.1103/PhysRevLett.100.120801). eprint: [arXiv:0801.1134](https://arxiv.org/abs/0801.1134).
- [56] Tatsumi Aoyama, Masashi Hayakawa, Toichiro Kinoshita, and Makiko Nio. “Tenth-Order QED Contribution to the Electron $g-2$ and an Improved Value of the Fine Structure Constant” (2012). DOI: [10.1103/PhysRevLett.109.111807](https://doi.org/10.1103/PhysRevLett.109.111807). eprint: [arXiv:1205.5368](https://arxiv.org/abs/1205.5368).
- [57] W.S. Cowland. “On Schwinger’s theory of the muon”. *Nuclear Physics* 8 (1958), pp. 397 – 401. ISSN: 0029-5582. DOI: [https://doi.org/10.1016/0029-5582\(58\)90171-8](https://doi.org/10.1016/0029-5582(58)90171-8). URL: <http://www.sciencedirect.com/science/article/pii/0029558258901718>.
- [58] G. F. Giudice, P. Paradisi, and M. Passera. “Testing new physics with the electron $g-2$ ” (2012). DOI: [10.1007/JHEP11\(2012\)113](https://doi.org/10.1007/JHEP11(2012)113). eprint: [arXiv:1208.6583](https://arxiv.org/abs/1208.6583).
- [59] Fred Jegerlehner and Andreas Nyffeler. “The Muon $g-2$ ” (2009). DOI: [10.1016/j.physrep.2009.04.003](https://doi.org/10.1016/j.physrep.2009.04.003). eprint: [arXiv:0902.3360](https://arxiv.org/abs/0902.3360).

- [60] T. D. Lee and C. N. Yang. “Question of Parity Conservation in Weak Interactions”. *Phys. Rev.* 104 (1 1956), pp. 254–258. DOI: [10.1103/PhysRev.104.254](https://doi.org/10.1103/PhysRev.104.254). URL: <https://link.aps.org/doi/10.1103/PhysRev.104.254>.
- [61] G. W. Bennett. “Measurement of the Negative Muon Anomalous Magnetic Moment to 0.7 ppm” (2004). DOI: [10.1103/PhysRevLett.92.161802](https://doi.org/10.1103/PhysRevLett.92.161802). eprint: [arXiv:hep-ex/0401008](https://arxiv.org/abs/hep-ex/0401008).
- [62] Muon, Collaboration, : and G. W. Bennett. “Final Report of the Muon E821 Anomalous Magnetic Moment Measurement at BNL” (2006). DOI: [10.1103/PhysRevD.73.072003](https://doi.org/10.1103/PhysRevD.73.072003). eprint: [arXiv:hep-ex/0602035](https://arxiv.org/abs/hep-ex/0602035).
- [63] Fred Jegerlehner. “Muon $g-2$ Theory: the Hadronic Part” (2017). DOI: [10.1051/epjconf/201816600022](https://doi.org/10.1051/epjconf/201816600022). eprint: [arXiv:1705.00263](https://arxiv.org/abs/1705.00263).
- [64] M. Passera. “The Standard Model Prediction of the Muon Anomalous Magnetic Moment” (2004). DOI: [10.1088/0954-3899/31/5/R01](https://doi.org/10.1088/0954-3899/31/5/R01). eprint: [arXiv:hep-ph/0411168](https://arxiv.org/abs/hep-ph/0411168).
- [65] A. Petermann. “Fourth order magnetic moment of the electron”. *Helv. Phys. Acta* 30 (1957), pp. 407–408.
- [66] Charles M. Sommerfield. “Magnetic Dipole Moment of the Electron”. *Phys. Rev.* 107 (1 1957), pp. 328–329. DOI: [10.1103/PhysRev.107.328](https://doi.org/10.1103/PhysRev.107.328). URL: <https://link.aps.org/doi/10.1103/PhysRev.107.328>.
- [67] H.H. Elend. “On the anomalous magnetic moment of the muon”. *Physics Letters* 20.6 (1966), pp. 682–684. ISSN: 0031-9163. DOI: [https://doi.org/10.1016/0031-9163\(66\)91171-1](https://doi.org/10.1016/0031-9163(66)91171-1). URL: <http://www.sciencedirect.com/science/article/pii/0031916366911711>.
- [68] J. A. Mignaco and E. Remiddi. “Fourth-order vacuum polarization contribution to the sixth-order electron magnetic moment”. *Il Nuovo Cimento A (1965-1970)* 60.4 (1969), pp. 519–529. ISSN: 1826-9869. DOI: [10.1007/BF02757285](https://doi.org/10.1007/BF02757285). URL: <https://doi.org/10.1007/BF02757285>.
- [69] R. Barbieri and E. Remiddi. “Sixth order electron and muon $(g-2)/2$ from second order vacuum polarization insertion”. *Physics Letters B* 49.5 (1974), pp. 468–470. ISSN: 0370-2693. DOI: [https://doi.org/10.1016/0370-2693\(74\)90638-8](https://doi.org/10.1016/0370-2693(74)90638-8). URL: <http://www.sciencedirect.com/science/article/pii/0370269374906388>.
- [70] R. Barbieri and E. Remiddi. “Electron and muon $12(g-2)$ from vacuum polarization insertions”. *Nuclear Physics B* 90 (1975), pp. 233–266. ISSN: 0550-3213. DOI: [https://doi.org/10.1016/0550-3213\(75\)90645-8](https://doi.org/10.1016/0550-3213(75)90645-8). URL: <http://www.sciencedirect.com/science/article/pii/0550321375906458>.
- [71] R. Barbieri, M. Caffo, and E. Remiddi. “A sixth order contribution to the electron anomalous magnetic moment”. *Physics Letters B* 57.5 (1975), pp. 460–462. ISSN: 0370-2693. DOI: [https://doi.org/10.1016/0370-2693\(75\)90268-3](https://doi.org/10.1016/0370-2693(75)90268-3). URL: <http://www.sciencedirect.com/science/article/pii/0370269375902683>.
- [72] S. Laporta and E. Remiddi. “The analytic value of the light-light vertex graph contributions to the electron $g-2$ in QED”. *Physics Letters B* 265.1 (1991), pp. 182–184. ISSN: 0370-2693. DOI: [https://doi.org/10.1016/0370-2693\(91\)90036-P](https://doi.org/10.1016/0370-2693(91)90036-P). URL: <http://www.sciencedirect.com/science/article/pii/037026939190036P>.
- [73] S. Laporta. “Analytical value of some sixth-order graphs to the electron $g-2$ in QED”. *Phys. Rev. D* 47 (10 1993), pp. 4793–4795. DOI: [10.1103/PhysRevD.47.4793](https://doi.org/10.1103/PhysRevD.47.4793). URL: <https://link.aps.org/doi/10.1103/PhysRevD.47.4793>.

- [74] S. Laporta. “The analytical value of the corner-ladder graphs contribution to the electron ($g - 2$) in QED”. *Physics Letters B* 343.1 (1995), pp. 421 –426. ISSN: 0370-2693. DOI: [https://doi.org/10.1016/0370-2693\(94\)01401-W](https://doi.org/10.1016/0370-2693(94)01401-W). URL: <http://www.sciencedirect.com/science/article/pii/037026939401401W>.
- [75] S. Laporta and E. Remiddi. “Progress in the analytical evaluation of the electron ($g - 2$) in QED; the scalar part of the triple-cross graphs”. *Physics Letters B* 356.2 (1995), pp. 390 – 397. ISSN: 0370-2693. DOI: [https://doi.org/10.1016/0370-2693\(95\)00822-3](https://doi.org/10.1016/0370-2693(95)00822-3). URL: <http://www.sciencedirect.com/science/article/pii/0370269395008223>.
- [76] S. Laporta and E. Remiddi. “The analytical value of the electron ($g - 2$) at order α^3 in QED”. *Physics Letters B* 379.1 (1996), pp. 283 –291. ISSN: 0370-2693. DOI: [https://doi.org/10.1016/0370-2693\(96\)00439-X](https://doi.org/10.1016/0370-2693(96)00439-X). URL: <http://www.sciencedirect.com/science/article/pii/037026939600439X>.
- [77] S. Laporta. “The analytical contribution of the sixth-order graphs with vacuum polarization insertions to the muon ($g-2$) in QED”. *Il Nuovo Cimento A (1965-1970)* 106.5 (1993), pp. 675–683. ISSN: 1826-9869. DOI: [10.1007/BF02787236](https://doi.org/10.1007/BF02787236). URL: <https://doi.org/10.1007/BF02787236>.
- [78] S. Laporta and E. Remiddi. “The analytical value of the electron light-light graphs contribution to the muon ($g-2$) in QED”. *Physics Letters B* 301.4 (1993), pp. 440 –446. ISSN: 0370-2693. DOI: [https://doi.org/10.1016/0370-2693\(93\)91176-N](https://doi.org/10.1016/0370-2693(93)91176-N). URL: <http://www.sciencedirect.com/science/article/pii/037026939391176N>.
- [79] Andrzej Czarnecki and Maciej Skrzypek. “The muon anomalous magnetic moment in QED: three-loop electron and tau contributions” (1998). DOI: [10.1016/S0370-2693\(99\)00076-3](https://doi.org/10.1016/S0370-2693(99)00076-3). eprint: [arXiv:hep-ph/9812394](https://arxiv.org/abs/hep-ph/9812394).
- [80] Stefano Laporta. “High-precision calculation of the 4-loop contribution to the electron $g-2$ in QED” (2017). DOI: [10.1016/j.physletb.2017.06.056](https://doi.org/10.1016/j.physletb.2017.06.056). eprint: [arXiv:1704.06996](https://arxiv.org/abs/1704.06996).
- [81] Tatsumi Aoyama, Masashi Hayakawa, Toichiro Kinoshita, and Makiko Nio. “Complete Tenth-Order QED Contribution to the Muon $g-2$ ” (2012). DOI: [10.1103/PhysRevLett.109.111808](https://doi.org/10.1103/PhysRevLett.109.111808). eprint: [arXiv:1205.5370](https://arxiv.org/abs/1205.5370).
- [82] Tatsumi Aoyama, Masashi Hayakawa, Toichiro Kinoshita, and Makiko Nio. “Tenth-Order QED Contribution to the Electron $g-2$ and an Improved Value of the Fine Structure Constant”. *Phys. Rev. Lett.* 109 (11 2012), p. 111807. DOI: [10.1103/PhysRevLett.109.111807](https://doi.org/10.1103/PhysRevLett.109.111807). URL: <https://link.aps.org/doi/10.1103/PhysRevLett.109.111807>.
- [83] Roman Jackiw and Steven Weinberg. “Weak-Interaction Corrections to the Muon Magnetic Moment and to Muonic-Atom Energy Levels”. *Phys. Rev. D* 5 (9 1972), pp. 2396–2398. DOI: [10.1103/PhysRevD.5.2396](https://doi.org/10.1103/PhysRevD.5.2396). URL: <https://link.aps.org/doi/10.1103/PhysRevD.5.2396>.
- [84] I. Bars and M. Yoshimura. “Muon Magnetic Moment in a Finite Theory of Weak and Electromagnetic Interactions”. *Phys. Rev. D* 6 (1 1972), pp. 374–376. DOI: [10.1103/PhysRevD.6.374](https://doi.org/10.1103/PhysRevD.6.374). URL: <https://link.aps.org/doi/10.1103/PhysRevD.6.374>.
- [85] G. Altarelli, N. Cabibbo, and L. Maiani. “The Drell-Hearn sum rule and the lepton magnetic moment in the Weinberg model of weak and electromagnetic interactions”. *Physics Letters B* 40.3 (1972), pp. 415 –419. ISSN: 0370-2693. DOI: [https://doi.org/10.1016/0370-2693\(72\)90833-7](https://doi.org/10.1016/0370-2693(72)90833-7). URL: <http://www.sciencedirect.com/science/article/pii/0370269372908337>.

- [86] W.A. Bardeen, R. Gastmans, and B. Lautrup. “Static quantities in Weinberg’s model of weak and electromagnetic interactions”. *Nuclear Physics B* 46.1 (1972), pp. 319–331. ISSN: 0550-3213. DOI: [https://doi.org/10.1016/0550-3213\(72\)90218-0](https://doi.org/10.1016/0550-3213(72)90218-0). URL: <http://www.sciencedirect.com/science/article/pii/0550321372902180>.
- [87] Kazuo Fujikawa, Benjamin W. Lee, and A. I. Sanda. “Generalized Renormalizable Gauge Formulation of Spontaneously Broken Gauge Theories”. *Phys. Rev. D* 6 (10 1972), pp. 2923–2943. DOI: [10.1103/PhysRevD.6.2923](https://doi.org/10.1103/PhysRevD.6.2923). URL: <https://link.aps.org/doi/10.1103/PhysRevD.6.2923>.
- [88] Friedrich Jegerlehner. “The Anomalous Magnetic Moment of the Muon”. *Springer Tracts Mod. Phys.* 274 (2017), pp.1–693. DOI: [10.1007/978-3-319-63577-4](https://doi.org/10.1007/978-3-319-63577-4).
- [89] T.V. Kukhto, E.A. Kuraev, A. Schiller, and Z.K. Silagadze. “The dominant two-loop electroweak contributions to the anomalous magnetic moment of the muon”. *Nuclear Physics B* 371.3 (1992), pp. 567–596. ISSN: 0550-3213. DOI: [https://doi.org/10.1016/0550-3213\(92\)90687-7](https://doi.org/10.1016/0550-3213(92)90687-7). URL: <http://www.sciencedirect.com/science/article/pii/0550321392906877>.
- [90] Andrzej Czarnecki, Bernd Krause, and William J. Marciano. “Electroweak corrections to the muon anomalous magnetic moment” (1995). DOI: [10.1103/PhysRevLett.76.3267](https://doi.org/10.1103/PhysRevLett.76.3267). eprint: [arXiv:hep-ph/9512369](https://arxiv.org/abs/hep-ph/9512369).
- [91] Andrzej Czarnecki, Bernd Krause, and William J. Marciano. “Electroweak Fermion-loop Contributions to the Muon Anomalous Magnetic Moment” (1995). DOI: [10.1103/PhysRevD.52.R2619](https://doi.org/10.1103/PhysRevD.52.R2619). eprint: [arXiv:hep-ph/9506256](https://arxiv.org/abs/hep-ph/9506256).
- [92] Andrzej Czarnecki, William J. Marciano, and Arkady Vainshtein. “Refinements in electroweak contributions to the muon anomalous magnetic moment” (2002). DOI: [10.1103/PhysRevD.67.073006](https://doi.org/10.1103/PhysRevD.67.073006). DOI: [10.1103/PhysRevD.73.119901](https://doi.org/10.1103/PhysRevD.73.119901). eprint: [arXiv:hep-ph/0212229](https://arxiv.org/abs/hep-ph/0212229).
- [93] Louis Bouchiat Claude et Michel. “La résonance dans la diffusion méson π - méson π et le moment magnétique anormal du méson μ ”. *J. Phys. Radium* 22 (1961), pp. 121–121. DOI: [10.1051/jphysrad:01961002202012101](https://doi.org/10.1051/jphysrad:01961002202012101).
- [94] Loyal Durand. “Pionic Contributions to the Magnetic Moment of the Muon”. *Phys. Rev.* 128 (1 1962), pp. 441–448. DOI: [10.1103/PhysRev.128.441](https://doi.org/10.1103/PhysRev.128.441). URL: <https://link.aps.org/doi/10.1103/PhysRev.128.441>.
- [95] M. Gourdin and E. De Rafael. “Hadronic contributions to the muon g-factor”. *Nuclear Physics B* 10.4 (1969), pp. 667–674. ISSN: 0550-3213. DOI: [https://doi.org/10.1016/0550-3213\(69\)90333-2](https://doi.org/10.1016/0550-3213(69)90333-2). URL: <http://www.sciencedirect.com/science/article/pii/0550321369903332>.
- [96] John F. Donoghue. *On the Marriage of Chiral Perturbation Theory and Dispersion Relations*. 1995. eprint: [arXiv:hep-ph/9506205](https://arxiv.org/abs/hep-ph/9506205).
- [97] J. F. Donoghue, E. Golowich, and Barry R. Holstein. “Dynamics of the standard model”. *Camb. Monogr. Part. Phys. Nucl. Phys. Cosmol.* 2 (1992). [Camb. Monogr. Part. Phys. Nucl. Phys. Cosmol.35(2014)], pp. 1–540. DOI: [10.1017/CB09780511524370](https://doi.org/10.1017/CB09780511524370).
- [98] Roman Zwicky. *A brief Introduction to Dispersion Relations and Analyticity*. 2016. eprint: [arXiv:1610.06090](https://arxiv.org/abs/1610.06090).
- [99] M. Davier, A. Hoecker, B. Malaescu, and Z. Zhang. *A new evaluation of the hadronic vacuum polarisation contributions to the muon anomalous magnetic moment and to $\alpha(m_Z^2)$* . 2019. eprint: [arXiv:1908.00921](https://arxiv.org/abs/1908.00921).

- [100] Alexander Keshavarzi, Daisuke Nomura, and Thomas Teubner. “The muon $g - 2$ and $\alpha(M_Z^2)$: a new data-based analysis” (2018). DOI: [10.1103/PhysRevD.97.114025](https://doi.org/10.1103/PhysRevD.97.114025). eprint: [arXiv:1802.02995](https://arxiv.org/abs/1802.02995).
- [101] Thomas Blum, Norman Christ, Masashi Hayakawa, Taku Izubuchi, Luchang Jin, Chulwoo Jung, and Christoph Lehner. “Connected and leading disconnected hadronic light-by-light contribution to the muon anomalous magnetic moment with physical pion mass” (2016). DOI: [10.1103/PhysRevLett.118.022005](https://doi.org/10.1103/PhysRevLett.118.022005). eprint: [arXiv:1610.04603](https://arxiv.org/abs/1610.04603).
- [102] Nils Asmussen, Antoine Gerardin, Jeremy Green, Oleksii Gryniuk, Georg von Hippel, Harvey B. Meyer, Andreas Nyffeler, Vladimir Pascalutsa, and Hartmut Wittig. “Hadronic light-by-light scattering contribution to the muon $g-2$ on the lattice” (2018). DOI: [10.1051/epjconf/201817901017](https://doi.org/10.1051/epjconf/201817901017). eprint: [arXiv:1801.04238](https://arxiv.org/abs/1801.04238).
- [103] Graziano Venanzoni. *The MUonE experiment: a novel way to measure the leading order hadronic contribution to the muon $g-2$* . 2018. eprint: [arXiv:1811.11466](https://arxiv.org/abs/1811.11466).
- [104] S. Eidelman and F. Jegerlehner. “Hadronic contributions to $(g - 2)$ of the leptons and to the effective fine structure constant $\alpha(M_Z^2)$ ” (1995). DOI: [10.1007/BF01553984](https://doi.org/10.1007/BF01553984). eprint: [arXiv:hep-ph/9502298](https://arxiv.org/abs/hep-ph/9502298).
- [105] B.E. Lautrup, A. Peterman, and E. de Rafael. “Recent developments in the comparison between theory and experiments in quantum electrodynamics”. *Physics Reports* 3.4 (1972), pp. 193–259. ISSN: 0370-1573. DOI: [https://doi.org/10.1016/0370-1573\(72\)90011-7](https://doi.org/10.1016/0370-1573(72)90011-7). URL: <http://www.sciencedirect.com/science/article/pii/0370157372900117>.
- [106] Matteo Fael and Massimo Passera. “Muon-electron scattering at NNLO: the hadronic corrections” (2019). DOI: [10.1103/PhysRevLett.122.192001](https://doi.org/10.1103/PhysRevLett.122.192001). eprint: [arXiv:1901.03106](https://arxiv.org/abs/1901.03106).
- [107] Marco Vitti. “Hadronic Contributions to Muon-Electron Scattering at NNLO”. MA thesis. Università degli Studi di Padova, Dipartimento di Fisica e Astronomia “Galileo Galilei”, 2018.
- [108] Matteo Fael. “Hadronic corrections to $\mu-e$ scattering at NNLO with space-like data” (2018). DOI: [10.1007/JHEP02\(2019\)027](https://doi.org/10.1007/JHEP02(2019)027). eprint: [arXiv:1808.08233](https://arxiv.org/abs/1808.08233).
- [109] P. van Nieuwenhuizen. “Muon-electron scattering cross section to order α^3 ”. *Nuclear Physics B* 28.2 (1971), pp. 429–454. ISSN: 0550-3213. DOI: [https://doi.org/10.1016/0550-3213\(71\)90009-5](https://doi.org/10.1016/0550-3213(71)90009-5). URL: <http://www.sciencedirect.com/science/article/pii/0550321371900095>.
- [110] T V Kukhto, N M Shumeiko, and S I Timoshin. “Radiative corrections in polarised electron-muon elastic scattering”. *Journal of Physics G: Nuclear Physics* 13.6 (1987), pp. 725–734. DOI: [10.1088/0305-4616/13/6/005](https://doi.org/10.1088/0305-4616/13/6/005). URL: <https://doi.org/10.1088%2F0305-4616%2F13%2F6%2F005>.
- [111] D. Bardin and L. Kalinovskaya. *QED Corrections for Polarized Elastic MU-E Scattering*. 1997. eprint: [arXiv:hep-ph/9712310](https://arxiv.org/abs/hep-ph/9712310).
- [112] Massimo Alacevich, Carlo M. Carloni Calame, Mauro Chiesa, Guido Montagna, Oreste Nicrosini, and Fulvio Piccinini. “Muon-electron scattering at NLO” (2018). DOI: [10.1007/JHEP02\(2019\)155](https://doi.org/10.1007/JHEP02(2019)155). eprint: [arXiv:1811.06743](https://arxiv.org/abs/1811.06743).
- [113] Z. Bern, L. Dixon, and A. Ghinculov. “Two-Loop Correction to Bhabha Scattering” (2000). DOI: [10.1103/PhysRevD.63.053007](https://doi.org/10.1103/PhysRevD.63.053007). eprint: [arXiv:hep-ph/0010075](https://arxiv.org/abs/hep-ph/0010075).

- [114] R. Bonciani, P. Mastrolia, and E. Remiddi. “Vertex diagrams for the QED form factors at the 2-loop level” (2003). DOI: [10.1016/j.nuclphysb.2004.08.009](https://doi.org/10.1016/j.nuclphysb.2004.08.009). eprint: [arXiv:hep-ph/0301170](https://arxiv.org/abs/hep-ph/0301170).
- [115] R. Bonciani, A. Ferroglia, P. Mastrolia, E. Remiddi, and J. J. van der Bij. “Planar box diagram for the ($N_F = 1$) 2-loop QED virtual corrections to Bhabha scattering” (2003). DOI: [10.1016/j.nuclphysb.2004.01.026](https://doi.org/10.1016/j.nuclphysb.2004.01.026). eprint: [arXiv:hep-ph/0310333](https://arxiv.org/abs/hep-ph/0310333).
- [116] T. Gehrmann and E. Remiddi. “Two-Loop Master Integrals for $\gamma^* \rightarrow 3$ Jets: The non-planar topologies” (2001). DOI: [10.1016/S0550-3213\(01\)00074-8](https://doi.org/10.1016/S0550-3213(01)00074-8). eprint: [arXiv:hep-ph/0101124](https://arxiv.org/abs/hep-ph/0101124).
- [117] R. Bonciani, P. Mastrolia, and E. Remiddi. “Master Integrals for the 2-loop QCD virtual corrections to the Forward-Backward Asymmetry” (2003). DOI: [10.1016/j.nuclphysb.2004.04.011](https://doi.org/10.1016/j.nuclphysb.2004.04.011). eprint: [arXiv:hep-ph/0311145](https://arxiv.org/abs/hep-ph/0311145).
- [118] R. Bonciani and A. Ferroglia. “Two-Loop QCD Corrections to the Heavy-to-Light Quark Decay” (2008). DOI: [10.1088/1126-6708/2008/11/065](https://doi.org/10.1088/1126-6708/2008/11/065). eprint: [arXiv:0809.4687](https://arxiv.org/abs/0809.4687).
- [119] R. Bonciani, A. Ferroglia, T. Gehrmann, D. Maitre, and C. Studerus. “Two-Loop Fermionic Corrections to Heavy-Quark Pair Production: the Quark-Antiquark Channel” (2008). DOI: [10.1088/1126-6708/2008/07/129](https://doi.org/10.1088/1126-6708/2008/07/129). eprint: [arXiv:0806.2301](https://arxiv.org/abs/0806.2301).
- [120] Kenneth G. Wilson and Michael E. Fisher. “Critical Exponents in 3.99 Dimensions”. *Phys. Rev. Lett.* 28 (4 1972), pp. 240–243. DOI: [10.1103/PhysRevLett.28.240](https://doi.org/10.1103/PhysRevLett.28.240). URL: <https://link.aps.org/doi/10.1103/PhysRevLett.28.240>.
- [121] C. Gnendiger, A. Signer, D. Stöckinger, A. Broggio, A. L. Cherchiglia, F. Driencourt-Mangin, A. R. Fazio, B. Hiller, P. Mastrolia, T. Peraro, R. Pittau, G. M. Pruna, G. Rodrigo, M. Sampaio, G. Sborlini, W. J. Torres Bobadilla, F. Tramontano, Y. Ulrich, and A. Visconti. “To d , or not to d : Recent developments and comparisons of regularization schemes” (2017). DOI: [10.1140/epjc/s10052-017-5023-2](https://doi.org/10.1140/epjc/s10052-017-5023-2). eprint: [arXiv:1705.01827](https://arxiv.org/abs/1705.01827).
- [122] D. B. Melrose. “Reduction of feynman diagrams”. *Il Nuovo Cimento A (1965-1970)* 40.1 (1965), pp. 181–213. ISSN: 1826-9869. DOI: [10.1007/BF02832919](https://doi.org/10.1007/BF02832919). URL: <https://doi.org/10.1007/BF02832919>.
- [123] G. 't Hooft and M. Veltman. “Scalar one-loop integrals”. *Nuclear Physics B* 153 (1979), pp. 365–401. ISSN: 0550-3213. DOI: [https://doi.org/10.1016/0550-3213\(79\)90605-9](https://doi.org/10.1016/0550-3213(79)90605-9). URL: <http://www.sciencedirect.com/science/article/pii/0550321379906059>.
- [124] Kirill Melnikov and Markus Schulze. “NLO QCD corrections to top quark pair production in association with one hard jet at hadron colliders” (2010). DOI: [10.1016/j.nuclphysb.2010.07.003](https://doi.org/10.1016/j.nuclphysb.2010.07.003). eprint: [arXiv:1004.3284](https://arxiv.org/abs/1004.3284).
- [125] W.L. van Neerven and J.A.M. Vermaseren. “Large loop integrals”. *Physics Letters B* 137.3 (1984), pp. 241–244. ISSN: 0370-2693. DOI: [https://doi.org/10.1016/0370-2693\(84\)90237-5](https://doi.org/10.1016/0370-2693(84)90237-5). URL: <http://www.sciencedirect.com/science/article/pii/0370269384902375>.
- [126] Z. Bern, L. Dixon, and D. A. Kosower. “Dimensionally Regulated One-Loop Integrals” (1992). DOI: [10.1016/0370-2693\(93\)90400-C](https://doi.org/10.1016/0370-2693(93)90400-C). eprint: [arXiv:hep-ph/9212308](https://arxiv.org/abs/hep-ph/9212308).
- [127] “Integration by parts: The algorithm to calculate β -functions in 4 loops”. *Nuclear Physics B* 192.1 (1981), pp. 159–204. ISSN: 0550-3213. DOI: [https://doi.org/10.1016/0550-3213\(81\)90199-1](https://doi.org/10.1016/0550-3213(81)90199-1). URL: <http://www.sciencedirect.com/science/article/pii/0550321381901991>.

- [128] Mario Argeri, Stefano Di Vita, Pierpaolo Mastrolia, Edoardo Mirabella, Johannes Schlenk, Ulrich Schubert, and Lorenzo Tancredi. “Magnus and Dyson Series for Master Integrals” (2014). DOI: [10.1007/JHEP03\(2014\)082](https://doi.org/10.1007/JHEP03(2014)082). eprint: [arXiv:1401.2979](https://arxiv.org/abs/1401.2979).
- [129] Hjalte Frellesvig. *Generalized Polylogarithms in Maple*. 2018. eprint: [arXiv:1806.02883](https://arxiv.org/abs/1806.02883).
- [130] Luca Mattiazzi. “Multiparticle Scattering Amplitudes at Two-Loop”. MA thesis. Università degli Studi di Padova, Dipartimento di Fisica e Astronomia “Galileo Galilei”, 2018.
- [131] Hans van Deurzen. “Automated evaluation of one-loop scattering amplitudes”. PhD thesis. Technische Universität München, Max-Planck-Institut für Physik (Werner-Heisenberg-Institut), 2015.
- [132] Hans van Deurzen. “Associated Higgs Production at NLO with GoSam”. *Acta Phys. Polon. B* 44.11 (2013), pp. 2223–2230. DOI: [10.5506/APhysPolB.44.2223](https://doi.org/10.5506/APhysPolB.44.2223).
- [133] Simon Badger, Hjalte Frellesvig, and Yang Zhang. “Hepta-Cuts of Two-Loop Scattering Amplitudes” (2012). DOI: [10.1007/JHEP04\(2012\)055](https://doi.org/10.1007/JHEP04(2012)055). eprint: [arXiv:1202.2019](https://arxiv.org/abs/1202.2019).
- [134] T. Hahn. “Generating Feynman Diagrams and Amplitudes with FeynArts 3” (2000). DOI: [10.1016/S0010-4655\(01\)00290-9](https://doi.org/10.1016/S0010-4655(01)00290-9). eprint: [arXiv:hep-ph/0012260](https://arxiv.org/abs/hep-ph/0012260).
- [135] Simon Badger, Hjalte Frellesvig, and Yang Zhang. “A Two-Loop Five-Gluon Helicity Amplitude in QCD” (2013). DOI: [10.1007/JHEP12\(2013\)045](https://doi.org/10.1007/JHEP12(2013)045). eprint: [arXiv:1310.1051](https://arxiv.org/abs/1310.1051).
- [136] Hjalte Axel Frellesvig. “Generalized Unitarity Cuts and Integrand Reduction at Higher Loop Orders”. PhD thesis. UNIVERSITY OF COPENHAGEN, FACULTY OF SCIENCE, 2014.
- [137] Dmitry Chicherin, Johannes Henn, and Vladimir Mitev. “Bootstrapping pentagon functions” (2017). DOI: [10.1007/JHEP05\(2018\)164](https://doi.org/10.1007/JHEP05(2018)164). eprint: [arXiv:1712.09610](https://arxiv.org/abs/1712.09610).
- [138] Samuel Abreu, Ben Page, and Mao Zeng. “Differential equations from unitarity cuts: nonplanar hexa-box integrals” (2018). DOI: [10.1007/JHEP01\(2019\)006](https://doi.org/10.1007/JHEP01(2019)006). eprint: [arXiv:1807.11522](https://arxiv.org/abs/1807.11522).
- [139] William Javier Torres Bobadilla. “Generalised Unitarity, Integrand Decomposition, and Hidden properties of QCD Scattering Amplitudes in Dimensional Regularisation”. PhD thesis. Università degli Studi di Padova, Dipartimento di Fisica e Astronomia “Galileo Galilei”, 2017.
- [140] D. Maitre and P. Mastrolia. “S@M, a Mathematica Implementation of the Spinor-Helicity Formalism” (2007). DOI: [10.1016/j.cpc.2008.05.002](https://doi.org/10.1016/j.cpc.2008.05.002). eprint: [arXiv:0710.5559](https://arxiv.org/abs/0710.5559).
- [141] Henriette Elvang and Yu tin Huang. *Scattering Amplitudes*. 2013. eprint: [arXiv:1308.1697](https://arxiv.org/abs/1308.1697).
- [142] Stefan Weinzierl. *Tales of 1001 Gluons*. 2016. eprint: [arXiv:1610.05318](https://arxiv.org/abs/1610.05318).
- [143] Jacob L. Bourjaily. *Efficient Tree-Amplitudes in N=4: Automatic BCFW Recursion in Mathematica*. 2010. eprint: [arXiv:1011.2447](https://arxiv.org/abs/1011.2447).
- [144] Simon Badger, Hjalte Frellesvig, and Yang Zhang. *Multi-loop integrand reduction techniques*. 2014. eprint: [arXiv:1407.3133](https://arxiv.org/abs/1407.3133).
- [145] Simon Badger, Gustav Mogull, and Tiziano Peraro. “Non-planar integrands for two-loop QCD amplitudes”. Oct. 2016, p. 006. DOI: [10.22323/1.260.0006](https://doi.org/10.22323/1.260.0006).
- [146] William Javier Torres Bobadilla. “T@M, a Mathematica Implementation of the Momentum-twistor Formalism”. Unpublished. 2016.
- [147] Emanuel Derman and William J Marciano. “Parity violating asymmetries in polarized electron scattering”. *Annals of Physics* 121.1 (1979), pp. 147–180. ISSN: 0003-4916. DOI: [https://doi.org/10.1016/0003-4916\(79\)90003-4](https://doi.org/10.1016/0003-4916(79)90003-4).

- [//doi.org/10.1016/0003-4916\(79\)90095-2](https://doi.org/10.1016/0003-4916(79)90095-2). URL: <http://www.sciencedirect.com/science/article/pii/0003491679900952>.
- [148] G. D'Ámbrosio. “Electron-muon scattering in the electroweak unified theory”. *Lettere al Nuovo Cimento (1971-1985)* 38.18 (1983), pp. 593–598. ISSN: 1827-613X. DOI: [10.1007/BF02782748](https://doi.org/10.1007/BF02782748). URL: <https://doi.org/10.1007/BF02782748>.
- [149] J. C. Montero, V. Pleitez, and M. C. Rodriguez. “Left-right asymmetries in polarized $e - \mu$ scattering” (1998). DOI: [10.1103/PhysRevD.58.097505](https://doi.org/10.1103/PhysRevD.58.097505). eprint: [arXiv:hep-ph/9803450](https://arxiv.org/abs/hep-ph/9803450).
- [150] F.V. Tkachov. “A theorem on analytical calculability of 4-loop renormalization group functions”. *Physics Letters B* 100.1 (1981), pp. 65 –68. ISSN: 0370-2693. DOI: [https://doi.org/10.1016/0370-2693\(81\)90288-4](https://doi.org/10.1016/0370-2693(81)90288-4). URL: <http://www.sciencedirect.com/science/article/pii/0370269381902884>.
- [151] Mario Argeri and Pierpaolo Mastrolia. “Feynman Diagrams and Differential Equations” (2007). DOI: [10.1142/S0217751X07037147](https://doi.org/10.1142/S0217751X07037147). eprint: [arXiv:0707.4037](https://arxiv.org/abs/0707.4037).
- [152] W. Beenakker and Ansgar Denner. “Infrared Divergent Scalar Box Integrals With Applications in the Electroweak Standard Model”. *Nucl. Phys. B* 338 (1990), pp. 349–370. DOI: [10.1016/0550-3213\(90\)90636-R](https://doi.org/10.1016/0550-3213(90)90636-R).
- [153] R. Keith Ellis and Giulia Zanderighi. “Scalar one-loop integrals for QCD”. *Journal of High Energy Physics* 2008.02 (2008), pp. 002–002. DOI: [10.1088/1126-6708/2008/02/002](https://doi.org/10.1088/1126-6708/2008/02/002). URL: <https://doi.org/10.1088/1126-6708/2008/02/002>.
- [154] Hjalte Frellesvig, Damiano Tommasini, and Christopher Wever. “On the reduction of generalized polylogarithms to Li_n and $Li_{2,2}$ and on the evaluation thereof” (2016). DOI: [10.1007/JHEP03\(2016\)189](https://doi.org/10.1007/JHEP03(2016)189). eprint: [arXiv:1601.02649](https://arxiv.org/abs/1601.02649).
- [155] F. del Aguila and R. Pittau. “Recursive numerical calculus of one-loop tensor integrals” (2004). DOI: [10.1088/1126-6708/2004/07/017](https://doi.org/10.1088/1126-6708/2004/07/017). eprint: [arXiv:hep-ph/0404120](https://arxiv.org/abs/hep-ph/0404120).